Wear of Hard-on-Hard Hip Prostheses: Influence of Head Size, Surgical Position, Material and Function

By

Mazen Al Hajjar

Submitted in accordance with the requirements for the degree of
Doctor of Philosophy

The University of Leeds
School of Mechanical Engineering

Leeds, UK

October, 2012

The candidate confirms that the work submitted is his own, except where work which has formed part of jointly-authored publications has been included. The contribution of the candidate and the other authors to this work has been explicitly indicated below. The candidate confirms that appropriate credit has been given within the thesis where reference has been made to the work of others.

Details of the jointly-authored publications- the work included in these publication were done by the candidate and the co-authors are the co-supervisors of the project:

- Mazen Al Hajjar, Ian J. Leslie, John Fisher, Sophie Williams, Joanne L. Tipper, Louise M. Jennings. Effect of cup inclination angle during microseparation and rim loading on the wear of BIOLOX$^®$ delta ceramic-on-ceramic total hip replacement. Journal of Biomedical Materials Research Part B: Applied Biomaterials. Wiley Subscription Services, Inc., A Wiley Company. 95B: 263-268.

- Manuscript in press: Mazen Al-Hajjar, John Fisher, Sophie Williams, Joanne L. Tipper, Louise M. Jennings. Effect of Femoral Head Size on the Wear of Metal on Metal Bearings in Total Hip Replacements under Adverse Edge Loading Conditions. Journal of Biomedical Materials Research: part B.

- Manuscript in press: Mazen Al-Hajjar, John Fisher, Sophie Williams, Joanne L. Tipper, Louise M. Jennings. Wear of 36mm BIOLOX Delta Ceramic-on-Ceramic Bearings in Total Hip Replacement under Edge Loading Conditions. Proceedings of Institute of Medical and Biological Engineering: Part H, Journal of Engineering in Medicine.

This copy has been supplied on the understanding that it is copyright material and that no quotation from the thesis may be published without proper acknowledgement.

Acknowledgements

Abstract

Edge loading in hip replacement bearings may occur due to rotational and translational mal-positioning. Rotational mal-positioning is easier to detect clinically which include steep inclination angle and excessive version/ante-version angles. Translational mal-positioning encompasses micro-separation of the centres of rotations of the head and the cup and could occur due to several clinical reasons, such as head offset deficiency, medialised cup, stem subsidence, impingement, subluxation and laxity of the joint/ soft tissue. Microseparation conditions were validated on the Physiological Anatomical Leeds Mark II Hip Joint Simulator against retrievals and shown to replicate stripe wear, and wear debris seen *in vivo*. The present thesis is focused on understanding the wear mechanisms of different sized ceramic-on-ceramic and metal-on-metal bearings under the different edge loading conditions and determining the contributions of rotational and translational mal-positioning to the increase in wear. The wear of ceramic-on-ceramic bearings did not increase due to rotational mal-positioning, however stripe wear and increase in wear rates occurred under translational mal-positioning conditions. On the other hand, the wear of metal-on-metal bearings was influenced by both rotational and translational mal-positioning with the latter having the more severe effect. There was clinically no difference in the wear of the 36mm bearings when compared to the 28mm bearings under translational mal-positioning conditions. However, with the larger bearings, edge loading due to rotational mal-positioning occurred at a steeper cup inclination angle. Edge loading caused severe wear features and roughening of the surface of metal-on-metal bearings with indications of increased corrosion rates. The new validated geometric measurement and analysis technique have helped determine the volumetric wear of ceramic and metal components and show three-dimensional representations of the wear areas, which could be applied for determining wear volumes and understanding wear features on retrieved explants. This thesis has emphasised the need for a more accurate surgical positioning and shown the necessity for testing hip replacement bearings under a wider range of clinical conditions that go beyond the current ISO standards. This should also include conditions which generate rotational and translational mal-positioning *in vivo*.

Table of Contents

List of Tables

List of Figures

Chapter 1 . INTRODUCTION

Total hip replacements have been used as a solution to hip joint disorders since 1938. The total hip replacement procedure involves separating the acetabulum from the femoral head by introducing a bearing surface between the two parts of the joint thus reducing pain and restoring motion. Several materials have been used as bearing surfaces since the start of the development of hip prostheses. The bearing couple used by surgeons can be metal-on-polyethylene (MoP) and ceramic-on-polyethylene (CoP), which are known as hard-on-soft bearings; and metal-on-metal (MoM), ceramic-on-ceramic (CoC) and ceramic-on-metal (CoM), which are known as hard-on-hard bearings.

Hard-on-soft bearings have suffered long term failure due to polyethylene wear debris induced osteolysis (Willert, 1977). Osteolysis is a result of biological and biomechanical interactions between the wear debris produced by the total hip arthroplasty and the environment. This is dependent on the wear volumes and size and shape of the wear debris produced. Small submicron polyethylene wear particles elicit more intense biological activities than larger particles (Green et al., 1998). There is an imperative to develop longer lasting prostheses that can be used for high demand younger and more active patients. This is and has been the main reason for the increased interest in polyethylene-free hard-on-hard bearings.

1.1 The Natural Hip Joint

The hip joint is a synovial joint that connects the lower limb to the trunk. It consists of a synovial ball (femoral head) and a socket (acetabulum), and as such allows a wide range of movements (Palastanga et al., 2006) (Figure 1.1A). The hip joint is capable of supporting the entire weight of the body while providing stability especially during the movement of the trunk on the femur, as happens during walking and running. The shape of the articular surface, the strength of the joint capsule, ligaments (Figure 1.1B) and muscles determine the stability of the hip joint.

Under low loading conditions, the contact area between the femoral head and the acetabulum is limited. This contact area increases when the loading is increased thus distributing the load over a greater area and as a result reducing excessive stress in the underlying cartilage. The contact stress or pressure are higher at the superior surfaces of the femoral head and the acetabulum relative to the other parts of the articulating surface. This difference in pressure distribution is due to the orientation of the femur relative to the pelvis. Consequently, the articular cartilage is thicker in the superior region than elsewhere.

The angle between the femoral neck and the shaft is called the angle of inclination in the frontal plane and the angle of anteversion in the horizontal plane. In an average adult, the angle of inclination of the femoral head is around 125° and the angle of anteversion is around 10°. These angles vary from one individual to another and they play an important role in the stability of the hip joint (Palastanga et al., 2006).

The hip joint allows movement in the three planes. In the sagittal plane, the hip joint has the largest range of motion of 165° (20° extension and 145° flexion). The extension of the hip is maximised to around 30° when the knee joint is extended. In the frontal plane, the range of motion is around 65° in which 40° is abduction and 25° is adduction. In the transverse plane, the medial and lateral rotations are of range of 70° and 90° respectively. A combination of movement about the different axis will limit the range of motions, for example, the range of the medial and the lateral rotation is minimised when the hip joint is fully extended (Palastanga et al., 2006).

The forces in the hip joint were estimated to range up to five times body weight during normal gait. During walking, the hip joint forces are maximal at heel strike and toe off and minimal during swing phase (Paul, 1966).

A

B
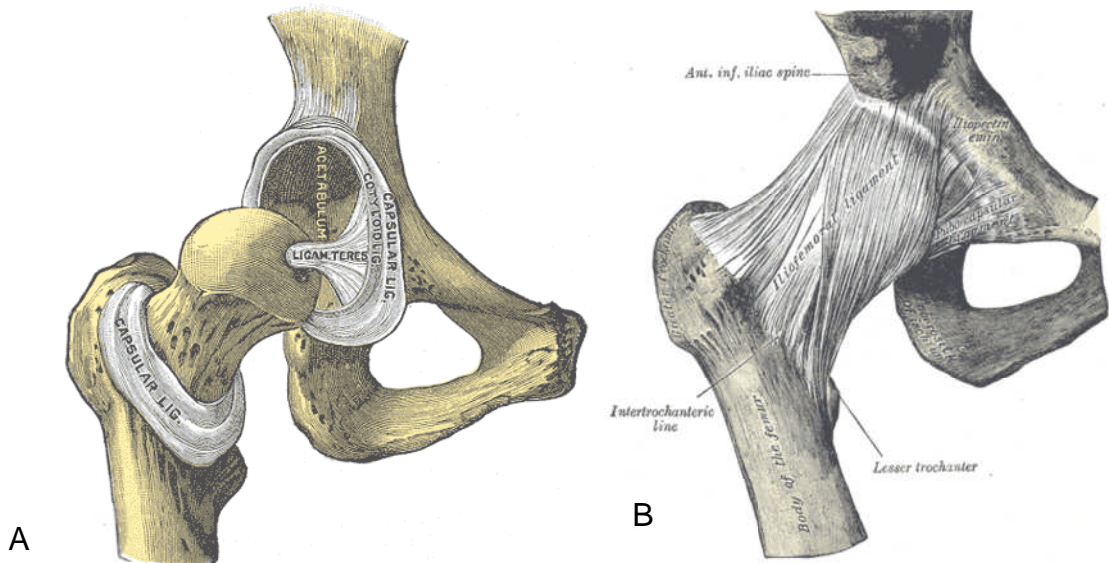
Figure 1.1: The natural hip joint (right hip). (A) capsule removed, anterior aspect, (B) showing the ligament (Gray, 2000).

1.1.1 Disorders of the hip joint

1.1.1.1 Osteoarthritis

Osteoarthritis is the degeneration of the articular cartilage especially in weight bearing joints such as hips, knees, spine, and ankles. The breakdown of cartilage tissue is dependent upon loss of the amorphous portion of the matrix and the collagen framework which results in either a local lesion, or a pattern of erosion that leads to the degeneration of articular cartilage lining. The breakdown of such tissue will lead to bones rubbing against each other in the joint that causes severe pain (Charlish, 1994).

Osteoarthritis mainly affects older people and can range from mild to severe conditions. The cause of osteoarthritis is not only age-related but it can be due to high levels of stresses in the joint due to extensive sport activities. There is also high correlation with obesity. Table 1.1 shows the prevalence of radiographic osteoarthritis in the hip joint of both sexes of different age range.

Table 1.1: Prevalence of radiographic osteoarthritis in the hip (Callaghan et al., 2007).

Age	Sex	Prevalence
<55	Men	1%
	Women	1%
55-65	Men	3%
	Women	2%
>65	Men	6%
	Women	4%

1.1.1.2   Rheumatoid Arthritis

Rheumatoid arthritis is a systemic inflammatory disorder that often progresses to cause destruction of the articular cartilage. The initial cause of such disease is not well understood, however immunity plays a vital role in its progression and chronicity. It usually initiates as inflammation in the synovium, which causes thickening of the membrane and proliferation of the synovial fluid and the connective tissue. This will lead to loss of stability, thinning of the articular cartilage and destruction of the joint (Charlish, 1994, Corr, 2003).

1.1.1.3   Avascular Necrosis

Avascular necrosis, also known as ischemic bone necrosis, is a disease resulting from the loss of blood supply to the bone. In the hip joint, as the disease progresses, the cells start to die and lead to the destruction of the articular cartilage and collapse of the joint. Alcoholism, excessive steroid use, and post trauma are the most common causes of such a disease that is

common in 30-70 year old individuals and affects the male more than the female population (Fagerson, 1998).

1.2 Artificial hip joint

Hip joint replacement can be described as the most successful achievement in orthopaedic surgery. The single largest indication for hip joint replacement surgery is osteoarthritis, recorded in 94% of cases (National Joint Registry for England and Wales, 5th Annual report, 2008). Hip joint replacements are also used in cases of rheumatoid arthritis, femoral neck fracture, and avascular necrosis. A conventional total hip prosthesis consists of a metallic stem and a femoral head articulating against an acetabular cup and only a head and cup in the case of the surface replacement. The aim is to reduce pain and restore function by separating the exposed bone and creating a low friction bearing. Fixation techniques and the type of bearing surfaces are the two main issues in the design of such prostheses. The components can either be fixated using bone cement (cemented prosthesis) or by using a porous sintered coating which allows bone growth (non-cemented prosthesis). The most common and widely used total hip replacements consist of a metal head articulating against a polyethylene cup (MoP) (Figure 1.2). The MoP bearing was first implanted by Charnley in 1958 and was called the low friction arthroplasty (LFA). The poor long term results of such bearing combinations due to polyethylene wear debris induced osteolysis (Willert, 1977), encouraged the use of polymer-free hard-on-hard bearing such as metal-on-metal (MoM), ceramic-on-ceramic (CoC), and ceramic-on-metal (CoM).
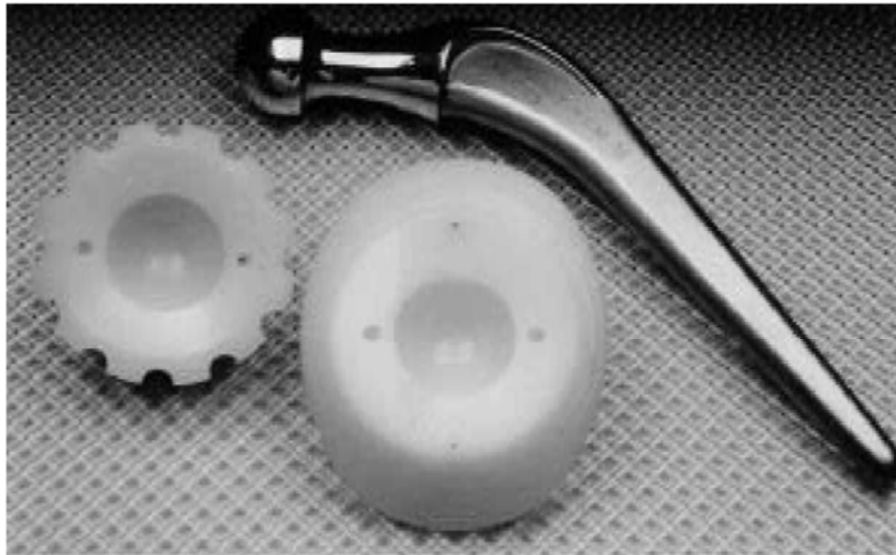
Figure 1.2: Monolithic stainless steel femoral stem and head with polyethylene acetabular cups (Dowson, 2001).

1.2.1 History of total hip replacement

In 1938, Philip Wiles (London) developed the first total hip replacement that consisted of a stainless steel cup and head. The cup was fixated using screws and the head was fixated using a stem, which was fixed to the neck of the femur by a bolt. Clinical results of this development were not known due to the intervention of World War II. Years later, metal-on-metal combinations were introduced by McKee, Farrar and Ring (UK) and Haboush, Urist and McBride (US). The results from such implants were not satisfactory due to loosening and high wear of the components as a result of increased frictional torque (Walker and Gold, 1971). These MoM prostheses were manufactured to give a matching femoral head and acetabular cup with no clearance (small space between the head and the cup). It was shown that introducing a small clearance between the two components could reduce friction between the components by creating a polar bearing (Walker and Gold, 1971).

It was not until 1958 when Sir John Charnley implanted the first metal-on-polymer total hip replacement. The first polymer Charnley chose was PTFE articulating against a stainless steel head, which only survived two years due to the rapid wear of PTFE. In 1961, he adopted ultra-high molecular weight

polyethylene (UHMWPE) which provided a low interfacial friction against a metal head. This prosthesis was called the 'Low Friction Arthroplasty' (LFA). Clinical results have encouraged the use of the Charnley prosthesis. Its concept is still being used to date in less active elderly patients (Charnley, 1982).

Metal-on-metal bearings were of great interest in the late 1980s after the long-term survivorship and the low wear of such prosthesis. It was thought that the improved tolerances and better surface finishes that can be achieved by better manufacturing technologies, would improve the outcome of metal-on-metal prostheses. The further developments of MoM prostheses will be discussed in subsequent sections.

In the early 1970s, Boutin, France, developed the first ceramic-on-ceramic (CoC) total hip replacement (Boutin et al., 1988). It was widely used in Europe after the promise of ceramics as a highly inert material and due to the good surface finish and excellent resistance to wear in vivo (Bizot et al., 2000). Although CoC have shown enhanced wear performance, there are still concerns about the incidental fracture of the ceramic material (Cales, 2000). The further developments of CoC prostheses will be discussed in subsequent sections.

A new developed bearing in total hip replacement is the ceramic-on-metal (CoM) combination. CoM consists of a ceramic head that articulates against cobalt chrome (CoCrMo) liner. This bearing offers enhanced wear performance which has been shown by Firkins et al. (2001b) in an in vitro hip simulator study. The smoothness of the ceramic head help reduce abrasive wear on the metallic liner. It also provides reduced risk of liner fracture that was seen in CoC bearings and reduced levels of ion concentrations compared to MoM bearings (Williams et al., 2007a).

1.2.2 Complications of total hip replacement

Total hip replacements have shown great success over the years with more than 62,000 procedures undergone every year in the UK (National Joint Registry for England and Wales, 5th Annual report, 2008). However, total hip replacements are not yet perfected and failure due to several reasons has been reported. Several complications that lead to revision of such

prostheses include osteolysis and loosening, dislocation, infection, leg length discrepancy, impingement, metallosis, adverse soft tissue responses, and pseudotumours.

1.3 Tribology of Hard-on-Hard Bearings in Total Hip Replacement

1.3.1 Principles of Tribology

1.3.1.1 Wear

Wear is defined as progressive removal of substance from the surface of a solid as a result of its motion relative to the adjacent moving part (Williams, 2005). There is no specific relation between wear and friction. Adding a lubricant to the moving surfaces can reduce wear. In most cases, harder and smoother surfaces wear less than soft and rougher surfaces. The studies of wear of bearing surfaces are not only focused on the volumes of material lost but also on the shape and size of the debris produced. Wear particles can cause adverse tissue reactions, osteolysis and loosening of the prosthesis. The wear in the joint can be some combinations of adhesive, abrasive, corrosive, or surface fatigue, which are described briefly in this section (Williams, 2005, Stachowiak and Batchelor, 2005).

The adhesive wear mechanism is the transference of material from one surface to another due to shearing of junctions between contacting asperities. The contact between the asperities is the actual or real contact area between the bearing surfaces. When a load is applied, deformation occurs until the contact area is large enough to support the applied force. Adhesive wear is the most common and least preventable wear mechanism in bearing couples.

Abrasive wear is the displacement of material due to harder particles trapped in the bearing surface or due to a hard material ploughing grooves into a softer one.

Surface fatigue wear is the loss of material due to cyclic stress variation. This can occur due to the transmission of repetitive stresses through the lubricant that separates both bearing surfaces (Halling, 1975). The severity

of the damage is related to the number of cycles the material has gone through, the level of stress it encountered and the friction acting at the surface during its lifetime.

Corrosive wear occurs due to the chemical interaction of the material with the surrounding environment. It is enhanced by the friction because this causes the removal of passivation layers and further corrosion of the materials surfaces.

1.3.1.2 Friction

Friction is defined as the resistance to motion when two bodies move tangentially over one another (Rabinowicz, 1965). Table 1.2 shows frictional factor values of materials used in bearing surfaces for total hip replacement.

The friction factor is a dimensional parameter defined as:

$$\mathbf{f} = \frac{T}{\mathbf{RW}}$$

where T is the frictional torque, R is the femoral head radius and W is the applied force.

Table 1.2: Typical friction factors for various bearings for artificial hip joints in the presence of 25% bovine serum (Jin et al., 2006b).

Bearing	Frictional factor
Metal-UHMWPE	0.06-0.08
Ceramic-UHMWPE	0.06-0.08
Metal-on-metal	0.22-0.27
Ceramic-on-ceramic	0.002-0.07
Ceramic-on-metal	0.002-0.07

1.3.1.3 Lubrication

Lubrication is the addition of a material, most often a liquid, to the bearing surface usually to reduce wear and friction. The mode of lubrication between

two moving surfaces can often be divided into three distinct regimes: fluid film, boundary and mixed lubrication modes. The mode of lubrication that any one bearing system is under, is dependent upon a number of factors which include the lubricant properties, roughness and stiffness of the bearing surfaces, sliding speed, and loading.

Table 1.3: Typical friction factors for various lubrication regimes in artificial joints in the presence of bovine serum (Jin et al., 2006b).

Lubrication regimes	Friction factor
Boundary Lubrication	0.1-0.7
Mixed Lubrication	0.01-0.1
Fluid-film lubrication	0.001-0.01

1.3.2   In Vitro Studies of Bearing Surfaces for Total Hip Replacement

In vitro studies of bearings for total hip replacement, which were more relevant to joint tribology, began in the early 1970s (Dowson, 2001). The most common testing techniques were friction and wear tests on pin-on-plate rigs and hip joint simulator machines. Hip simulator studies have been used extensively in the past 15 years to evaluate the performance of new prostheses. Some of these publications are: (Brummitt and Hardaker, 1996, Chan et al., 1996, Streicher et al., 1996, Farrar and Schmidt, 1997, Barbour et al., 1999, Goldsmith and Dowson, 1999a, Goldsmith and Dowson, 1999b, Tipper et al., 1999, Barbour et al., 2000, Cales, 2000, Clarke et al., 2000, Goldsmith et al., 2000, Nevelos et al., 2000, Anissian et al., 2001, Dowson, 2001, Firkins et al., 2001b, Firkins et al., 2001a, Firkins et al., 2001c, Nevelos et al., 2001a, Rieker et al., 2001, Scholes et al., 2001, Smith et al., 2001, Spector et al., 2001, Stewart et al., 2001, Butterfield et al., 2002, Fisher et al., 2002, Stewart et al., 2002, Good et al., 2003, Stewart et al., 2003a, Stewart et al., 2003b, Williams, 2003, Williams et al., 2003a, Williams et al., 2003b, Dowson et al., 2004a, Dowson et al., 2004b, Fisher et al.,

2004, Rieker et al., 2004a, Williams et al., 2004b, Affatato et al., 2005, Aust, 2005, Bowsher et al., 2005, Saikko, 2005, Vassiliou, 2005, Affatato et al., 2006, Bowsher et al., 2006a, Bowsher et al., 2006b, Brockett et al., 2006, Pavoor et al., 2006, Vassiliou et al., 2006, Williams et al., 2006, Angadji et al., 2007, Gispert et al., 2007, Williams et al., 2007a, Leslie et al., 2009). These studies have provided researchers, engineers, and designers with the data that allowed further improvement of existing prostheses and development of new ones. It also provided clinicians with an indication of expected wear rates in vivo.

Different laboratories have used different methods for hip simulation. These include loadings, kinematics, lubrication, test period, measurement points, fixturing, and measurement methods. These variations have made it difficult to compare results obtained from different labs. In the laboratory at Leeds University, a walking gait cycle has generally been employed, with a twin peak loading of 3 kN and a swing load of 0.3 kN, flexion/extension of -15°/+30° and internal/external rotation of -10°/+10°. Abduction/adduction were not applied in the loading regime of the new developed hip simulators due to the complexity of hip simulator model and the findings of Barbour et al. (1999) which highlighted the minimal effects abduction/adduction had on the wear of metal-on-polyethylene bearings.

Wide ranges of different conditions have also been employed in the same laboratory (University of Leeds) on the hip simulators. Barbour et al. (1999) and Firkin et al. (2001a) investigated the influence of different kinematics on the wear performance of MoP, CoP and MoM combinations. The influence of loading regimes (swing phase load) was investigated by Williams et al. (2004b, 2006).

Different concentrations of lubricants have been used in different laboratories. Chan et al. (1999) used 95% (v/v) calf serum as lubricant. In the laboratory at the University of Leeds, 25% (v/v) new-born calf serum is used. The rationale behind dilution of the serum to this level was to try and match the protein concentration with that found in human synovial fluid (Saari et al., 1993). The lubricant is generally supplemented with sodium azide to try and inhibit bacterial growth by scavenging oxygen in the solution.

Some laboratories use ethylenediamine tetraacetic acid (EDTA) in their lubricant to avoid the development of calcium phosphate layer on the bearing surfaces, which could cause reduction in wear of the test components. However, the laboratory at Leeds University does not add EDTA to the lubricant, when testing hard-on-hard bearings, based on the findings of Mckellop et al. (1996) who reported formation of such films on retrieved MoM bearings.

Gravimetric analysis is the most common method in determining the cumulative wear of test components. This is done by taking the components off the simulator machine, and cleaning them carefully before using a high accuracy balance to weigh them. One of the challenging issues with this technique is the effort needed to remove all protein precipitate from the wear area using a very soft material to avoid scratching or damaging the components. In addition, the accuracy of the balance (accuracy up to 0.01 mg) is a limitation in this technique especially in the very low wearing ceramic components. Bills et al. (2007) used a coordinate measuring machine (CMM) to assess the wear of the test components. This method is very effective and advantageous in assessing the wear of polyethylene due to high penetration and wear. However, the CMM measurements are not accurate enough to determine the wear in hard-on-hard bearings which often have linear penetration of around 1µm (Brummitt and Hardaker, 1996).

Cumulative volumetric wear has been a common assessment of the performance of different bearing surfaces. However, recently it has been shown that osteolysis is dependent on the shape and size of the debris and the resultant biological activity (Green et al., 1998, Ingram et al., 2004). Thus, characterising the wear debris and determining their relative biological activities (Tipper et al., 1999, Firkins et al., 2001c, Fisher et al., 2001, Tipper et al., 2001, Endo et al., 2002) in combination with the volumetric wear rate allowed direct comparisons of the overall tribological and biological performances of different bearing surfaces.

1.3.3   In Vivo Wear Assessment of Total Hip Replacement

The wear of hard-on-hard bearing couples can be too low to be measured using clinical radiographs in situ. So in vivo wear assessment of such

bearings can only be done on retrieved components. Generally, a coordinate measuring machine (CMM) was used to quantify the amount of wear. The machine could assess the sphericity of the bearing surface relative to a perfect sphere. The deviation of sphericity measured would be the combination of both wear and original manufacturing deviations. For this reason, only positive deviations of the cup profile and negative deviations of the head profile are considered to be due to wear (Mckellop et al., 1978, McKellop et al., 1996, Schmalzried et al., 1996b).

The volumetric wear can then be determined by integrating the depth of multiple individual points on the worn part of the bearing surface. The wear scar on the head can be located with reference to the stem orientation. However, it is challenging to find a reference point on the acetabular component unless impingement wear is present so it can be used as a reference point.

In vivo wear assessment is challenging due to the number of variables that contribute to wear. These variables can be related to individual patients and hip reconstructions, which affect the kinematics and kinetics the prosthesis is exposed to, the lubrication modes and third body wear mechanisms, thus affecting the wear rate of the bearing surface. These variables include: age, gender, weight, general health, activity of patient, implanted materials, design and manufacturing of prosthesis, biomechanical considerations, and fixation techniques.

Wear assessment techniques also play a role in the variations of in vivo results. Thus, comparison of results from different groups could be limited.

Unlike in vitro studies, where the wear rates of the bearing couples are expressed per number of cycles, in vivo results are expressed per year. Schmalzried et al. (2000) has clearly stated and showed that the wear is a function of use, not time. Therefore, these limitations of in vivo results have to be considered when assessing the wear of retrieved prostheses.

It has been suggested that elderly patients walk an average of about 1 million steps per year (Seedhom and Wallbridge, 1985). The Seedhom et al. (1985) study was based on nine healthy elderly people on vacation. The results showed a huge variability in the number of gait cycles recorded due

to the activities of each patient. The most active patient from that study averaged 3.2 million steps per year. A more recent study by Silva et al. (2002) on patients of mean age of 71 years averaged 2 million gait cycles per year. It is also clear that there is a correlation between the number of gait cycles and age (Silva et al., 2002). So younger more active patients could easily exceed 4 million gait cycles per year and this has to be considered when assessing new developed prostheses in in vitro studies.

1.3.4 Tribology of Ceramic-on-Ceramic Total Hip Replacement

1.3.4.1 Ceramic materials

Ceramic material is defined as a non-metallic and inorganic material. The end product of ceramic material is dependent upon the purity of the material and the manufacturing process applied. The machining process is important to avoid any residual cracks that can lead to fracture of the product. Hot isostatic Pressing allows minimisation of residual stresses within the ceramic material which has been introduced during the 1990s and resulted in huge improvements in the strength and reliability of the ceramic components.

1.3.4.2 Developments and issues of alumina ceramics in total hip replacements

Alumina-on-alumina ceramic bearings for total hip replacement were introduced by Boutin in the early 1970s. They were introduced to address the problems of friction and wear in MoM and MoP bearings surfaces. The first generation of alumina ceramic showed low friction and low wear rates. However, this material faced a few limitations including risk of fracture, squeaking noise, and difficulty to obtain stable fixation of the femoral head and the acetabular cup.

Alumina ceramic heads are harder than titanium and cobalt chrome alloys used in femoral stem manufacturing (Cuckler et al., 1995). When the alumina head is impacted onto the metal taper, tensile stress is generated in the ceramic head that can sometimes cause its. The risk of fracture of the ceramic head could be reduced by careful manufacturing and proper

surgical techniques. It has also been reduced by the development of the second-generation alumina ceramic, which has fewer impurities and higher fracture toughness.

The fracture of ceramic prostheses is correlated with its fracture toughness. So avoiding the fracture of such prostheses could be achieved by improving the properties that are correlated to fracture toughness. This was the aim when developing the third generation alumina ceramics which was hot isostatic pressed (HIPed) subsequent to the process of sintering. This product was developed by CeramTec AG (Germany) and it is commercially known as BIOLOX$^{®}$ Forte. Laser engraving was used instead of mechanical engraving to avoid initiation of weak stress areas. The hot isostatic pressing process enabled optimisation of the material density and microstructure. Also, the use of lower temperatures with the HIP process compared to the sintering process minimised grain growth and resulted in smaller grain size in the end product.

Further innovations in ceramic materials for orthopaedic implants have led to the development of the fourth generation alumina matrix composite (AMC, CeramTec AG, Germany) which is commercially known as the BIOLOX$^{®}$ Delta. This material consists of 72.5% alumina, 25.5% zirconia and 2% mixed oxides (Masson, 2009). AMC makes use of the stable monoclinic phase transformation of the zirconia grains in the microstructure, which makes the material more resistant to severe mechanical overloading as it impedes microcracking. The mechanical characteristics of different generations of ceramic materials are shown in Table 1.4.

Table 1.4: Mechanical characteristics of different alumina ceramics (Masson, 2009).

Properties of ceramics	Alumina ceramics; ISO 6474 (1994)	1st and 2nd generations alumina	3rd generation HIPed alumina; (BIOLOX® Forte)	4th generation alumina matrix composite; AMC (BIOLOX® Delta)
4-point bending strength (MPa)	400	500	580	>1000
Average grain size (µm)	<4.5	<3.2	<1.8	<1.5
Density (g/cm^3)	3.94	3.96	3.98	4.37
Fracture toughness K_{1c} (MPa.m$^{1/2}$)	>2.5	4-5	4-5	6.5-8.5

Squeaking is another issue for ceramic-on-ceramic bearings in total hip replacement. Capello *et al.* (2008) have reported squeaking in 0.8% of ceramic-on-ceramic bearings at 8 years follow up, which the author described as "occasional and transient in nature". Some other publications have reported similar if not lower squeaking rates but others reported a significant percentage of squeaking incidents (Table 1.5).

Table 1.5: Squeaking incidents in ceramic-on-ceramic total hip replacements.

Reference	Product name and company	Type of ceramics	% of squeaking incidents	Follow up (years)
(Capello et al., 2008)	ABC & Trident alumina ceramic, Stryker orthopaedics	Alumina-on-Alumina	0.8%	8
(Lusty et al., 2007)	BIOLOX® forte, CeramTec AG, Germany	HIPed Alumina-on-Alumina	0.3%	5
(Walter et al., 2007)	BIOLOX® forte, CeramTec AG, Germany	HIPed alumina-on-alumina	0.6%	8
(Jarrett et al., 2007)	Not provided	Alumina-on-alumina	7%	3
(Keurentjes et al., 2008)	Not provided	Alumina-on-alumina	20.9%	4

1.3.4.3 *In vivo* wear of ceramic-on-ceramic bearings

In vivo wear assessment of ceramic-on-ceramic bearings is done on retrieved components from which the prostheses have failed due to various reasons. Some of the reasons for revision are: loosening of either or both of the femoral and the acetabular components, fracture and infection.

1st and 2nd generation alumina ceramics

Several publications reported *in vivo* wear rate of early generations ceramic-on-ceramic bearings with high variation between the results. Boutin *et al.*

(1988) and Mittlemeier and Heisel (1992) reported a linear wear rate of 5-9 μm/ year and 10μm/ year respectively. However, Nevelos *et al.* (1999) reported an increased linear wear of up to 953μm on both components combined of one prosthesis after 1 year of implantation.

Nevelos *et al.* (1999) conducted an analytical study on 11 retrieved alumina ceramic-on-ceramic bearing couples. These components were retrieved from a 16-year series of Mittlemeier implants implanted between 1980 and 1996. The reason for revision was either aseptic loosening of the acetabular component, loosening of the femoral components or both. However, one prosthesis was thought to be loose until proven otherwise during the surgery and only the head was replaced. The wear penetration measured varied from 4μm to 2946μm for the acetabular cup and between 27μm and 1967μm for the femoral head. The volumetric wear rate of the femoral head ranged between <1mm^3/year to approximately 262 mm^3/ year. The components were split into three categories of wear: severe (four cases), stripe (six cases) and low (one case). Steep acetabular cup inclination angle was associated with high wear rate of ceramic-on-ceramic bearings. A 'stripe' like wear shaped area was observed on the femoral heads with a corresponding wear area on the acetabular cups. Stripe wear was defined as a narrow and elongated wear area on the femoral heads formed as a consequence of edge loading. Low wear was found in normally functioning prostheses.

3rd generation HIPped alumina ceramics

Walter *et al.* (2004) analysed 16 retrieved 3rd generation alumina ceramic-on-ceramic bearings couples (16 heads and 12 cups). The reasons for revision were: psoas tendonitis, infection, periprosthetic fracture of the femur and dislocation. Stripe wear was observed on 11 out of the 16 heads retrieved and four bearing couples showed no visible wear. The average volumetric wear rates of the heads and liners were 0.4 mm^3/ year and 0.3 mm^3/ year respectively. The maximum volumetric wear rates reported for one retrieved bearing couple were 1.9 mm^3/ year and 1.6 mm^3/ year for the head and cup respectively.

It is important to note the difference in the maximum volumetric wear rate reported by Nevelos *et al*. (1999) for the 2nd generation alumina CoC bearing couples (262 mm^3/ year) and that by Walter *et al*. (2004) for the 3rd generation alumina CoC bearing couples (1.9mm^3/year).

Lusty *et al.* (2007) analysed 7 retrieved 3rd generation alumina CoC bearing couples after more than six months of implantation. Stripe wear was observed on five heads and the remaining two heads showed no macroscopic wear. The average wear rate of the femoral heads was 0.3mm^3/year with a maximum wear rate of 0.7mm^3/year measured on two heads revised due to osteolysis.

The wear rate of CoC bearings is extremely low for the well-functioning prostheses. The *in vivo* wear rate of the 3rd generation alumina CoC bearings was lower than that reported for earlier generations. Also stripe wear was consistent for retrieved CoC bearings.

1.3.4.4 *In vitro* wear of ceramic-on-ceramic bearings

Ceramic-on-ceramic bearing couples have shown extremely low wear rates under standard simulator conditions compared to other bearings couples such as MoM, MoP and CoP. Nevelos *et al*. (2001b) reported a volumetric wear rate of 0.15mm^3/ million cycles for 2nd generation alumina CoC and 0.09mm^3/million cycles for 3rd generation HIPed alumina CoC bearings couples under standard simulator conditions.

Wear rate of CoC under standard simulator conditions did not replicate wear rates and patterns observed on retrievals. Nevelos *et al*. (2001b) investigated the effect of elevated swing phase load on the wear of CoC bearings, finding no difference in wear rates compared to standard conditions.

Several groups have investigated the effect of cup inclination angle on the wear rate of ceramic-on-ceramic bearings *in vitro*. Refior *et al*. (1997) reported a 25% to 65% increase in wear rate of 2nd generation alumina CoC

bearings when the cup inclination angle was increased from 45° to 55°. Affatato *et al.* (2004) found no significant difference in the wear rate of 3rd generation alumina CoC bearings for cup inclination angles of 23°, 45° and 63°. The same conclusion was reported by Nevelos *et al.* (2001a) for cup inclination angles of 45° versus 60° for the 3rd generation alumina CoC.

Stripe wear reported on retrieved CoC femoral heads could not be replicated under standard hip simulator conditions and steep cup inclination angles. Nevelos et al. (2000) modified Leeds Mark II physiological Anatomical Hip Simulator to replicate microseparation of the joint. This was based on fluoroscopic studies that showed separation of the head and cup during swing phase of walking for MoP hip prosthesis (Mallory et al., 1999). Nevelos *et al.* (2000) tested 2nd and 3rd generations alumina CoC bearing under microseparation conditions. Stripe-like wear area was observed on all the heads with a corresponding wear area on the cups. Besides, the wear rates obtained were comparable to those seen clinically.

Microseparation is associated with edge loading at heel strike and is caused by head offset deficiency or joint laxity. The contact mechanics of ceramic-on-ceramic hip implants was altered by the microseparation of the femoral head where the femoral head contacted the superolateral rim of the acetabular cup (Mak et al., 2002).

Stewart *et al.* (2001) compared the wear rate of 3rd generation HIPed alumina CoC under standard conditions and, mild and severe microseparation conditions. The severity of the microseparation condition was adjusted by changing the swing phase load of the two-peak loading cycle with lower swing phase load resulting in more severe conditions. The mean bedding-in wear rates were 0.11 mm^3/million cycles, 0.55 mm^3/million cycles and 4.0 mm^3/million cycles for standard, mild microseparation and severe microseparation conditions respectively. The mean steady state wear rates were 0.05 mm^3/million cycles, 0.1 mm^3/million cycles and 1.3 mm^3/million cycles for standard, mild microseparation and severe microseparation conditions respectively. The overall wear rate under the severe microseparation condition was 1.84 mm^3/million cycles which was

comparable to wear rates reported by Walter *et al.* (2004), 0.7 mm^3/year, and Lusty *et al.* (2007), 0.3 mm^3/year on femoral head only.

Stewart *et al.* (2001, 2003b, 2003a) reported the wear rate of different ceramic bearings combination under hip simulator microseparation conditions. The 4th generation alumina matrix composite (AMC), zirconia heads (ZrO$_2$) and the 3rd generation alumina ceramic (HIPed Al) were used. The combinations were AMC-on-HIPed Al, AMC-on-AMC, and ZrO$_2$-on-HIPed Al. AMC-on-HIPed Al and AMC-on-AMC showed a total wear rate of 0.61 mm^3/million cycles and 0.16 mm^3/million cycles respectively (Stewart et al., 2003a), which were significantly lower than that of HIPed Al-on-HIPed Al (1.87 mm^3/million cycles) reported previously (Stewart et al., 2001). A catastrophic result was reported for the ZrO$_2$-on-HIPed Al combination with the fracture of the zirconia head in one case and a mean wear rate of 6.8 mm^3/million cycles (10.6 mm^3/million cycles bedding-in and 1.8 mm^3/million cycles steady state) obtained. Stripe wear was reported on all heads tested under microseparation conditions with corresponding wear area on the acetabular liner.

Manaka *et al.* (2004) studied the wear of 3rd generation alumina CoC under microseparation conditions. However, the microseparation condition applied on the simulator was slightly different from that of Stewart *et al.* (2001) and Nevelos *et al.* (2000). Stewart *et al.* achieved microseparation (edge loading) by applying a 0.5mm displacement in the horizontal plane, using a spring force during swing phase, where the vertical load was dropped to approximately 70N. Manaka *et al.* applied the same displacement using a spring load, but applied a negative vertical load during swing phase, which resulted in 1mm vertical distraction creating an inferior peripheral wear scar on the head as well as a superior wear scar due to edge loading at heel strike. This scenario assumed that the femur was pulled away from the pelvis during swing phase creating complete separation which makes this method less clinically relevant than the method applied by Stewart *et al.* (2001). The study by Manaka *et al.* (2004) showed a 3 to 6-fold increase for the bedding-in wear and a 14 to 59-fold increase for the steady-state wear under microseparation conditions compared to standard condition. This

study also showed an increase in the wear rate with increasing the head diameter with mean wear rates of 0.4, 0.51, and 1.02 mm^3/million cycles for bearings sizes of 28, 32, and 36 mm respectively.

1.3.5   Tribology of Metal-on-Metal Total Hip Replacement

1.3.5.1   Conventional Metal-on-Metal Bearings

The long-term failure of metal-on-polyethylene due to the polyethylene wear debris induced osteolysis (Willert, 1977) encouraged the re-introduction of metal-on-metal bearings after it was abandoned in the 1970s due to concerns regarding metal sensitivity and high frictional torques. Early metal-on-metal design was re-introduced by Muller in the early 1980s. The femoral head and the acetabular cups were made up of CoCrMo and were coated with titanium nitride (TiN) and titanium carbide (TiC) respectively. However, this design was abandoned by Muller due to concerns regarding the durability of the coating (Muller, 1995). Sulzer and Weber were also responsible for the re-introduction of metal-on-metal bearings in the 1980s. Sulzer used high carbon CoCrMo with no coating. The manufacturing technique and the material structure allowed the surface to be highly polished thus reducing the frictional torque, which was present in earlier designs. Weberalso used the CoCrMo without any coatings but he designed the acetabular cup embedded in a polyethylene backing covered with a titanium shell. The tribology of metal-on-metal bearings and clinical findings are discussed in later sections of the introduction.

1.3.5.2   Surface Replacement Arthroplasty

1.3.5.2.1   Development of Surface replacement arthroplasty

Total hip replacement is an effective operation for restoring motion and function of the hip joint. However, this surgery has several inherent shortcomings, which involves sacrificing the femoral head and neck. Replacement of such prostheses, when they fail, is challenging and not always possible and can result in an unstable joint and leg discrepancy. Also, the load distribution in the joint is totally changed with the introduction

of the femoral stem and this might result in loss of bone around the implant and subsequently, loosening (Wagner, 1978).

Surface replacements (CoCrMo-on-CoCrMo) were re-introduced by McMinn and Wagner as an alternative to metal-on-metal total hip replacement. Surface replacement is an option for younger and more active patients that offer them joint stability and wider range of motion due to the large diameter of the femoral component (40-65mm) compared to the conventional metal-on-metal total hip replacement (28-36mm) (Bartz et al., 2000). The surgery involves reshaping the femoral head, with removing as little bone as possible, and placing a metallic femoral head on top, articulation against a metallic acetabular cup. This allows easier revision surgery, had the prostheses failed (Schmalzried et al., 1996b).

The concept of resurfacing was first introduced as an alternative to total hip replacement, which consisted of a metallic head (CoCrMo) articulating against a polyethylene cup (UHMWPE). Failure rates due to loosening of the acetabular cup were extremely high. The MoP surface replacement had a larger head diameter which resulted in a thinner polyethylene liner and an increased wear rate (Livermore et al., 1990). The increased wear rate of such design and material combination resulted in loosening of the implant and thus failure (Schmalzried et al., 1996b, McMinn et al., 1996).

After the success of metal-on-metal total hip replacement, McMinn and Wagner developed the MoM surface replacement (Figure 1.3). McMinn described the important issues that have been taken into consideration when designing the MoM (CoCrMo) surface replacement. Four essential features were considered: "(1) Thin components to avoid undue resection of the femoral head or acetabular bone stock; (2) the articulation of a large diameter head femoral component against a socket without excessive production of wear debris; (3) use of materials and design criteria with a known track record in clinical use; and (4) technique and instrumentation to avoid femoral neck notching and varus placement of the femoral component" (McMinn et al., 1996).
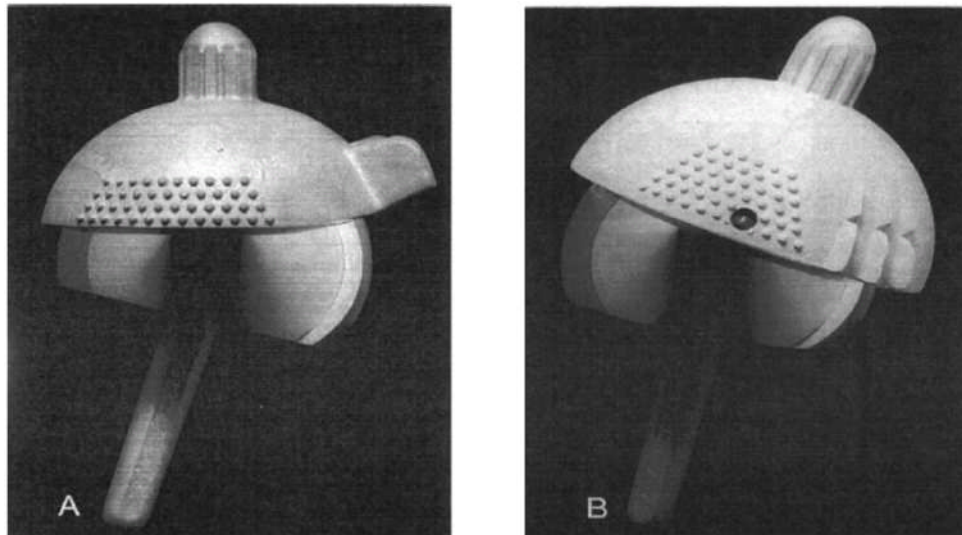
Figure 1.3: (A) Press fit femoral component and press fit acetabular component with superolateral fins. (B) Hybrid design with femoral component for cemented use and hydroxyapatite coated acetabular component (McMinn et al., 1996).

McMinn et al. (1996) reported a total of 9 failures out of 70 surface replacements, implanted in 66 patients, after 50.2 months follow up. Three hips in two patients had to be revised due to infection. Six patientscomplained of pain and their hips were revised due to aseptic loosening. Amstutz (2004) reported 94.4% survival rate at 4 years follow up. This study also showed that rate of survival, for patients with surface arthroplasty of risk index of >3, was 89%, compared to 97% for patients with risk index of <3, indicating that not all patients are suitable for surface replacement arthroplasty.

Further development of surface replacement have been encouraged after the short term promising results. New systems have been developed, such as the Articular Surface Replacement (ASR™, DePuy), the Birmingham Hip Resurfacing System (BHR™, Smith and Nephew), the Cormet (Corin) and many others.

1.3.5.3   Materials in metal-on-metal bearings

The choice of material and the manufacturing process has been a challenge in the development of MoM bearings. Cobalt chromium molybdenum

(CoCrMo) alloys have been used in MoM due to their corrosion resistance and toughness, which is due to the firm adherent of the carbides to the metal matrix (Schmalzried et al., 1996a). The primary content of these alloys are Cr, Co and Mo. High levels of chromium content provide the alloy with a good corrosion resistance. Carbon-rich compounds of metal alloys are formed during manufacturing which in turn affects the size and distribution of the carbides. Different manufacturing processes (heat treatment, cast, wrought) and different carbon levels have been investigated in the development of MoM bearings for total hip replacements. The first generation MoM bearings were cast CoCrMo alloys (ASTM, F-75) with high carbon content of 0.2% to 0.3%. Current MoM bearings can either be wrought, as cast or heat-treated and with different carbon contents depending on the orthopaedic company. (Dowson et al., 2004a) described the effect of carbon content and manufacturing process (wrought and cast) on the wear of MoM bearings. The low-carbon cast metal materials exhibited higher wear than high-carbon cast or wrought metal materials whereas little difference was found in the bedding-in wear volumes generated by high-carbon wrought or cast materials.

1.3.5.4   Wear rates of metal-on-metal

The wear of MoM bearings can typically be divided into two phases. The bedding-in phase during which a higher volumetric wear rate is obtained, then a steady state phase, which is a sustained period of lower wear rate. This is supported by *in vitro* (Goldsmith et al., 2000, Rieker et al., 2001, Scholes et al., 2001, Dowson et al., 2004b, Fisher et al., 2004) and *in vivo* (McKellop et al., 1996, Schmidt et al., 1996, Sieber et al., 1999b, Rieker et al., 2004a) studies. Chan *et al.* (1999) reported a mean bedding in wear rate of 0.4mm^3 /million cycles under standard gait hip simulator study, which then dropped to a steady state rate of 0.08mm^3/ million cycles. Retrieval studies have shown a mean linear wear rate of about 0.004mm/ year with a volumetric wear rate of around 1.5mm^3/ year (McKellop et al., 1996, Schmidt et al., 1996, Kothari et al., 1996). One should bear in mind that direct comparison of *in vivo* and *in vitro* studies should be carefully assessed.

1.3.5.5   Friction and lubrication regime in MoM bearings

The lubrication mode in MoM bearing couples seemed to be a mixed-film lubrication. Fluid film thickness can be dependent on the properties of the lubricant and can be influenced by other factors such as the properties of the bearing material, the geometry of the bearing surface as a function of head diameter and diametrical clearance, and the surface finish of the metal components (Schey, 1996). The contact area between the two bearing couples is mostly the contact between the tips of the asperities. The lubricant plays an important role in separating these asperities and significantly reducing wear. During the early stages of wear, the contact area between these tips increases, "bedding in", until a more favourable micro-geometry for the lubricant film to form and separate the two surfaces and reduce wear, "steady state", (Medley et al., 1996). Unlike MoP, wear could be reduced by increasing the head diameter of MoM bearings (Smith et al., 2001, Dowson, 2001). Fluid-film lubrication is promoted by maximising the head diameter and minimising the clearance of MoM bearings.

The coefficient of friction of MoM bearings is generally higher than that of MoP bearings and this difference is amplified for larger diameter couples. However, frictional torque has not been established to be a crucial measure in the instigation of aseptic loosening of either the femoral head or the acetabular cup. Wear is a more important factor in demonstrating the survivorship of such prostheses and large diameter bearings can have a long term success if the wear rate is sufficiently low (Mai et al., 1996).

1.3.5.6   Effect of clearance on the performance of MoM bearings

Contact area between the bearing couples could be increased by increasing the diameter of the bearing or by decreasing the clearance. The clearance is the gap between the two bearing surfaces and is determined by taking the difference between the diameters of the femoral head and the acetabular cup. If the head and the cup have the exact same diameter then the clearance will be equal to zero and a maximal contact area is achieved. Small clearances might result in equatorial contact, high frictional force and

high torque, which lead to loosening and failure of the prosthesis. Large clearances will result in smaller contact areas and thus high contact stresses, and loss of fluid film lubrication, which lead to high wear rates.

When these bearings are implanted, the contact area between the head and cup is minimal. As the material is worn away (bedding-in), an optimum contact area is reached where the wear rate becomes very low (steady state) (Hu et al., 2004). So the larger the initial clearance is, the more material will wear away during bedding-in to reach the optimum contact area. Therefore, an optimum clearance should be achieved when manufacturing MoM bearings. Another factor that has to be taken into account is the deformation of the acetabular cup when implanted (Udofia et al., 2007, Jin et al., 2006a, Yew et al., 2006). This would result in smaller operating clearance than aimed for, leading to equatorial bearings which may have been a factor associated with failure of early MoM bearings in total hip replacements (Kothari et al., 1996).

The importance of clearance on the lubrication mode of the bearing surfaces in total hip replacements has been demonstrated *in vitro* (Jin et al., 1997). *In vitro* results showed that large clearances would result in longer bedding-in periods and higher bedding-in wear rates (Chan et al., 1999, Dowson et al., 2004b, Rieker et al., 2005b). Table 1.6 shows some bedding-in wear rates of different size MoM bearings with difference clearances. Also, it has been suggested that increasing the clearance will result in thinner fluid film lubrication, higher friction and higher incidents of squeaking in MoM bearings (Brockett et al., 2007). A study done by Farrar and Schmidt (1997) showed reduction in wear of 28mm MoM with decreasing the clearance from 322μm to 80μm. Scholes *et al.* (2001) obtained a reduction in wear when reducing the clearance from 80μm to 44μm.

An *in vivo* study by Rieker *et al.* (2004a) on 172 retrieved bearing couples (head and cup) showed correlation between the clearance and the linear wear rate which support the *in vitro* studies. This is a study that was done on retrieved prostheses, which were revised due to several reasons such as

dislocation and loosening. Assessment of such correlation in situ is not possible due to the difficulty of assessing the wear rate of MoM bearing.

Table 1.6: In vivo wear rates of some MoM bearings surfaces for hip replacement with different clearances.

Author, year	Bearing diameter (mm)	Diametrical Clearance (μm)	Bedding-in wear rate (mm^3/ million cycles)
(Chan et al., 1999)	28	100	0.76
		65	0.24
		56	0.21
(Dowson et al., 2004b)	36	142-146	3.51
		123-124	2.81
		105	2.32
	55	254-307	3.28
		83-129	0.76
(Rieker et al., 2005a) values were taken from a graph	38	90-100	<1
		275-285	3
	50	135-145	1
		260-270	4
	56	50-60	0.5
		235-245	2

1.3.5.7   Effect of head size and clearance on the performance of MoM bearings

Unlike MoP bearings, the wear rate of MoM bearing surfaces tends to decrease with increased head diameter (Smith et al., 2001, Hu et al., 2004, Dowson et al., 2004b, Affatato et al., 2006). It has been suggested that increasing the head diameter increases the entrainment velocity and

therefore improves the lubrication regime in MoM bearing surfaces, which leads to lower wear rates (Liu et al., 2006). Smith *et al.* (2001) compared sizes 16, 22.5 and 28 mm diameter bearings and found a great decrease in wear rate for the larger size bearings. Affatato *et al.* (2006) compared sizes 28, 36 and 54 mm diameter bearings and found a decrease in wear for size 36 mm compared to 28 mm, but no further decrease for size 54 mm. Bowsher *et al.* (2005) obtained similar results, with a reduction in wear for size 40 mm bearing compared to size 28 mm, but an increase in wear for size 56 mm bearings. However, the clearances for larger size bearing are bigger than those of smaller ones and this would tend to contribute to an increase in wear rate in larger bearings. Leslie *et al.* (2008) investigated the wear of size 55mm and size 39mm diameter MoM surface replacement bearings with similar radial clearances. The findings show a reduction in wear for the larger bearing surfaces which can be explained by the reduction in inlet pressure gradient with increased head size.

In vivo studies investigating the effect of head sizes on wear are limited. Mckellop *et al.* (1996) reported a 50% reduction in wear rate for larger bearing surfaces (42mm compared against 35mm), however the clearance was a variable in this study which might have affected the results. McBryde *et al.* (2009) have shown that for every millimetre increase in femoral head size there was 0.89 times reduction in risk of revision concluding that the reason for increased revision of surface replacements was due to size and not gender. One should also bear in mind that *in vivo* studies on MoM especially surface replacements are done on retrievals that have been revised due to several complications and the long term performance of such prostheses are not yet known.

1.3.5.8 Wear of MoM under severe testing conditions

Early hip simulator studies have focused on replicating a standard walking cycle and testing bearing surfaces for millions of cycles. However, hip replacements are subjected to different conditions in the body including, walking, standing, sitting, running, jumping and stair climbing. Also head offset, cup inclination angle and joint laxity are issues associated with

surgical technique and anatomical variation between individuals. All these conditions can affect the performance of any bearing surface and have to be taken into consideration when developing bearing surfaces for hip replacements.

Williams *et al.* (2006) investigated the effect of varying the swing phase load on the wear of MoM hip replacements. The study showed a ten-fold increase in the mean wear rate when increasing the swing phase load from 100N to 280N. This might be due to the diminishing of fluid film lubrication due to high swing phase load (280N).

Roter *et al.* (2002), Chan *et al.* (1999) and Pare *et al.* (2003) investigated the sensitivity of MoM bearings to motion interruptions. The study involved stopping and re-starting the hip simulator several times. It was reported that there was a significant increase in wear rate of MoM bearings. These finding contradicted with the findings of Wimmer *et al.* (2001) who found no increase in wear under a pin-on-ball set up conditions.

Retrieval studies of CoC bearings have shown evidence of edge loading while in situ. Edge loading was associated with high cup inclination angle and microseparation. It was thought that MoM bearings would be less prone to the effect of head-cup rim contact due to their ability to self-polish. However retrieval studies have shown the formation of stripe wear area on the metallic femoral head and evidence of edge loading (Morlock et al., 2006b). Morlock *et al.* (2006b) reported a mean wear rate of 4.16 mm^3/ year from one retrieval study. This mean wear rate dropped to 1.17 mm^3/year when excluding components for which edge loading was obvious, concluding that edge loading does increase the wear rate of MoM bearings in vivo.

Angadji *et al.* (2007) tested MoM bearings under different cup inclination angle conditions (35°, 50° and 60°). The results showed no significant difference between the wear rates during bedding-in. During steady state, the wear rate significantly increased when comparing cup inclination angles of 35° with 65° and 50° with 65° but no significant difference between 35°

and 50°. Steep cup inclination angle is associated with head-rim contact and increased cup inclination angle of 50° might not be high enough to provide rim loading and high wear rates. Reports should mention if rim contact has occurred and comparison should be between components where the contact area was away from the rim of the acetabular cup and components where edge loading (head-rim contact) has occurred regardless of the inclination angle.

Williams *et al.* (2008) reported a fivefold increase in the steady state wear rate of 28mm MoM bearings when increasing the cup inclination angle from 45° to 55°. The increase in wear rate was associated with the head-cup contact area approaching the superior rim of the acetabular cup, which may have resulted in the depletion of the fluid film lubrication. Another study reported by Williams *et al.* (2008) showed a fivefold increase in the steady state wear rate when microseparation was introduced to the gait cycle.

Williams *et al.* (2008) also tested 39mm MoM surface replacement under steep cup inclination angle (55°) and introducing microseparation to the gait cycle. The results showed a tenfold increase in wear rate compared to the same size bearing tested under standard gait condition at 45° cup inclination angle. The test ran for 2 million cycles with no sign of steady state phase under the severe testing conditions. Further studies should be done for longer periods under these severe conditions to investigate if the wear rate decreases and reaches a steady state phase. Furthermore, these results indicated that cup inclination angle and microseparation conditions are important factors in the determinant of wear in the development of MoM bearings.

1.4   Wear Products of Hard-on-Hard bearings

1.4.1   Wear debris

The biological reaction of the body towards the wear debris produced by THR bearings affects the performance and the survival of such prostheses. Polyethylene wear debris is considered to induce osteolysis in MoP THR

bearings (Amstutz et al., 1992). Wear rate of THR bearings in vitro is not always sufficient to determine the performance of such prostheses *in vivo*. The size and number of wear debris produced by bearing surfaces could affect the biological reactions and the inflammatory responses in the body. Although, the wear rate of MoM bearings is significantly lower compared to MoP bearings, the number of wear particles produced was estimated to be up to 100 times higher (Tipper et al., 1999, Firkins et al., 2001c).

Different size polyethylene wear particles induce different inflammatory responses by activating or failing to activate macrophages. Polyethylene wear particles produced by THR bearings tend to have a variety of different morphologies and sizes including submicron granules and large flakes (>50μm) (Tipper et al., 2001). Green *et al.* (1998) reported that polyethylene wear particles of mean sizes of 0.21μm, 7.2μm and 88μm tend to induce lower rates of cytokines release than wear particles of mean sizes of 0.49μm and 4.3μm. So polyethylene wear particles in the range of 0.3 and 5μm in size tend to activate macrophages and induce biological activities.

Unlike polyethylene wear debris, the wear debris produced by MoM and CoC bearings tend to be very uniform in size and round and oval in shape (Tipper et al., 2001, Catelas and Wimmer, 2011). The mode of the size distribution of metal wear debris was 30nm and that of ceramic wear debris was 9nm (Tipper et al., 2001). However, some authors have reported some needle shaped particles as well as oval and round shaped particles when characterising metal wear particles (Bowsher et al., 2005, Catelas et al., 2006). The different outcomes from different labs might be due to different reasons such as isolation techniques, imaging techniques, different hip simulator and different testing conditions. However, Firkins *et al.* (2001c) and Brown *et al.* (2006) obtained consistent results with those reported by Tipper *et al.* (2001) with no observations of any needle shaped particles despite their different isolation and imaging techniques. In addition, Bowsher *et al.* (2006a) reported threefold increase in the number of needle shaped particles under fast-jogging simulation compared to walking simulation,

suggesting that the production of needle shaped particle is dependent on the testing conditions.

Leslie e*t al.* (2008) compared the wear debris generated from different size surface replacement MoM bearings (39 mm vs 55 mm). The study showed no significant difference ($p > 0.05$) in the mean particle size between the different bearing size groups with size range from 8-108 nm being reported.

The introduction of microseparation condition to the gait cycle on a hip simulator resulted in the production of larger size ceramic wear particles (Stewart et al., 2003a). The wear debris generated under standard gait cycle conditions were uniform and in the range of 10nm whereas the wear debris generated under microseparation conditions were in the range between 10 and 1000nm (Stewart et al., 2003a).

1.4.2   Ion release in metal-on-metal bearings

Cobalt (Co) and Chromium (Cr) metal ions release is a primary concern related to metal-on-metal bearing surfaces in total hip replacements. The *in vivo* performance of metal-on-metal bearing can be determined by measuring the urine and blood metal ion concentrations. The long-term effects of the metal ion released into the body are not known.

Liao and Hanes (2006) showed a strong correlation between the wear of MoM bearings and serum ion levels in an *in vitro* study. The wear of MoM reaches a steady state phase in which the ion release is very low. However, this does not match the data obtained in *in vivo* studies. Savarino *et al.* (2003) found no reduction in ion levels from patients that had their MoM total hip prostheses for 2 and 4.4 years. One explanation for this could be the necessity for removing the serum every few hundreds of thousands of cycles on the hip simulator and replacing it with fresh-ion-free serum.

The effects of head size and cup inclination angles have been investigated. Clinically, steep cup inclination angle results in high patient metal ion levels (De Haan et al., 2008, Brodner et al., 2004). Femoral head size had no

influence on the level of metal ions released by the implant (Clarke et al., 2003, Daniel et al., 2006).

1.4.3   Tribocorrosion in metal-on-metal bearings

Wear and corrosion of MoM bearings couples have been considered key issues for their long-term performance (Jacobs et al., 1994). Metal bearings usually rely on a stable passive film for their biocompatibility. This film protects the bearing surface from the surrounding environment. However, when damage to the surface occurs, the film gets disrupted leading to increased corrosion rates. The protein contents in the surrounding environment adversely affect the corrosion resistance of metal alloys (Yan et al., 2006). It has been shown that corrosion accounts for between 21.6% and 46.7 % of the total wear volume of metal-on-metal articulation with the remainder being down to mechanical wear (Yan et al., 2006). Yan *et al.* (2006) showed increased wear rate caused by pitting and blistering of the bearing surface due to corrosion.

1.4.4   Cytotoxicity of metal debris

The formation of necrotic tissue is not uncommon following a MoM hip replacement. The prevalence of tissue necrosis in the periprosthetic tissue of long-term MoM hip replacement patients have been studied by Doorn *et al.* (1996). In this study, all three types of necrosis were observed in the nine patients examined. Four patients were diagnosed with necrobiosis with the presence of visible wear debris. Three patients were diagnosed with conventional necrosis and one with conventional necrosis surrounded by layers of histiocytes.

Another abnormal periprosthetic soft tissue mass related to MoM hip implants which is neither malignant nor infective in nature has been observed and described as 'pseudotumour' (Pandit et al., 2008). Pseudotumours have not been observed following a conventional MoM total hip replacement but are directly related to MoM hip resurfacing (Pandit et al., 2008). The cause of symptomatic pseudotumours is still not clear and can

be multifactorial and it has been estimated that 1% of patients with MoM hip resurfacing will develop pseudotumours within 5 years (Pandit et al., 2008).

Kwon *et al.* (2009) studied the prevalence of asymptomatic pseudotumours and their potential association with ion levels in 123 patients with 160 MoM hip replacements. Pseudotumours were observed in six patients (5%). This prevalence was higher than that reported previously for the symptomatic pseudotumours (1%). The prevalence of pseudotumour was also associated with high ion levels. The concentrations of cobalt and chromium ions and the inferior Oxford hip score for patients with pseudotumours were compared to the rest of the patients (Table 1.7). There was a six-fold increase in serum cobalt and chromium and twelve-fold increase in hip aspirate levels of cobalt and chromium in the six patients diagnosed with pseudotumours.

Table 1.7: Cobalt and chromium ions concentrations for patients with and without asymptomatic pseudotumours (Kwon et al., 2009).

	Pseudotumours patients	Pseudotumours-Free patients
Serum cobalt (μg/L)	9.2	1.9
Serum chromium (μg/L)	12.0	2.1
Hip aspirate cobalt (μg/L)	1182.0	86.2
Hip aspirate chromium (μg/L)	883.0	114.8
Inferior Oxford hip score	23	14

Germain *et al.* (2003) studied the toxicity of clinically relevant CoCrMo and alumina ceramic wear particles. Different concentrations of cobalt-chrome particles were used, 5 μm^3/cell and 50 μm^3/cell. A concentration of 5 μm^3/cell reduces the viability of U937 and L929 cells by 42% and 73 % respectively. Increasing the concentration to 50 μm^3/cell reduced the viability

even more, 97 % for U937 cells and 95% for L929 cells. 50 μm^3/cell clinically relevant alumina ceramic particles reduced the viability of U937 cells by 18 %. These findings show the high level of toxicity of metal wear particles compared to ceramic particles.

1.4.5 Hypersensitivity due to metal debris

Corrosion most definitely occurs when metal gets in contact with a biological environment (Jacobs et al., 1994). The ions released by the metal implants can combine with the proteins in the body and activate the immune system as antigens and elicit hypersensitivity responses (Hallab et al., 2001). Nickel, cobalt and chromium are very common sensitizers in humans (Hallab et al., 2001). Metal sensitivity is very common, affecting approximately 10-15% of the population with Nickel having the highest prevalence of 14% (Basketter et al., 1993). The elevated release of ions by metal implants can lead to the development of hypersensitivity.

Hypersensitivity caused by ions released from metal implants are generally delayed cell-mediated responses (Hallab et al., 2001). The activation of macrophages occurs as a result of cytokines released by the sensitized T Lymphocyte. Metal implant-related hypersensitivity has been reported in several studies (Hallab et al., 2001, Gawkrodger, 2003, Antony and Holden, 2003). Some publications have reported specific histological changes in the surrounding tissue of modern metal-on-metal hip prostheses (Al-Saffar, 2002, Davies et al., 2005, Willert et al., 2005). The surrounding tissue contained lymphocytic infiltration and showed significant ulceration of the pseudosynovial surface. Davies *et al.* (2005) found no correlation between the occurrence and the severity of the immunological reaction and the amount of the metal wear debris produced by the implant. The clinical implications of these histological findings are not yet clear as the number of these cases is a fraction of the number of metal-on-metal prostheses revised. The prevalence of metal sensitivity is approximately 25% of a well-functioning metal-on-metal implants and approximately 60% among patients with failed or poorly functioning implants (Silva et al., 2007). It is not clear if

metal implant-related hypersensitivity causes implant failure or vice versa (Hallab et al., 2001).

1.4.6 Carcinogenic concerns

There are concerns that wear debris generated by metal-on-metal implant could cause cancer. However, there is no direct association between cancer and the presence of MoM implants in the body. The outcomes of the epidemiologic studies investigating the association of cancer with metal prosthesis are conflicting. Some studies that have been done in animal models have shown that Co and Cr induce carcinoma (Freeman et al., 1969), which gave rise to concern regarding the effect of such ions on human tissue.

Visuri *et al.* (1996) classified Cr and Ni produced by CoCrMo alloy as a carcinogens and proven to increase the risk of throat cancer if inhaled. Epidemiological study showed no apparent increased risk of cancer and sarcoma development after the implantation of metal-on-metal hip systems (Visuri et al., 1996). However, the same study showed a relative risk of hematopoietic cancer to be 1.59 after a metal-on-metal surgery and 3.77 for leukaemia when MoM implants were compared to MoP hip replacements. In addition, patients with MoM hip prostheses were found to have higher risk of developing cancer than patients with MoP hip prosthesis. A later study that was done by Visuri *et al.* (2003) showed no increase in the risk of developing leukaemia and lymphoma after MoM hip replacement. A study by Onega *et al.* (2006) showed no increased risk of developing cancer for patients with MoM, MoP, CoP and CoC hip replacements.

1.5 Aims and Objectives

1.5.1 Rationale

Hard-on-soft bearings have suffered long-term failure due to polyethylene wear debris induced osteolysis (Willert, 1977). Osteolysis is a result of biological and biomechanical interactions between the wear debris produced by the total hip arthroplasty and the environment. This is dependent on the

wear rate and the size of the wear debris produced by prosthesis. Third body damage to the femoral head in MoP bearings couples have been associated with increased wear rate and osteolysis (Barbour et al., 2000). Besides, small submicron size polyethylene wear debris have been found to elicit intense inflammatory response in macrophages (Green et al., 1998). Tipper *et al.* (2000) reported the wear rate of a retrieved MoP bearings couples to be 60 mm^3/year with a total wear volume of 785 mm^3 at a mean lifetime at failure of 12 years.

Hard-on-hard (CoC, MoM and CoM) bearings have been developed and encouraged to be used due to many reasons. The high demand of younger and more active patients with longer life expectancy and higher level of activities have made MoP bearings insufficient to meet such requirements. The increased interest in the use of larger bearing surfaces to provide wider range of motion and improve stability have made hard-on-hard bearings more favourable over hard-on-soft bearings ((Crowninshield et al., 2004)). Unlike MoP, the wear rate of MoM decreases with increased head diameter due to improved fluid lubrication.

Hip simulator studies have been carried out to support research and development of new bearing systems for hip prostheses (Barbour et al., 1999, Barbour et al., 2000, Chan et al., 1996, D'Lima et al., 2003, Leslie et al., 2008). Most hip simulator studies investigated the wear rate under walking conditions. However, the mismatch between the results obtained from retrieval studies and simulator studies have led some groups to increase the severity of hip simulator testing. The influence of kinematics (Barbour et al., 1999, Firkins et al., 2001a), stop/start motion (Roter et al., 2002), varying level of peak load (Nevelos et al., 2001b) and swing phase load (Williams et al., 2006) and the introduction of microseparation to the gait cycles (Leslie et al., 2009, Nevelos et al., 2000, Stewart et al., 2001, Stewart et al., 2003b, Stewart et al., 2003a, Williams et al., 2004a, Williams et al., 2008, Clarke et al., 2007) have been investigated and compared to clinical retrievals.

Characterisations of the size and shape of the wear debris produced by different bearing surfaces and the resultant biological and chemical activities, besides the volumetric wear rates, are key issues in determining the performance of alternative bearings (Tipper et al., 2001). Polyethylene wear particles in the range of 0.3 and 5μm in size tend to activate macrophages and induce biological activities (Green et al., 1998). The small size of metal particles generated by MoM bearings can allow them to migrate away from the periprosthetic tissue and cause inflammatory or toxic reaction. Also, the large number of wear debris produced can increase the level of corrosion due to increased surface area. Wear debris characterisation have focused on size 28 mm bearings and the benefit of larger size bearings is still to be determined.

Retrieval studies of early generation ceramic-on-ceramic bearings showed stripe-like wear on the femoral head with rim wear on the acetabular cup; evidence of edge loading (Nevelos et al., 1999, Nevelos et al., 2001c). There was a good correlation between this wear mechanism and steep cup inclination angle (Nevelos et al., 1999). Excessive cup inclination angle (rotational malposition) allowed the contact area between the head and the cup to intersect with the edge of the acetabular cup (rim) and increase the contact stresses. In vitro studies, however, showed no increase in wear when the acetabular cup of the ceramic-on-ceramic bearing was set up at a steeply inclined angle (65°) (Nevelos et al., 2001a). Edge loading that resulted in the formation of stripe wear similar to that seen on retrievals was achieved when the centres of rotation of the head and the cup were separated; a condition defined as microseparation (translational mal-positioning) (Nevelos et al., 2000). Microseparation conditions may occur when the centres of the head and the cup are mismatched by a value greater than the radial clearance. It was shown that microseparation conditions (0.4-0.5mm) generated wear rates, wear mechanisms and wear particles similar to those seen in retrievals (Hatton et al., 2002, Nevelos et al., 2000, Nevelos et al., 1999, Nevelos et al., 2001c, Tipper et al., 2002, Stewart et al., 2001). This was the only laboratory condition where bimodal micrometre and nanometre sized ceramic wear particles were generated,

which have been observed in tissue retrieved at revision (Hatton et al., 2002, Tipper et al., 2002). Edge loading due to microseparation conditions could occur clinically due to head offset deficiency, medialised cup, impingement, subluxation, stem subsidence, or laxity of the joint. In addition to the validation study mentioned above (Nevelos et al., 2000), microseparation conditions have caused the fracture of 3Y-TZP zirconia femoral heads, which was also observed in vivo (Stewart et al., 2003b). Finally, edge loading resulted in the elevation of wear rates and simulation of wear mechanisms in metal-on-metal bearings, similar to those observed in retrievals (Morlock et al., 2008, Leslie et al., 2010). The effect of this condition on larger size bearings compared to smaller size bearings with the same design is still to be determined.

The fourth generation alumina matrix composite (AMC), also known as BIOLOX® Delta have shown improved performance under severe simulator conditions compared to earlier generation ceramics. The influence of the combination of cup inclination angle and microseparation on such improved material is still unknown. Also, the benefit of larger size heads is still to be determined.

High wear of MoM bearings have been associated with steep cup inclination angle in *in vivo* (Morlock et al., 2006a) and *in vitro* (Williams et al., 2008, Angadji et al., 2009) studies. It was thought that MoM bearings are less susceptible to edge loading, however Morlock *et al.* (2006a) reported increased wear rate and the formation of wear stripe on retrieval MoM studies. *In vitro* studies have also shown increased wear rates of MoM bearings with the introduction of microseparation however, the wear rates were lower than that reported *in vivo* (Williams et al., 2008). The effect of the combination of both steep cup inclination angle and microseparation conditions on MoM bearings and the benefit of larger size bearings are yet to be determined.

Wear (wear debris) and corrosion (ion release) of MoM bearings couples have been considered key issues for their long-term performance. Metal bearings usually rely on a stable passive film for their biocompatibility. This

film protects the bearing surface from the surrounding environment. However, when damage to the surface occurs (wear scar), the film gets disrupted leading to increased corrosion rates. Under microseparation conditions, the damage to the bearing surfaces is excessive to the damage that occurs under standard condition. The effect of cup inclination angle and microseparation of the tribo-chemical levels is still to be determined.

1.5.2   Hypothesis

Increased wear in hard-on-hard bearings is associated with edge loading contributed to by steep acetabular cup inclination angle (rotational mal positioning) and microseparation conditions (translational mal positioning). The combination of these two conditions will result in a more severe condition, which will elevate the wear rate even higher. The adverse effects of these conditions may be reduced in larger size bearings and the use of the fourth generation alumina matrix composite, BIOLOX$^®$ Delta.

1.5.3   Aims

The primary aim of this study was to investigate the influence of head size, head position, and cup angle in a hip joint simulator on the wear, wear debris, ion levels and tribo-corrosion of metal-on-metal bearings and wear and wear debris of ceramic-on-ceramic bearings. This study also aimed to determine the benefits of larger bearings and the use of ceramic material.

1.5.4   Objectives

The aims of this study were achieved by completing the following objectives:

- To determine the effect of both rotational and translational mal-positioning on the wear and wear mechanisms of size 28mm BIOLOX$^®$ delta ceramic-on-ceramic hip replacement bearings. (Chapter 3)

- To determine the effect of rotational and translational mal-positioning on the wear and wear mechanism of size 28mm metal-on-metal hip replacement bearings. (Chapter 4)

- To determine the effect of increasing the femoral size on the wear and wear mechanisms of ceramic-on-ceramic bearings under adverse hip simulator conditions simulating rotational and translational mal-positioning. (Chapter 5)

- To determine the effect of increasing the femoral size on the wear and wear mechanisms of metal-on-metal bearings under adverse hip simulator conditions simulating rotational and translational mal-positioning. (Chapter 6)

- To perform electrochemistry experiments to understand the corrosion regimes on the surface of the metal articulating bearings under standard gait and adverse (rotational and translational mal-positioning) hip simulator conditions. (Chapter 7)

- To validate a geometric measurement technique to determine the volumetric wear on ceramic-on-ceramic and metal-on-metal bearing surfaces using a coordinate measuring machine. (Chapter 8)

CHAPTER 2. MATERIALS AND METHODS

Hip simulator studies were undertaken to assess the wear of different sized metal-on-metal and ceramic-on-ceramic total hip replacement bearings under different simulator conditions.

2.1 Materials

Two bearing combinations were used for the hip simulator studies; ceramic-on-ceramic and metal-on-metal bearings. The ceramic bearing materials were the fourth generation ceramics, alumina matrix composite (AMC), which is commercially known as BIOLOX$^®$ delta (CeramTec , Germany). This material consisted of 72.5% alumina, 25.5% zirconia and 2% mixed oxides. The metal bearings were high carbon (>0.2%), heat treated cobalt chrome alloys (CoCrMo). Two bearing materials were tested in like-on-like configurations and both bearing sizes were used; 28mm and 36mm.

2.2 Hip Joint Simulator

In vitro hip joint simulator studies are used to predict the wear performance of hip joint replacement bearings under different kinematics and kinetics conditions. The Leeds Mark II Physiological Anatomical hip joint simulator (Figure 2.1) was used in all the wear studies. This simulator consists of six identical stations that simulate dynamic vertical loading, flexion/extension and internal/external rotation as described in the ISO standard 14242-1 (2002). It has also been modified to simulate adverse condition that will be described in this chapter. It has been used extensively for over a decade for a range of published studies (Leslie et al., 2009, Nevelos et al., 2000, Nevelos et al., 2001a, Nevelos et al., 2001b, Stewart et al., 2001, Stewart et al., 2003b, Stewart et al., 2003a).

Figure 2.1: Leeds Mark II Physiological Anatomical Six Station Hip Joint Simulator.

2.2.1 Simulator Kinetics and Kinematics

The Leeds II simulator has six identical stations that can generate multi-directional motion between the femoral head and the acetabular component (Figure 2.2). It is a three axis machine, a single vertical load axis and two independently controlled axes of motion, extension/flexion (-15° to +30°) and internal/external rotation (+/- 10°). The flexion/extension and internal/external rotation were 90° out of phase to generate an open elliptical wear path. The load was applied vertically from above through the acetabular component and the centre of the femoral head. Under standard gait conditions, running at a frequency of 1Hz, a twin peak loading cycle with a peak load of 3kN and swing phase load of 0.3kN were applied as recommended by ISO14242-1 (2002).

Nevelos *et al* (2000) showed that standard ISO conditions do not replicate all clinically relevant conditions and it is necessary to investigate the wear of hip replacement bearings under adverse conditions. The Leeds II hip simulator was modified to simulate edge loading conditions that replicated stripe wear. This simulator condition was termed "microseparation". Microseparation was introduced to the normal gait cycle by the medial and superior translation of the cup relative to the head. This was achieved by applying a lateral to medial force using a spring as described previously by Nevelos *et al.* (2000)

and Stewart *et al.* (2001). The spring force was adjusted manually to produce a medial displacement of around 0.4-0.5mm during the swing phase at each of the six stations. The swing load was dropped from 300N to approximately 50N in order to achieve the desired displacement. This provided the severe microseparation condition previously described by Stewart *et al.* (Stewart et al., 2001). The microseparation displacement was measured using a calibrated Linear Variable Differential Transformer (LVDT) position sensor. An oscilloscope was used to visualise the displacement of the cup on the screen when adjusting the spring to obtain the desired displacement. The displayed graph on the screen of the oscilloscope showed that the microseparation occurred when the load was minimal (swing phase). The LVDT measurements were acquired and analysed using a LabView^{TM} programme (Figure 2.3).
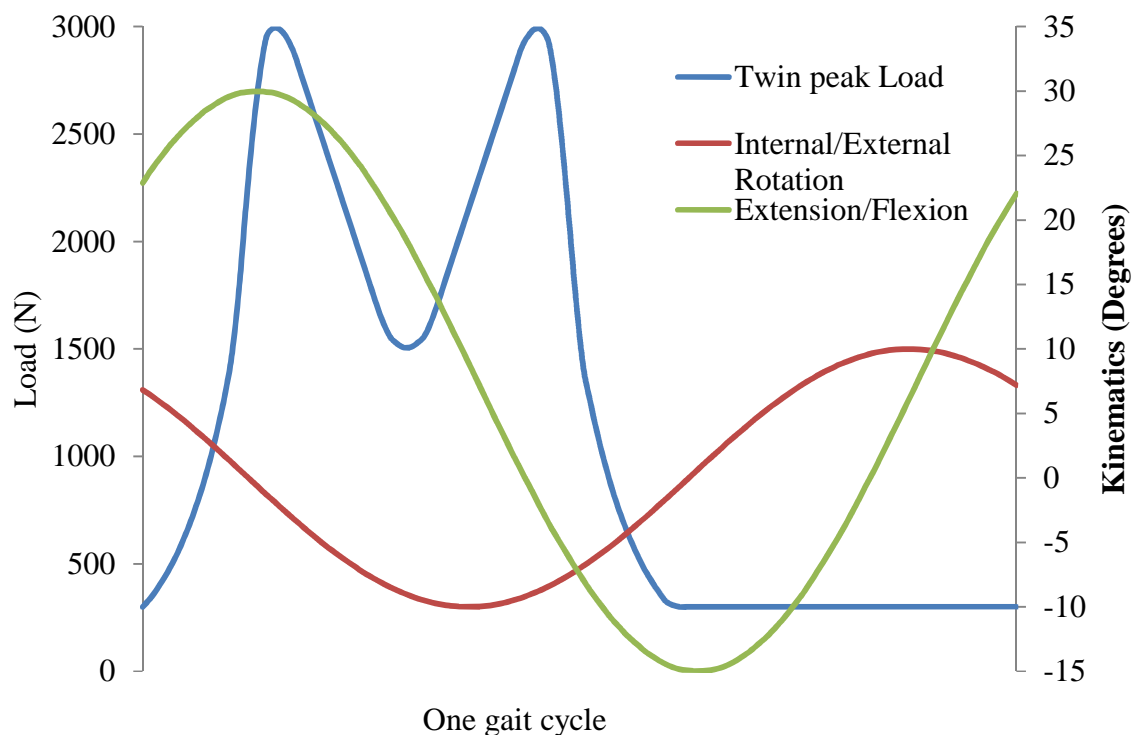
Figure 2.2: Loading and motion on the Leeds II hip simulator. One gait cycle takes 1 second to complete.
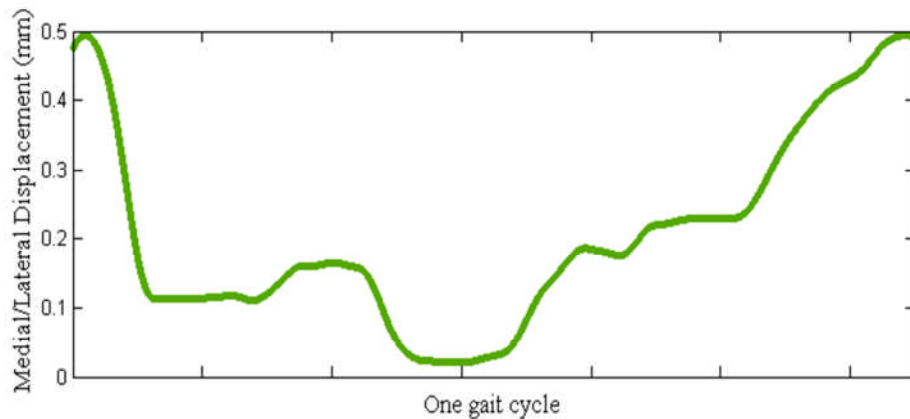
Figure 2.3: Medial lateral Displacement of Cup relative to the femoral head introduced under microseparation conditions. The timing of this figure is synchronised with Figure 2.

2.2.2 Set up

It is important when setting up the components on the machine for the centres of rotation of the femoral head and acetabular cup to coincide with the centre of rotation of the machine itself. Also the positioning of the cup is important as different inclination or version angles could affect the wear of the bearing couple. Inclination angles were investigated in this study while the version angle was kept constant.

Two fixation methods were employed to mount the acetabular components in a stainless steel cup holder. The liners were either mounted directly in the cup holder using PMMA resin, for metal-on-metal studies, or taper locked to a metallic shell that was mounted to the cup holder using PMMA resin, for ceramic-on-ceramic studies. With the metal cup, a keyway was machined on the back of the cup to avoid any rotation in the cup holder. Stainless steel locking rings were utilised to hold the cups in place. The set-up was done so that the liners could be easily removed from the cup holders for measurement. With the ceramic liners, the metal shells were securely mounted in the cup holder with a hole drilled from the back and blocked with a grub screw for the liner to be pushed out when needed for measurement. It was during mounting up when the cups were positioned at the desired inclination angles using a bespoke fixturing jig.

There is a 10° transposition between the body and the simulator set-up which is due to the direction of the applied force. During gait, the direction of the force vector in the body is approximated as 10° medial, however in the hip joint simulator, the force vector is applied vertically (Figure 2.4). Hence, cup inclination angles of 35°, 45° and 55° on the hip joint simulator represent clinical cup inclination angles of 45°, 55° and 65° respectively.
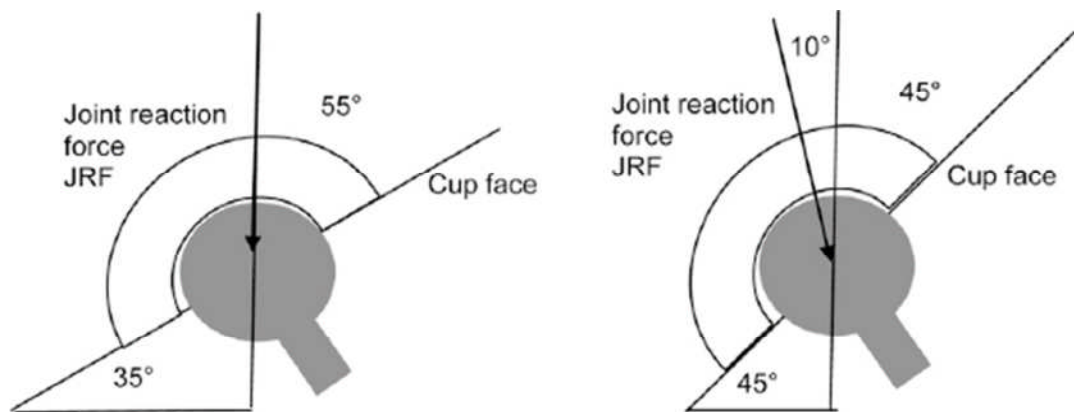
Figure 2.4: Schematic of cup inclination angle on the simulator and in vivo. (A) Cup inclination angle of 35° in the laboratory hip simulator representing a clinical angle of 45°. (B) Clinical representation of cup inclination angle of 45° (Williams et al., 2008).

The femoral heads were positioned on total hip replacement stems. The stems were mounted in stainless steel holders using PMMA resin applied carefully to avoid any air bubbles that might cause the failure of the cement mantle. An alignment jig was used to make sure the stems were mounted centrally and vertically in the holder. The holders were securely attached in the machine making sure the centre of the femoral heads was positioned on the centre of rotation of the machine through which the load was applied. The advantage of positioning the femoral head on a THR stem mounted in PMMA resin was the deflection achieved when the peak load was applied. This deflection was representative of *in vivo* conditions and was very important when microseparation conditions were applied.

The components and the fixtures were marked with matching alignment marks and numbers so the components could be placed in the same station

and in the exact same position after they had been removed for measurements.

2.2.3 Lubrication

New-born calf serum (Harlan, UK and SeraLab, UK), was used as a lubricant in the hip simulator studies. It was diluted to 25% in concentration using de-ionised water and supplemented with 0.03% (v/v) sodium azide solution to minimise bacterial growth. The protein content in the lubricant after dilution was approximately 15g/L. The serum was contained in an open bath that allowed evaporation of fluid, so 0.03% sodium azide solution was used to top up the serum in the bath to the right level. The serum was changed every 330,000 cycles and stored in individual bottles which were frozen at -18°C for further wear debris, for metal-on-metal and ceramic-on-ceramic studies, and ion level analysis for metal-on-metal studies. The serum was replaced with a freshly prepared batch after cleaning the components and baths using detergent water, disinfectant (Trigene), then deionised water. The colour of serum throughout the MoM studies was monitored by taking images at every serum change. The serum tended to be darker when the wear volume was higher due to the presence of wear debris (Pria, 2007).

2.2.4 Volumetric wear analysis

2.2.4.1 Gravimetric wear analysis

The wear of the test components was assessed gravimetrically at each measurement point. The components were removed from the hip simulator fixturing, cleaned then weighed to determine the weight of material loss and therefore the volumetric wear.

2.2.4.2 Cleaning

The test components were carefully removed from the fixturing then cleaned as described below:

The components were cleaned in situ using detergent water then soaked in 1% Trigene solution for 30 minutes.

The components were then removed from the machine and washed in detergent water to remove all visible serum and contaminants on the surface.

Then, they were soaked in detergent water and ultrasonicated for 10 minutes.

They were then rinsed with deionised water and ultrasonicated for 10 minutes in 70% (v/v) isopropanol.

The components were then left to dry and then placed in the weighing room (temperature and humidity controlled) for 12 hours before weighing them.

Cleaning of the test components was challenging due to the precipitation of protein on and around the wear scar especially between tiny scratches on the metal components.

2.2.4.3 Weighing

The components were weighed in a temperature and humidity controlled environment using Mettler AT201 balance (Leicester, UK) (for components of weight less than 200g) and Sartorius comparator balance CC500 (Germany) (for components of weight more than 200g), which are accurate to 0.01mg. The components were weighed five times and an average weight was determined. A reference weight was also weighed to make sure the difference of weight of components was not due to any other factors but wear. Cumulative volumetric wear was calculated using the following equation:

$Volume = \dfrac{Weight}{density}$, (density of cobalt chrome (CoCrMo): 0.00833 g/mm^3 (Black and Hastings, 1998), density of BIOLOX$^®$ Delta: 0.00437 g/mm^3 (Masson, 2009)).

Then the mean wear rates and 95% confidence limits were determined. One way ANOVA was performed and significance taken at $p < 0.05$.

The wear rates were calculated according to the following equations:

$$Wear\ rate\ at\ x\ million\ cycles = \frac{Total\ wear\ volume\ at\ x\ million\ of\ cycles}{x\ million\ of\ cycles}$$

2.2.5   Geometric wear analysis

The continuing developments of hip joint replacement bearings to be more wear resistant have been successful over the years. With these improvements, it is becoming more challenging to accurately determine the *in vitro* wear rates using gravimetric methods. Several issues contribute to the difficulty of the measurements which are: the accuracy of the balance, the control of humidity and temperature of the environment, protein deposition on the bearing surfaces and metal transfer from metallic parts on to the ceramic bearings that are hard to remove using current validated cleaning methods.

Geometric measurements are used mostly to determine the wear volume on retrievals. However with the improvements in the accuracy and resolution of current coordinate measuring machines, it has become of interest to investigate the potential of measuring very low wear rates using geometric techniques.

A coordinate measuring machine (CMM, Legex 322, Mitutoyo, UK) was used to determine the volumetric wear of *in vitro* tested hip replacement bearings. The machine has a resolution of 0.8µm; however, this value increased depending on the probe/stylus combination and measurement parameters. Three-dimensional representations of the surface of the femoral head or the acetabular cup were reconstructed by taking several thousand data points on the surface of the measured components. The number of data points was different depending on the component size and type. For the 36mm metal-on-metal bearings measured, 2,844 data points were taken on the femoral heads in the form of 36 traces. The traces were taken at intervals of 10° rotation about the vertical axis (Figure 2.5). Each trace started at the pole using and ended 7mm below the equator of the head. There was a 0.5mm spacing between each measurement point in each trace. The acetabular cups were measured by taking 2,052 points in the form of 36 traces rotated by 10 degrees from each other about the vertical axis. Each trace consisted of 57 points with a pitch of 0.5mm starting at the pole and finishing at the rim of the cup. The last three points of each trace were on the chamfer of the

rim. A 5-star stylus configuration was used with styli diameters of 2mm to measure the femoral head and a single straight stylus configuration was used to measure the acetabular cups.

For the ceramic-on-ceramic bearings, it was possible to reach the wear area on the femoral head using the 3mm single stylus configuration. The 28mm ceramic femoral heads were measured and three-dimensional reconstructions of the surfaces were done by taking 9,864 data points in the form of 72 traces rotated by 5 degrees from each other about the vertical axis. Each trace consisted of 137 points with a pitch of 0.2mm starting at the pole and finishing 3mm below the equator. The 36mm femoral heads were measured and three-dimensional reconstructions of the surfaces were done by taking 12,024 data points in the form of 72 traces rotated by 5 degrees from each other about the vertical axis. Each trace consisted of 167 points with a pitch of 0.2mm starting at the pole and finishing 3mm below the equator.
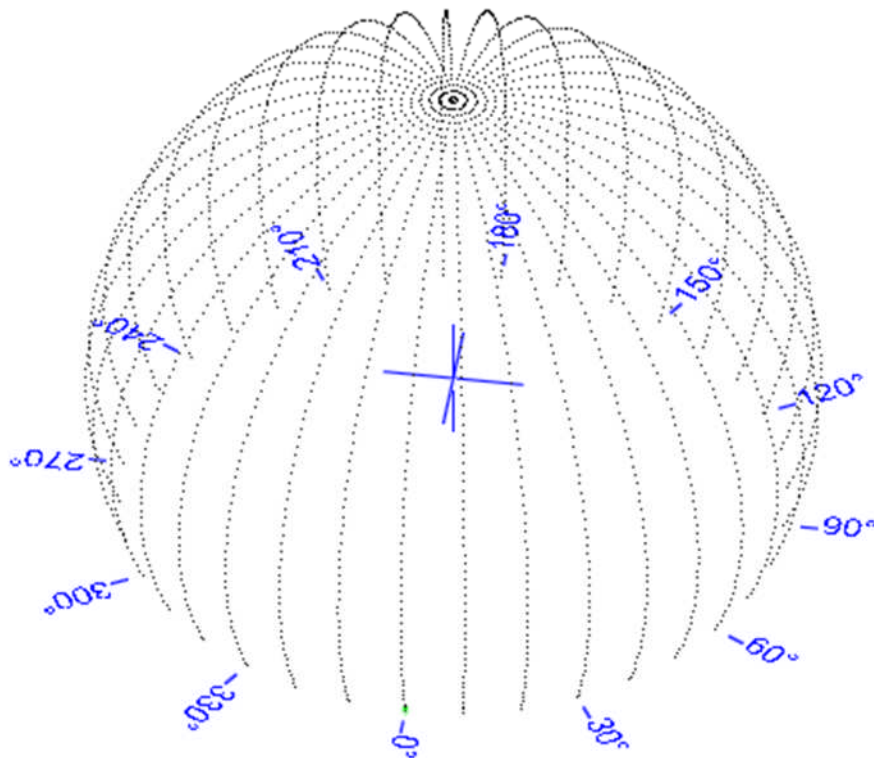
Figure 2.5: Data points taken on the surface of a femoral head using the CMM.

The data was exported to SR3D software (Tribosol, UK) to determine the wear volume and depth.

It was possible to visualise the wear area on the reconstructed surface. The unworn surface of the measurement was used to accurately estimate the position of the centre of the nominal sphere of the component, and then an average of several traces over the unworn region was determined and revolved around the vertical axis through the centre of the nominal sphere. This reconstructed surface was taken as an estimate of the unworn original surface of the measured component. The SR3D software was used to determine the volumetric wear by using the unworn surface as a reference.

2.2.6 Surface topography analysis

2.2.6.1 Surface roughness

A two-dimensional contacting profilometry (Form Talysurf series, Taylor-Hobson, UK) was used to assess the surface of the bearing couples. Before the hip simulator test, the roughness of the bearing surface was determined by taking three traces on each component; p1, p2 and p3 as shown in

Figure 2.6. Traces p1 and p2 were normal to each other and passed through the pole (highest point of the head and lowest point of the cup) of the components. The femoral head was positioned on its side so trace p3 could be taken. The acetabular cup was tilted approximately 45° so trace p3 could be taken. Before each measurement the stylus was "crested"; adjusted in the horizontal plane until a maximum (for the femoral head) or a minimum (for the acetabular cup) vertical value was reached. This point was the mid-point of the measurement trace. The lengths of the traces were taken as one sixth of the circumference of the sphere so they were dependent upon the diameter of the component (Table 2.1) and were determined using the following equation:

Trace length= (1/6) x πD, where D is the diameter of the component.

Table 2.1: Trace length for different bearing sizes

Bearing diameter (mm)	Trace length (mm)
28	15
36	19

The data was analysed using least squares arc with Gaussian filter with the appropriate cut off. The cut off is a filter that uses mathematical or electronic means to reduce or even remove unwanted data in order to look at wavelength in the region of interest. A cut off with 100:1 bandwidth as recommended by ISO 4288 (1997) for the characterisations of orthopaedic implant surfaces was used as indicated in Table 2.2.

Table 2.2: Recommended cut offs for different surface finish.

Recommended cut off (ISO 4288- 1996)

Cut off λc (mm)	R_z (µm)	R_a (µm)
0.08	≤0.1	≤0.02
0.25	>0.1-0.5	>0.02-0.1
0.8	>0.5-10	0.1-2
2.5	>10-50	>2-10
8	>50	>10

Surface roughness (R_a), the skewness (R_{sk}), and the maximum peak to valley height (R_z) were determined. R_a is the universally recognised international parameter for roughness and it is the arithmetic mean of

absolute departures of the roughness profile from the mean line. R_{sk} is the measure of symmetry of the profile about the mean line. The two parameters chosen (R_a and R_{sk}) determined the roughness of the surface with indication to the amplitude of the asperities. R_z is the mean peak to valley height, which is the sum of R_p (height of peak), and R_v (height of the valley). R_p and R_v were of high values if deep scratches existed on the measured surface. Surface measurements over the wear scar were carried out before and after the completion of each test.
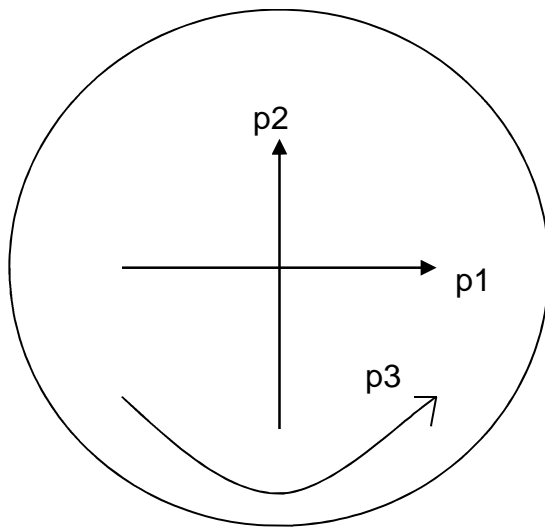
Figure 2.6: Traces p1, p2 and p3 were taken to determine the pre-test roughness of the surface.

2.2.6.2   Penetration

When microseparation condition was applied, a stripe-like wear scar was formed on the femoral head with corresponding wear area on the acetabular cup. Three traces (p1, p2 and p3) were taken across the wear scar formed due to edge loading to determine the area and penetration depth (Figure 2.7). A primary analysis using a least square arc with no filter was applied to each measurement. The analysis was done using Talymap Universal 3.1 Taylor Hobson software Mountains™ by which the form was removed excluding the wear scar area. The area and maximum depth under the mean line was determined using the 'surface of hole or peak' option under 'Studies' tab.
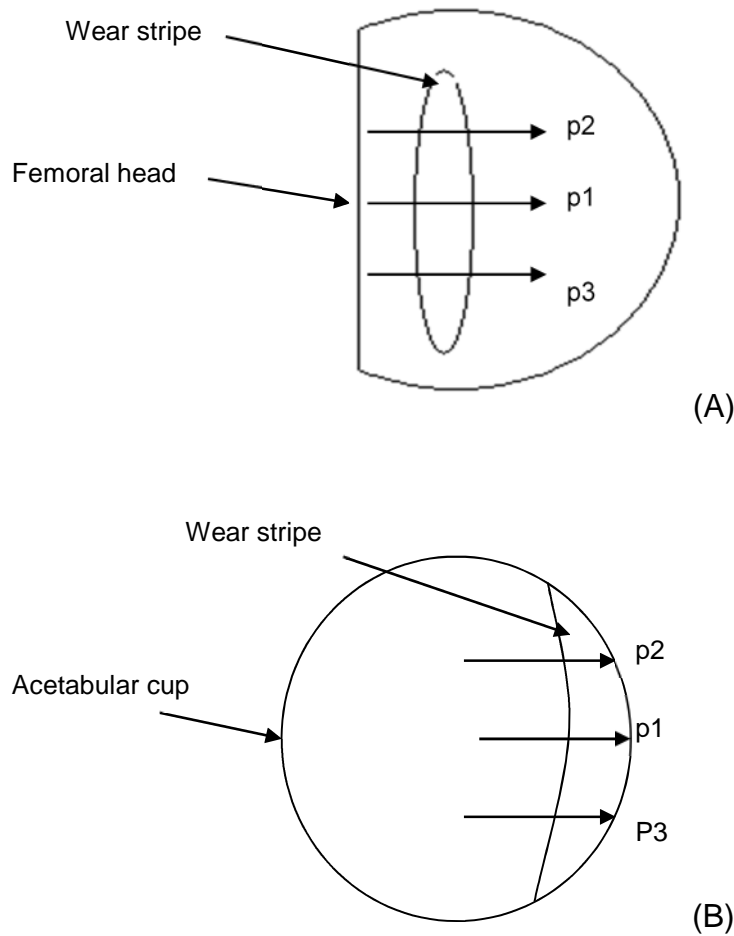
Figure 2.7: Traces p1, p2 and p3 were taken to determine the penetration depth of the wear stripe on the femoral head (A) and the acetabular cup (B) after introducing microseparation to the gait cycle.

2.2.6.3   Scanning electron microscopy

A high resolution field emission scanning electron microscope (LEO) was used to take high magnification images over the wear area of the bearing surface to identify the main features of the wear mechanism. As the specimen imaged needed to be conductive, the ceramic components were coated with a gold coating prior to imaging. As CoCrMo alloy is conductive, the metal specimen was not coated.

2.2.7   Diameter and form measurements

Two coordinate measuring machines (CMM, Kemco, UK and Legex, Mitutoyo, UK) were used to measure the diameter and the form of the components. The QCT-200, Inspect 2CAD software (Quality central

Technology Ltd, UK) was used to analyse the data. Twenty five measurement points were made for each component using the 'measure a sphere' option. One point was taken at the pole, a ring of 10 points at approximately 20 latitude and a ring of 14 points at approximately 110 latitude. The clearances were calculated by subtracting the diameter of the head from the diameter of the cup. For the metal components, the combination of the femoral heads and the acetabular cups were selected so that the range of clearances was as minimal as possible due to the large tolerance of the components. The ceramic femoral and acetabular components were randomly matched.

2.3 Wear Debris Analysis

2.3.1 Isolation of wear debris from simulator serum

The isolation procedure was based on the method developed by Brown *et al.* (2006). This method involved using a series of enzymatic digestions to reduce the amount of proteins surrounding the wear debris generated in 25% new-born calf serum on the Leeds II hip joint simulator. As protein-based enzymes were used, the shape and size of the debris were preserved compared to isolation methods using alkaline digestions.

2.3.2 Chemicals and Reagents

The following chemicals were used in the isolation process of wear debris from serum:

Table 2.3: Chemical used in the isolation procedure of wear debris from the serum.

Supplier	Chemical/ reagent
Sigma-Aldrich Ltd., Poole, Dorset, UK	3-(N-morpholino) propanesulphonic acid (MOPS)
	β-mercaptoethanol
	Tris (2-carboxyethyl) phosphine (TCEP, 93284)
	Sodium dodecyl (lauryl) sulphate (SDS)
	Papain
VWR International Ltd, Lutterworth, Leicestershire, UK	Acetone
	Proteinase K
Fisher Scientific, Loughborough, UK	Ethanol
	Tris-HCl
	Sodium azide

2.3.3 Method

The serum collected from the hip simulator studies was allowed to thaw at room temperature before being centrifuged at 15,000g for 30 minutes at 4^oC using the Sorval Evolution RC Superspeed centrifuge (Thermo Scientific, UK). The pellets were rehydrated in 0.05% (w/v) sodium azide in 0.1M MOPS for 24 hours before supernatant removed (after centrifuging) and 2% (w/v) SDS and 5% (v/v) β-mercaptoethanol in MOPS added and boiled for 10 minutes to denature the protein contents. The pellets were then washed in 0.1M MOPS, 80% acetone and 0.1M MOPS respectively to remove any

traces of the β-mercaptoethanol. The samples were centrifuged and the supernatant removed after each washing step.

The protein contents in the pellets were then digested using two enzymes for the MoM studies and four enzymes for the CoC studies. Before adding the first enzyme (papain, final concentration of 0.21mg/ml), the pellets were sonicated for 30 minutes in 9mM of TCEP in 0.1M of MOPS. The samples were placed in a water bath set at 55°C for 24 hours. The second enzyme was proteinase K (final concentration of 0.34mg/ml) and it was added after sonicating the pellets for 30 minutes in 50mM Tris-HCl (pH 7.8). The samples were placed in a water bath set at 55°C for 24 hours. The third enzyme (only used for ceramic particles) was yeast lytic enzyme (20U.ml^{-1} in 1.1M Sorbitol in HEPES buffer, pH 7.4). The samples were placed for 2 hours in an oven set at 37°. The fourth enzyme (only used for ceramic particles) was Zymolyase 100T (250U.ml^{-1} in 0.1.M sodium phosphate buffer, pH 7.0, containing 50 mM (v/v) b-mercaptoethanol. The samples were placed for 2 hours in an oven set at 37°. All enzyme digestions were repeated three times. The samples were boiled in 2% (w/v) SDS for 10 minutes and washed three times in 0.1M MOPS before and after using proteinase K.

The samples were then washed with deionised water and sonicated in 5ml of 100% ethanol for 1 hour before being filtered onto 0.015μm pore size polycarbonate filters. The filters were left to dry under infrared lamps for at least 4 hours.

2.3.4   Imaging the wear debris

A Field Emission Gun Scanning Electron Microscopy (FEGSEM) was used to image the wear particles prepared onto the polycarbonate filter. The polycarbonate filter was sectioned and placed on an aluminium stub, which was then coated with 5-10nm platinum. Three images were taken at randomly chosen fields of view at three different magnifications (60K, 90K and 150K X).

2.3.4.1 Analysis of Images taken by FEGSEM

Image Pro Plus software (Media Cybernetics, USA), was used to size and count the particles. A minimum of 200 particles were measured per image if possible. The particles were sized using the 'size and measure' object tools where the maximum and the minimum diameters, the area and the perimeter were set as measurements. The data was exported to excel using the 'DDE to excel' function then it was sorted into different size ranges (0-10, 10-20, 20-30, 30-40, 40-50, 50-60, 60-70, 70-80, 80-90, 90-100, 100-110, 110-120, 120-130, 130-140, 140-150, 150-1000 nm). The number of particles in each size range was then divided by the field of view for the analysed image (N/A) and the average area of particles (A/P) determined. Statistical analysis was done by calculating arc sin of the percentage of particles in each size range for different samples and mean values and 95% confidence limits calculated for each set of conditions. Size and volume distribution graphs were drawn after back transforming the mean values and 95% confidence limits.

2.4 Ion level analysis

Co and Cr ion release is a primary concern related to MoM bearings. Clinically, high serum and blood ion levels are an indication that the prosthesis is not functioning as it should. Although ion concentrations measured in a hip simulator study cannot be compared directly to blood ion levels in patients with MOM implants, it is important to determine the concentration of ions released by implants under different *in vitro* simulator conditions. Ion level (Co and Cr) analysis was carried out on all the serum batches collected from the MoM hip simulator studies.

2.4.1 Sample preparation

2.4.1.1 Chemicals and reagents

New born calf serum collected from the hip simulator studies

Nitric acid (Science Lab, SLN1963, SLN1549)

De-ionised water

Cobalt in 2% (abs) HNO_3 (Inorganic Ventures, MSCO-10PPM)

Chromium (+3) in 1.4% (abs) HNO3 (Inorganic Ventures, MSCR(3)-10PPM)

2.4.1.2 Method

The serum was left to thaw at room temperature. For each replicate, 3 x 1ml of serum was transferred to 3 micro-test tubes and centrifuged for 5 minutes at 13,000rpm. 0.9ml of supernatant from each micro-test tube was transferred to a clean microtest tube leaving the pellets (containing wear debris, proteins and microbes) behind. 0.1ml of 10% (v/v) nitric acid was added to the supernatant and placed in the water bath for 10 minutes set at $70^{o}C$ to digest the protein content. The samples were then centrifuged for 10 minutes at 13,000rpm. 0.5ml of the supernatant from each microtest tube was transferred to a 20ml tube and 13.5ml of dH_2O was added. The final sample was 9% dilution of the original 25% serum collected from the hip simulator study. For the control sample, fresh 25% serum was digested following the same method then adding known concentration of Co or Cr and then topped up with dH_2O to make a 15ml sample.

2.4.2 Ion level measurements

The measurements were done using an inductively coupled plasma mass spectroscopy (ICP-MS) in Earth and Environmental Sciences department at the University of Leeds, UK. Five replicates were measured for each sample and an average was taken. Measurements were compared to background measurements of digested fresh 25% serum containing known amount of Co or Cr and calibrated samples of Co and Cr. These were used to check if the machine was measuring the right concentrations and the digestion process was valid. Using the ICP the solution was aspirated into aerosol then passed through argon plasma. This procedure transforms the atoms of the metal elements into ions. These ions are then separated and detected by the mass spectrometer (MS).

2.5   Tribocorrosion study

Tribocorrosion measurements were carried out at the end of each MoM hip simulator test. It is hypothesised that a voltage potential between passive articulating surfaces would be close to zero, however, as the contact between the two bearing surfaces is increased under certain conditions, then the voltage potential will become more negative.

The bearing components were rotated by 180° in the fixtures so the contact occurred between undamaged surfaces of the two components. This was done so the effect of microseparation and cup inclination angle could be determined during the bedding in of MoM bearings.

The rate of corrosion reaction could be determined using an accelerated electrochemical test techniques which were based on the use of a three-electrode cell (Figure 2.8). The three-electrode cell consists of a working electrode, reference electrode and a counter electrode. In these hip simulator studies, the bearing surface was the working electrode. The reference electrode (Ag/AgCl) was placed in the serum bath to provide a stable datum against which the potential of the working electrode is measured. A potentiostat was used to control the three-electrode cell and data was acquired using a computer software.
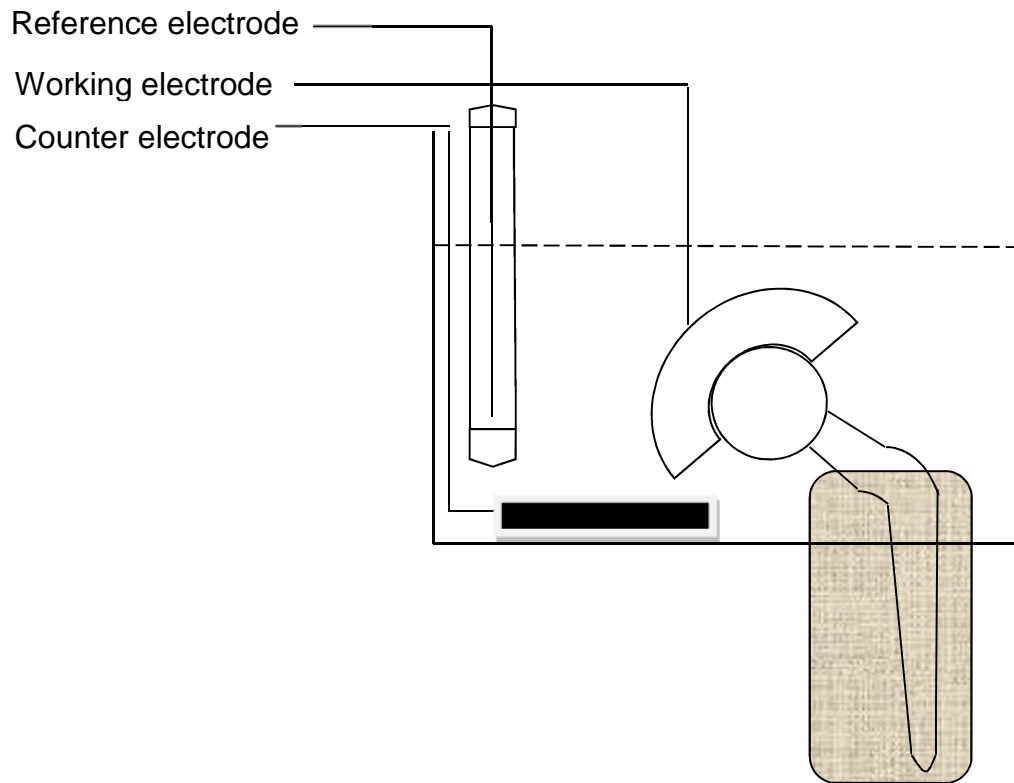
Figure 2.8: Schematic of the three-electrode cell set-up.

2.5.1 OCP measurements

The open circuit potential (OCP) is the potential of the working electrode relative to the reference electrode when no potential or current is being applied to the cell. The OCP for a passive material is low as the flow of electrons is minimal. However, as the surface is activated and the flow of electrons between surfaces increases the OCP becomes more negative. The OCP under standard and microseparation conditions was assessed and compared for individual stations; the correlation between the change in wear rate between standard and microseparation conditions and the difference in OCP drop was determined.

2.5.2 OCP measurements over one gait cycle

The OCP under both standard and microseparation conditions over one gait cycle was matched with the loading cycle and compared.

CHAPTER 3. EFFECT OF EDGE LOADING DUE TO STEEP CUP INCLINATION ANGLE AND MICROSEPARATION CONDITIONS ON THE WEAR OF 28mm BIOLOX® *DELTA* CERAMIC-ON-CERAMIC TOTAL HIP REPLACEMENT

3.1   Introduction

Ceramic-on-ceramic (CoC) bearings have become of great interest in total hip replacement after the long-term failure of metal-on-polyethylene (MoP) due to polyethylene wear debris induced osteolysis (Willert, 1977). Ceramic materials currently used for total hip replacement have been improved significantly from earlier generations. The third generation alumina ceramic was hot isostatic pressed (HIPed), which resulted in reducing the grain size, removing porosity and improving the strength of alumina. Despite these treatments to alumina, some problems associated with rim chipping (Hasegawa et al., 2003) and head fracture (Park et al., 2006) have continued to exist. In the latest development, the introduction of zirconia nano-particles and other oxides into the alumina matrix (alumina matrix composite, AMC) increased the strength and toughness to levels seen in pure zirconia whilst preserving stability (Kuntz et al., 2006). The key to the improved performance of such materials was the elevated hardness and toughness properties, low surface roughness due to smaller grain sizes and high wettability, which provides better fluid-film lubrication.

Retrieval studies of CoC prostheses have shown lower volumetric wear rates compared to other bearing combinations such as metal-on-metal, metal-on-polyethylene (MoP) and ceramic-on-polyethylene (CoP). Ceramic wear particles were found to be less biologically active than particles produced by other types of bearings and *in vivo* wear volumes might not be large enough to elicit adverse inflammatory responses (Tipper et al., 2001). The tribological performance of CoC bearings which are available in 28mm and 36mm sizes might meet the functional requirements of 100 million cycles for younger and more active patients (Fisher et al., 2006).

Ceramic-on-ceramic total hip replacements have shown extremely low wear rates under standard gait conditions in hip simulator studies (Essner et al., 2005, Refior et al., 1997, Stewart et al., 2003a, Nevelos et al., 2001b, Nevelos et al., 2001a). However, some clinical retrievals have shown higher wear rates and the formation of stripe wear on the femoral head (Nevelos et al., 2000, Nevelos et al., 1999). It was shown that steep cup inclination angle conditions did not produce stripe wear in *in vitro* simulator studies (Nevelos et al., 2001a), but the introduction of microseparation and edge loading produced stripe wear, elevated wear rates and a bimodal particle distribution replicating clinical wear rates, wear patterns and wear particles (Nevelos et al., 2000, Nevelos et al., 1999). Nevelos *et al.* (1999, 2000) were the first to show the necessity introducing microseparation and edge loading to replicate stripe wear seen in retrievals. Subsequently, this was repeated by other groups in the form of retrieval (Walter et al., 2004) and laboratory studies (Manaka et al., 2004, Affatato et al., 2004).

Clinically, fluoroscopy studies have demonstrated microseparation of the centres of rotation of the head and insert during gait (Dennis et al., 2001, Glaser et al., 2008). Microseparation occurs during swing phase when the load is minimal and has been associated with different factors such as laxity of the joint, femoral head offset deficiency or medialised cups. These factors cause the femoral head to be positioned laterally relative to the acetabular insert at swing phase. When the load increases rapidly at heel strike, edge loading occurs as the femoral head contacts the rim of the acetabular insert while sliding back into the centre of rotation resulting in stripe wear and elevated wear rates (Nevelos et al., 1999). Hip simulator studies have shown that introducing microseparation to the gait cycle can reproduce clinically relevant wear rates, wear mechanics and wear debris and can lead to the formation of a wear stripe on the femoral head with a corresponding wear area on the rim of the acetabular insert (Nevelos et al., 2000, Stewart et al., 2001).

Stewart *et al.* (Stewart et al., 2003a) have compared the wear rate of HIPed alumina CoC couples against that of alumina matrix composite CoC couples (AMC) under microseparation conditions and it was shown that the wear rate of AMC bearings was significantly lower than that of HIPed alumina bearing

couples. Stewart *et al.* (2003a) achieved microseparation (edge loading) by applying a 0.4-0.5mm displacement in the horizontal plane, using a spring force during swing phase, where the vertical load was dropped to approximately 50N. AMC (commercially known as BIOLOX® *delta*) had better wear resistance under the more severe microseparation conditions than HIPed alumina (commercially known as BIOLOX® *forte*) that might be due to the optimised toughening mechanism of its microstructure. Subsequently, Clarke *et al.* (Clarke et al., 2006) have confirmed Stewart *et al.*'s (2003a) findings. Clarke *et al.* (2006) achieved microseparation by applying the same displacement using a spring load, but applied a negative vertical load during swing phase which resulted in 1 mm vertical distraction creating an inferior peripheral wear scar on the head as well as a superior wear scar due to edge loading at heel strike.

It has been shown that increased *in vitro* wear in CoC bearings is associated with head-cup rim contact. Head-cup rim contact or edge loading could occur due to rotational or translational mal-positioning. In vitro studies have shown that increased cup inclinational angle (rotational mal-positioning) without microseparation (translational mal-positioning) does not increase wear in ceramic-on-ceramic bearings and stripe wear was reproduced only when microseparation conditions were present. However the effect of different cup angles on wear during microseparation conditions is not known. The aim of this study was to investigate the effect of cup angle coupled with microseparation conditions on the wear of ceramic matrix composite bearing couples. Four different testing conditions were applied in this study and the following questions were addressed: What is the influence of increasing the cup inclination angle and microseparation on the wear of BIOLOX® *delta* ceramic-on-ceramic bearings? What is the combined influence of steep cup inclination angle and microseparation on the wear of BIOLOX® *delta* ceramic-on-ceramic bearings?

3.2 Materials and Methods

A commercially available AMC ceramic material (BIOLOX® *delta*, CeramTec AG, Germany) was used in this study. This material consisted of 72.5%

alumina, 25.5% zirconia and 2% mixed oxides (Pria, 2007). Size 28mm CoC bearing couples were investigated.

The six-station Leeds Mark II Physiological Anatomical Hip Joint Wear Simulator was used in this study. Three bearing couples were mounted to provide a clinical inclination angle of 55° and the remaining three were mounted to provide a steep clinical inclination angle of 65°. The rationale for these cup inclinations originated from the findings of Nevelos *et al.* (Nevelos et al., 1999), who showed that clinically steep acetabular cup inclination angles ($>55^o$) were associated with high wear rates of retrieved alumina CoC total hip replacements.

The simulator study was performed for a total of 7 million cycles. The first 4 million cycles were performed under standard gait conditions. The 'severe' microseparation conditions, described previously by Nevelos *et al.* (2000) and Stewart *et al.* (2001), were introduced to the six stations for the subsequent 3 million cycles. The lubricant used was 25% new-born calf serum, supplemented with 0.03% sodium azide to inhibit microbial growth. The lubricant was changed every 330,000 cycles. The wear volume was ascertained through gravimetric analysis, which was undertaken every million cycles. The samples were cleaned using a standard operating procedure and placed in a temperature and humidity controlled environment for a minimum of 12 hours prior to weighing on a Mettler AT201 balance (Leicester, United Kingdom) (0.01mg resolution). Each sample was weighed five times in a consistent manner and the mean calculated.

Surface measurements of the samples were undertaken at the beginning and the end of each gait protocol using two-dimensional contacting profilometer (Form Talysurf series, Taylor Hobson, UK). Further wear stripe analysis was undertaken at every measurement point when the microseparation condition was introduced. Three two-dimensional Talysurf measurements were taken on each head and cup across the wear scar 5mm apart and there were three test components for each condition. The average penetration depths of the wear stripe were determined. Statistical analysis was performed using one-way ANOVA (significance taken at $p < 0.05$) and 95% confidence limits were calculated.

A coordinate measuring machine (CMM, Legex 322, Mitutoyo, UK) was used to reconstruct three dimensional representations of the wear stripes on the femoral heads. This machine had a 0.8μm resolution, however, this changed depending on the size of the stylus and the set-up configuration of the measuring probe. All six 28mm femoral heads were measured by taking 72 traces over the femoral heads surfaces with 5 degrees spacing about the vertical axis (Figure 3.1). Each trace started at the pole of the component and had a 0.2mm pitch resulting in a total number of points. SR3D software (TriboSol, UK) was used to visualise the size, shape and penetration depth of the wear areas.

Statistical analysis was performed using one-way ANOVA (significance taken at $p < 0.05$) and 95% confidence limits were calculated.
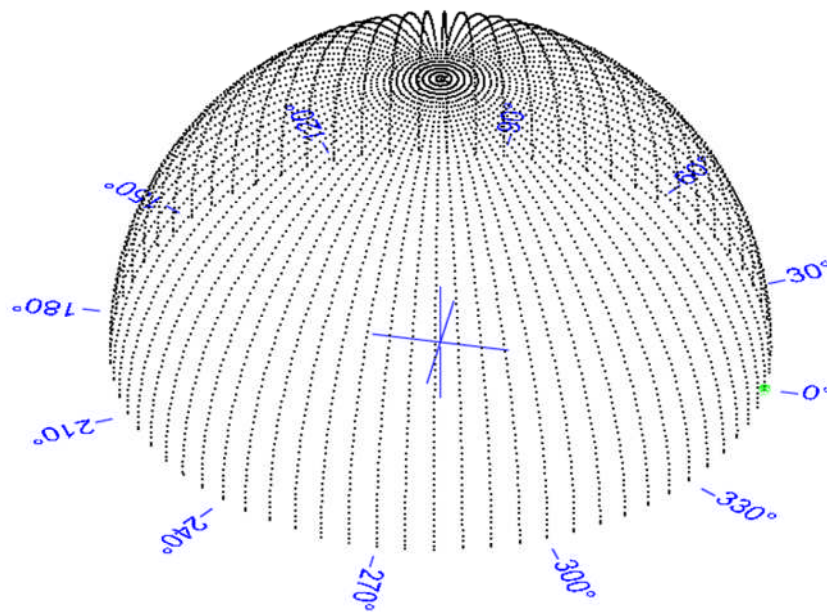
Figure 3.1: Data points taken on the surface of a femoral head consisting of 72 traces. Each trace had several points with 0.3mm spacing (pitch) between each point, starting at the pole and ending 3.5mm below the equator.

Scanning Electron Microscopy (SEM, Philips XL30) was used to take high magnification images of the surface of the ceramic femoral head. The ceramic head was coated with approximately 20nm thick gold coating. Two

images were taken over the stripe wear area at magnifications of 4000x and 8000x, lower magnification images showing the border line between the worn and unworn surface, and one image was taken over the unworn surface at a magnification of 4000x.

Wear debris analysis was performed on serum samples collected from the simulator however, it was not possible to visualise enough particles on the filters to count and size, after the serum has been digested using the method details in Chapter 2. This was thought to be due to the very low wear volume of the ceramic-on-ceramic bearings.

3.3   Results

3.3.1   Wear

During the first two million cycles of test under standard conditions, the components gained weight due to metal transfer from the metal shell and stem onto the back of the liner and head respectively. So the wear volume could not be determined. After the initial two million cycles, the weight of the components started to decrease and it was possible to determine the wear rates under standard conditions for the subsequent two million cycles (Figure 3.2).
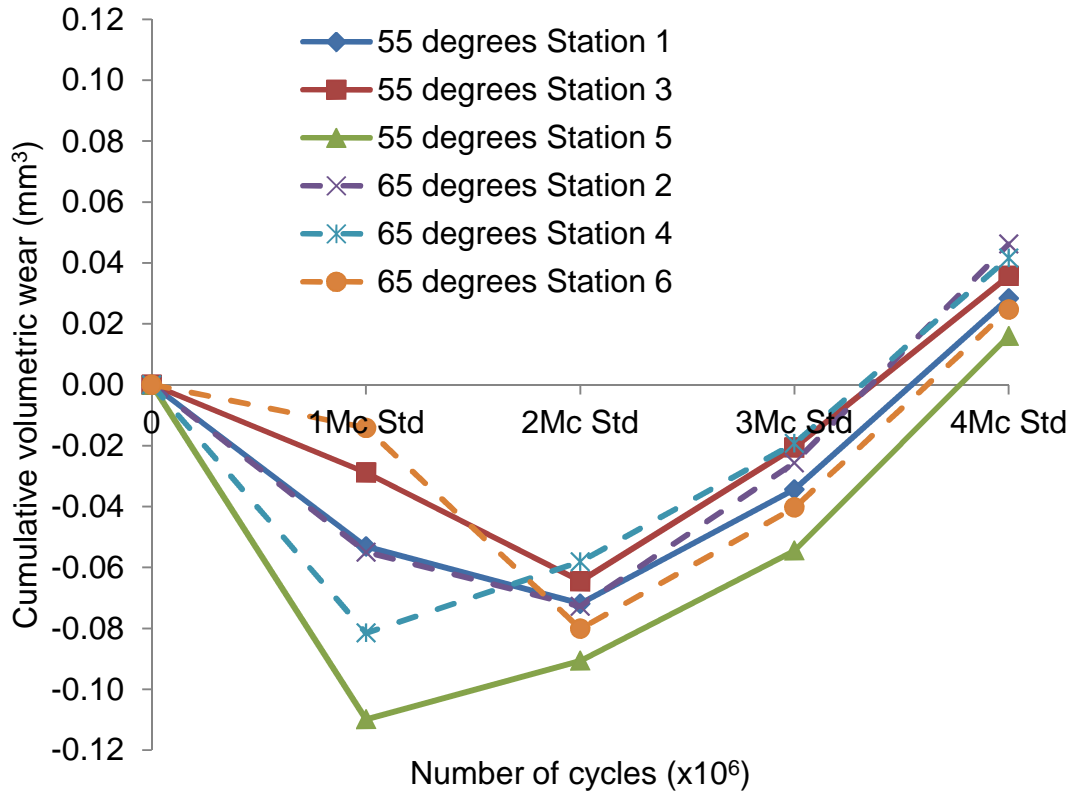
Figure 3.2: Cumulative wear volume of size 28mm BIOLOX® delta ceramic-on-ceramic bearings under standard gait conditions for both cup inclination angles. Negative slopes indicate weight gain due to metal transfer.

There were increased wear volumes and variation in the results when the microseparation conditions were introduced to the gait cycle (Figure 3.3). There was no distinctive reduction in wear rate as the test progressed under microseparation conditions.
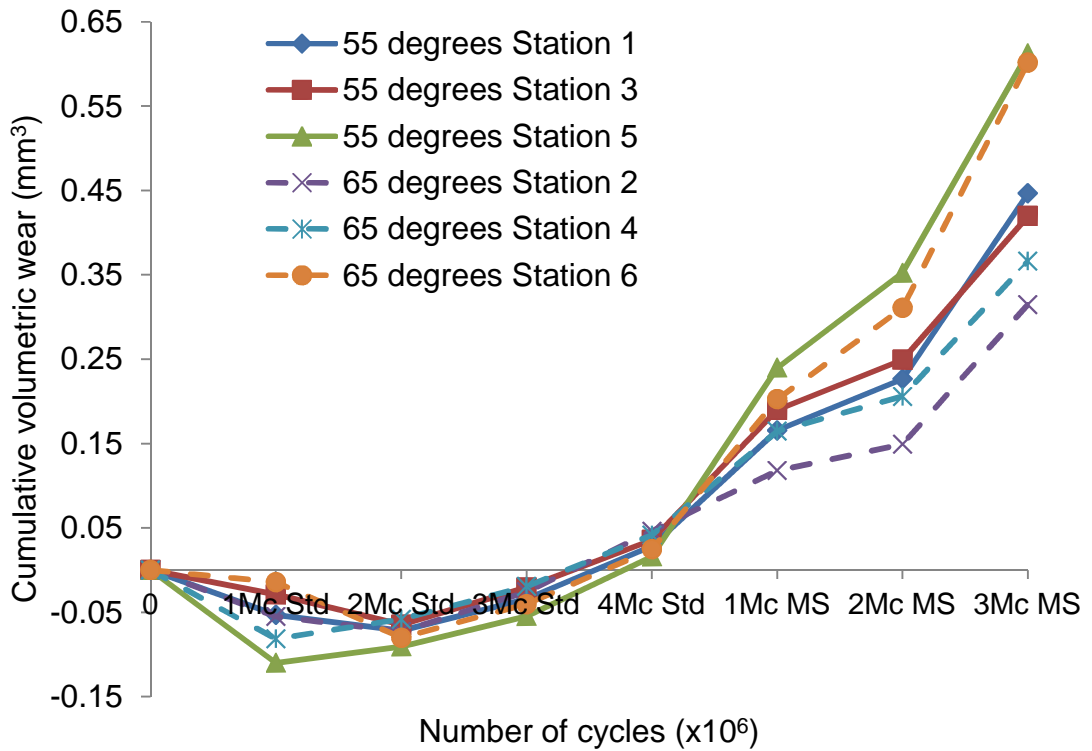
Figure 3.3: Cumulative wear volume of size 28mm BIOLOX® delta ceramic-on-ceramic bearings under standard gait and microseparation conditions for both cup inclination angles. Mc=million cycles, Std= standard and MS=Microseparation.

Increasing the cup inclination angle from 55° to 65° had no statistically significant effect on the mean wear rate of BIOLOX® *delta* CoC bearings either under standard gait (p=0.42) or microseparation (p=0.55) conditions (Figure 3.4). Under standard gait conditions, the wear rate for both cup inclination angles was 0.05 mm^3/million cycles (Figure 3.4).
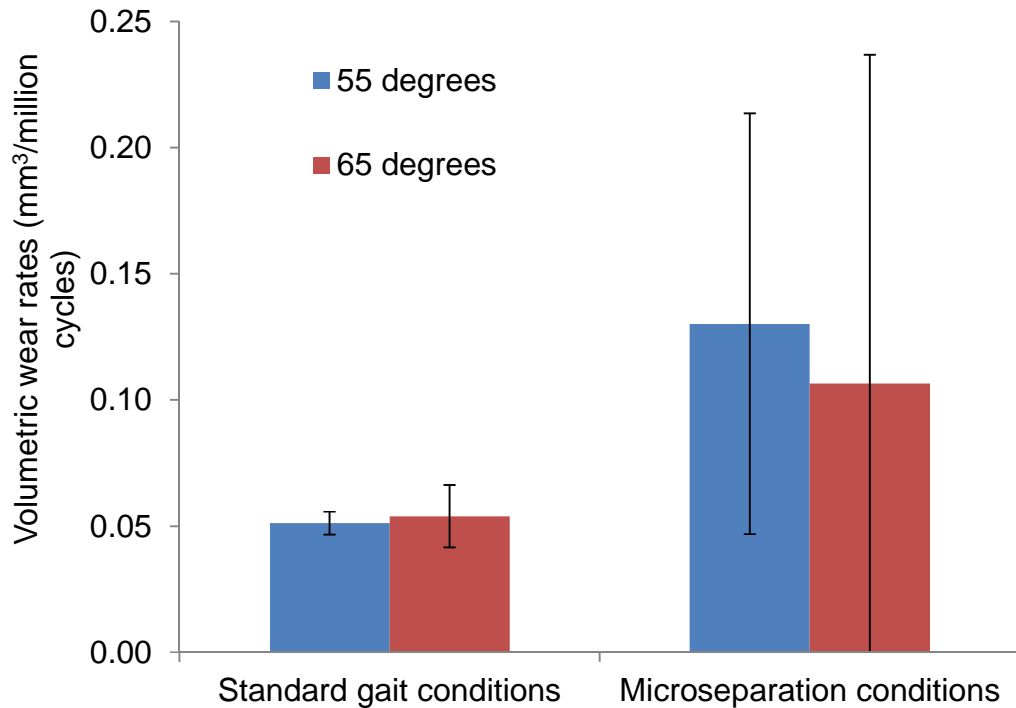
Figure 3.4: Volumetric wear rates of size 28mm BIOLOX® delta ceramic-on-ceramic bearings under standard gait and microseparation conditions for both cup inclination angles. The first two million cycles under standard conditions were not included. Error bars represent 95% confidence limit.

Under microseparation conditions, the wear rate significantly increased, compared to standard conditions (p=0.02), to 0.13 mm^3/million cycles for cup inclination angle of 55°. Under combined adverse conditions (steep cup inclination angle and microseparation), the wear rate increased from 0.05mm^3/ million cycles to 0.11 mm^3/ million cycles, however this increase was not significant (p=0.16) due to the large variation in the wear (standard deviation of 0.05 mm^3/million cycles) when the microseparation condition was introduced to the gait cycle (Figure 3.4). While the wear rate was elevated with microseparation for both cup inclination angle conditions, there was no difference in the wear rates between the two cup inclination angles with microseparation conditions (p=0.55). As the cup inclination angle had no statistically significant effect on the wear under microseparation conditions, the wear rates from the six samples under standard conditions and microseparation conditions were compared. For the six bearing couples

tested, the wear rates significantly (p<0.01) increased from 0.05mm^3/ million cycles under standard conditions to 0.12mm^3/ million cycles.

Throughout the test, the percentage of wear was slightly higher on the cups than the heads with an average of 53% of wear on the cups and 47% of wear on the heads (Figure 3.5). There was an exception of one sample where the wear on the head was 75% of the total wear between two and three million cycles under standard conditions, which influenced the mean percentage wear volumes at three million cycles under standard conditions (Figure 3.5).
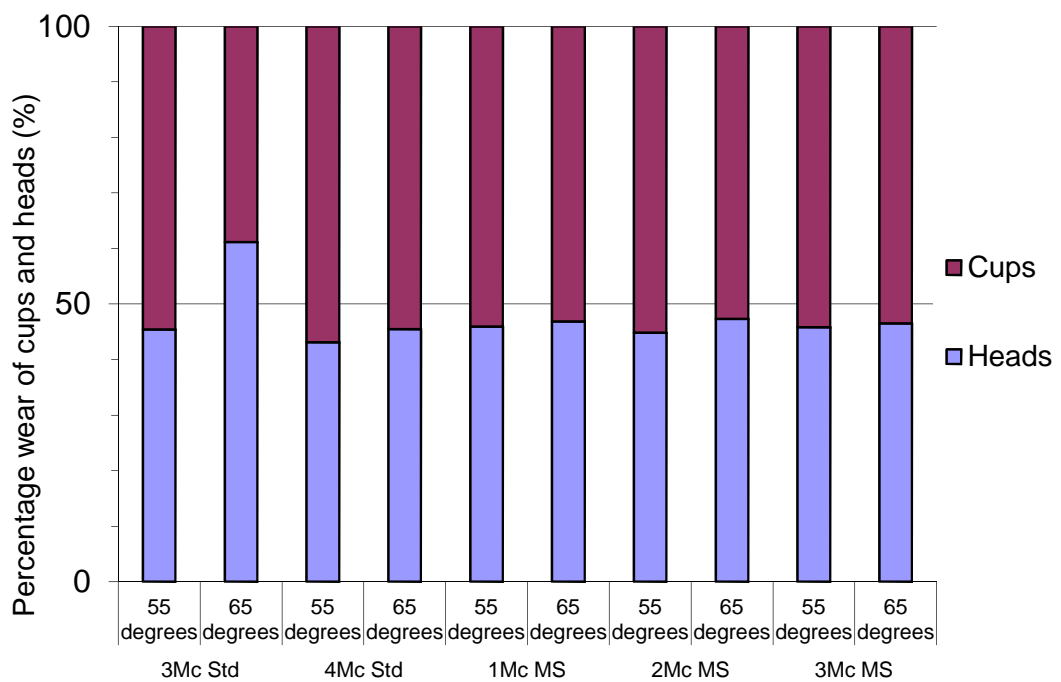
Figure 3.5: Percentage of wear on head and cups at every measurement points for both cup inclination angles under standard gait and microseparation conditions. The first two million cycles under standard conditions were not included as no wear volume was measured. Mc=million cycles, Std= standard and MS=Microseparation.

3.3.2   Surface Roughness Analysis

The introduction of microseparation to the gait cycle resulted in the formation of stripe-like wear on the femoral head and a corresponding wear scar on

the acetabular cup (Figure 3.6). The surface roughness around the wear area was not changed however edge loading due to microseparation conditions caused a significant increase ($p<0.01$) in the surface roughness (Ra) from around 0.005µm to approximately 0.021µm (Table 3.1).

Figure 3.6: The wear stripe on the ceramic femoral head and the rim wear of the acetabular cup formed after testing under microseparation conditions. The wear areas were marked with pencil rubbing for clarity (the grey colour was not due to the wear test).

Table 3.1: The mean surface characterisation parameters before and after the microseparation conditions for the femoral heads under both cup inclination angle conditions. Post- test measurements were taken over the wear stripe area.

	Pre-test		Post-test	
	55 degrees	65 degrees	55 degrees	65 degrees
Ra (µm)	0.005	0.005	0.020	0.023
Rp (µm)	0.013	0.012	0.052	0.061
Rv (µm)	0.035	0.017	0.114	0.144
Rsk	-0.500	-0.480	-1.153	-1.207

3.3.3 Penetration depth

Surface measurements show the depth and the width of the wear stripe formed due to the introduction of microseparation conditions (Figure 3.7 &Figure 3.8). The horizontal parts of the graphs represent the unworn surface of the components with the spherical form removed from the actual trace so the wear area can be assessed. The grey shaded area of the graphs shows the depth and the width of the wear scar.

Maximum depth :   10.2 µm Area of the hole :   10760 µm2
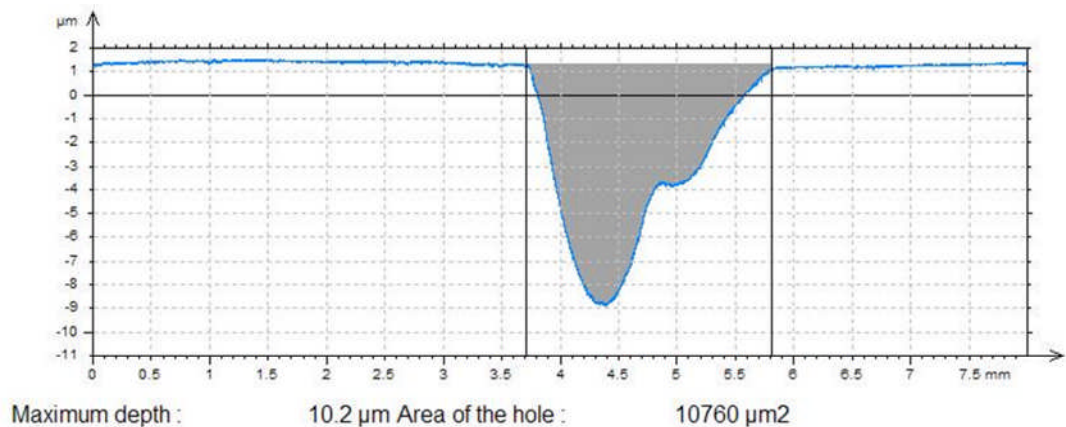
Figure 3.7: An analysed trace taken by a 2D profilometer (Talysurf) showing the penetration depth and width of a 2D line over the wear stripe on the ceramic femoral head after three million cycles of edge loading under microseparation conditions.

Maximum depth :   8.84 µm Area of the hole :   3460 µm2
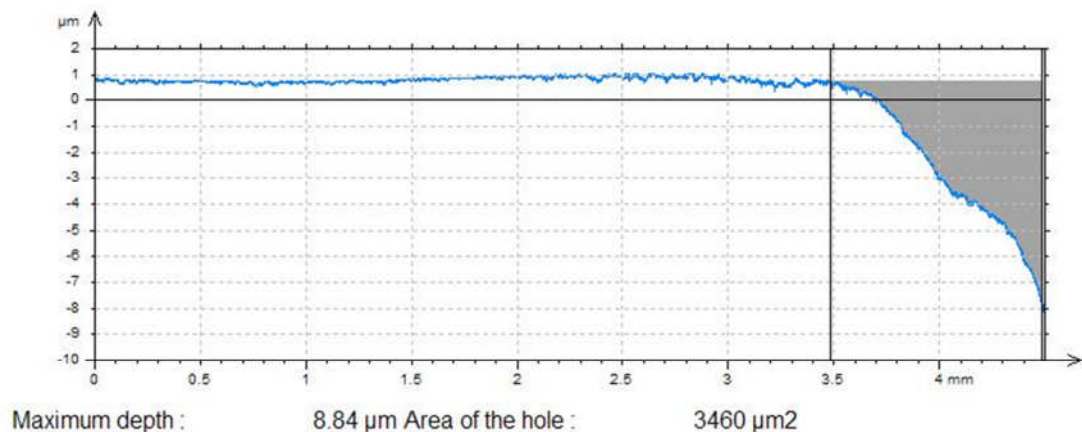
Figure 3.8: An analysed trace taken by a 2D profilometer (Talysurf) showing the penetration depth and width of a 2D line over the wear area adjacent to the rim of the acetabular cup after three million cycles of edge loading under microseparation conditions.

There was no statistically significant difference (p=0.60) in the penetration depth of the femoral heads between the two cup inclination angle conditions over the three million cycles of microseparation conditions. The extent of the damage increased as the test progressed under microseparation conditions. After three million cycles of test, the mean maximum penetration depth was 7.8 μm for the 55° cup inclination angle condition and 7.3 μm for the 65° cup inclination angle condition (Figure 3.9).
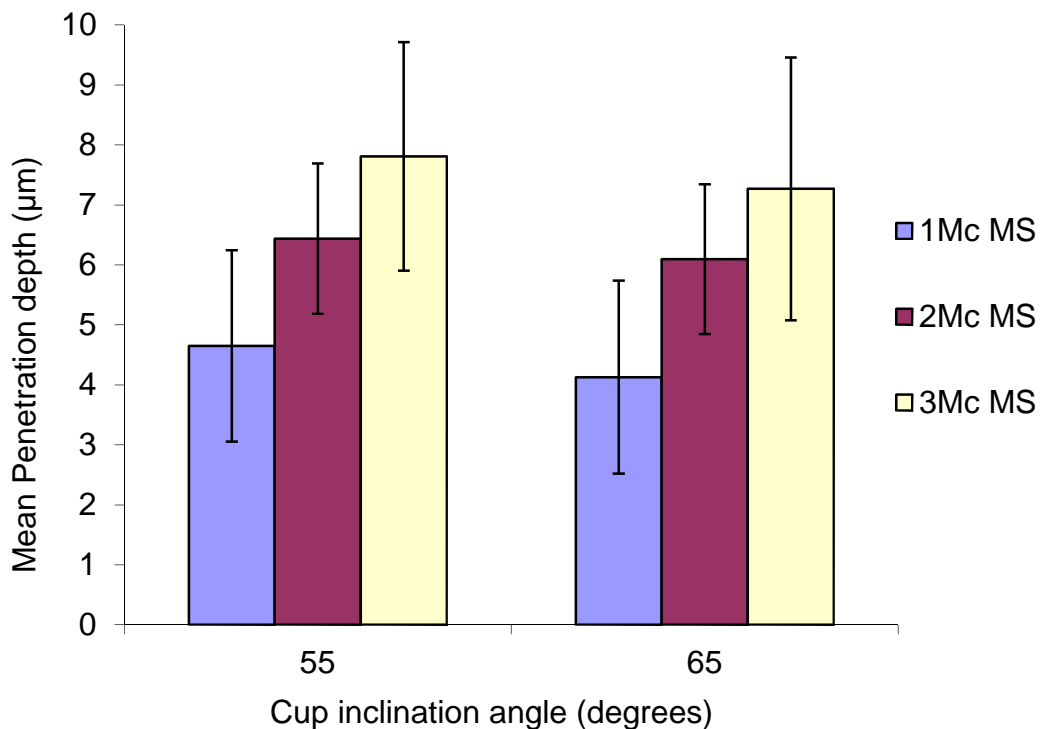
Figure 3.9: Mean Penetration depth over the wear stripe on the femoral heads after 3 million cycles of testing under microseparation conditions. Error bars represent 95% confidence limits. Mc= million cycles and MS=microseparation conditions.

3.3.4 Stripe analysis

An unworn ceramic femoral head showed a sphericity deviation (form error) of +/-2µm, which was a combination of form errors of both the stylus and the ceramic head (Figure 3.10). This meant a wear area with a penetration depth below 2µm could not be accurately detected. The coordinate measuring machine measurements have shown the size and shape of the wear stripes produced under the edge loading conditions due to

microseparation (Figure 3.11 and Figure 3.12). All the femoral heads showed a stripe of wear with penetration depth greater than the sensitivity of the measurement techniques. The maximum penetration occurred when the head was in contact with the rim of the acetabular cup during heel strike, at the position of the highest flexion (30°) and an external rotation of 2° of the gait cycle. These correspond to the left part of the wear stripes formed on all the femoral heads. There was no statistically significant (p=0.5) difference in the maximum penetration depth between the two cup inclination angle conditions. There was also no significant difference in the lengths and widths of the wear scars under both cup inclination angles (Table 3.2).

Table 3.2: The lengths and widths of the wear stripes on the 28mm femoral heads after 3 million cycles of testing under microseparation conditions.

	Length		Width	
	55°	66°	55°	66°
Sample 1	24.2	27.4	2.4	2.0
Sample 2	24.0	27.1	2.0	1.5
Sample 3	28.0	28.0	2.4	2.3
Mean	**25.4**	**27.5**	**2.3**	**1.9**
Significance (p value)	0.19		0.28	
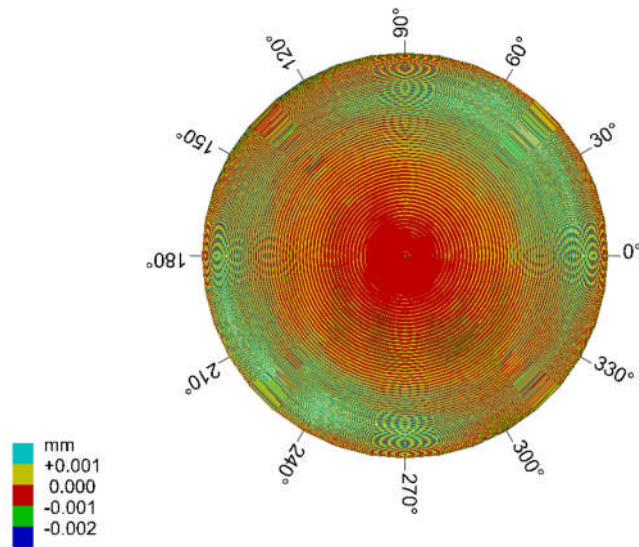
Figure 3.10: Three dimensional reconstruction of an unworn ceramic head. The contours shown are relative to a perfect sphere.
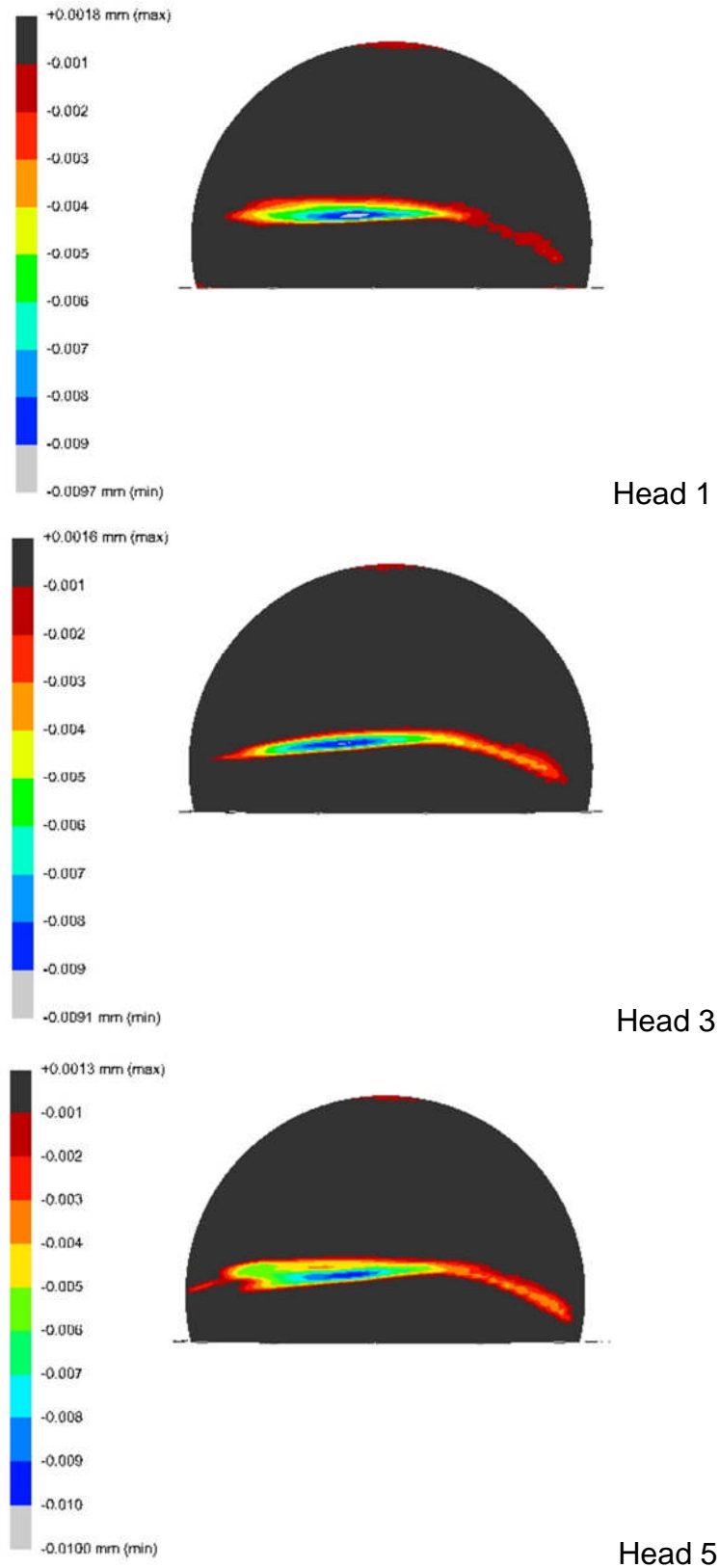
Figure 3.11: Three dimensional reconstruction of the wear stripe area over the three femoral heads articulated against acetabular cups inclined at 55º.

Head 2

Head 4

Head 6
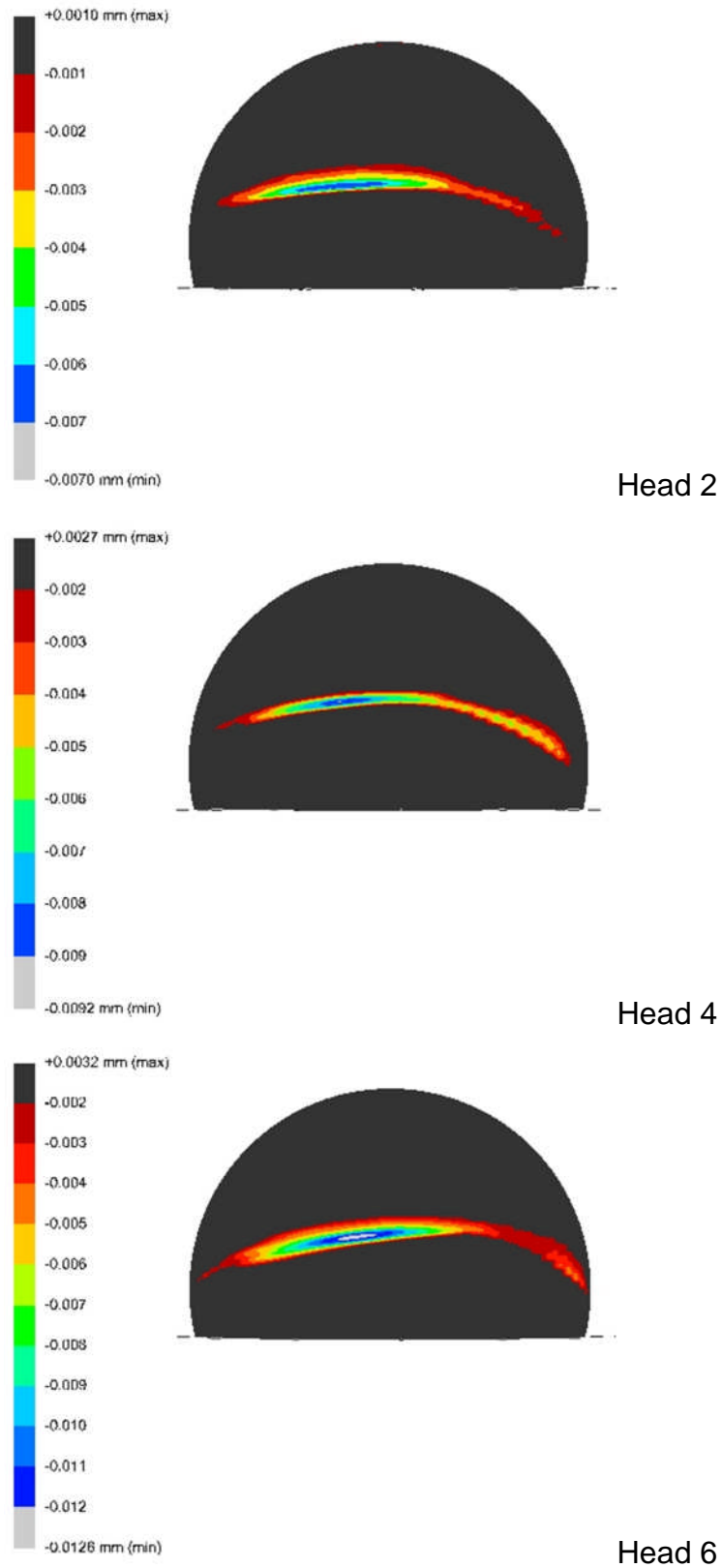
Figure 3.12: Three dimensional reconstruction of the wear stripe area over the three femoral heads articulated against acetabular cups inclined at 65⁰.

3.3.5   Surface Analysis

A high magnification micrograph over the unworn area of the femoral head showed a smooth uniform surface (Figure 3.13). Whereas, the stripe wear area had a rough surface with round pores up to $2\mu m$ in diameter due to grain removal (Figure 3.14, Figure 3.15 and Figure 3.16).
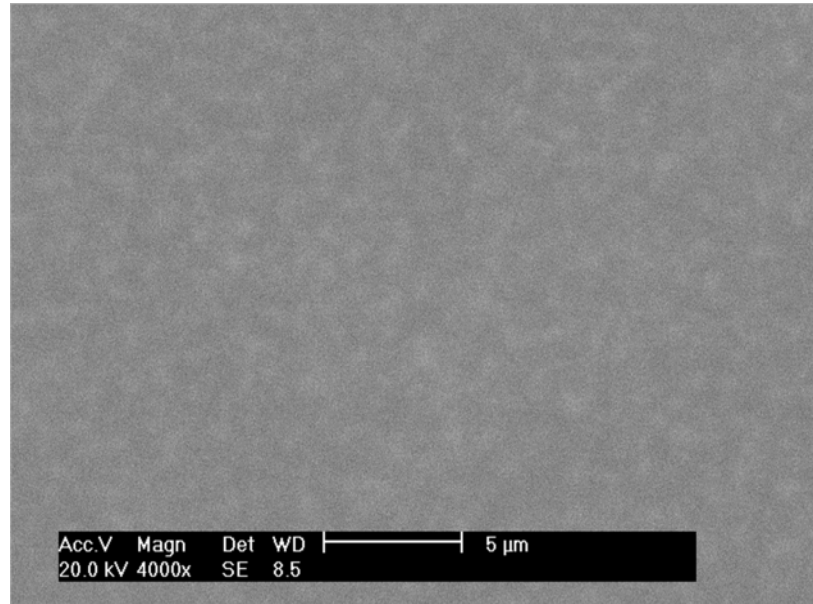
Figure 3.13: High magnification image(x4000) over the unworn surface of the ceramic femoral head taken using a scanning electron microscope (SEM).
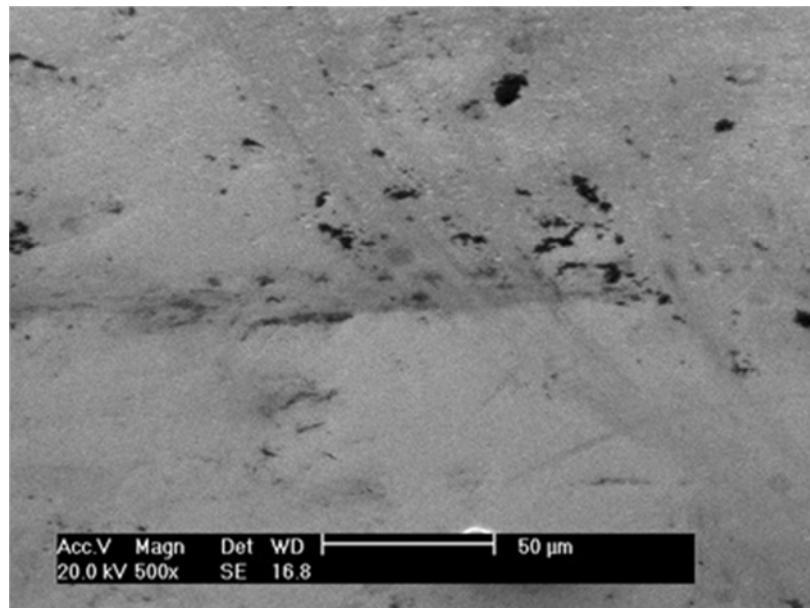
Figure 3.14: SEM image (x500) on the border line between worn (top half of image) and unworn (bottom half of image) regions on the surface of the ceramic femoral head.
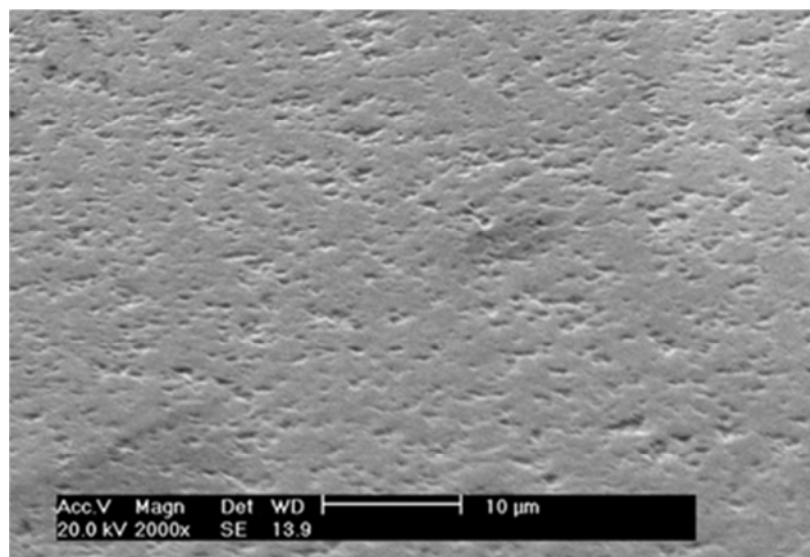
Figure 3.15: High magnification image(x2000) over the worn surface of the ceramic femoral head taken using a scanning electron microscope (SEM).
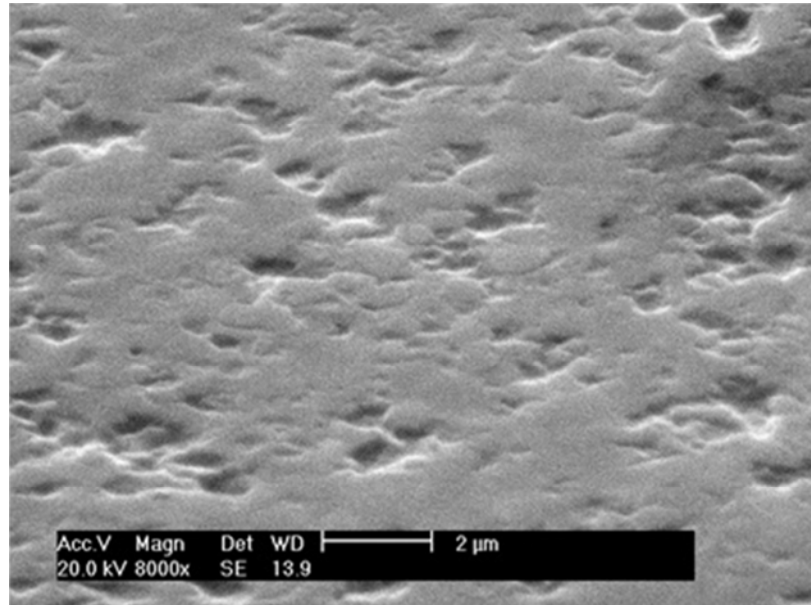
Figure 3.16: High magnification image(x8000) over the worn surface of the ceramic femoral head taken using a scanning electron microscope (SEM).

3.4 Discussion

Ceramic-on-ceramic bearings produce very low wear volumes under standard gait hip simulator studies. However, clinically, relatively high wear rates compared to *in vitro* results under standard gait, and formation of stripe of wear on the femoral head with a matching wear area on the cup have been reported (Nevelos et al., 1999). Stripe-like wear has been associated with edge loading (Nevelos et al., 1999, Nevelos et al., 2000), that is believed to be associated with microseparation. *In vitro* studies have shown that steep cup inclination angle did not produce stripe wear and high wear rates (Nevelos et al., 2001a), however, the introduction of microseparation to the gait cycle produced clinically relevant wear patterns and wear rates (Nevelos et al., 2000). The effect of cup position on wear during microseparation and rim loading conditions has not been previously studied. In this study, increasing the cup inclination angle from 55° to 65° had no statistically significant effect on the wear rate of size 28mm BIOLOX® *delta* CoC THR under standard or microseparation condition. This was consistent with previous studies reported by Nevelos *et al.* (2001a) that cup inclination

angle has no statistically significant effect on the wear rate of BIOLOX[®] *forte* CoC bearings under standard gait simulation.

The introduction of microseparation to the gait cycle increased the wear rate of BIOLOX[®] *delta* CoC bearings. These findings were consistent with previous *in vitro* hip simulator studies of CoC THR (Nevelos et al., 2000, Stewart et al., 2003a). This highlights the importance of surgical technique in positioning the centre of the head in the centre of the axis of rotation to avoid the lateral/medial displacement and thus avoid edge loading.

Analysis of retrieved alumina CoC bearings by Nevelos *et al.* (1999) have shown that steep inclination angle facilitates edge loading that can lead to higher wear rates in CoC THR. In this study, the wear rate of BIOLOX[®] *delta* CoC bearings under combined microseparation and steep cup angle conditions was similar to that under microseparation condition alone. Clinically, a high cup angle potentially facilitates microseparation as smaller displacement and lower forces are required for the head to microseparate and come into contact with the rim of the cup resulting in higher wear rates. In our simulation the microseparation lateral displacement was controlled to be the same for both cup angle tests, so this may not fully replicate the increased instability found with steep cups in vivo.

Although microseparation increased the wear rate of the BIOLOX[®] *delta* CoC bearings, the wear rate measured was still very low at a mean of 0.13mm^3/million cycles compared to 1.84mm^3/million cycles for HIPed third generation alumina ceramic (BIOLOX[®] *forte*) reported by Stewart *et al.* (Stewart et al., 2001) under the same conditions. This wear rate is extremely low compared to *in vitro* wear rates of MoP and MoM under standard conditions. Typical *in vitro* wear rates previously reported for metal-on-historical polyethylene were in the range of 35-50 mm^3/million cycles (Smith and Unsworth, 1999, Bigsby et al., 1997), that of metal-on-cross-linked polyethylene were in the range of approximately 5 to 10 mm^3/million cycles (Galvin et al., 2007), and that for MoM ranged between 1 and 4 mm^3/million cycles (Bowsher et al., 2004, Liao and Hanes, 2006, Williams et al., 2006, Leslie et al., 2008).

The change in surface roughness (Ra) was from approximately 5nm (unworn surface) to approximately 20nm (wear area) which was not significant relative to the surface roughness increase of HIPed alumina ceramic from < 10nm to between 140 and 300 nm (Stewart et al., 2001) under the same microseparation conditions.

It was possible, using the CMM and SR3D software, to visualise the shape, depth and orientation of the wear stripes on the femoral heads. This method provided an effective way of determining the linear wear (and volumetric wear which will be discussed in Chapter 8) on the surfaces of the femoral heads. Previously, when the 2 dimensional profilometry (Talysurf) was used, only three traces were taken across the wear area, giving very little information about the wear area which was overcome using this geometric technique.

High stresses caused by edge loading due to microseparation conditions have resulted in the removal of micron sized ceramic grains off the bearing surfaces as shown on the micrographs taken by the scanning electron microscope. However, the micro-pitting formed on the BIOLOX® delta ceramic materials used in this study were not as severe as the deformation on the surface of the HIPed alumina (BIOLOX® forte) bearings tested under the same edge loading conditions (Figure 3.17).
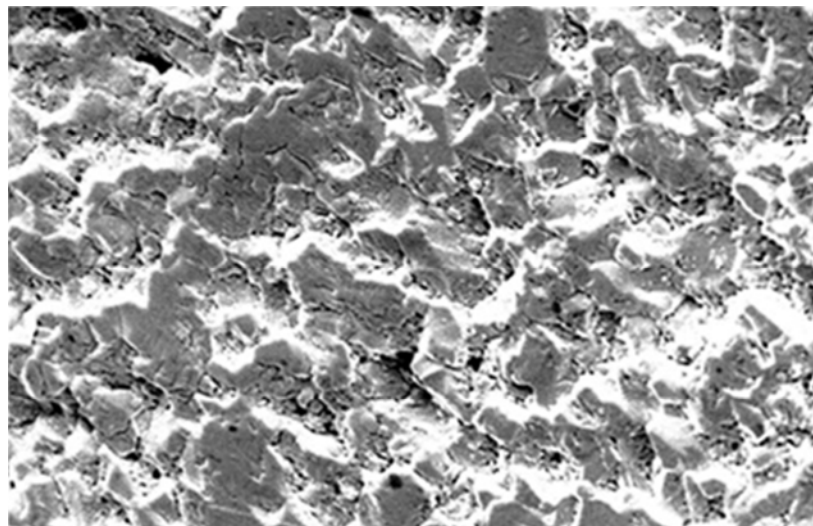
Figure 3.17: SEM image over the wear stripe area of the BIOLOX® forte ceramic femoral head tested under microseparation conditions (Nevelos et al., 2000).

In conclusion, this study has shown that increasing the cup inclination angle from 55° to 65° had no influence on the *in vitro* wear rate of BIOLOX$^®$ *delta* CoC bearings under either standard gait or microseparation conditions. It has also been demonstrated in this study that the introduction of microseparation (head offset deficiency) condition to the gait cycle increased the wear rate of such bearing surfaces and combining microseparation conditions with steep cup angle did not increase the wear rate any further. Although microseparation increased the wear rate of BIOLOX$^®$ *delta*, the wear rates obtained were still very low compared to the HIPed third generation alumina ceramic (BIOLOX$^®$ *forte*) reported by Stewart *et al.* (2001) under the same adverse conditions.

CHAPTER 4. THE INFLUENCE OF CUP INCLINATION ANGLE AND HEAD POSITION ON THE WEAR OF 28mm METAL-ON-METAL BEARINGS IN TOTAL HIP REPLACEMENTS

4.1   Introduction

Up until recently, metal-on-metal (MoM) bearings in total hip replacements (THRs) have been used as an alternative to metal-on-polyethylene (MoP) due to the polyethylene particles induced osteolysis (Willert, 1977). One retrieval analysis of MoM bearings have reported a low steady state wear rate of 5 μm/year (Sieber et al., 1999a). However, more recent retrieval studies of MoM bearings in THRs have shown a wide range in clinical wear rates (Rieker et al., 2004b) and wear mechanisms (Howie et al., 2005). High wear rates measured on retrievals, including surface replacements, have been widely reported (Rieker et al., 2004b, Campbell et al., 2006, Morlock et al., 2008, Langton et al., 2011).

High wear rates have been associated with many clinical complications that lead to complicated revision surgeries. ALVALs, pseudotumours, and pain are consequences of high wearing metal-on-metal bearings. These high wear rates could be related to the level of patient activities and surgical factors such as cup and head positions and laxity of the surrounding tissues and muscles that can lead to edge loading. One study has correlated the development of pseudotumours in patients with MoM bearings with the occurrence of edge loading conditions (Kwon et al., 2010).

High wearing MoM surface replacements (SR) retrievals have been associated with steep cup inclination angle and edge loading mechanisms (Morlock et al., 2008, Kwon et al., 2010). Also, high levels of metal ions have been measured in patients with steeply-inclined metal acetabular component (De Haan et al., 2008). *In vitro* studies have shown that increasing the cup inclination angle of MoM bearings resulted in elevation of wear rates (Williams et al., 2004a, Angadji et al., 2009, Leslie et al., 2009), however not to levels similar to those observed in retrievals.

High cup inclination angles coupled with microseparation conditions have replicated similar high *in vivo* wear rates in MoM SR (Leslie et al., 2009). Metal-on-metal bearings in THRs have shown low *in vitro* wear rates under standard hip simulator conditions which correlate with well positioned prostheses (Chan et al., 1999, Firkins et al., 2001c, Goldsmith et al., 2000). However, *in vivo*, steeply inclined cups or head offset deficiency can cause higher wear rates and failure of prostheses. The aim of this study was to investigate the effect of cup angle coupled with microseparation conditions on the wear of MoM bearings in THRs. Four different testing conditions were applied in this study and the following questions were addressed: What is the influence of increasing the cup inclination angle and the introduction of microseparation to the gait cycle on the wear of MoM bearings? What is the combined influence of steep cup inclination angle and microseparation on the wear of MoM bearings?

4.2 Materials and Methods

The wear of MoM bearings in THRs was investigated under different cup inclination angles during standard gait and microseparation conditions. Six 28mm diameter cobalt chrome alloy (CoCrMo) femoral heads and acetabular cups were custom manufactured by Corin Ltd UK, and tested using the six station Leeds II Physiological Anatomical Hip Joint Wear simulator. The components were all high carbon (>0.2% C) and heat treated. The mean diametrical clearance of all couples was 40µm. Three acetabular cups were mounted to provide an inclination angle equivalent to 45° *in vivo* and three other cups were mounted to provide an inclination angle equivalent to 65° *in vivo*. A twin peak loading of 3kN peak load was applied and two independently controlled axes of motion, flexion/extension (-15° to +30°) and internal/external rotation (+/- 10°) were applied.

The first 3 million cycles out of a total of six million were performed under standard gait conditions. The 'severe' microseparation conditions, described in previous studies (Nevelos et al., 2000, Stewart et al., 2001), were introduced to all six stations for the subsequent 3 million cycles. Microseparation condition was achieved by applying a lateral movement of

approximately 0.5 mm to the acetabular cup relative to the head, which resulted in edge loading at heel strike. The set-up allowed comparison between four different testing conditions summarised in Table 4.1.

Table 4.1: The four testing condition investigated in this study.

	Cup inclination angle (in vivo equivalence)	
	45°	65°
Standard gait cycle	Standard conditions	Steep cup inclination angle conditions
Microseparation introduced to gait cycle	Microseparation conditions	Steep cup inclination angle under microseparation conditions

The lubricant, 25% new born calf serum supplemented with 0.03% sodium azide, was changed every 330,000 cycles and wear measurements were under taken every one million cycles. The wear volume was ascertained through gravimetric analysis. The components were weighed using a Mettler AT201 balance (Leicester, United Kingdom) (0.01mg resolution).

A two-dimensional contacting profilometer (Form Talysurf series, Taylor Hobson, UK) was used to measure the surface roughness of the components before and after testing. The penetration depth over the wear stripe produced due to edge loading was measured using the Talysurf. Three traces were taken across the wear scar 5mm apart. The CMM methodology was not developed when this study was performed so CMM measurements were not done on the 28mm metal-on-metal components.

Scanning Electron Microscopy (SEM, Philips XL30) was used to take high magnification images over the wear area of the acetabular components.

The ion level measurements were done using an inductively coupled plasma mass spectroscopy (ICP-MS) in Earth and Environmental Sciences

department at the University of Leeds, UK. At each measurement point, 0-0.33Mc, 0.33-0.66Mc, 0.66-1Mc, 1-2Mc and 2-3Mc, five 3ml-samples were taken from each station and underwent nitric acid digestion and centrifuging processes to eliminate proteins, contaminants and wear debris. Measurements were compared to background measurements of digested fresh 25% serum containing known amount of Co or Cr and calibrated samples of Co and Cr. These were used to check if the machine was measuring the right concentrations and the digestion process was valid. Using the ICP the solution was aspirated into aerosol then passed through argon plasma. This procedure transforms the atoms of the metal elements into ions. These ions are then separated and detected by the mass spectrometer (MS).

Statistical analysis was performed using one-way ANOVA (significance taken at $p < 0.05$) and 95% confidence limits were calculated.

4.3 Results

4.3.1 Wear

Under standard gait conditions with cup inclination angle of 45°, there was two distinct phases of wear, a bedding in phase over the first 2 million cycles then a relatively reduced wear phase between 2 and 3 million cycles (Figure 4.1). The wear rates significantly ($p = 0.04$) decreased from a mean of 1.26 mm^3/million cycles (95% confidence limit: 0.79 mm^3/million cycles) between 0 and 2 million cycles to a mean of 0.44 mm^3/million cycles (95% confidence limit: 0.82 mm^3/million cycles) between 2 and 3 million cycles of testing.
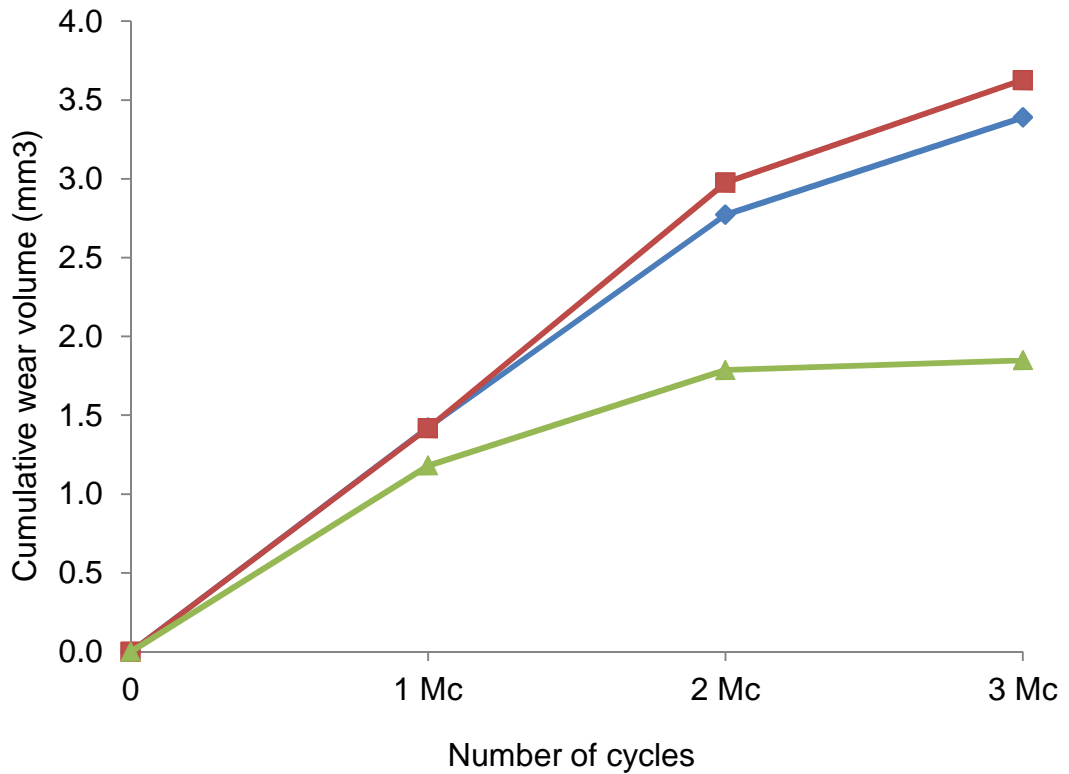
Figure 4.1:Cumulative wear volume of the three individual MoM samples tested under standard gait conditions with a cup inclination angle of 45° over the 3 million cycles. Mc= million cycles.

Under standard gait conditions with the cup steeply inclined (65°), the components did not show any sign of bi-phasic wear mechanisms (Figure 4.2). Over the 3 million cycles of testing, the wear rate significantly (p=0.003) increased from an overall wear rate of 0.99 mm^3/million cycles under 45° cup inclination angle to 2.65 mm^3/million cycles under 65° cup inclination angle. The wear area of the three bearing couples tested under steeply inclined angle intersected with the rim of the acetabular cup showing signs of edge loading.
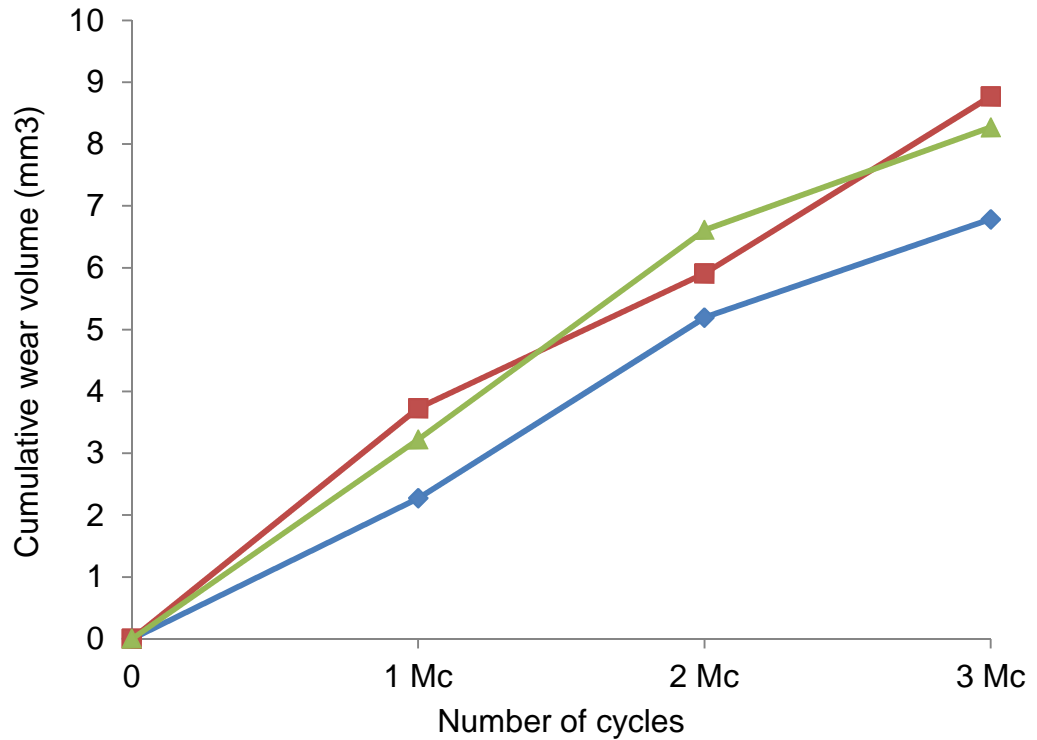
Figure 4.2: Cumulative wear volume of the three individual MoM samples tested under standard gait conditions with steep cup inclination angle of 65° over the 3 million cycles. Mc= million cycles.

The introduction of microseparation conditions to the gait cycle significantly increased the wear rate to 4.62 mm^3/million cycles for cup inclination angle of 45° (p=0.001) and to 4.44 mm^3/million cycles for cup inclination angle of 65° (p=0.003) (Figure 4.3).However increasing the cup inclination angle from 45° to 65° under microseparation conditions did not influence (p=0.7) the wear rate of MoM bearings in THR (Figure 4.3). There was also no sign of bi-phasic wear mechanisms under microseparation conditions showing a linear increase in wear over the 3 million cycles of testing (Figure 4.4 and Figure 4.5).
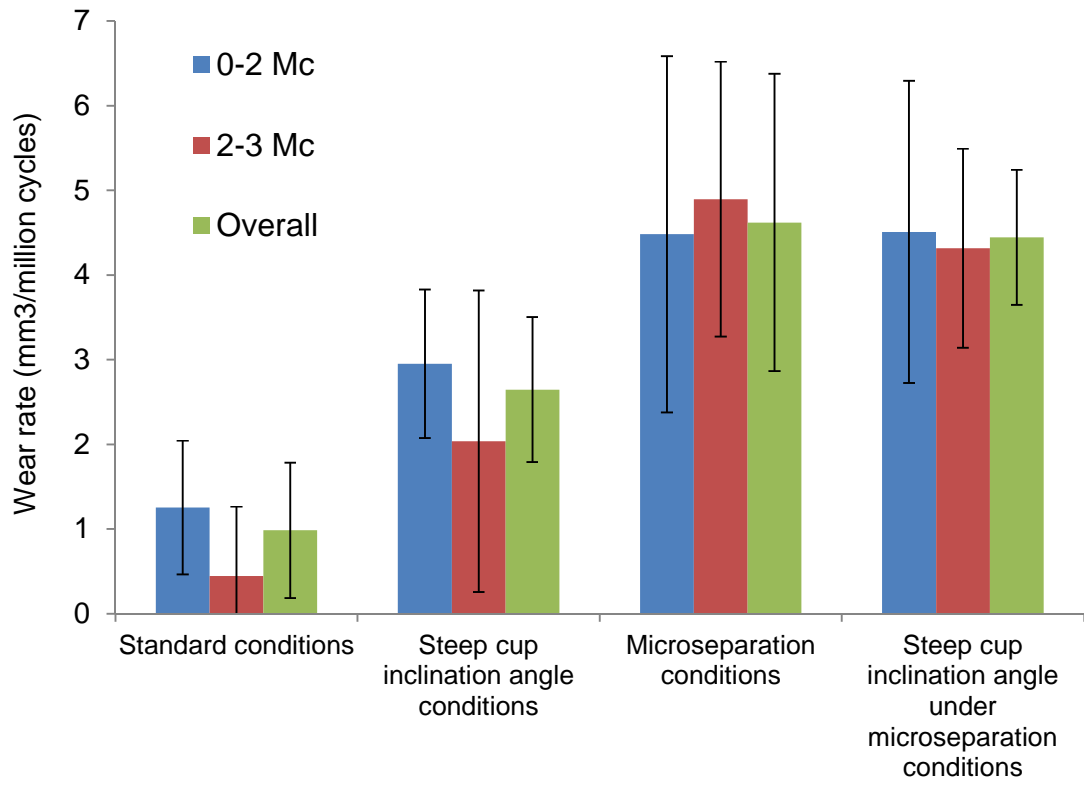
Figure 4.3: The mean wear rates at different stages of the test under the four different testing conditions. Error bars represent the 95% confidence limits. Mc= million cycles.
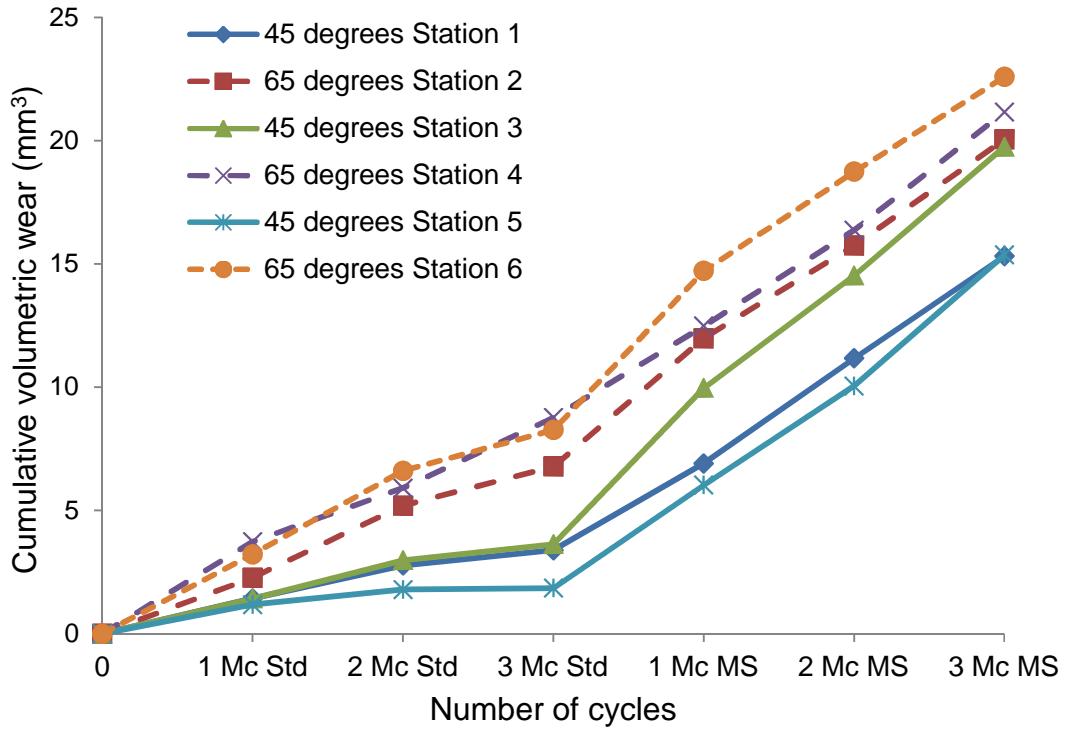
Figure 4.4: Cumulative wear volume for the six individual MoM samples tested under standard gait and microseparation conditions for both cup inclination angles. Mc= million cycles, Std= Standard conditions, MS= Microseparation conditions.
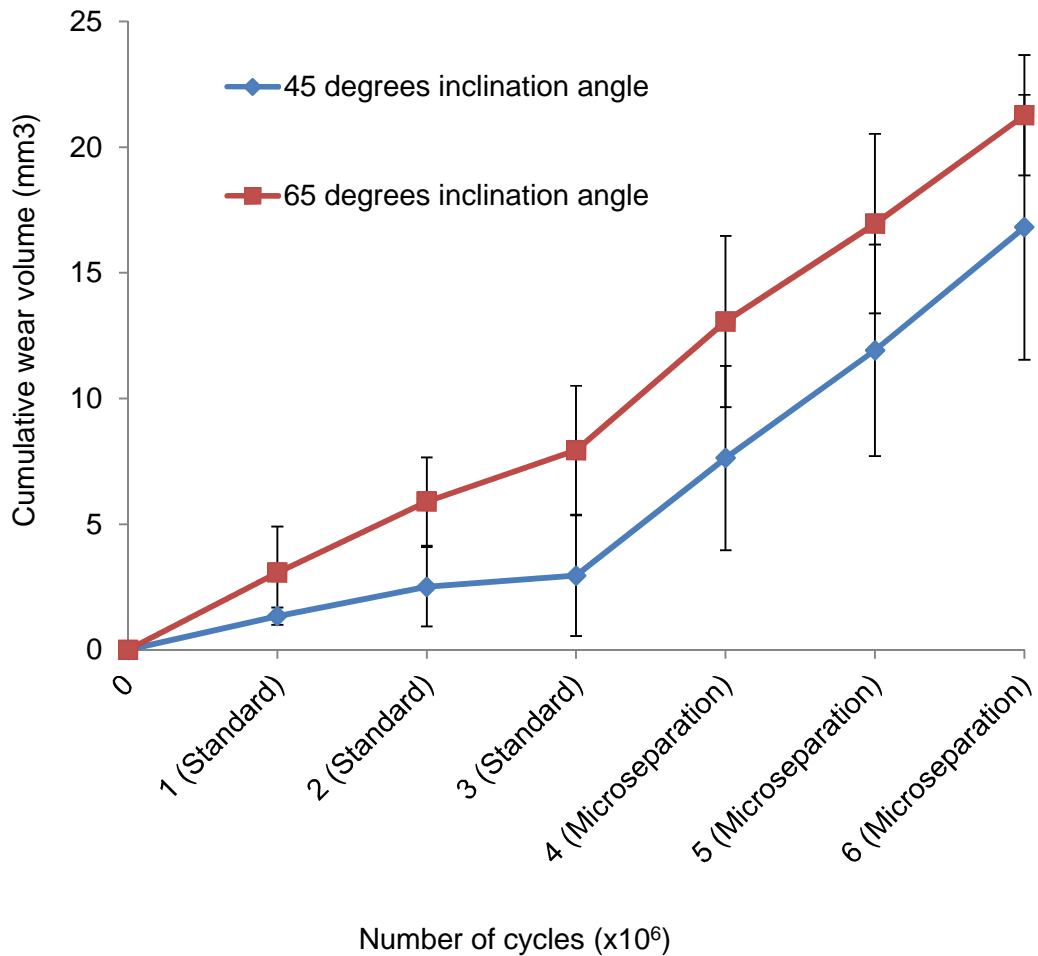
Figure 4.5: Mean cumulative wear volume after 6 million cycles of test; 3 million cycles under standard gait conditions and 3 million cycles under microseparation conditions. Error bars represent 95% confidence limit.

4.3.2 Serum colour

The rapid release of metal wear debris have darkened the serum colour during the bedding in stage of the test under standard gait conditions (Figure 4.6, top). Towards the end of the test, the lubricant from the stations where the cup was inclined at an in vivo angle equivalent of 45° had become lighter in colour, indicating less presence of wear debris (steady state phase; Figure 4.6, bottom). However, under steep cup inclination angle the serum became even darker with no sign of steady state phase (Figure 4.6). This was also the case under microseparation conditions where the serum colour remained dark throughout the three million cycles of testing (Figure 4.7).

Figure 4.6: Serum colour for all stations at 0.68 million cycles of test (top) and 2.65 million cycles of test (bottom) under standard gait conditions. Stations 1, 3 and 5 had the cups inclined at 45° and 2, 4 and 6 had the cups inclined at 65°.

Figure 4.7: Serum colour for all stations at 0.66 million cycles of test (top) and 3 million cycles of test (bottom) under microseparation conditions. Stations 1, 3 and 5 had the cups inclined at 45° and 2, 4 and 6 had the cups inclined at 65°.

4.3.3 Ion level analysis

The cobalt and chromium ions concentrations followed the same pattern as the wear volumes that were measured gravimetrically (Figure 4.8 and Figure 4.9). There was a good correlation between the wear volume and cobalt ion concentration under all conditions tested (R^2=0.90, Figure 4.10). However the correlation between the volumetric wear and the chromium ions was weaker (R^2=0.76, Figure 4.11) especially under high wear volume conditions (Figure 4.11 and Figure 4.12).
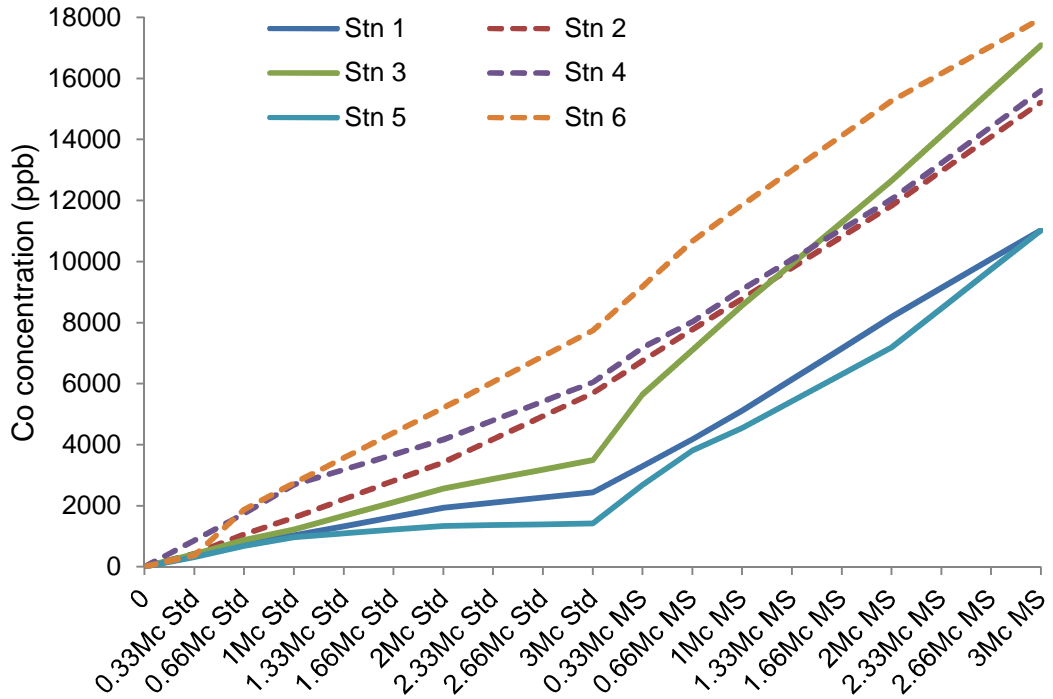
Figure 4.8: Cobalt ion concentration throughout the six million cycles of test; three under standard conditions and three under microseparation conditions. The odd numbered station had the cups inclined at 45° and the even numbered stations had the cups inclined at 65°.
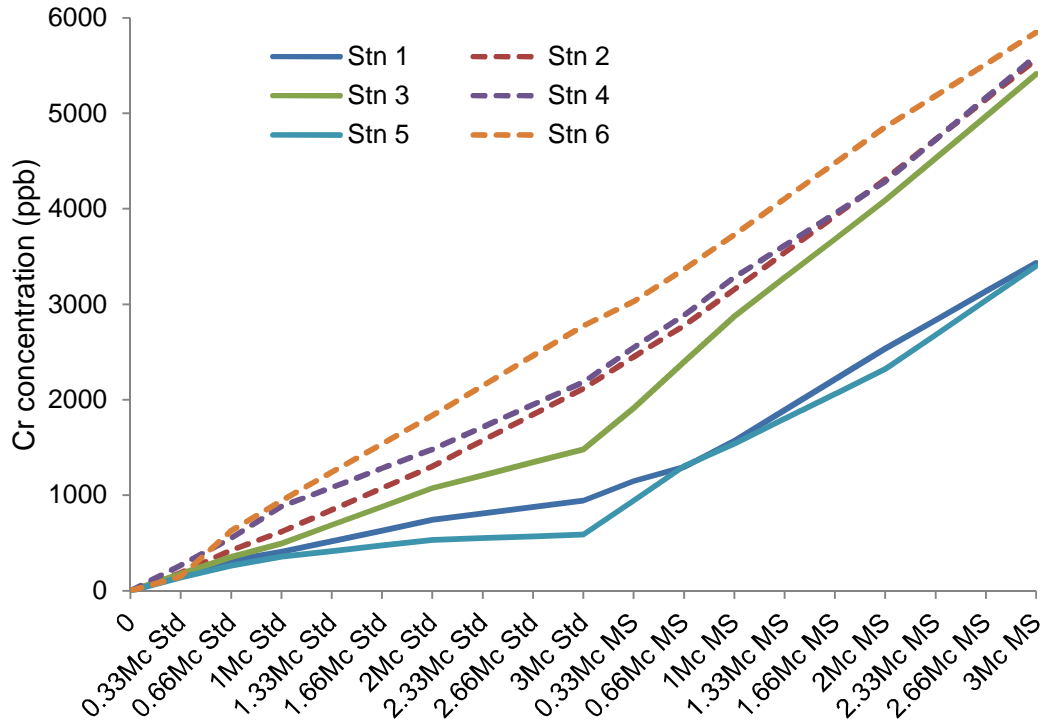
Figure 4.9: Chromium ion concentration throughout the six million cycles of test; three under standard conditions and three under microseparation conditions. The odd numbered station had the cups inclined at 45° and the even numbered stations had the cups inclined at 65°.
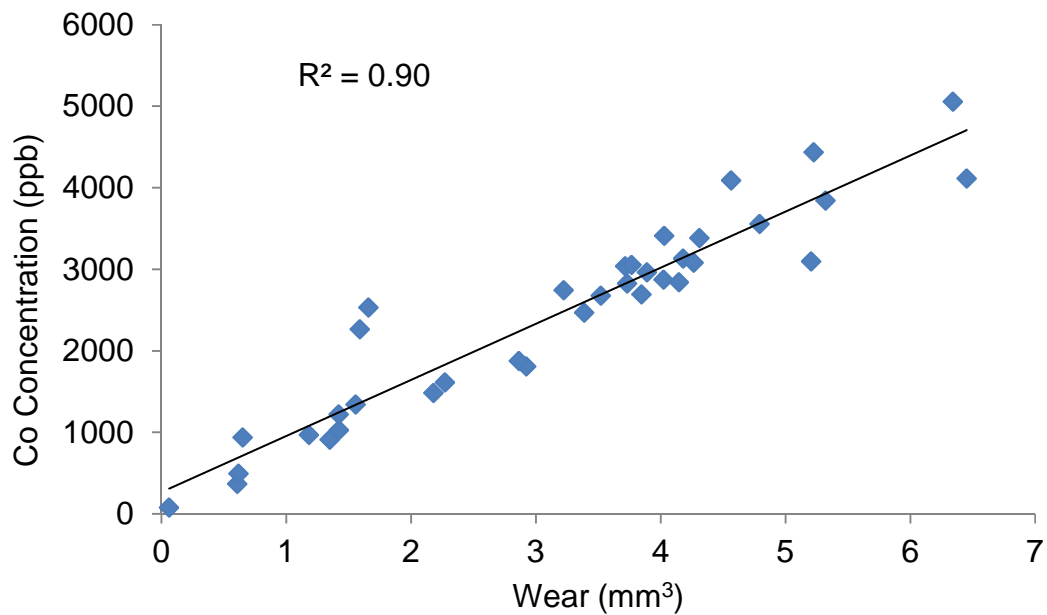
Figure 4.10: Correlation between Co ion concentration and volumetric wear throughout the hip simulator test.
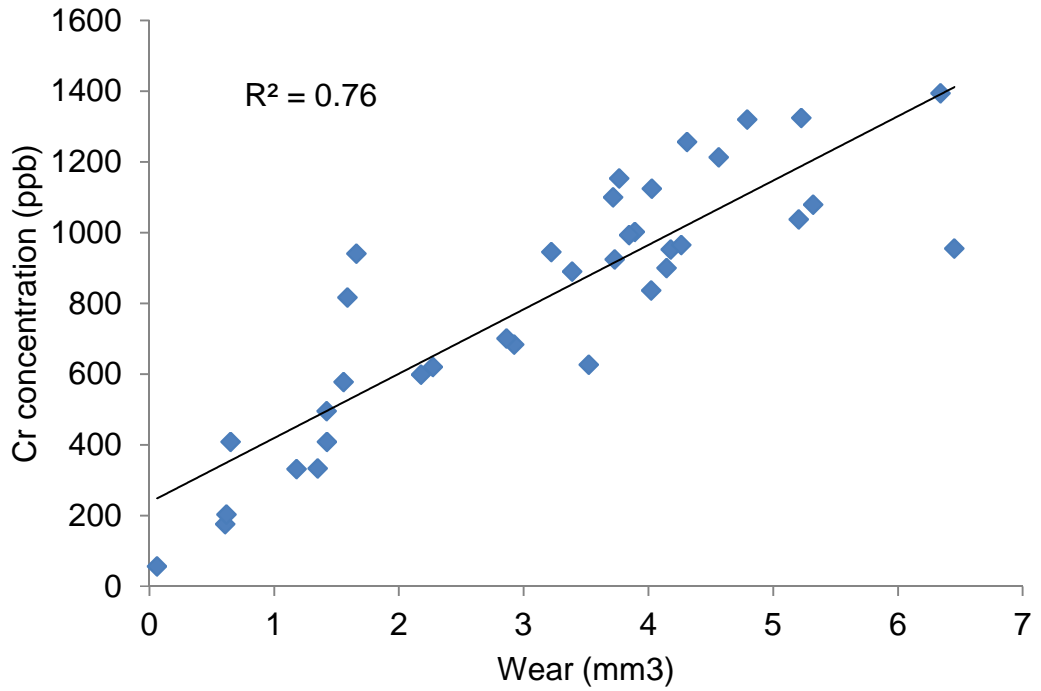
Figure 4.11: Correlation between Cr ion concentration and volumetric wear throughout the hip simulator test.
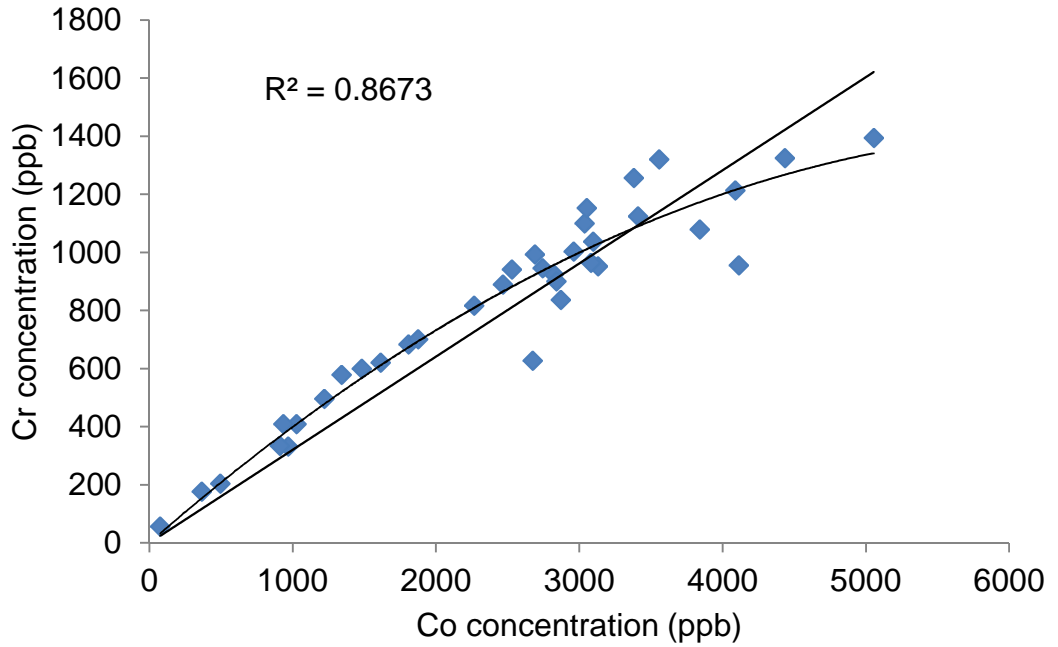
Figure 4.12: Correlation between Co ion concentration and Cr ion concentration throughout the hip simulator test.

4.3.4 Penetration depth

A stripe of wear on the metal heads (Figure 4.13) with a corresponding wear area on the lateral edge of the acetabular cup (Figure 4.14) have been observed when microseparation conditions were introduced to the gait cycle. The mean penetration depth on the femoral heads was 57 μm under the standard cup inclination angle condition and 74 μm under the steep cup inclination angle condition (Figure 4.15 and Figure 4.16). There was no statistically significant difference (p= 0.2) between the two cup inclination angle conditions. The mean penetration depth on the acetabular cups was 228 μm under the standard cup inclination angle condition and 286 μm under the steep cup inclination angle condition (Figure 4.17 and Figure 4.18). There was no statistically significant difference (p= 0.4) between the two cup inclination angle conditions.
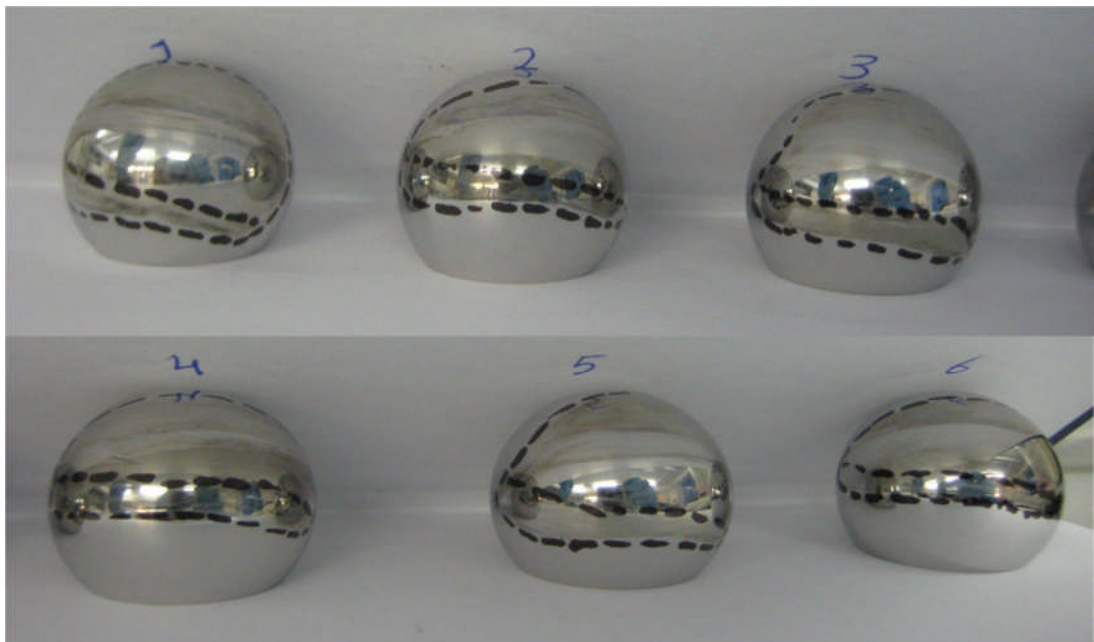
Figure 4.13: Images of the six femoral heads after six million cycles of testing. Ink marking show two distinct wear areas, a rough wear stripe at the bottom and a smoother wear area on the top.

Figure 4.14: Images of the 6 acetabular cups after 6 million cycles of testing. Ink marking show two distinct wear areas; a smooth wear area at the bottom with a rougher wear area adjacent to the rim of the acetabular cup.

Maximum depth 54.8 µm Area of the hole 0.237 mm2

Maximum depth 79.9 µm Area of the hole 0.313 mm2

Maximum depth 76.0 µm Area of the hole 0.289 mm2
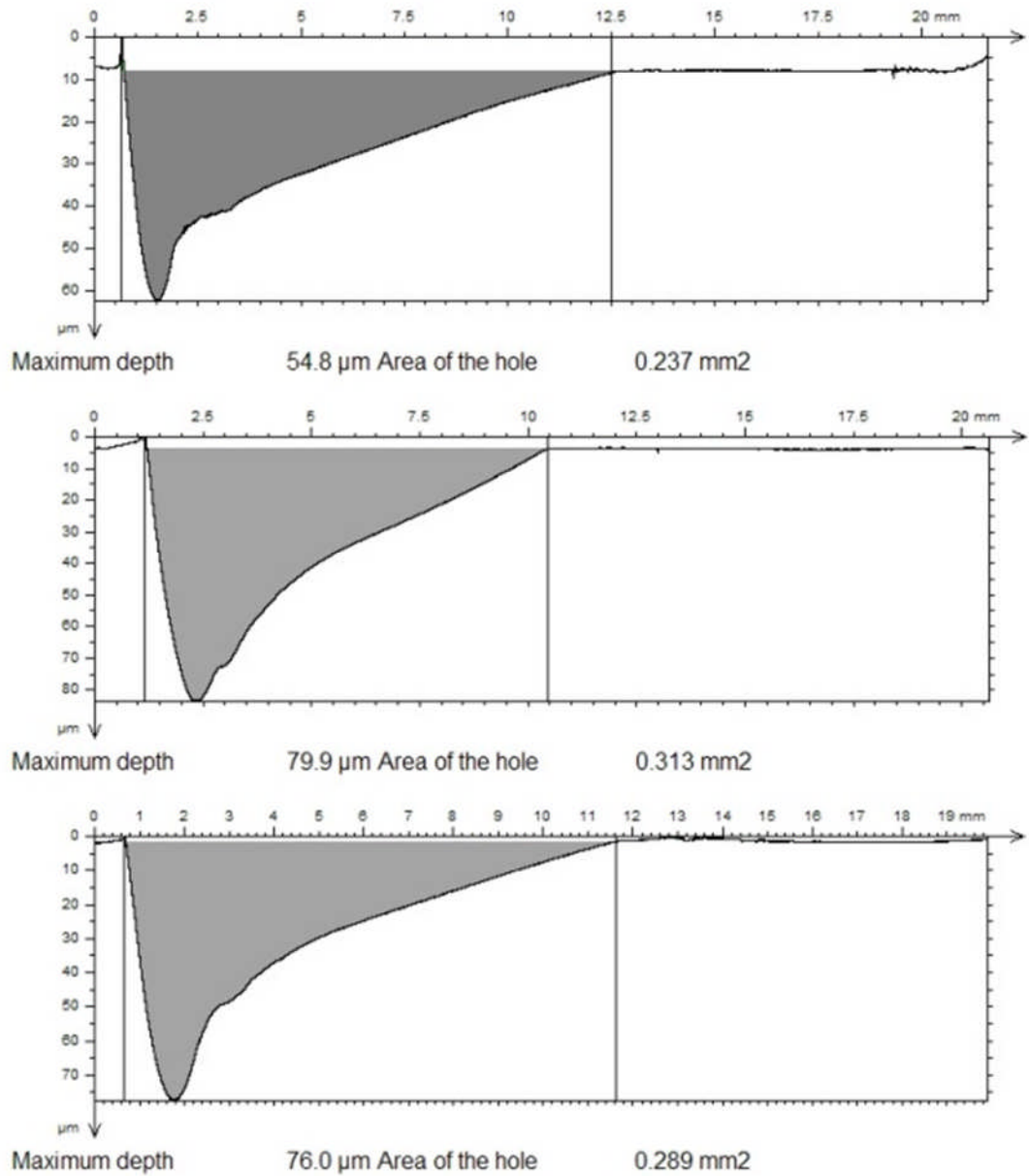
Figure 4.15: Two dimensional form Talysurf traces across the wear stripe on the femoral heads under 45° cup inclination angle condition. A Least square arc was removed from the curve fit so the horizontal part of the curves represent the unworn surfaces.

Maximum depth   65.6 µm Area of the hole   0.454 mm2

Maximum depth   86.1 µm Area of the hole   0.504 mm2

Maximum depth   71.7 µm Area of the hole   0.495 mm2
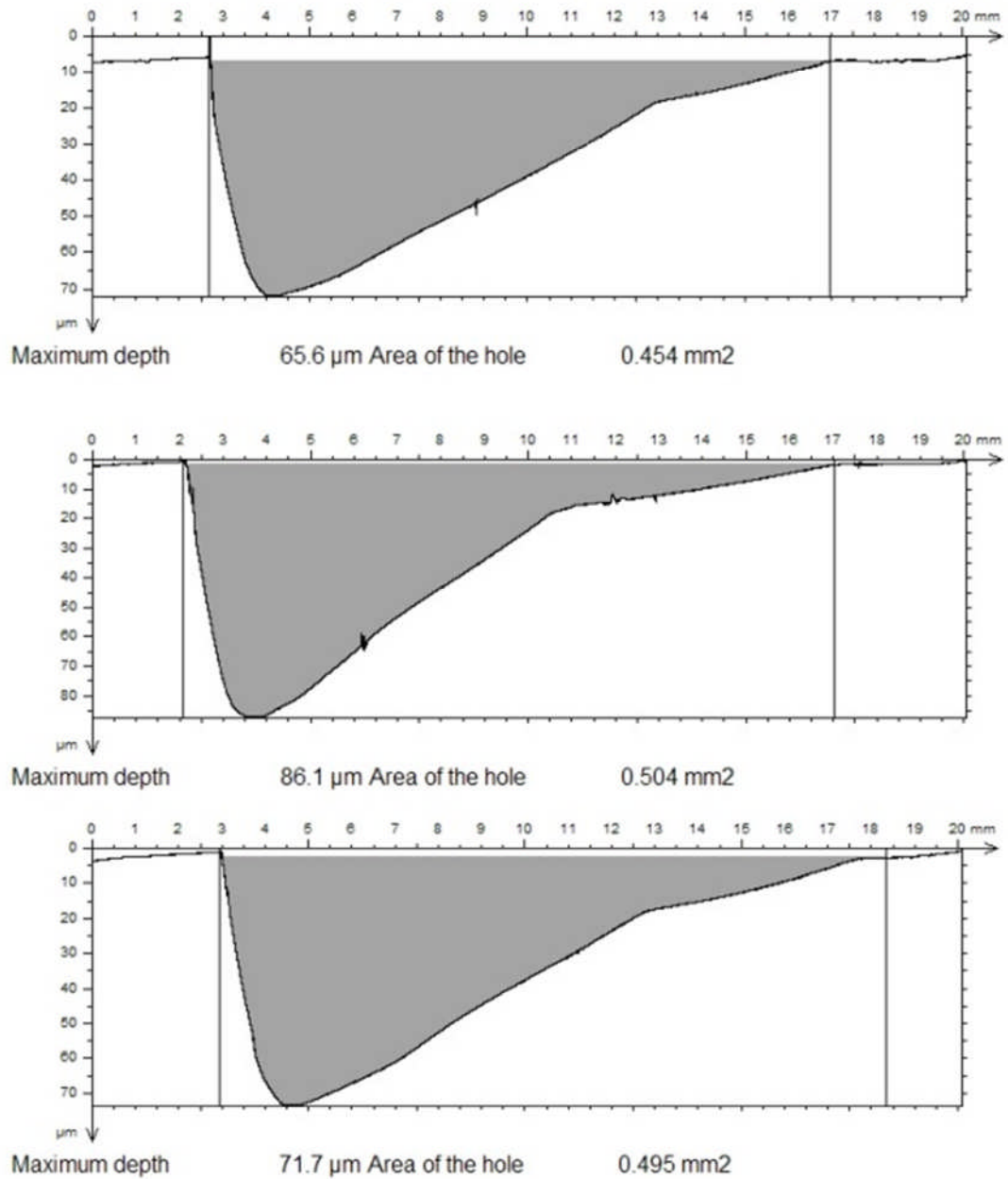
Figure 4.16: Two dimensional form Talysurf traces across the wear stripe on the femoral heads under 65° cup inclination angle condition. A Least square arc was removed from the curve fit so the horizontal part of the curves represent the unworn surfaces.

Maximum depth   156 µm Area of the hole   0.170 mm2

Maximum depth   241 µm Area of the hole   0.277 mm2

Maximum depth   294 µm Area of the hole   0.414 mm2
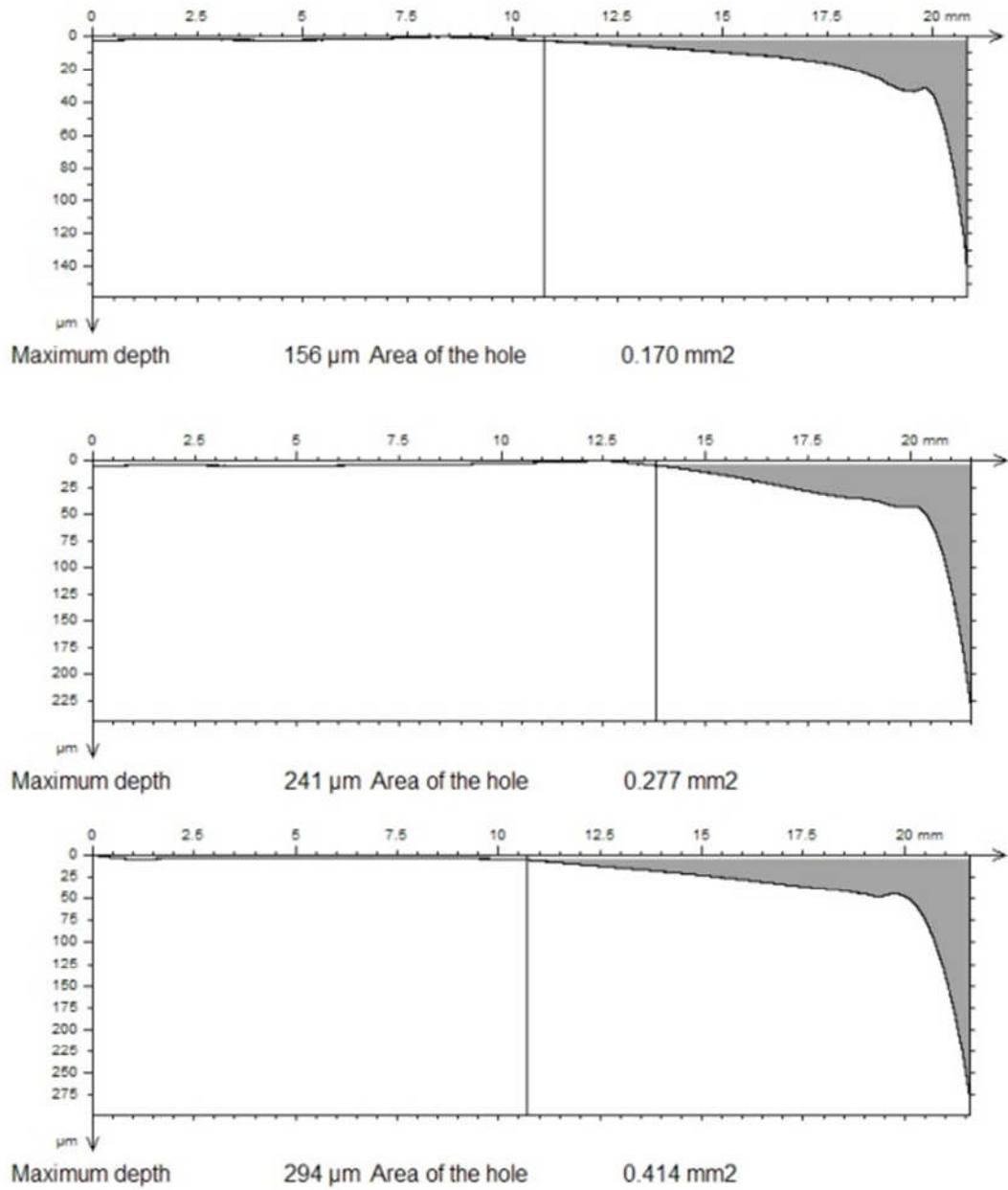
Figure 4.17: Two dimensional form Talysurf traces across the wear area near the rim of the acetabular cups under 45° cup inclination angle condition. A Least square arc was removed from the curve fit so the horizontal part of the curves represent the unworn surfaces.

Maximum depth   189 µm Area of the hole   0.443 mm2

Maximum depth   273 µm Area of the hole   0.676 mm2

Maximum depth   241 µm Area of the hole   0.588 mm2
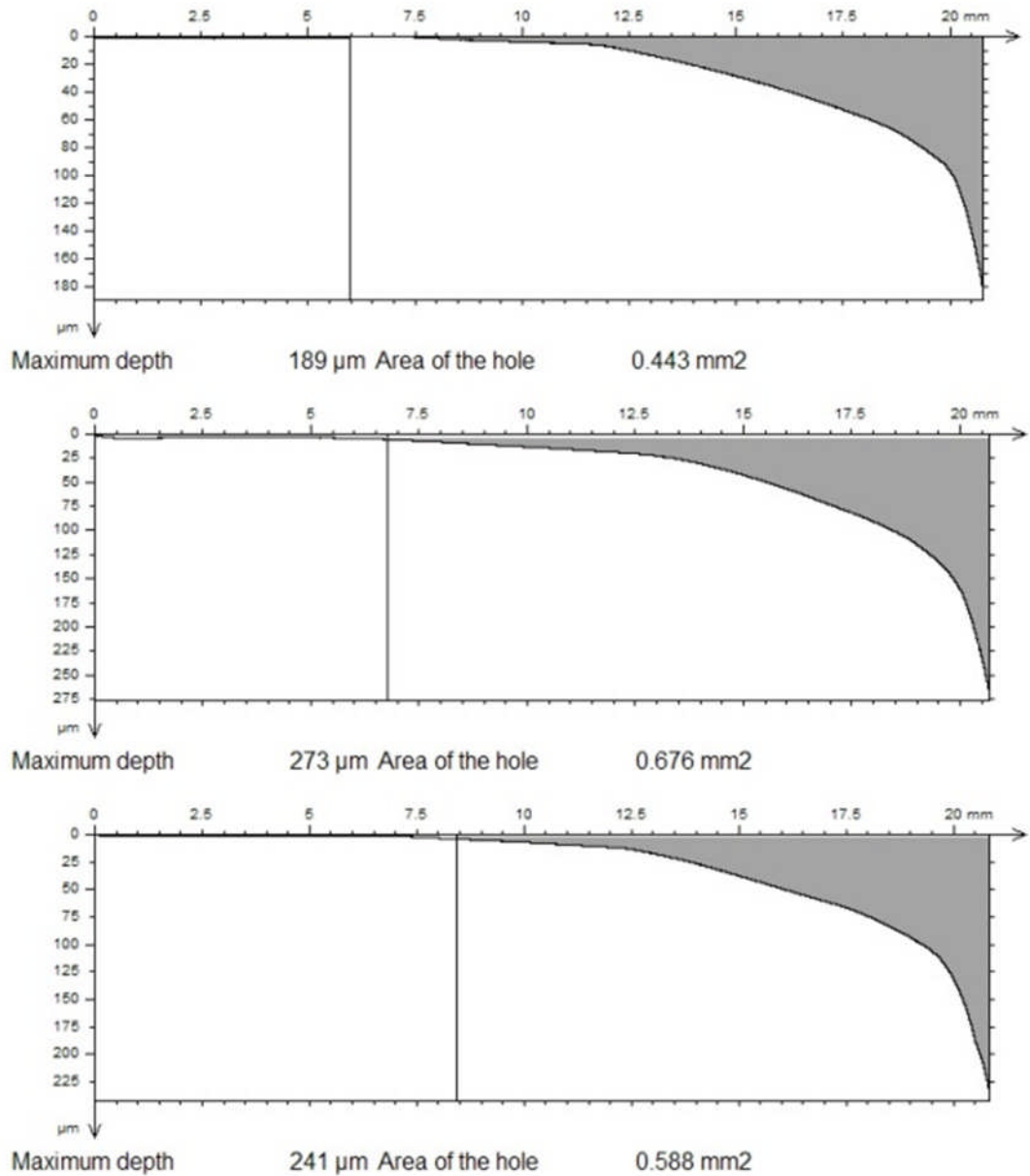
Figure 4.18: Two dimensional form Talysurf traces across the wear area near the rim of the acetabular cups under 65° cup inclination angle condition. A Least square arc was removed from the curve fit so the horizontal part of the curves represent the unworn surfaces.

4.3.5 Roughness and wear features

Under standard conditions, the surface roughness changed from a mean of 36.8 nm (29.0-49.5 nm) to a mean of 23.6 nm (15.5-32.7 nm) for the heads and from a mean of 14.2 nm (10.9-20.7 nm) to a mean of 18.8 nm (10.9-33.0 nm) for the cups. High magnification image showed evidence of micro-pitting over the wear area of the cup (Figure 4.19).
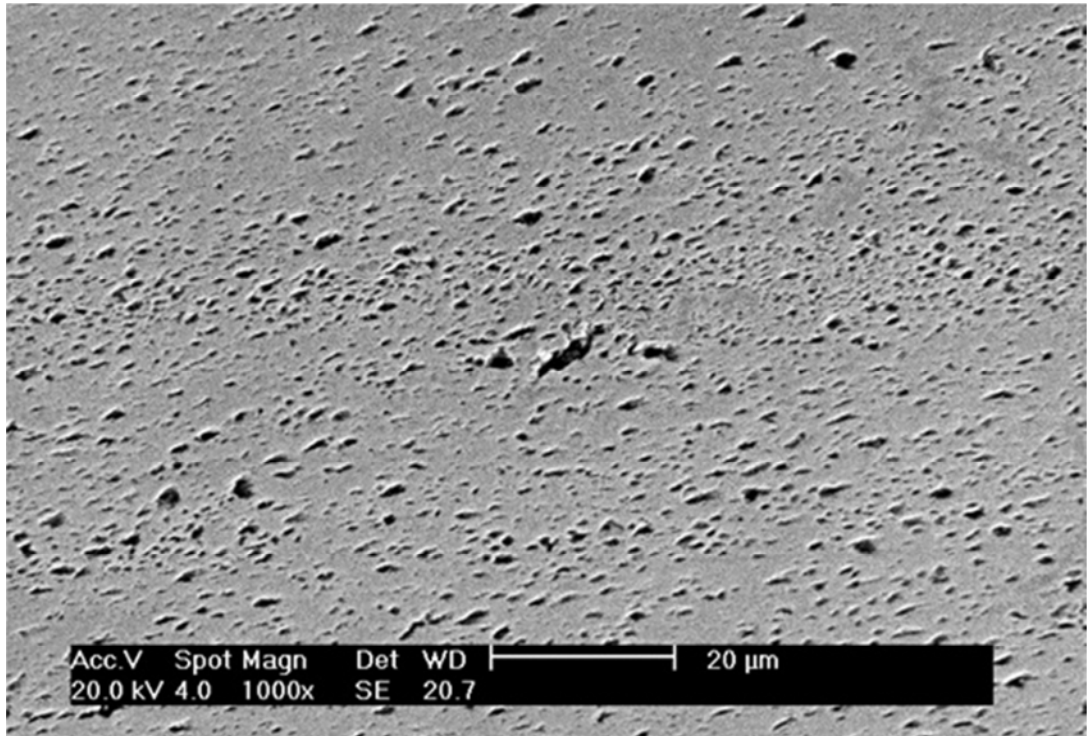
Figure 4.19: Example of surface texture over the wear area of the acetabular cup under standard conditions after 3 million cycles of testing (x 1000 magnification).

Under steep cup inclination angle condition, there was evidence of head-cup rim contact. Over the wear area, away from the rim contact area, the mean roughness value decreased to 18.7 nm (11.1-33.1 nm) for the heads and to 13.8nm (10.1-18.1 nm) for the cups. However, near the rim of the cup and where the head contacted the rim of the cup, the mean roughness value increased to 95.0 nm (54.8-142.3 nm) for the heads and to 39.0 nm (34.3-48.2 nm) for the cups. High magnification images over the wear area away from the rim of the cup showed similar wear patterns as that under standard conditions. However, high magnification images near the rim of the cup

showed scratches along the rim with elongated pits of different sizes (Figure 4.20).
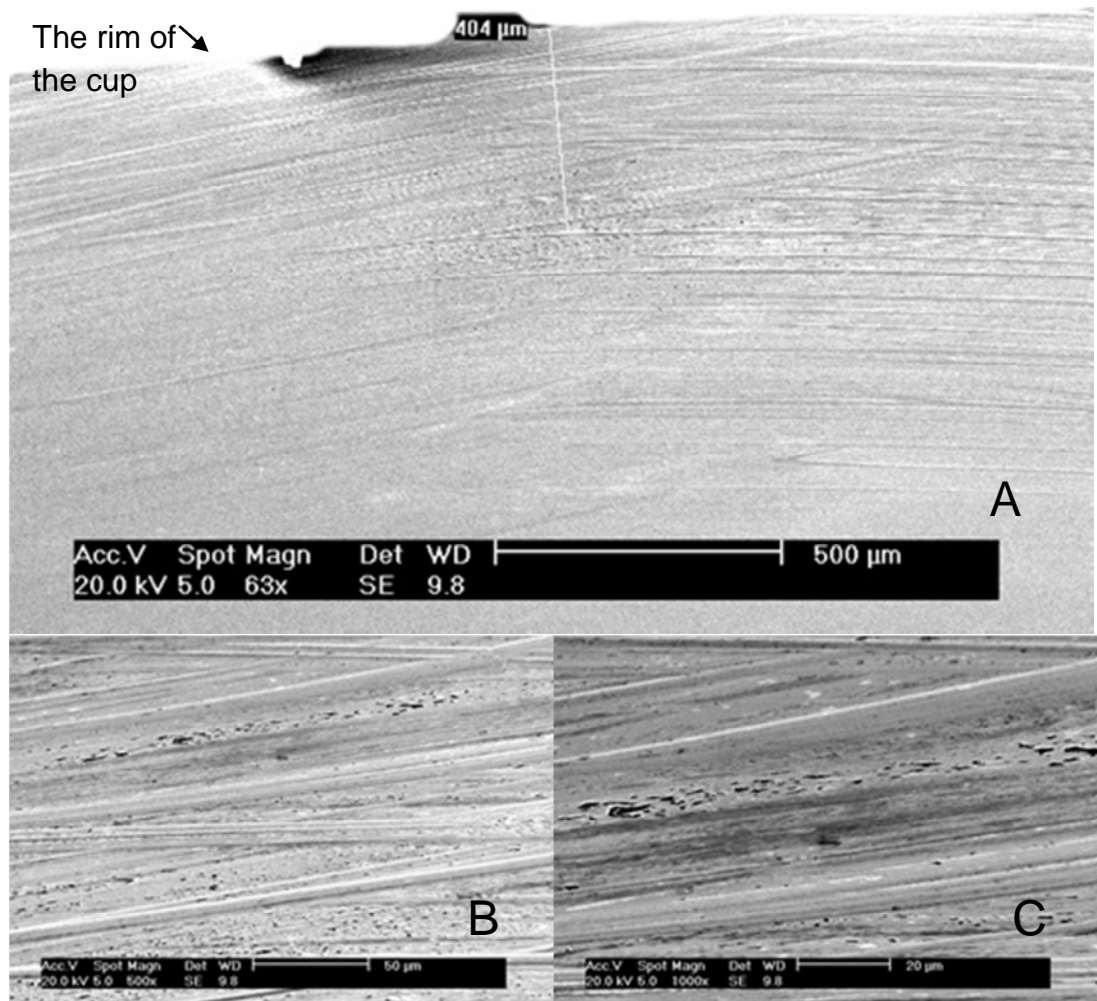
Figure 4.20: Example of surface damaged near the rim of the cup under steep cup inclination angle condition. (A) is a low magnification image (x 63) showing the scratches near the rim of the cup. (B&C) are high magnification images showing a detailed texture of the surface.

Under microseparation conditions, over the wear area, away from the rim contact area, the mean roughness value changed to 23.6 nm (17.8-32.2 nm) for the heads and to 18.4 nm (15.7-20.7 nm) for the cups. However, near the rim of the cup and where the head contacted the rim of the cup, the mean roughness value increased to 94.8 nm (80.6-119.9 nm) for the heads and to 114.5 nm (72.3-151.7 nm) for the cups. High magnification images showed

scratches in several directions and several wear patterns such as abrasive wear, micropitting and polishing of the surface (Figure 4.21).
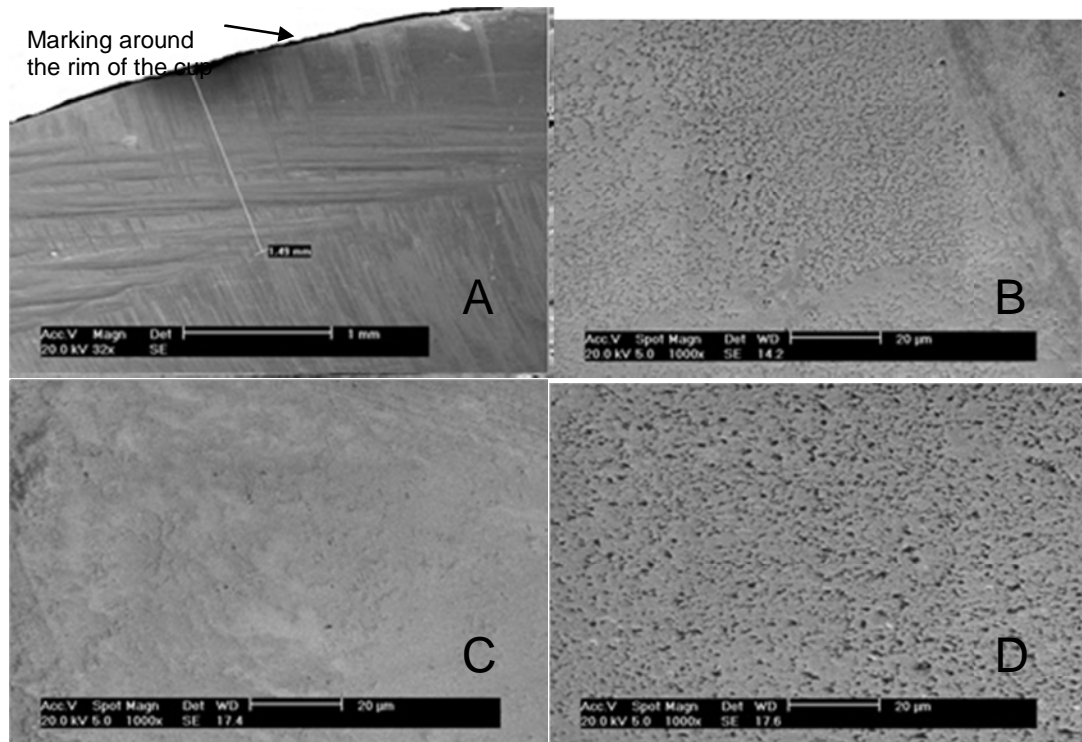
Figure 4.21: Examples of surface damaged near the rim of the cup under microseparation conditions. (A) is a low magnification image (x 32) showing the scratches near the rim of the cup; scratches are in different directions. (B, C & D) are high magnification images showing a detailed texture of the surface damage. A range of wear patterns are observed on the surface under microseparation conditions.

For the steep cup inclination angle under microseparation conditions, over the wear area, away from the rim contact area, the mean roughness value changed to 31.4 nm (24.9-36.9 nm) for the heads and to 14.6 nm (11.4-20.4 nm) for the cups. However, near the rim of the cup and where the head contacted the rim of the cup, the mean roughness value increased to 50.1 nm (49.4-50.6 nm) for the heads and to 40.2 nm (23.4-72.1 nm) for the cups.
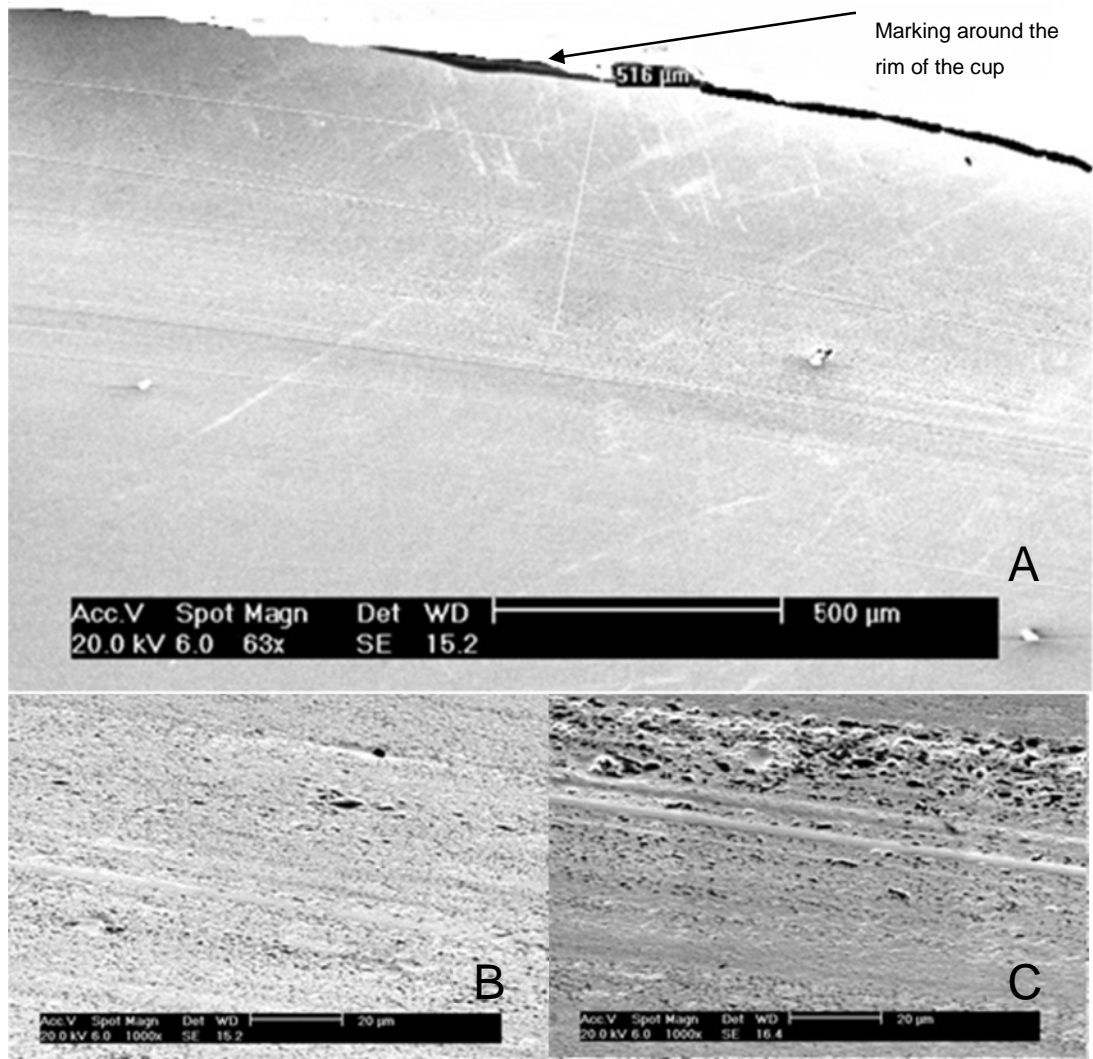
Figure 4.22: Examples of surface damaged near the rim of the cup under microseparation conditions with steeply-inclined cup. (A) is a low magnification image (x 63) showing the damage near the rim of the cup and (B and C) are high magnification image over different areas showing elongated pits. A range of wear patterns are observed on the surface under microseparation conditions.

4.4 Discussion

High wear rates (Morlock et al., 2008, De Haan et al., 2008, Langton et al., 2011) and ion levels (De Haan et al., 2008) in patients with metal-on-metal bearings have been associated with steep acetabular cup inclination angles. However, *in vitro* studies with steeply inclined acetabular cups (Angadji et al., 2009, Williams et al., 2008) have not replicated the level of increase in wear rates that have been observed in retrievals. This indicates that other

conditions or factors are influencing or causing the high levels of wear *in vivo*. *In vitro* studies with CoC bearings where microseparation conditions were introduced to the gait cycle leading to edge loading have replicated *in vivo* wear rates, wear mechanisms and bimodal nano- and micron-sized wear particles (Nevelos et al., 2001c, Nevelos et al., 2000, Tipper et al., 2002, Hatton et al., 2002). Fisher (Fisher, 2011) explained the adverse conditions that may produce edge loading and increased wear. These could occur due to either rotational or translational mal-positioning of the bearing couple. Rotational mal-positioning of the acetabular cup resulting in excessive inclination or version angles causes the femoral head to contact the acetabular cup rim. Translational mal-positioning where the centres of the head and the cup are displaced relative to one another (microseparation) can occur due to several reasons such as head offset deficiency, medialised cup, stem subsidence, impingement and laxity of the soft tissues. Microseparation conditions do not necessarily mean a physical separation of the surfaces of the head and the acetabular cup but a translational displacement between the centres of the head and the cup higher than the radial clearance (<0.5mm). This study aimed to investigate the influence of head size under adverse rotational mal-positioning (increased cup inclination angle) and translational mal-positioning (microseparation conditions) independently and in combination and to assess their relative contributions to increasing the wear of the implants under these different conditions.

Under standard gait conditions when the cup inclination angle was at 45°, the wear rate was split into two phases, a bedding in phase and a steady state phase (Dowson, 2001). In this study, the steady state wear rate for the 28mm bearings was 0.44 mm^3/ million cycles, which is consistent with previous studies for 28mm bearings, tested with a 300N ISO standard swing phase load (Firkins et al., 2001a). Ion level analysis showed a similar pattern to the wear results, with the steady state phase reached between 1 and 2 million cycles. As the serum collected between 1 and 2 million cycles was pooled together, it was not possible to determine at what point between 1 and 2 million cycles the steady state phase was reached.

When the cup inclination angle was increased to 65°, the contact area between the head and the cup, for the 28mm bearings, decreased and the

head contacted the superior rim of the acetabular cup resulting in high contact stresses, reduction in lubrication and hence an increased wear rate and no evidence of a steady state phase after three million cycles. For the standard condition testing, when the 45° cups reached steady state wear between 1 and 2 million cycles, there was a 4.6-fold increase in the wear rate between 2 and 3 million cycles when the cup inclination angle was increased to 65°. This was consistent with previous studies that showed increased wear rate in MoM bearings with increased cup inclination angle (Angadji et al., 2009, Leslie et al., 2009, Williams et al., 2008). The relative increases in wear could have been influenced by the different prosthesis designs used, especially the acetabular cup rim profile, as well as cup inclination angle. Another study on 39mm MoM SR showed a 9-fold increase in the wear rate when the cup angle was increased from 45° to 60° (Leslie et al., 2009). The surface replacement cup used was larger in size and had a smaller inclusion angle and a different rim profile than the metal cup used in the current study, which again may have contributed to the higher wear rates under steeply inclined cup conditions.

A cup design with hemispherical included angle (180°) will have better tolerance to rotational mal-positioning however, this will restrict the range of motion and increase the incidence of impingement (Wang et al., 2011). Decreasing the acetabular coverage will increase the range of motion but will increase the chance of edge loading due to rotational mal-positioning. These results shows that increased wear due to rotational mal-positioning only occurs when edge loading occurs, which in turn is dependent on the combination of several factors such as steep cup inclination angles, excessive version or ante-version angles, and acetabular cup geometries and component size.

When microseparation conditions were introduced to the gait cycle, there were significant increases in wear rates and a stripe of wear was formed on the femoral head with a corresponding wear area at the superior rim of the acetabular cup. The wear rate throughout the three million cycles of testing under microseparation conditions was steady, showing no evidence of bedding in and steady state phases. The results showed no statistically significant differences in the wear rate between the two cup inclination angle

conditions under microseparation conditions indicating that edge loading due to microseparation conditions dominates the effect of head-rim contact due to steeply inclined acetabular cups.

The previous *in vitro* study which tested 39mm MoM SR under microseparation conditions (Leslie et al., 2009) showed comparable wear values to retrieved surface replacement bearings that have experienced edge loading conditions (Morlock et al., 2008). It is clear from the literature there is a wide range of wear rates observed *in vivo*, as well as cup position, inclination and version, soft tissue tension, impingement and microseparation may affect wear rates. But in addition, under adverse rim loading conditions, other design factors such as rim geometry and cup included angle may also impact on the increase in wear for different designs.

Serum cobalt ion concentrations measured in this study showed a strong correlation with the wear volumes measured gravimetrically. However, chromium ion concentrations showed a weaker correlation with wear volume especially at high wear volumes. Under microseparation and edge loading conditions, metal-on-metal bearings produce micrometer sized particles as well as nanometer sized particles (Leslie et al., 2009). These relatively large particles are rich in chromium oxide and are removed by centrifuging when preparing samples for ion level measurement (Catelas et al., 2006). Centrifuging was necessary to get rid of all the digested proteins from the serum as this could interfere with ICP-MS measurements. This could explain the lower than expected chromium ion level at high wear volumes which were obtained under edge loading conditions.

Surface analysis indicated two distinct wear areas under adverse simulator conditions. A wear area similar to that obtained under standard gait cycle conditions and another wear area where the head contacted the rim of the cup under edge loading conditions. Under steep cup inclination angle conditions, the contact between the head and the rim of the cup resulted in a stripe of wear featuring elongated micro-pits along the rim with scratches running alongside. Under the microseparation and edge loading conditions, however, the stripe of wear showed a large variation in the wear features

including abrasive wear, micro-pitting, polishing and multidirectional scratches.

Ceramic-on-ceramic bearings, unlike metal-on-metal bearings, showed no increase in wear due to head-rim contact under increased cup inclination angle (Nevelos et al., 2001a, Al-Hajjar et al., 2010). However, microseparation and edge loading conditions have resulted in stripe wear and increased wear in ceramic-on-ceramic bearings (Nevelos et al., 2001a, Stewart et al., 2001, Al-Hajjar et al., 2010, Nevelos et al., 2001b, Stewart et al., 2003b, Stewart et al., 2003a, Manaka et al., 2004). For 28mm BIOLOX$^{®}$ Delta ceramic-on-ceramic bearings, the wear rate under microseparation conditions was 0.12mm^3/ million cycles; approximately 40 times lower than the wear rate of metal-on-metal bearings under the same conditions using the same simulator (Al-Hajjar et al., 2010). The mean penetration over the wear stripe on the ceramic femoral heads over three million cycles of testing was below 8µm (Al-Hajjar et al., 2010), compared to a mean of approximately 65µm for the same sized metal-on-metal bearings tested in this study.

The results of this study suggest that high wear rate and variations in the wear mechanisms are influenced by edge loading due to microseparation. *In vivo*, steep cup inclination angles and other factors such as impingement stem subsidence, tissue laxity around the prosthesis and head position could facilitate microseparation and edge loading leading to various complications and implant failure. This study highlights the importance of prosthesis design and the accurate positioning of the implant in its optimum position during surgery.

CHAPTER 5. WEAR OF 36MM BIOLOX® DELTA CERAMIC-ON-CERAMIC BEARING IN TOTAL HIP REPLACEMENTS UNDER EDGE LOADING CONDITIONS

5.1 Introduction

The latest development of ceramic materials has taken advantage of the good properties of alumina and zirconia materials to create an alumina matrix composite (BIOLOX delta) (Burger and Richter, 2000). This new innovation has extended the design flexibility of the ceramic-on-ceramic bearings by allowing the production of larger size femoral heads. Size 28mm bearing is designed to allow a range of motion of at least 120° which is required to comfortably perform standard daily activities. However, with a small bearing, there is high probability of impingement, subluxation or luxation of the joint. Increasing the head size increases the range of motion and reduces the chance of failure and meets the demand of active patients. A clinical study has shown a significant reduction in dislocation when using 36mm bearings compared to 28mm bearings (Zagra and Giacometti Ceroni, 2007).

Chapter 3 has investigated the influence of edge loading due to increased cup inclination angle and microseparation condition on the wear of size 28mm zirconia-platlet toughned alumina (ZPTA, BIOLOX® Delta) (Al-Hajjar et al., 2010). The results showed no increase in wear under edge loading due to increased cup inclination angle, however, increased wear rate and stripe wear were achieved under edge loading due to microseparation conditions. The aim of this study was to investigate the influence of increasing the femoral head size on the wear of BIOLOX Delta ceramic-on-ceramic bearings under standard and edge loading conditions using the same simulator and methodology as the 28mm study. Edge loading was achieved by rotational mal-positioning (steep cup inclination angle), translational mal-positioning (microseparation), and the combination of both conditions.

5.2 Materials and Methods

Six 36mm ceramic-on-ceramic bearings (BIOLOX® *Delta*, CeramTec, Germany) were tested under different adverse *in vitro* conditions using the Leeds II Physiological Anatomical Hip Joint Simulator. The six bearing couples had diametrical clearances in the range of 76-85μm. Four *in vitro* conditions were investigated including standard gait condition, steep cup inclination angle (rotational mal-positioning), microseparation conditions (translational mal-positioning) and the combination of the latter two conditions. Two clinical cup inclination angles were considered, *in vivo* equivalence of 45° (n=3) and 65° (n=3). The first three million cycles ran under standard gait conditions and a subsequent three million cycles ran under microseparation conditions (Nevelos et al., 2000, Stewart et al., 2001). A standard gait cycle included a twin peak load (peak load of 3000N), extension/flexion (-15°/+30°) and internal/external rotation (±10°). Microseparation was achieved by applying a 0.4-0.5mm medial displacement to the cup relative to the head during the swing phase of the standard gait cycle resulting in edge loading at heel strike. The lubricant was 25% (v/v) new-born calf serum supplemented with 0.03% (v/v) sodium azide to retard bacterial growth. The lubricant was changed approximately every 330,000 cycles and replaced with fresh serum. The wear volume was ascertained through gravimetric analysis every million cycles using the Mettler AT201 (Mettler-Toledo Ltd, UK)) balance (0.01mg resolution).

Surface measurements of the components were undertaken at the beginning and the end of each gait protocol using two-dimensional contacting profilometer (Form Talysurf series, Taylor Hobson, UK). Further wear stripe analysis was undertaken when the microseparation conditions were introduced; three two-dimensional Talysurf measurements were taken on each head and cup across the wear scar 5mm apart. The mean maximum penetration depths of the wear stripe were determined.

A coordinate measuring machine (CMM, Legex 322, Mitutoyo, UK) was used to reconstruct three dimensional representations of the wear stripes on the

femoral heads. A single straight configuration 3mm diameter stylus was used to measure all six 36mm femoral heads. The heads were measured by taking 12,024 data points in the form of 36 traces rotated by 5 degrees from each other about the vertical axis. Each trace consisted of 167 points with a pitch of 0.2mm starting at the pole and finishing 3mm below the equator. SR3D software (TriboSol, UK) was used to visualise the size, shape and penetration depth of the wear areas.

Statistical analysis was performed using one-way ANOVA (significance taken at $p<0.05$) and 95% confidence limits were calculated.

5.3   Results

5.3.1   Wear

Under standard gait conditions, the wear rates of the 36mm CoC bearings were very low (<0.02 mm^3/million cycles, within the resolution of measurement method; ±0.05 mm^3/million cycles) under both cup inclination angles (Figure 5.1). Increasing the cup inclination angles from 45° to 65° had no effect on the wear rates under standard gait conditions (Figure 5.2). However, after introducing the microseparation conditions to the gait cycles, stripes of wear were formed on the femoral heads with a corresponding wear area at the rim of the acetabular cups (Figure 5.3), and the wear rates significantly ($p=0.02$) increased to 0.23 mm^3/million cycles for the 45° cup inclination angle condition and 0.20 mm^3/million cycles for the 65° cup inclination angle (Figure 5.4). There was no statistically significant difference ($p=0.5$) in the wear rates for both cup inclination angles under microseparation conditions (Figure 5.4). The percentage of wear was split equally on the cups and heads with an average of 51% of wear on the cups and 49% of wear on the heads (Figure 5.5).

There was a wide variation in the wear volumes of the six bearing surfaces when tested under microseparation conditions with no sign of bi-phasic (bedding in and steady state) wear mechanisms (Figure 5.6).

The mean wear rate under standard gait conditions was 0.05mm^3/ million cycles for the 28mm bearings and significantly lower ($p=0.003$) for the 36mm

bearings (Figure 5.7) which could be due to improved lubrication regime. Under microseparation conditions, the wear rate of size 36mm bearings was significantly higher (p=0.004) than that for size 28mm bearings. This was thought to be due to the larger contact area for the larger bearings and deprived lubrication under edge loading conditions.
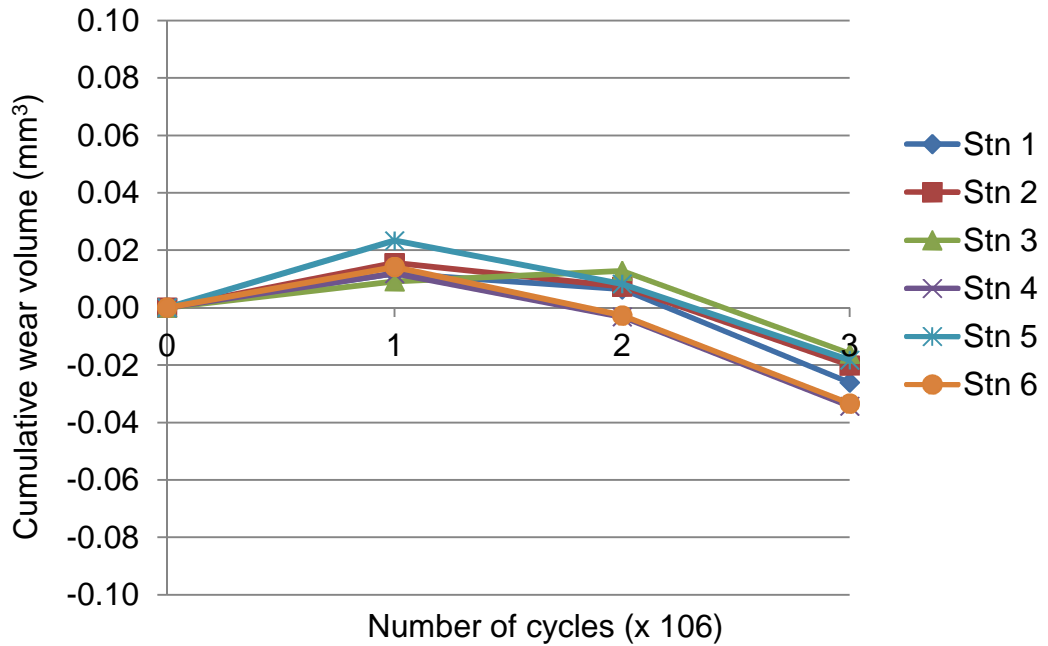
Figure 5.1: Cumulative wear volume of 36mm ceramic-on-ceramic bearings (BIOLOX® delta) under standard simulator conditions. The wear volume measured is within the resolution of the measurement technique (0.05mm³).
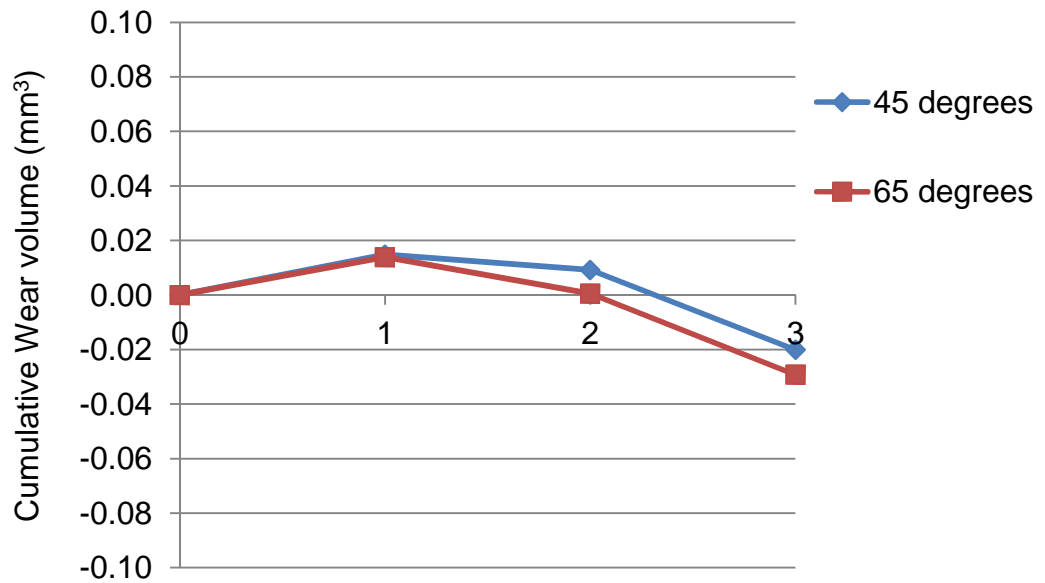
Figure 5.2: Mean Cumulative wear volume of 36mm ceramic-on-ceramic bearings (BIOLOX® delta) under both cup inclination angle conditions with standard simulator gait conditions. The wear volume measured is within the resolution of the measurement technique.
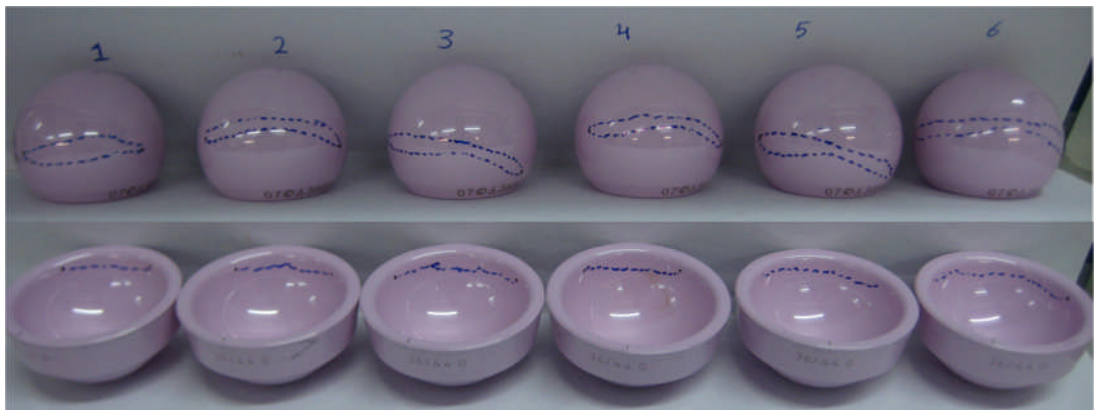
Figure 5.3: Stripe-like wear areas formed on all the femoral heads after introducing microseparation to the gait cycle, with a corresponding wear area near the rim of the acetabular cup.
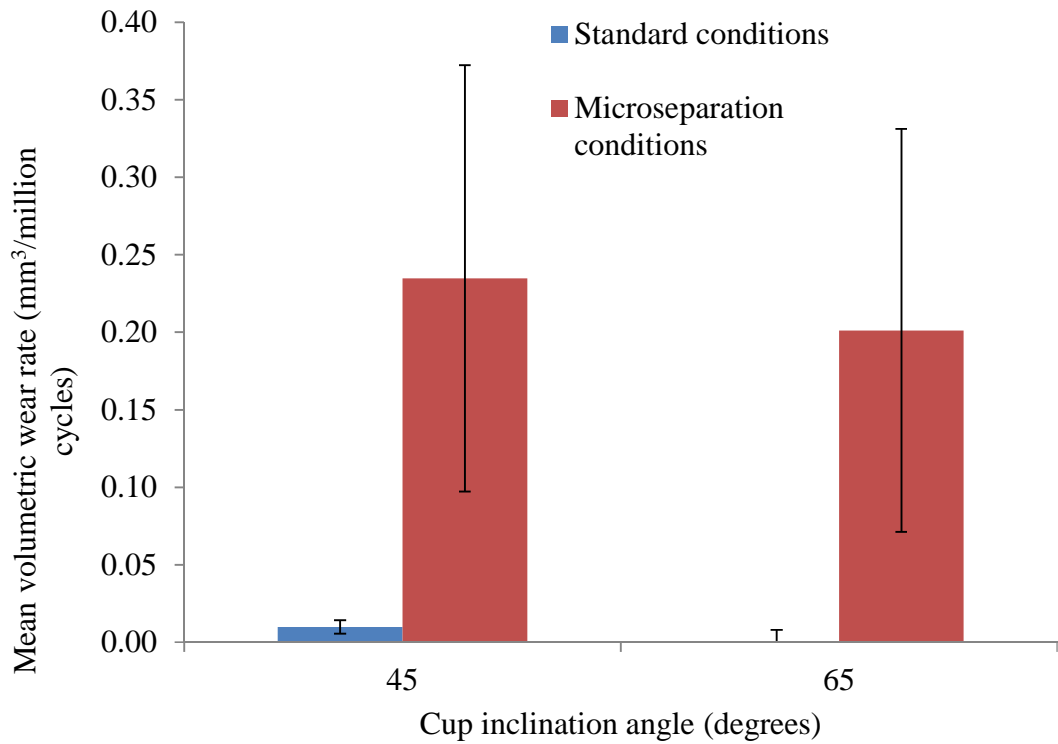
Figure 5.4: Mean volumetric wear rates for the 36mm ceramic-on-ceramic BIOLOX® Delta bearings for the different cup inclination angles under standard (2 million cycles) and microseparation conditions (3 million cycles). Error bars represent 95% confidence limit.
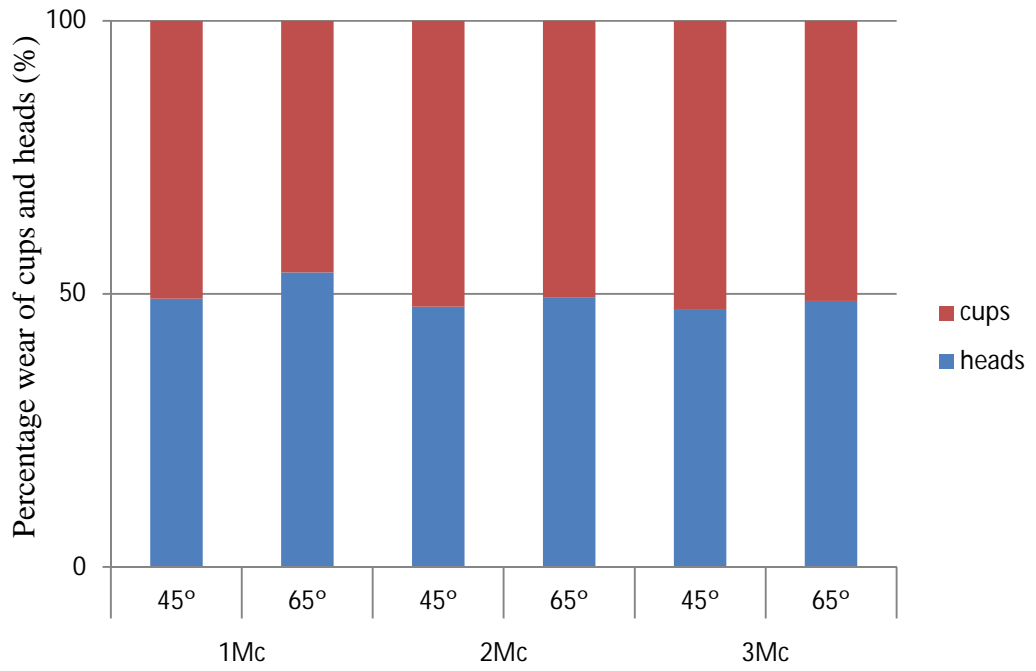
Figure 5.5: Percentage of wear on head and cups at every measurement points for both cup inclination angles under microseparation conditions. Mc=million cycles.
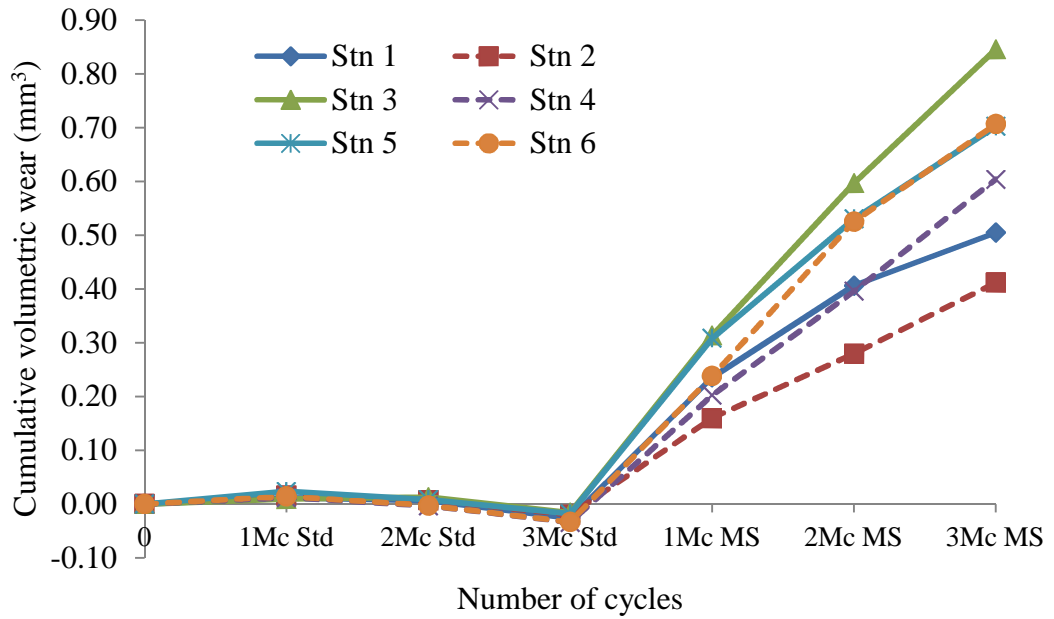
Figure 5.6: Cumulative wear volume under standard and microseparation conditions for individual stations. Odd numbered stations included components with 45° cup inclination angles (solid lines) and even numbered stations included components with 65° cup inclination angles. Mc= million cycles, Std= standard, MS= microseparation.
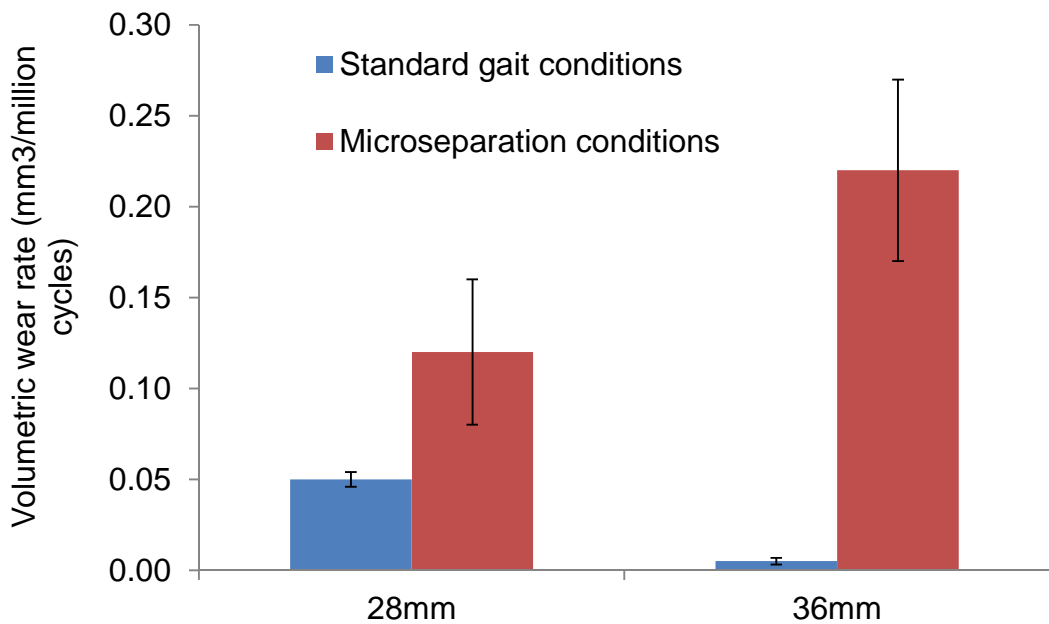
Figure 5.7: Volumetric wear rates of the 28mm (n=6) and 36mm (n=6) under standard and microseparation conditions. Error bars represent 95% confidence limits.

5.3.2 Surface Roughness Analysis

The surface roughness did not change after three million cycles of test under standard gait conditions however, under microseparation conditions, the surface roughness over the wear stripe had significantly (p=0.001) increased from a mean below 0.010µm Ra to 0.016µm Ra for both cup inclination angle conditions.

Table 5.1: Surface Roughness parameters over the heads and cups pre-test and over the wear stripe after 3 million cycles under microseparation conditions.

			Roughness parameters			
			Ra (µm)	Rp (µm)	Rv (µm)	Rsk
Pre-test	45⁰	Heads	0.008	0.048	0.039	-0.605
		Cups	0.007	0.023	0.025	-0.092
	65⁰	Heads	0.008	0.030	0.035	-0.393
		Cups	0.007	0.024	0.033	0.009
Over wear stripe at 3Mc MS	45⁰	Heads	0.015	0.035	0.074	-1.376
		Cups	0.017	0.040	0.099	-1.968
	65⁰	Heads	0.016	0.037	0.074	-1.237
		Cups	0.015	0.037	0.087	-1.899

5.3.3 Wear stripe analysis

Under edge loading conditions the mean penetration depth measured by the two dimensional form Talysurf, over the wear stripe of the femoral head was 7.0µm for 45° cup inclination angle conditions and 7.2µm for 65° cup inclination angle condition; with no statistically significant difference between the two cup inclination angle conditions (p=0.9).

The coordinate measuring machine measurements have shown the size and shape of the wear stripes produced under the edge loading conditions due to microseparation (Figure 5.8, Figure 5.9 and Table 5.2). The CMM provided more information about the depth of the wear scan than the 2 dimensional profilometry (Talysurf). The Talysurf penetration values is an average of

three 2D traces taken across the wear scar, however, the CMM measurement are able to pinpoint where the maximum penetration is and its value. All the femoral heads showed a stripe of wear with penetration depth greater than the sensitivity of the measurement techniques. There was no statistically significant ($p=0.5$) difference in the maximum penetration depth between the two cup inclination angle conditions, however the wear stripes on the heads articulating against the steeply inclined acetabular cups (Figure 5.9) were slightly closer to the pole of the heads than the ones articulating against the shallower acetabular cups (Figure 5.8). The average length of the stripes on the 28mm heads was 94.5% of that of the diameter (26.5mm) and that on the 36mm head was 94.6% of that of the diameter (34.1mm/36mm). the average width of the stripes on the 28mm and 36mm heads was 7.5% of the diameter (2.1mm/28mm and 2.7mm/36mm).

Table 5.2: The lengths, widths and maximum penetration of the wear stripes on the 36mm femoral heads after 3 million cycles of testing under microseparation conditions.

	Length		Width		Penetration depth (µm)	
	45°	65°	45°	65°	45°	65°
Head 1(45°) & 2(65°)	31.5	34.1	4.5	2.0	5.6	10.3
Head 3(45°) & 4(65°)	34.4	34.5	2.8	2.1	11.2	10.7
Head 5(45°) & 6(65°)	34.4	35.5	3.0	1.8	8.6	11.1
Mean	**33.4**	**34.7**	**3.4**	**2.0**	**8.4**	**10.7**
Significance (p value)	0.30		0.05		0.24	

Head 1

Head 3

Head 5
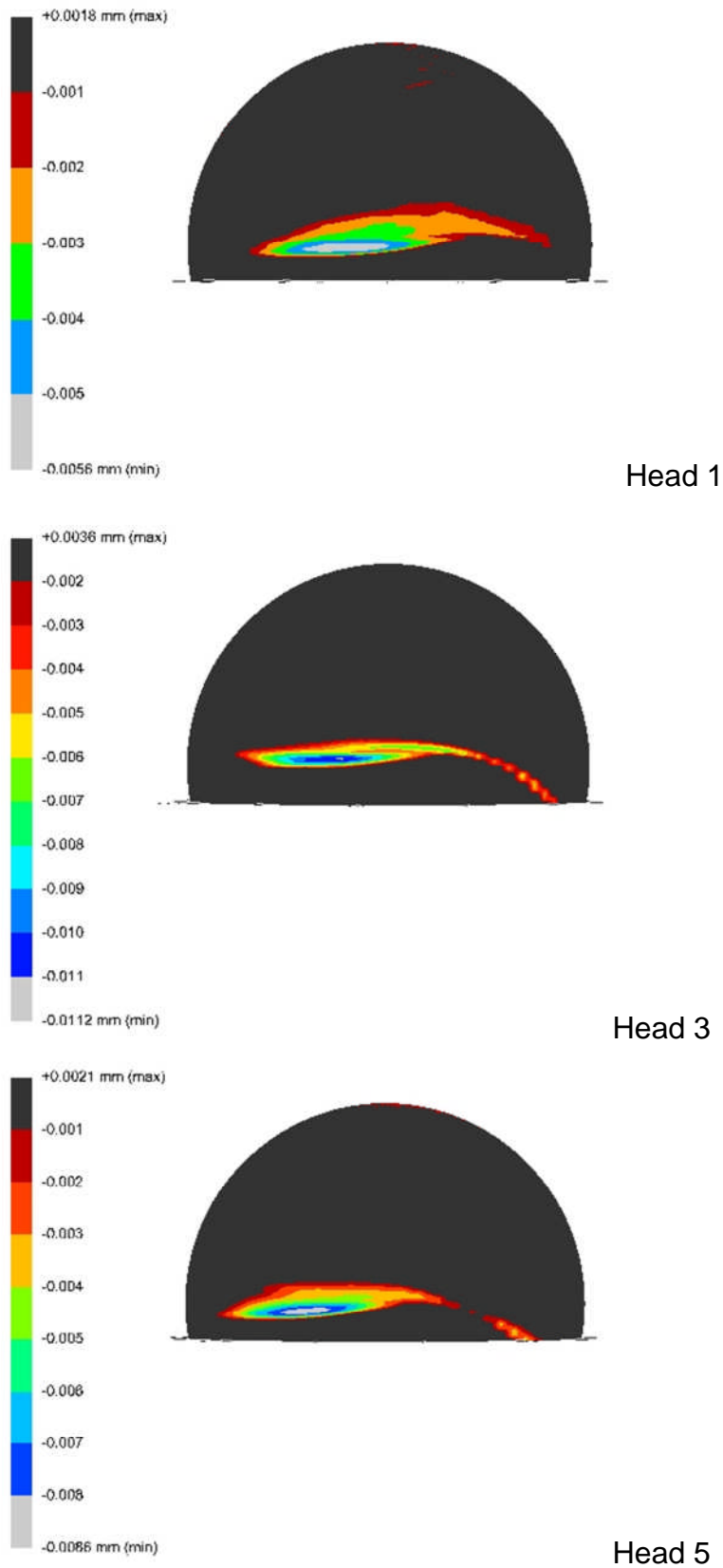
Figure 5.8: Three dimensional reconstruction of the wear stripe area over the three femoral heads articulated against acetabular cups inclined at 45⁰.

Head 2

Head 4

Head 6
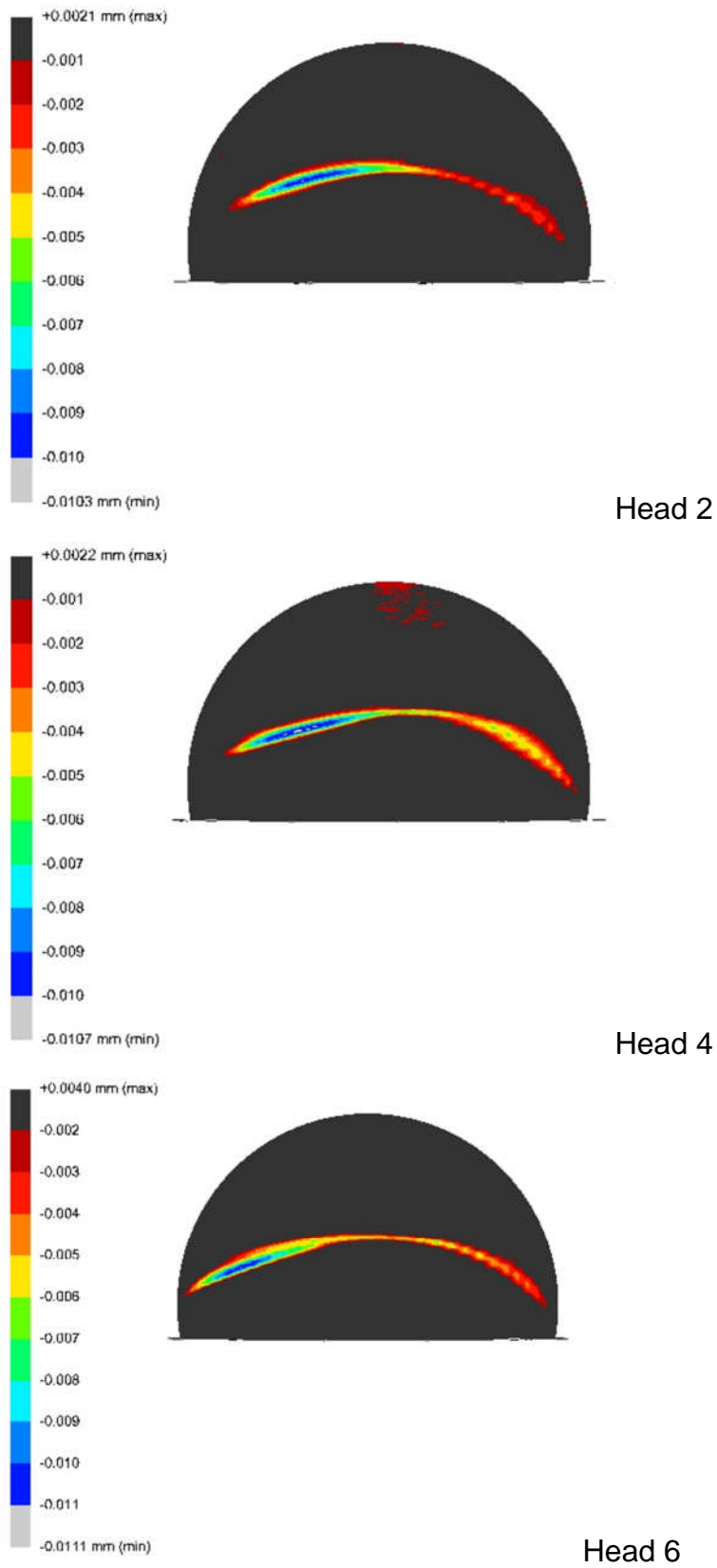
Figure 5.9: Three dimensional reconstruction of the wear stripe area over the three femoral heads articulated against acetabular cups inclined at 65⁰.

5.4 Discussion

Larger ceramic-on-ceramic bearings offer larger range of motion thus reducing the risk of impingement and subluxation providing more flexibility for the active patients (Zagra and Giacometti Ceroni, 2007). The wear of ceramic-on-ceramic bearings is very low under standard in vitro simulator testing conditions (Nevelos et al., 2001c, Nevelos et al., 2001a, Clarke et al., 2000). However, retrieval studies have shown stripe wear that was not replicated using these standard conditions (Nevelos et al., 1999). Stripe wear was replicated under edge loading conditions which resulted from translational mal-positioning, a condition termed "microseparation" (Nevelos et al., 2000). The aim of this study was to investigate the wear resistance of large diameter (36mm) BIOLOX$^®$ delta ceramic-on-ceramic bearings under the microseparation edge loading conditions and compare their performance to the 28mm BIOLOX$^®$ delta ceramic-on-ceramic bearings tested under the same set of adverse conditions (Chapter 3) (Al-Hajjar et al., 2010).

In this study cup inclination angle did not influence the wear of ceramic-on-ceramic bearings under either standard gait or microseparation conditions. Under standard gait conditions, the wear rate of size 36mm bearings was significantly lower than size 28mm bearings tested on the same simulator (Al-Hajjar et al., 2010). This was reversed when microseparation conditions were introduced to the gait cycle, where the wear rate of the larger size bearings was approximately twice as high (0.23mm^3/million cycles for the 36mm bearing compared to 0.12mm^3/million cycles for the 28mm bearing). This was thought to be due to the larger contact area for the larger bearings and deprived lubrication under edge loading conditions.

The wear stripes formed on the 36mm heads were similar in shape, orientation and depth to that formed on the 28mm heads. The wear stripes on the 28mm and 36mm heads had mean maximum penetration depths of 9μm and 10μm respectively (p=0.6) measured using the CMM. The lengths of the wear stripes were proportional to femoral head size covering similar percentage areas. Hence, the higher wear rate of the larger size bearing was due to the larger wear area on the larger bearing.

The wear rate of BIOLOX® *Delta* bearings under microseparation conditions was much lower (<0.25mm³/million cycles) compared to the third generation ceramic-on-ceramic bearings (Stewart et al., 2001) (1.84mm³/million cycles) and other bearings materials such as metal-on-metal bearings (Williams et al., 2004b, Williams et al., 2008, Leslie et al., 2009) (2-9mm³/million cycles). Also the mean penetration of the wear stripe was lower for the BIOLOX® delta ceramic bearings tested in this study (7µm at 3 million cycles) compared to the alumina-on-alumina bearing tested under the same in vitro conditions (~90µm at 5 million cycles) (Stewart et al., 2001). A metal on metal bearing showed linear penetration of approximately 41µm on the femoral head at 2 million cycles when tested under the same conditions (Leslie et al., 2009).

The improved wear properties of the fourth generation ceramic materials under adverse conditions, even with a larger head size, highlight the resistance of the material to the harsher conditions which, younger and more active patients may exert on a hip prosthesis. It also showed that this material, where wear is concerned, is more forgiving to surgical mal-positioning than metal-on-metal bearings. BIOLOX® delta ceramic-on-ceramic bearings showed no increase in wear under rotational mal positioning and improved wear rates under translational mal positioning when compared to earlier generation ceramics (Al-Hajjar et al., 2010, Stewart et al., 2001). Whereas metal-on-metal bearings showed significant increase in wear rates under edge loading conditions due to both rotational (steep cup inclination angles) and translational (microseparation) mal positioning (Angadji et al., 2007, Leslie et al., 2009, Williams et al., 2004a).

Although BIOLOX® delta ceramic-on-ceramic bearings have shown improved wear resistance, with both bearing sizes under adverse conditions, optimum component positioning cannot be over-emphasised. Current clinical reports related to ceramic-on-ceramic fracture are mainly related to alumina ceramics, and further clinical data is needed to determine the relative fracture risk of this improved material, however early results are encouraging (Hamilton et al., 2010).

5.5 Conclusion

This study has shown that increasing the femoral head size of ceramic-on-ceramic bearings resulted in increased wear rates only under microseparation conditions from 0.12 mm^3/million cycles for the 28mm bearings to 0.22 mm^3/million cycles for the 36mm bearings. BIOLOX$^®$ delta showed superior wear performance when compared to earlier generations ceramic materials and current metal-on-metal bearing and this was only distinguishable when advance adverse microseparation conditions was used as a testing methodology.

CHAPTER 6. THE EFFECT OF INCREASING HEAD SIZE ON THE WEAR OF METAL-ON-METAL HIP REPLACEMENT BEARINGS UNDER ROTATIONAL AND TRANSLATIONAL MAL-POSITIONING

6.1 Introduction

Larger head size in metal-on-metal bearings have the benefits of increasing the range of motion of the prosthesis. This benefits younger and more active patients and increase the options of activities they can perform, whilst reducing the risk of impingement. Increasing the femoral head size from 28mm to 36mm would increase the range of motion from approximately 123° to 136°. These values were calculated and assumed perfect component positioning and did not take into account patients factor such as joint anatomy and soft tissue around the joints.

Mckellop *et al.* (1996) reported a 50% reduction in wear rate for larger bearing surfaces (42mm compared against 35mm), however the clearance was a variable in this study which might have affected the results. McBryde *et al.* (2009) have shown that for every millimetre increase in femoral head size there was 0.89 times reduction in risk of revision concluding that the reason for increased revision of surface replacements was due to size and not gender. In addition, more recent findings by the National Joint Registry for England and Wales (NJR, 2011 annual report) showed higher failure rates with large diameter metal on metal bearings in total hip replacement compared to smaller size metal-on-metal bearings (≤36mm).

The wear rates of MoM bearing surfaces tend to decrease with increased head diameter (Smith et al., 2001, Hu et al., 2004, Dowson et al., 2004b, Affatato et al., 2006). It has been suggested that increasing the head diameter increases the entrainment velocity and therefore improves the lubrication regime in MoM bearing surfaces, which leads to lower wear rates (Liu et al., 2006). Smith *et al.* (2001) have compared sizes 16, 22.5 and 28

mm diameter bearings and found a great decrease in wear rate for the larger size bearings. Affatato *et al*. (2006) compared sizes 28, 36 and 54 mm diameter bearings and found a decrease in wear for size 36 mm compared to 28 mm, but no further decrease for size 54 mm. Bowsher *et al*. (2005) obtained similar results, with a reduction in wear for size 40 mm bearing compared to size 28 mm, but an increase in wear for size 56 mm bearings. However, the clearances for larger size bearing are bigger than those of smaller ones and this might have contributed to the increase in wear rate in larger bearings. Leslie *et al*. (2008) investigated the wear of size 55mm and size 39mm diameter MoM surface replacement bearings with similar radial clearances. The findings show a reduction in wear for the larger bearing surfaces.

So it is clear that under standard gait conditions, where the components are positioned perfectly, increasing the head size from 28mm to 36mm would result in reduction in wear. The aim of this study was to investigate the effect of increasing the head size while keeping the component design the same, on the wear of metal-on-metal bearings under rotational (steep inclination angle) and translational (microseparation conditions) mal-positioning, independently and in combination.

6.2   Materials and Methods

Six 36mm metal-on-metal bearings were tested on the Leeds II simulator for a total of 6 million cycles. The first three million cycles of simulation were under standard gait cycles conditions and the subsequent three million cycles were under microseparation condition. The method and the components set up were identical to that summarised in Chapter 4. Also, all the cobalt chrome alloy (CoCrMo) femoral heads and acetabular cups were custom manufactured by Corin Ltd (Cirencester, UK). The components were all high carbon alloys (>0.2% (w/w) Carbon) and all components were heat treated. All bearing couples had a diametrical clearance that ranged between 40 and 60μm consistent with the 28mm components studies in Chapter 4. The acetabular cups used had an outer diameter of 54mm, a coverage angle (inclusion angle) of 160°, and a rim radius of 0.5mm which

were identical to the dimension of the 28mm bearings. The thickness of the 36mm acetabular cups was smaller than that of the 28mm .
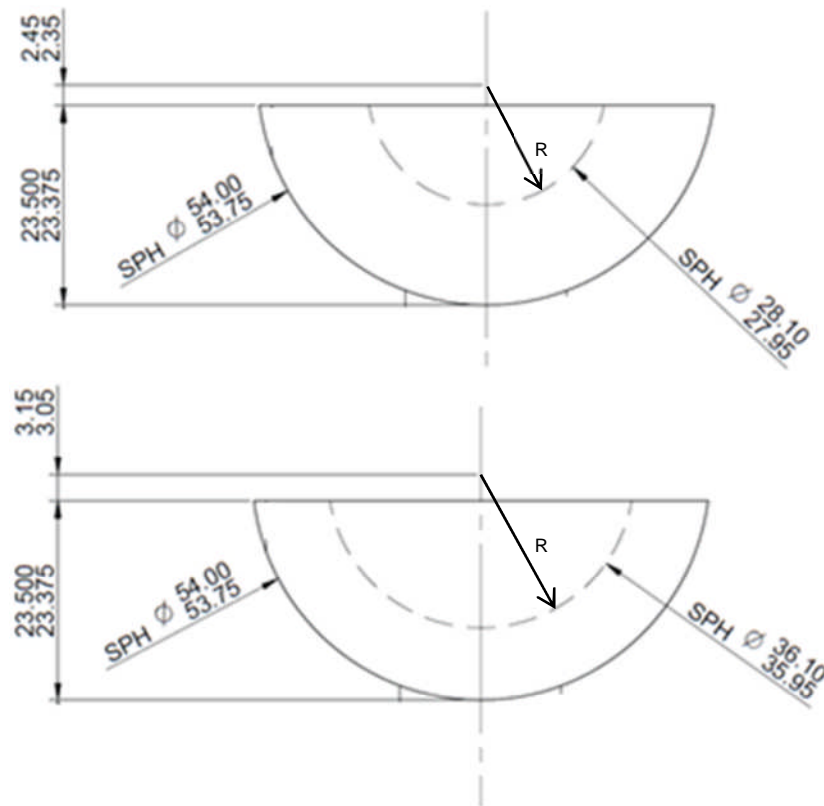
Figure 6.1: Engineering drawing showing the differences in the acetabular cup dimensions used for the 28mm MoM study (Chapter 4) and the current 36mm MoM study, R= inner radius.

Three acetabular cups were mounted to provide an inclination angle equivalent to 45° *in vivo* and three other cups were mounted to provide an inclination angle equivalent to 65° *in vivo*. A twin peak loading of 3kN peak load was applied and two independently controlled axes of motion, flexion/extension (-15° to +30°) and internal/external rotation (+/- 10°) were applied.

The first 3 million cycles out of a total of 6 million were performed under standard gait conditions. The 'severe' microseparation conditions, described in previous studies (Nevelos et al., 2000, Stewart et al., 2001), were introduced to all six stations for the subsequent 3 million cycles. Microseparation condition was achieved by applying a lateral movement of

approximately 0.5 mm to the acetabular cup relative to the head, which resulted in edge loading at heel strike.

The lubricant, 25% new born calf serum supplemented with 0.03% sodium azide, was changed every 330,000 cycles and wear measurements were under taken every one million cycles. The wear volume was ascertained through gravimetric analysis. The components were weighed using a Mettler AT201 balance (Leicester, United Kingdom) (0.01mg resolution).

The ion level measurements were done using an inductively coupled plasma mass spectroscopy (ICP-MS) in Earth and Environmental Sciences department at the University of Leeds, UK. At each measurement point, 0-0.33Mc, 0.33-0.66Mc, 0.66-1Mc, 1-2Mc and 2-3Mc, five 3ml-samples were taken from each station and underwent nitric acid digestion and centrifuging processes to eliminate proteins, contaminants and wear debris. Measurements were compared to background measurements of digested fresh 25% serum containing known amount of Co or Cr and calibrated samples of Co and Cr. These were used to check if the machine was measuring the right concentrations and the digestion process was valid. Using the ICP the solution was aspirated into aerosol then passed through argon plasma. This procedure transforms the atoms of the metal elements into ions. These ions are then separated and detected by the mass spectrometer (MS).

The femoral head and the acetabular cups were measured using the CMM (Legex 322, Mitutoyo, UK) after completing the 6 million cycles of testing on the simulator. The femoral head were measured by taking 2808 data points taken in the form of 36 traces rotated by 10 degrees from each other about the vertical axis. Each trace consisted of 78 points with a pitch of 0.5mm starting at the pole and finishing 7mm below the equator. A 5-star 2mm stylus configuration was used to measure the femoral heads. Analysis of the unworn part of the femoral heads showed form deviations of ±10µm. The acetabular cups were measured by taking 2,052 points in the form of 36 traces rotated by 10 degrees from each other about the vertical axis. Each trace consisted of 57 points with a pitch of 0.5mm starting at the pole and finishing at the rim of the cup. The last three points of each trace lay on the

chamfer of the rim. A straight 2mm stylus configuration was used to measure the acetabular cups. Three dimensional reconstructions of the femoral head surfaces and the acetabular cups surfaces were obtained using the SR3D software (Tribology solutions Ltd, UK).

Statistical analysis was performed using one-way ANOVA (significance taken at p<0.05) and 95% confidence limits were calculated.

6.3 Results

6.3.1 Wear

Increasing the cup inclination angle from 45° to 65° did not statistically significantly (p=0.9) increase the wear of the 36mm metal-on-metal bearings. The wear rates over the first 3 million cycles under standard gait conditions were 0.35 mm^3/ million cycles and 0.37 mm^3/ million cycles for 45° and 65° cup inclination angles respectively (Figure 6.2). There was sign of bedding in and steady state phases under microseparation conditions (Figure 6.3). Under the 65° inclination angle condition, the wear patch approached the rim of the acetabular cup but it still did not intersect with the rim avoiding edge loading and elevation of wear rate (Figure 6.4). Comparing this to the 28mm bearings tested in Chapter 4, the wear patch under the 65° cup inclination angle condition did intersect with the rim of the acetabular cup increasing the wear rate (Figure 6.5 and Figure 6.6).

Under standard gait conditions, the wear rates of the 36mm bearings could be split into 2 stages, a bedding stage between 0 and 1 million cycles and a steady state stage between 1 and 3 million cycles. The bedding in stage for the 36mm bearings was shorter than that of the 28mm bearings which lasted up to two million cycles (Figure 6.6).

When the microseparation conditions were introduced to the gait cycles, edge loading occurred and stripe like wear areas were formed on the femoral heads with corresponding wear areas at the rim of the acetabular cups. The wear rates significantly increased under both cup inclination angle conditions from below 0.5mm^3/million cycles to 5.47mm^3/million cycles for

the 45° cup inclination angle condition (p<0.01) and to 4.14mm^3/ million cycles for the 65° cup inclination angle condition (p<0.01) (Figure 6.2).

Under microseparation conditions, there was no significant difference (p=0.42) in the wear rates of the 28mm and the 36mm bearings under both cup inclination angle conditions (Figure 6.6).

Increasing the cup inclination angle from 45° to 65° under microseparation conditions did not cause a statistically significant (p=0.7) change in the wear rate of the 36mm MoM bearing (Figure 6.2), consistent with the 28mm bearings.

The wear rates during the first million cycles under microseparation conditions for both cup inclination angle conditions were lower that the wear for the subsequent million cycles (Figure 6.2).

The percentage of the wear volume under standard gait conditions was slightly higher on the acetabular cups compared to the femoral head (60:40). However, under microseparation conditions the percentage of the wear volume was equally split between the heads and cups (Figure 6.7).
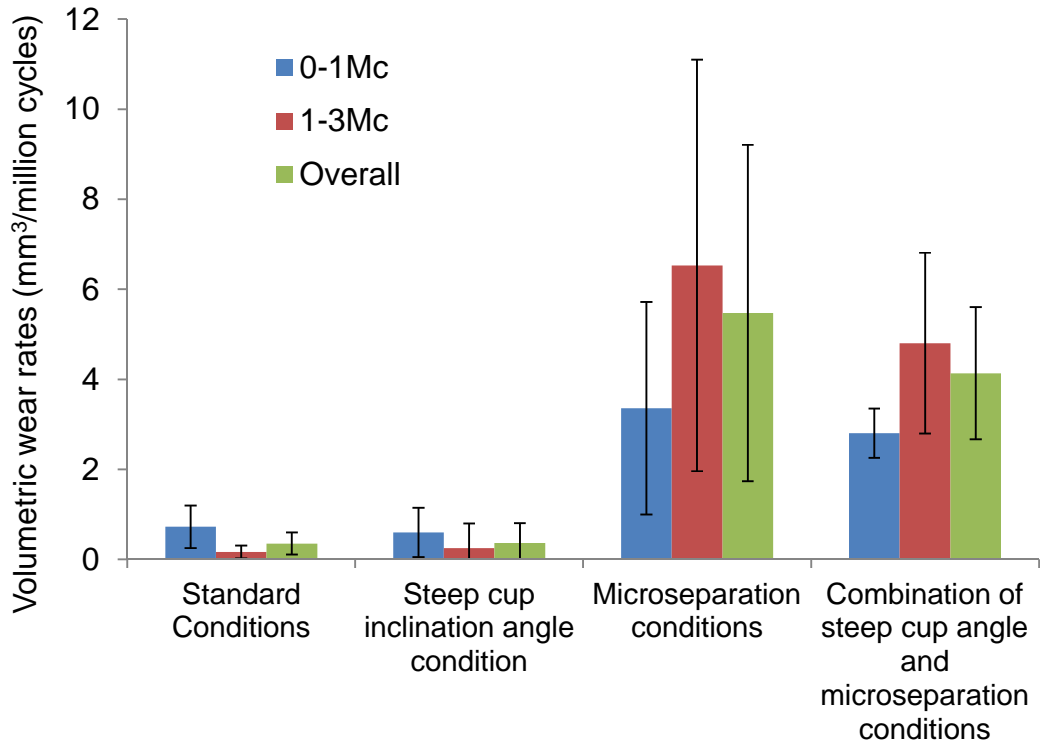
Figure 6.2: The mean wear rates at different stages of the test under the four different testing conditions. Error bars represent the 95% confidence limits. Mc= million cycles.
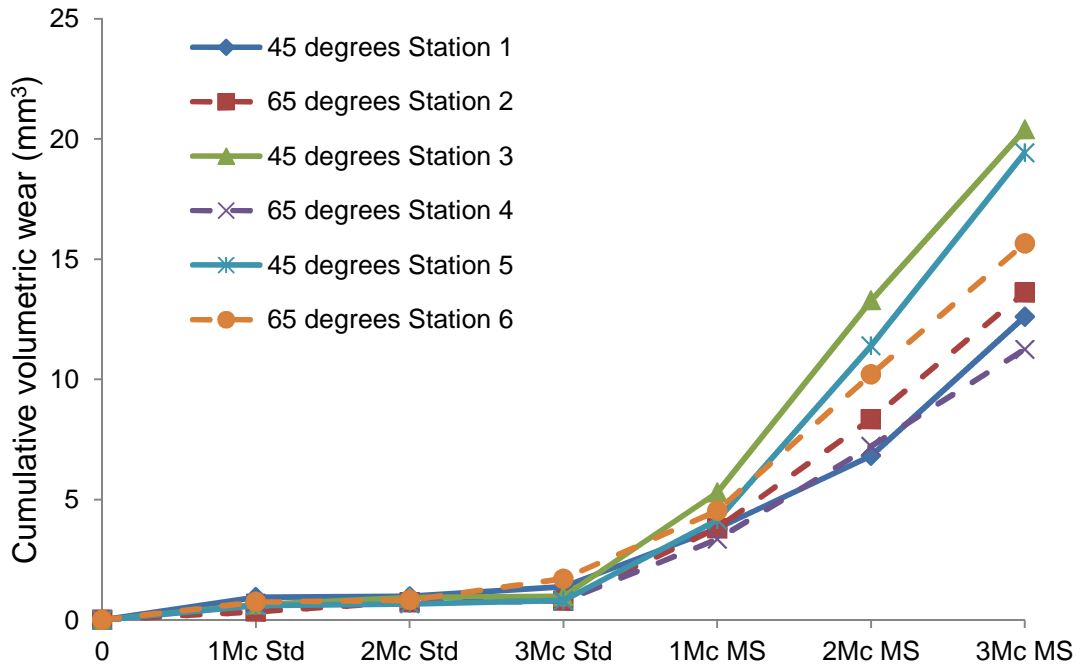
Figure 6.3: Cumulative wear volume under standard and microseparation conditions for individual stations for the 36mm MoM bearings. Mc= million cycles, Std= standard, MS= microseparation.

Figure 6.4: Photographs of the 36mm inner diameter acetabular cups showing the wear area (within dotted line) under standard conditions with 45° inclination angle (left) and the wear area under steep inclination angle (right). Under steep inclination angle the wear area approached the rim of the acetabular cup but it did not intersect with the rim after 3 million cycles of test under standard gait conditions.

Figure 6.5: Photographs of the 28mm inner diameter acetabular cups showing the wear area (within dotted line) under standard conditions with 45° inclination angle (left) and the wear area under steep inclination angle (right). Under steep inclination angle the wear area intersected with the rim of the acetabular cup.
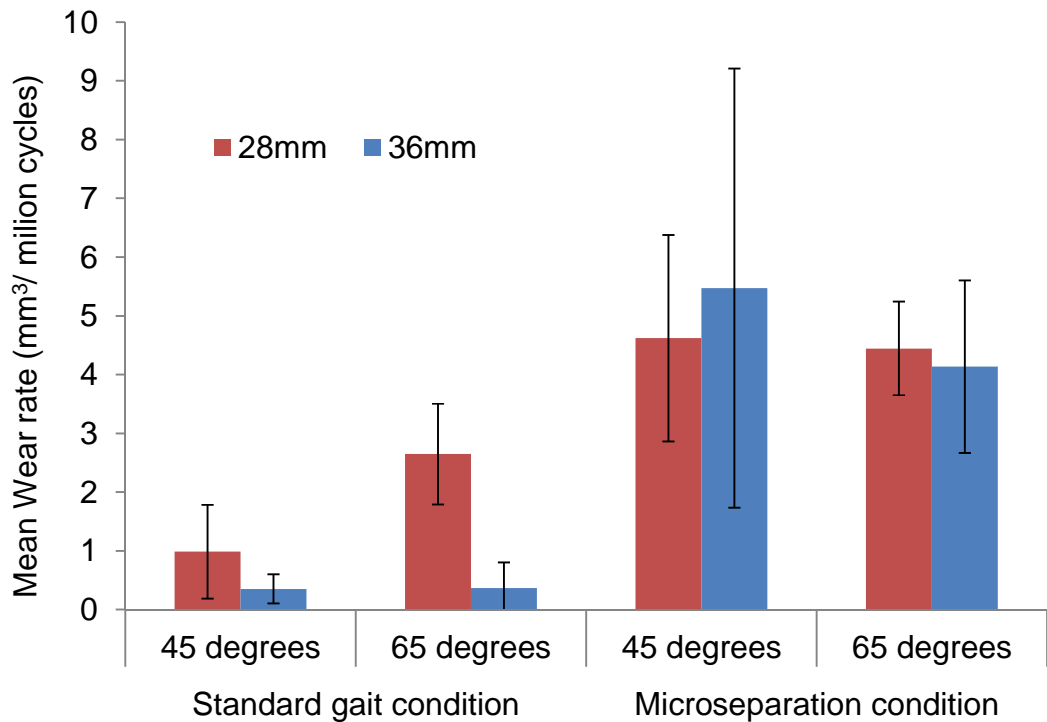
Figure 6.6: The mean wear rates of the 28mm and 36mm metal-on-metal bearings under the four different testing conditions. Error bars represent the 95% confidence limits.
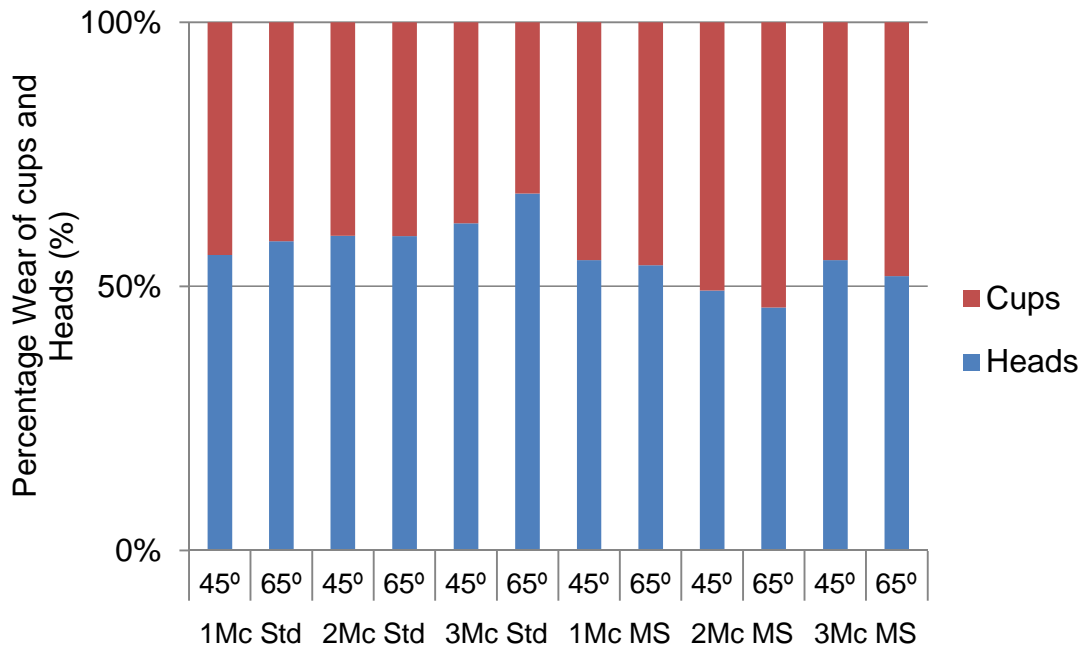
Figure 6.7: Percentage of wear on head and cups at every measurement points for both cup inclination angles under standard gait and microseparation conditions. Mc=million cycles, Std= standard and MS=Microseparation conditions.

6.3.2   Ion level Analysis

The cobalt and chromium ions concentrations followed the same pattern as the wear volumes that were measured gravimetrically (Figure 6.8, Figure 6.9and Figure 6.10). There was a good correlation between the wear volume and cobalt ion concentration under all conditions tested (R^2=0.97, Figure 6.11), however the correlation between the volumetric wear and the chromium ions was weaker (R2=0.81, Figure 6.12), especially under high wear volume conditions (Figure 6.12and Figure 6.13).
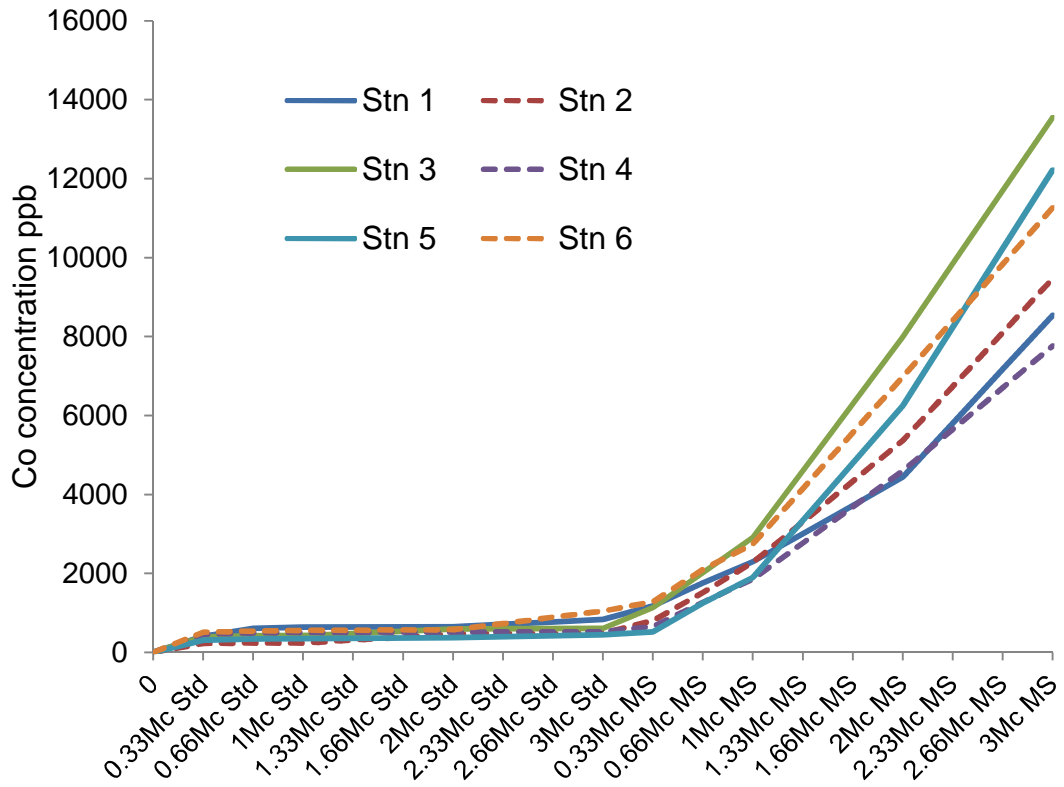
Figure 6.8: Cobalt ion concentration throughout the six million cycles of test; three under standard conditions and three under microseparation conditions. The odd numbered station had the cups inclined at 45° and the even numbered stations had the cups inclined at 65°. Mc= million cycles, Std=Standard conditions, MS= Microseparation conditions.
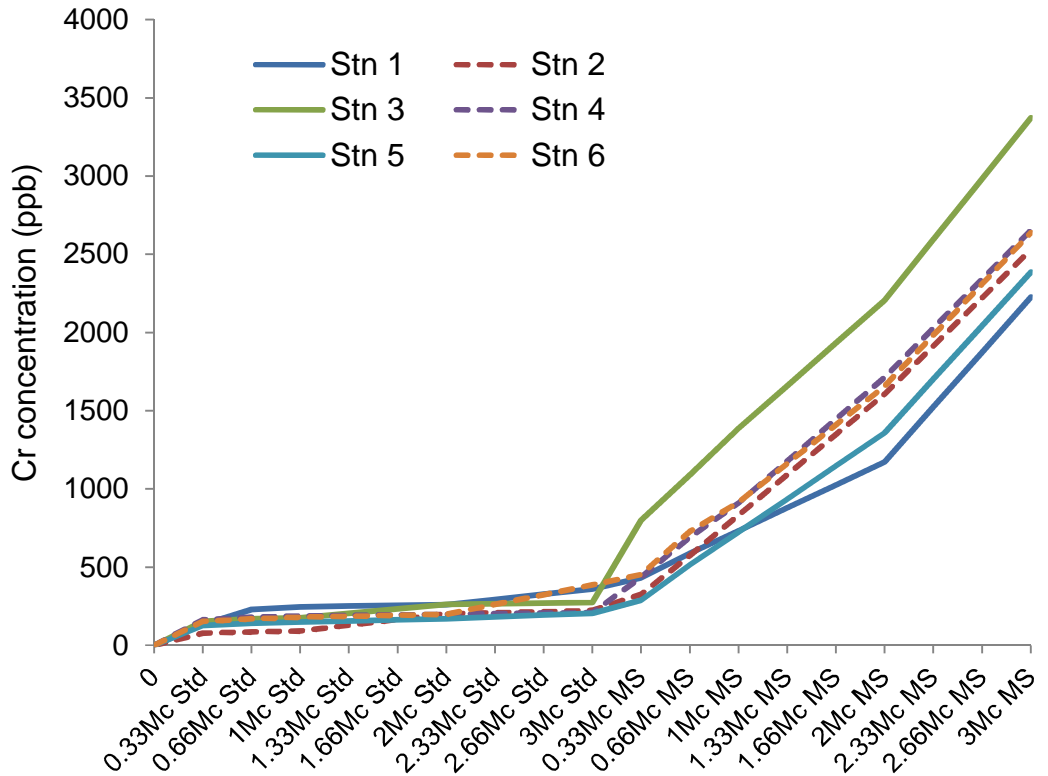
Figure 6.9: Chromium ion concentration throughout the six million cycles of test; three under standard conditions and three under microseparation conditions. The odd numbered station had the cups inclined at 45° and the even numbered stations had the cups inclined at 65°. Mc= million cycles, Std=Standard conditions, MS= Microseparation conditions.
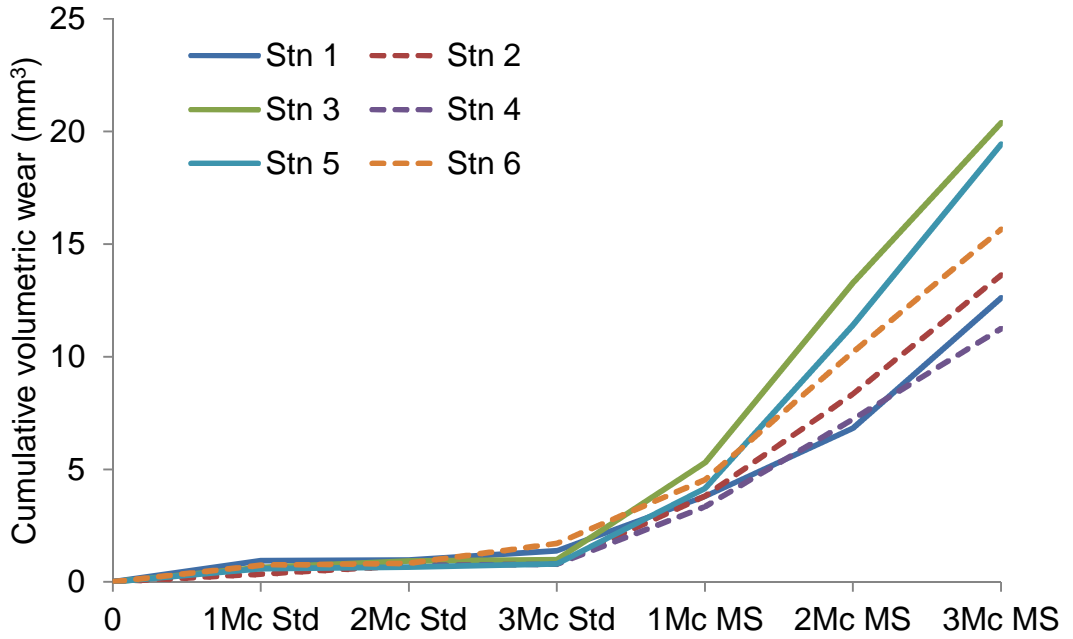
Figure 6.10: Cumulative wear volume of individual bearing couples throughout the six million cycles of testing under standard gait and microseparation conditions. Mc= million cycles, Std=Standard conditions, MS= Microseparation conditions.
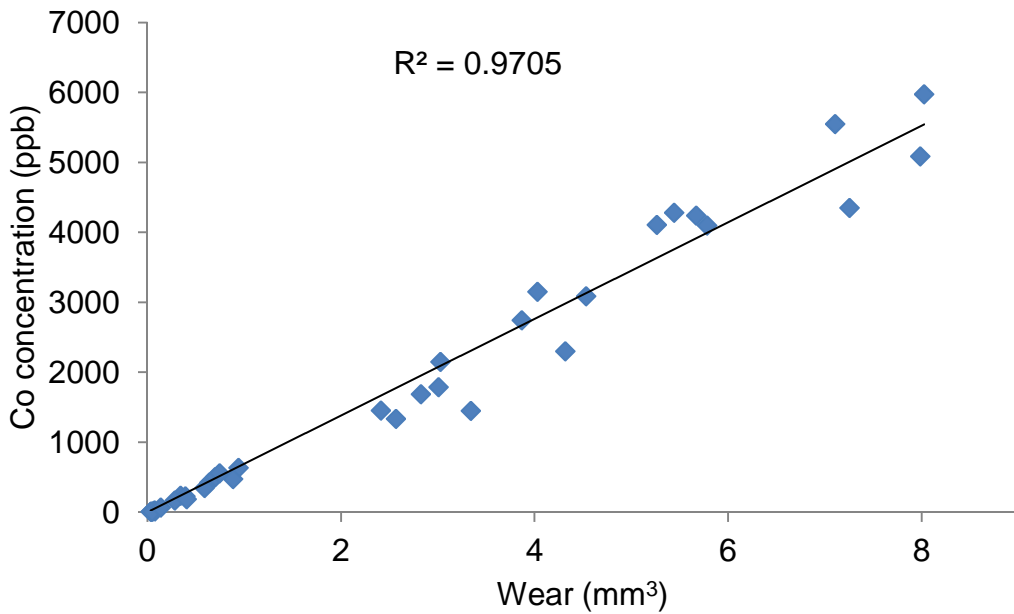
Figure 6.11: Correlation between Co ion concentration and volumetric wear throughout the hip simulator test.
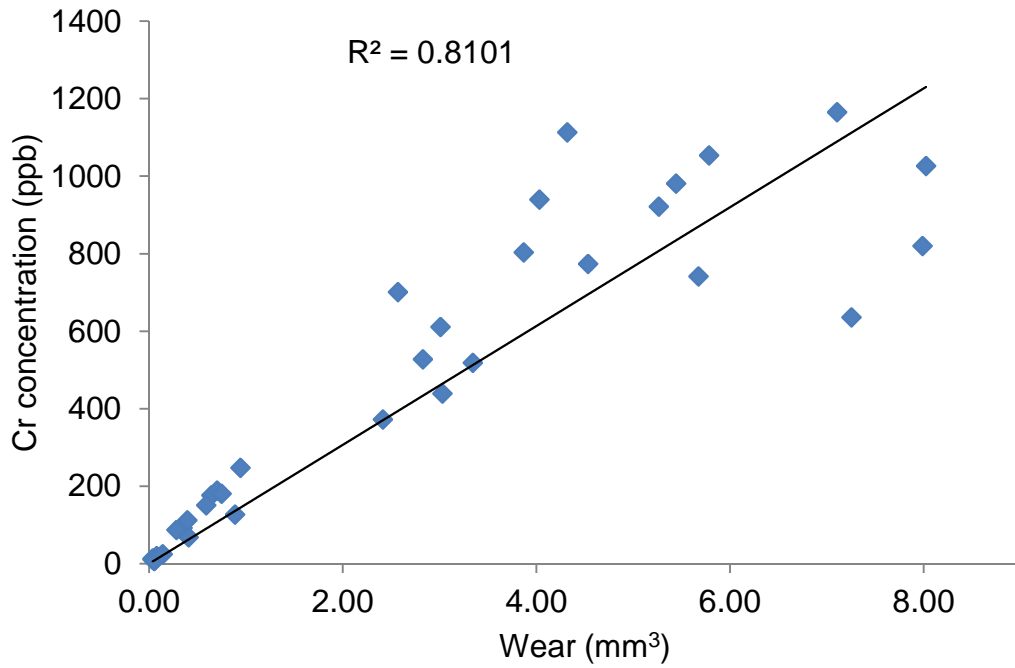
Figure 6.12: Correlation between Cr ion concentration and volumetric wear throughout the hip simulator test.
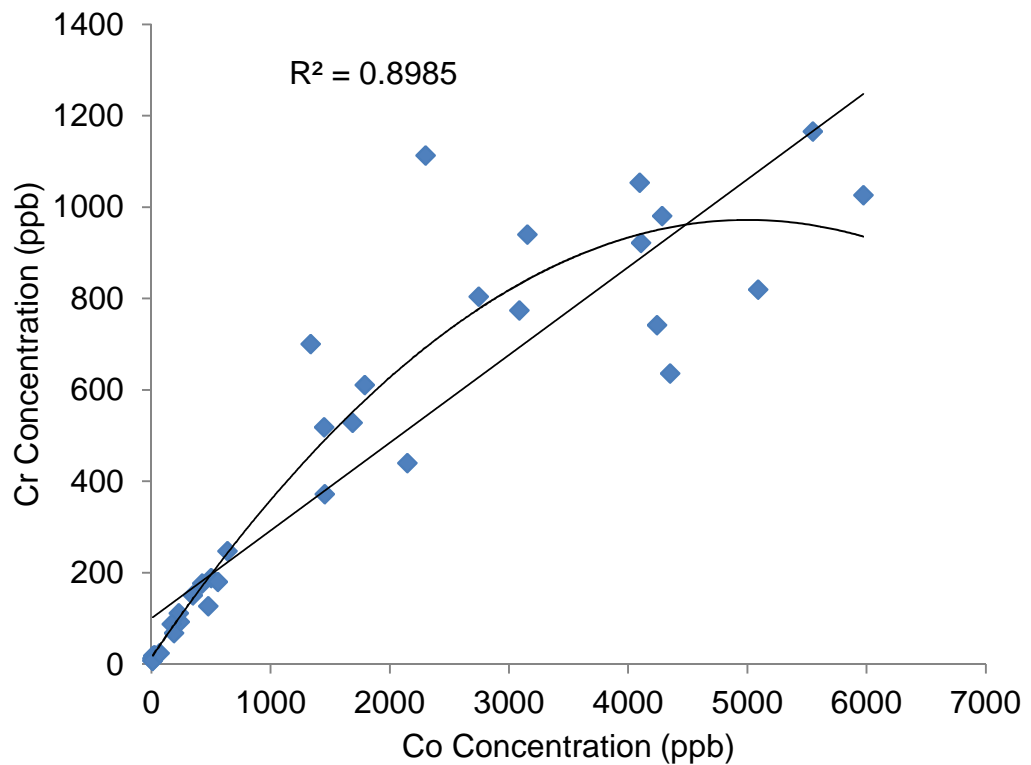
Figure 6.13: Correlation between Co ion concentration and Cr ion concentration throughout the hip simulator test.

6.3.3   Penetration

A stripe of wear on the metal heads with a corresponding wear area on the superior lateral edge of the acetabular cup were observed when microseparation conditions were introduced to the gait cycle. For the 28mm bearings, the mean maximum penetration depth on the femoral heads was 57 µm under the standard cup inclination angle condition, and 74 µm under the steep cup inclination angle condition. These measurements were done using the 2 dimensional profilometry (Talysurf, Taylor Hobson, UK). For comparison using the Talysurf, the 36mm bearings, the mean penetration depth on the femoral heads was 55 µm under the standard cup inclination angle condition and 48 µm under the steep cup inclination angle condition.

The 36mm bearings were also measured using the CMM and it was possible to reconstruct 3D representations of the surfaces of the femoral heads (Figure 6.14) and the acetabular cups (Figure 6.15). The reconstructed surfaces showed the size, shape, and location of the maximum depth of the wear areas. The wear area on the femoral heads that articulated against acetabular cups with 45° inclination angles were oriented downwards with most of the wear area below the equator. However, the wear areas of the femoral heads, that articulated against acetabular cups included at 65°, were more superior, located above the equator. The dimension of the wear stripe area caused by edge loading were determined and summarised in Table 6.1 and Table 6.2. There were statistically significant differences in the lengths, widths, and penetrations of the wear stripes on the femoral head between the two cup inclination angles conditions.

Table 6.1: The lengths, widths and maximum penetration depth (using CMM) of the wear stripes on the 36mm femoral heads after 3 million cycles of testing under microseparation conditions.

	Length (mm)		Width (mm)		Maximum Penetration depth (µm)	
	45°	65°	45°	65°	45°	65°
Head 1(45°) & 2(65°)	35.0	34.0	4.3	3.6	50.8	43.8
Head 3(45°) & 4(65°)	36.0	33.5	5.7	3.5	64.6	35.4
Head 5(45°) & 6(65°)	36.0	34.5	5.0	3.6	63.0	44.7
Mean	**35.7**	**34.0**	**5.0**	**3.6**	**59.5**	**41.3**
Significance (p value)	0.02		0.02		0.03	

Table 6.2: The lengths, widths and maximum penetration depth (using CMM) of the wear area near the rim on the 36mm acetabular cups after 3 million cycles of testing under microseparation conditions.

		Length (mm)		Width (mm)		Maximum Penetration depth (μm)	
		45°	65°	45°	65°	45°	65°
Cup 1(45°) & 2(65°)		33.0	36.0	6.9	2.9	100	120
Cup 3(45°) & 4(65°)		36.0	36.0	4.7	2.5	120	85
Cup 5(45°) & 6(65°)		36.0	36.0	6.4	3.5	160	135
Mean		**35.0**	**36.0**	**6.0**	**3.0**	**126.7**	**113.3**
Significance (p value)		0.37		0.01		0.59	
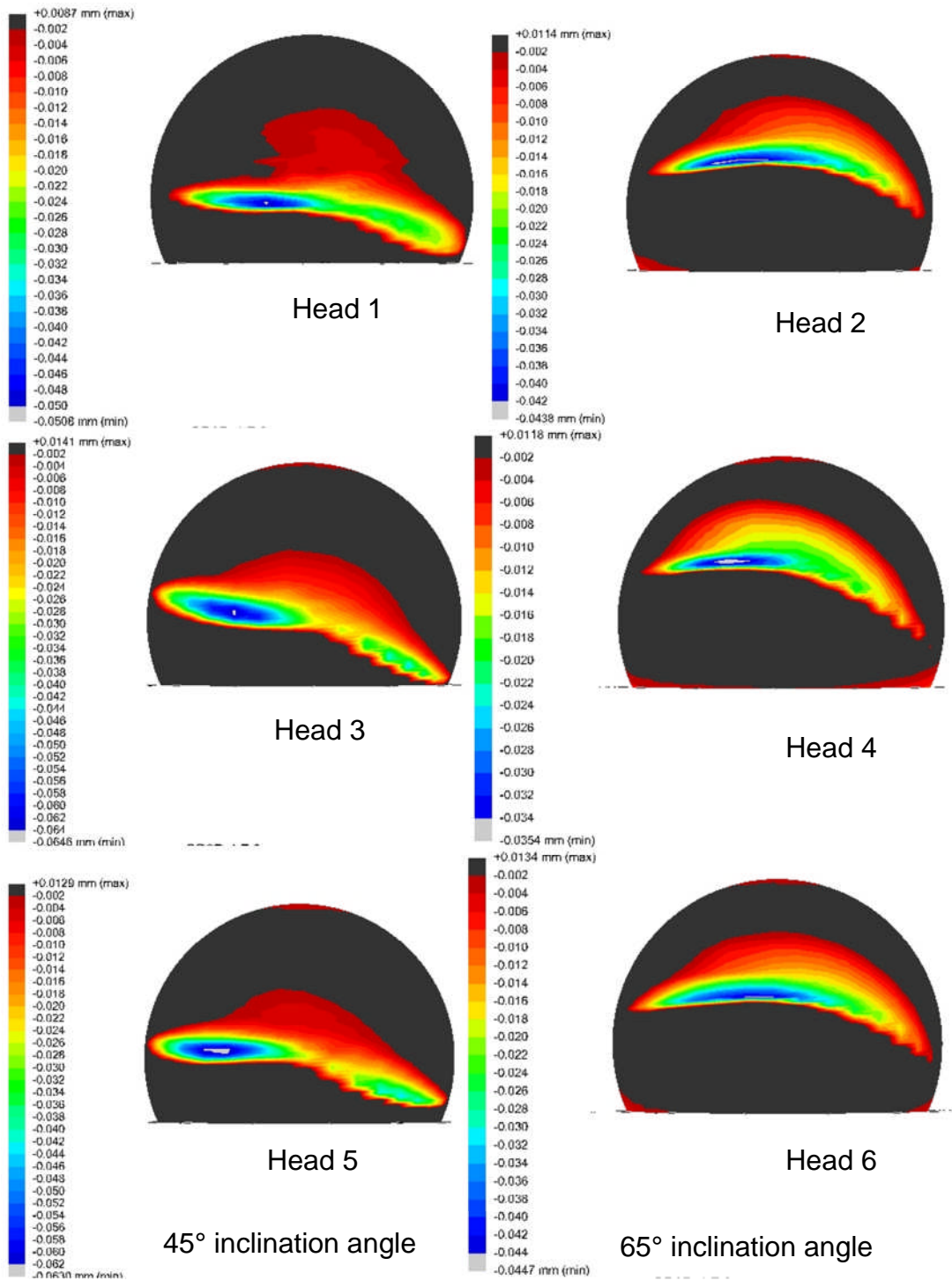
Figure 6.14: Three dimensional reconstruction of the wear are on the femoral heads using the 5 star stylus. The dark grey region represents the unworn area on the femoral head or an area with small penetration which was within the accuracy of the measurement technique.
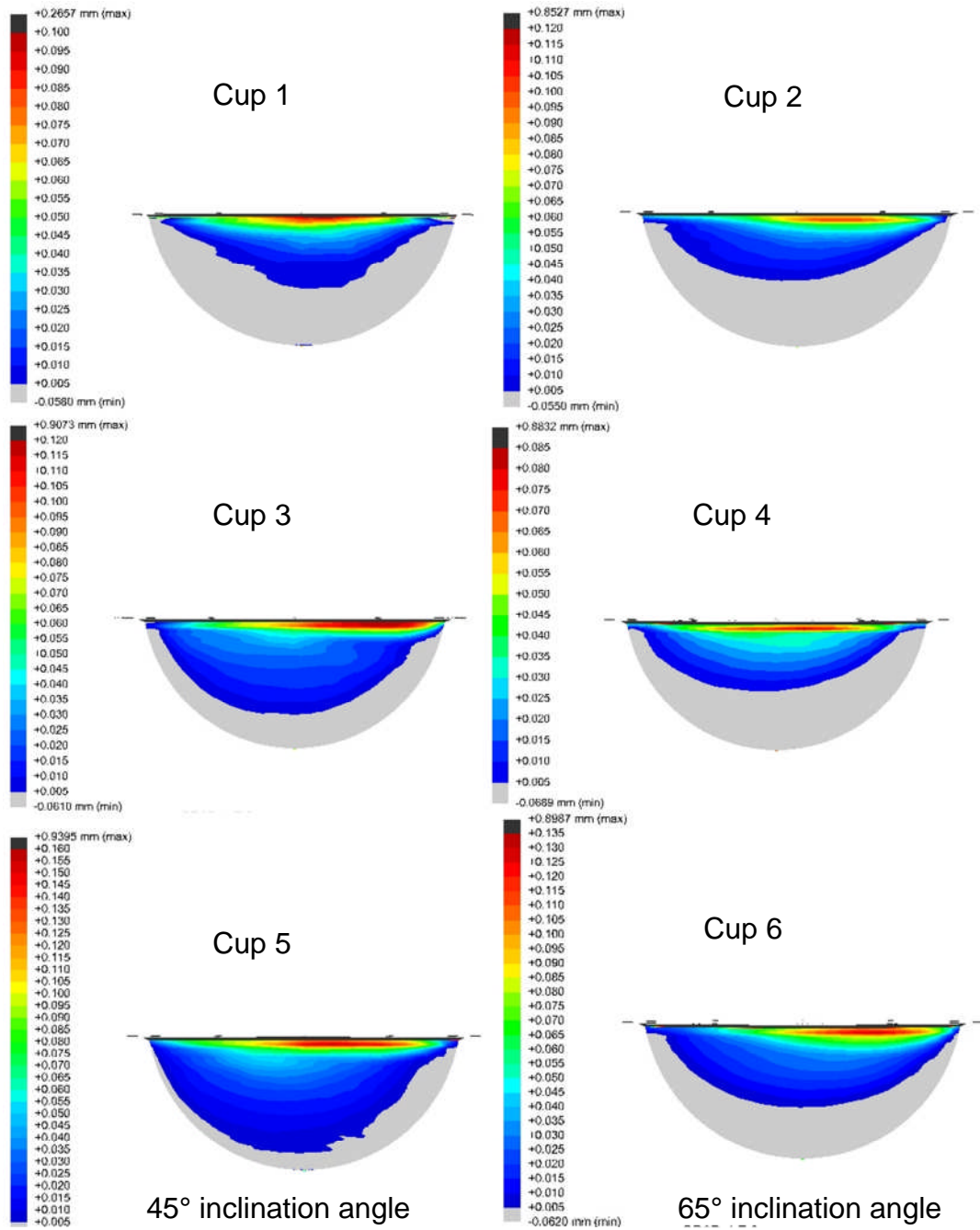
Figure 6.15: Three dimensional reconstruction of the wear area on the acetabular cup using 2mm straight stylus. The light grey region represents the unworn area on the surface of the cup or an area with small penetration which was within the accuracy of the measurement technique.

6.4 Discussion

In this study, the wear rates obtained under standard conditions were lower than previously reported for the 36mm MoM bearings (Williams et al., 2007b). This could be due to the reduced diametrical clearance used in this study (40µm) compared to approximately 80µm in the previous study. Farrar et al. (1997) have shown that decreasing the diametrical clearance reduces the bedding in wear of MoM articulations.

The 36mm bearings showed no increase in wear rate when the cup inclination angle was increased from 45° to 65°. As the inclination angle increased, the contact area approached the rim of the acetabular cup but no head-rim contact occurred. Both the 28mm (Chapter 4) and the 36mm (this Chapter) metal-on-metal bearings had an inclusion angle (cup coverage) of 160°. A cup designed with a hemispherical inclusion angle (180°) will have better tolerance to rotational mal-positioning however, this will restrict the range of motion and increase the incidence of impingement (Wang et al., 2011). Decreasing the acetabular coverage will increase the range of motion but will increase the chance of edge loading due to rotational mal-positioning. These results showed that increased wear due to rotational mal-positioning only occurs when edge loading occurs, which in turn is dependent on the combination of several factors such as steep cup inclination angles, excessive version or ante-version angles, and acetabular cup geometries and component size.

When microseparation conditions were introduced to the gait cycle, there were significant increases in wear rates and a stripe of wear was formed on the femoral head with a corresponding wear area at the superior rim of the acetabular cup. The wear rate throughout the three million cycles of testing under microseparation conditions for both bearing sizes was steady, showing no evidence of bedding in and steady state phases. The results showed no statistically significant differences in the wear rate between the two cup inclination angle conditions under microseparation conditions indicating that edge loading due to microseparation conditions dominates the effect of head-rim contact due to steeply inclined acetabular cups. These

results were consistent with those obtained on the 28mm bearings presented in Chapter 4.

Under standard conditions, the wear rates decreased with increasing head size due to improved lubrication regimes. However, when edge loading occurred under microseparation conditions, the wear rate of the 36mm bearings was similar to the 28mm bearings. It is postulated that this was due to a change in the lubrication regime from mixed lubrication, which gave the larger bearings their superior wear resistance under standard gait conditions, to boundary lubrication. The wear rate obtained for both bearing sizes under microseparation and edge loading conditions was lower than that reported previously for 39mm MoM surface replacement bearings tested under similar conditions (Leslie et al., 2009). This difference may be due to the different prosthesis design, in particular the inclusion angle of the cup or the rim design. The previous in vitro study which tested 39mm MoM SR under microseparation conditions (Leslie et al., 2009) showed comparable wear values to retrieved surface replacement bearings that had experienced edge loading conditions (Morlock et al., 2008). It is clear from the literature that there is a wide range of wear rates observed in vivo, as well as cup position, inclination and version, soft tissue tension, impingement and microseparation may affect wear rates. But in addition, under adverse rim loading conditions, other design factors such as rim geometry and cup inclination angle may also impact on the increase in wear for different designs.

Serum cobalt ion concentrations measured in this study showed a strong correlation with the wear volumes measured gravimetrically, consistent with the 28mm study (Chapter 4). However, chromium ion concentrations showed a weaker correlation with wear volume, especially at high wear volumes. Under microseparation and edge loading conditions, metal-on-metal bearings produce micrometer sized particles as well as nanometer sized particles (Leslie et al., 2009). These relatively large particles are rich in chromium oxide and are removed by centrifuging when preparing samples for ion level measurement (Catelas et al., 2006). This could explain the lower than expected chromium ion levels at high wear volumes, which were obtained under edge loading conditions.

Geometric measurement of the femoral head and acetabular cups using the CMM provided better understanding of the wear mechanisms between the two cup inclination angles conditions. The microseparation conditions were achieved by introducing a medial lateral displacement to the cup relative to the head while the gait cycle was running. This displacement was achieved by spring forces in the medial- lateral axis and was always kept constant at 0.5mm regardless of the cup inclination angle. However with a low cup inclination angle, there was a better conformity between the femoral head and the cup and a larger force was needed to separate the components. A smaller stripe (lower penetration) on the right hand side of the femoral head was formed while the cup was separating from the femoral head (Figure 6.16). This was not shown on the heads that articulated against cups inclined at 65°, which only formed a single continuous stripe indicating that the head was edge loading for most of the gait cycle (Figure 6.14).

Main stripe created due to edge loading at heal strike

Stripe created at the beginning of the swing phase when the cup was separating away from the head
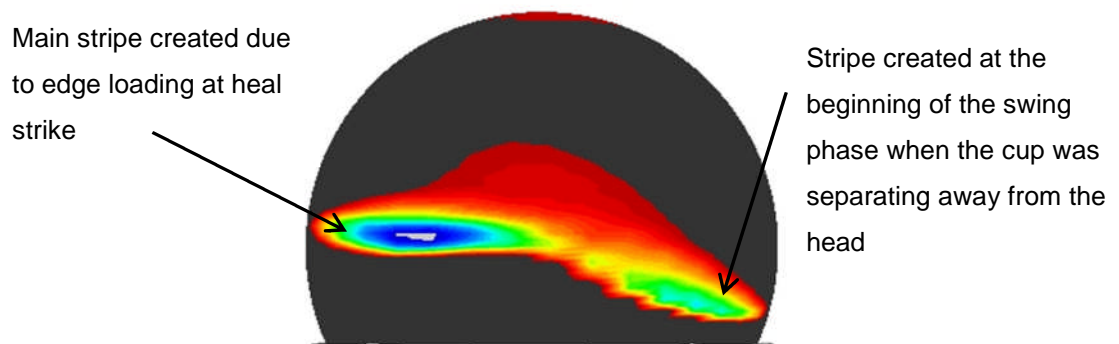
Figure 6.16: Stripes formed on a 36mm femoral head articulating against an acetabular cup inclined at 45°.

6.5 Conclusion

This study showed that with the larger size bearings, head-rim contact (edge loading due to rotational malposition) occurs at a steeper cup inclination angle (>65°) providing an advantage over smaller bearings. Edge loading due to microseparation conditions caused excess damage and wear to the bearing surfaces. In vivo, steep cup inclination angles and other factors such

as impingement, stem subsidence, tissue laxity around the prosthesis and head position could facilitate microseparation and edge loading leading to various complications and implant failure. This study highlights the importance of prosthesis design and the accurate positioning of the implant in its optimum position during surgery. The effects of edge loading were more dominant with microseparation conditions to that of edge loading due to increased cup inclination angle alone. Finally, under microseparation conditions, there were no statistically significant differences in the wear rates of the 28mm and the 36mm size bearings.

CHAPTER 7. THE EFFECT OF EDGE LOADING CONDITIONS ON THE CORROSION OF METAL-ON-METAL BEARINGS IN TOTAL HIP REPLACEMENT

7.1   Introduction

The release of cobalt and chromium ions in metal-on-metal bearings is a major clinical concern (Jacobs et al., 1994, Jacobs et al., 1998, Jacobs et al., 1999) and very little is known about the long-term effect of these metallic ions on patients' health. Thus, the aim in metal-on-metal bearing technology is to minimise the release of ions into the surrounding tissue. They are released by the metal bearings through two different processes; corrosion of the surface itself activated by the tribological contact, or by the dissolution of the wear particles produced due to mechanical wear of the bearing surface (Yan et al., 2005).

The cobalt chrome alloy used in hip replacement bearings is highly corrosion resistant possessing a chromium rich passive layer. This passive layer prevents the release of ions into the surrounding environment. However, when sliding and loading are introduced to the bearing, mechanical wear occurs leading to the removal of the protective layer, activating the surface (Yan et al., 2006). The more active the surface is the higher the corrosion rate and release of ions into the surrounding environment .

The wear of metal on metal bearings under standard hip simulator conditions has been widely reported and it showed a biphasic wear mechanism (Dowson, 2001); a relatively higher bedding in wear rate then a relatively low steady state wear rate. This mechanism is dependent on the lubrication regime and the protein constituent of the lubricant (Dowson et al., 2000). The protein constituent has been shown to play an important role in the electrochemistry of the metal surfaces. It has been postulated that the chromium rich passive layer originally present at the surface of the bearing is removed due to the mechanical wear when the two bearing surfaces contact under sliding and loading regimes (Yan et al., 2005). This layer is then

replaced by a more complex protective layer called the tribofilm. This tribofilm is made up of organic materials and cobalt and chromium oxides. It is this tribofilm layer, that can act as a solid lubricant, alongside the lubrication regimes that explain the low steady state wear behaviour of metal on metal bearings (Yan et al., 2010b).

So due to the tribocorrosion processes that goes on the surface of the bearings, the total material loss of metal on metal bearings can be split into mechanical wear and corrosion wear (Yan et al., 2005). However, there are synergistic effects between the two phenomena; the corrosion-enhanced wear and the wear-enhanced corrosion. The total material loss can be explained in the following equation:

$$T = W + C + \Delta W + \Delta C$$

Where T is the total material loss, W is wear, C is corrosion, ΔW is corrosion-enhanced wear and ΔC is wear-enhanced corrosion.

It has been shown in Chapters 4 and 6 that edge loading causes significant increase in wear rate and ion release. So as well as understanding the wear behaviour of metal on metal bearings under adverse conditions, it is important to understand the tribocorrosion behaviour of such bearings under normal gait conditions and adverse edge loading conditions.

The aim of this study was to assess the corrosion regime of different size metal on metal bearing in a total hip simulator machine under physiological conditions and determine the effect of rotational and translational mal positioning on the corrosion mechanism.

7.2   Materials and Methods

Metal on metal bearings were used in this study. Six 28mm and six 36mm diameter cobalt chrome alloy (CoCrMo) femoral heads and acetabular cups were custom manufactured by Corin Ltd UK, and tested using the six-station Leeds II Physiological Anatomical Hip Joint Wear simulator. These were the same components used in Chapters 4 and 6. They were rotated around by 180 degrees so the contact areas were over the unworn regions of the bearings surfaces. The components were all high carbon (>0.2% C) and

heat treated. The diametrical clearances of all couples were in the range of 40-60 (μm).

The simulator set up used in this study was identical to the set up used for the wear studies reported in Chapters 4 and 6. Three acetabular cups were mounted to provide an inclination angle equivalent to 45° *in vivo* and three other cups were mounted to provide an inclination angle equivalent to 65° *in vivo*. A twin peak loading of 3kN peak load was applied and two independently controlled axes of motion, flexion/extension (-15° to +30°) and internal/external rotation (+/- 10°) were applied.

The metallic cup holder was isolated from the acetabular cup by using a delrin spacer between the locking ring and the surface of the acetabular cup. The femoral head was not isolated from the titanium stem. A two-electrode cell was set up by using the acetabular cup as the working electrode. A silver/ silver chloride (Ag/AgCl) electrode was used as the reference electrode to provide a stable datum against which the potential of the working electrode was measured (Figure 2.8). A potentiostat was used to measure the potential of the working electrode versus the stable reference electrode (Yan et al., 2010a).

The machine was run using one single station at any one time measuring the open circuit potential (OCP) under standard then microseparation conditions before moving to the next station. For the 28mm bearings, the test ran for at least 150,000 cycles (around 48 hours) under standard conditions and 150,000 cycles under microseparation conditions. However, for the 36mm bearings it was decided to run the test for longer reaching 330,000 cycles (around 72 hours) under standard conditions and 330,000 cycles under microseparation conditions.

The OCP was monitored for 20 minutes before the machine was started. This was done to record the static free potential between the acetabular cup and the Ag/AgCl reference electrode to determine the corrosion regime. After 20 minutes the machine was started while the OCP was being recording capturing the initial drop in potential. After one hour, the OCP was measured for 60 seconds using a high acquisition rate at 100 data points per second. This was done to visualise the measured potential in detail over one

gait cycle. Then the OCP was measured at a rate of one data point every five minutes for the remainder of the test. At the end of the test, the OCP was monitored for one hour after the machine was stopped.

The test was carried out in 25% (v/v) new-born calf serum which was supplemented with 0.03% (v/v) sodium azide to retard bacterial growth. The lubricant was changed at the end of the measurements under standard conditions and before starting the test under microseparation conditions.

The mean static free corrosion, the mean initial shift in OCP when the machine was started and the mean of the maximum shift in OCP throughout the test under all four different testing conditions for the 28mm and 36mm bearings were determined and standard deviations calculated. Statistical analysis was done using one way ANOVA with the significance taken at 0.05.

7.3   Results

Before any motion or loading was applied to the metal-on-metal bearings, the free static OCP was in the range of 0 to -0.1V. However, as the sliding and loading were introduced to the system, the OCP suddenly shifted to a more negative value indicating depassivation of the surfaces for both the 28mm (Figure 7.1) and the 36mm (Figure 7.2) bearings. For both bearing sizes, the initial shift in OCP from the free static potential was higher under microseparation conditions compared to the standard conditions (Figure 7.1and Figure 7.2).
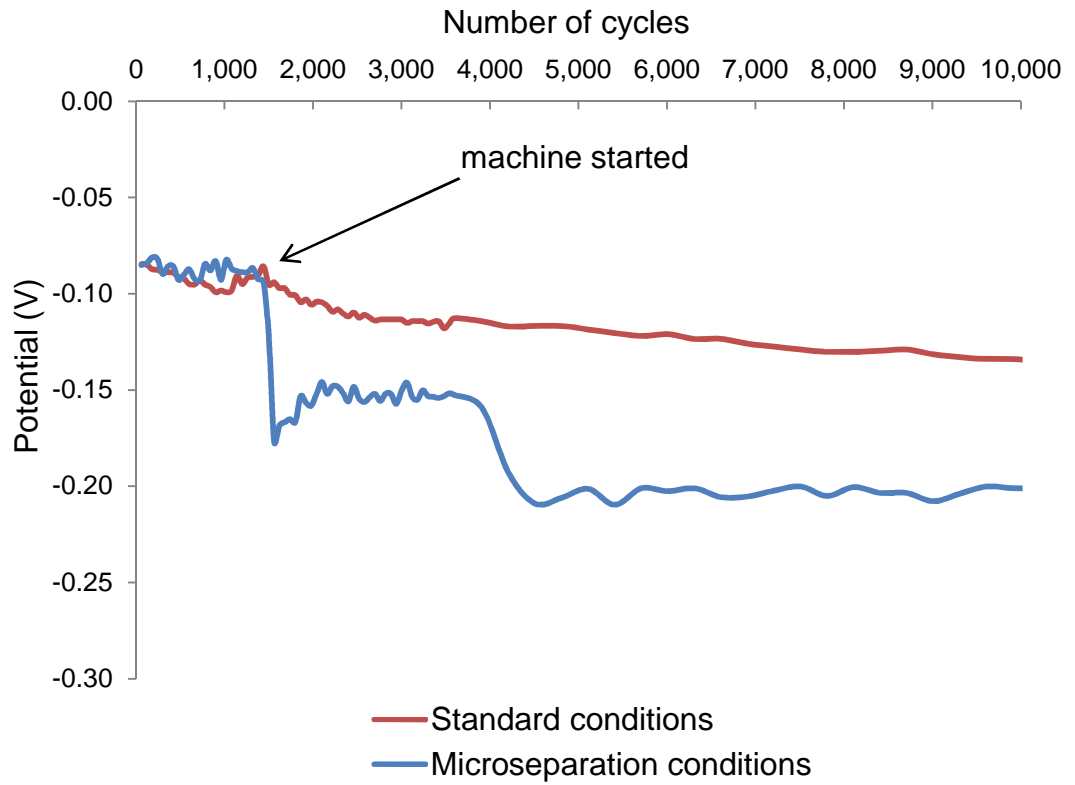
Figure 7.1: Initial drop in OCP when sliding and loading were applied to a 28mm MoM bearing under standard and microseparation conditions.
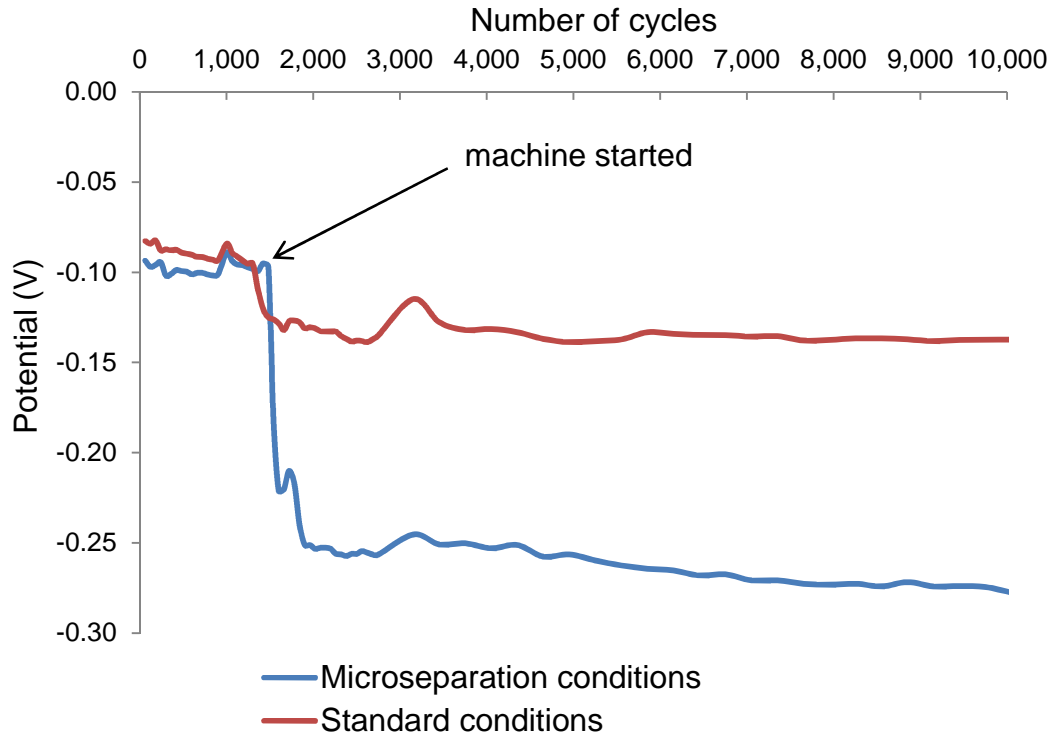
Figure 7.2: Initial drop in OCP when sliding and loading were applied to a 36mm MoM bearing under standard and microseparation conditions.

Over one gait cycle under both standard and microseparation conditions, the OCP measurements resembled a twin peak profile similar to that of the loading profile (Figure 7.3 and Figure 7.4). The change in potential was very low (approximately 0.01V) over the one gait cycle under both loading conditions. However, under microseparation conditions there was a spike in the open circuit potential which might be due to edge loading of the head on the rim of the cup (Figure 7.4).
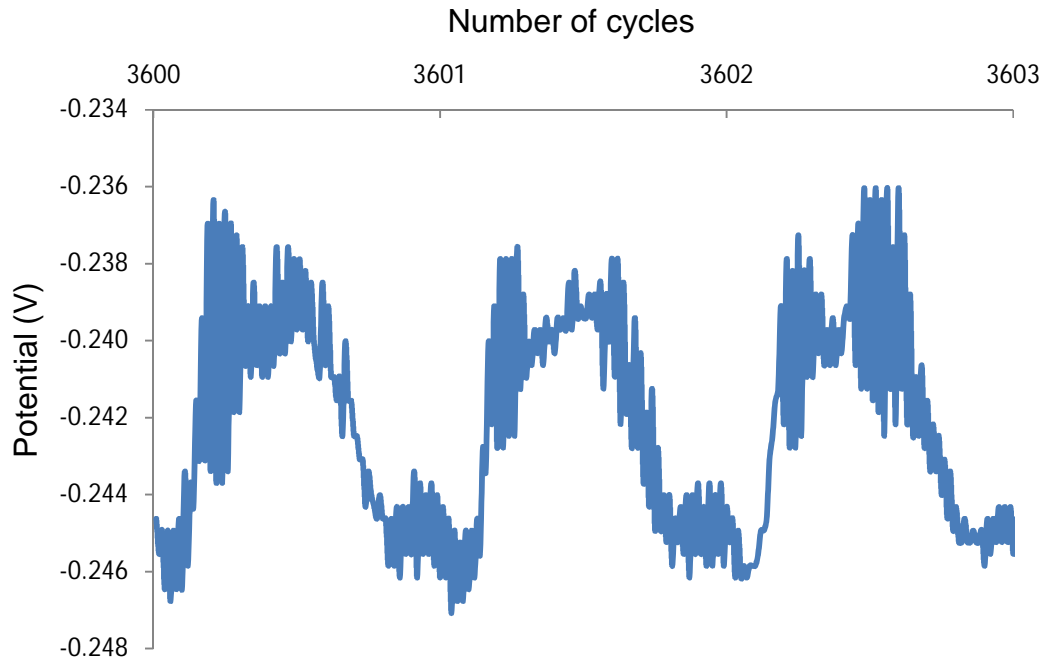
Figure 7.3: OCP measurement over three gait cycles under standard gait conditions.
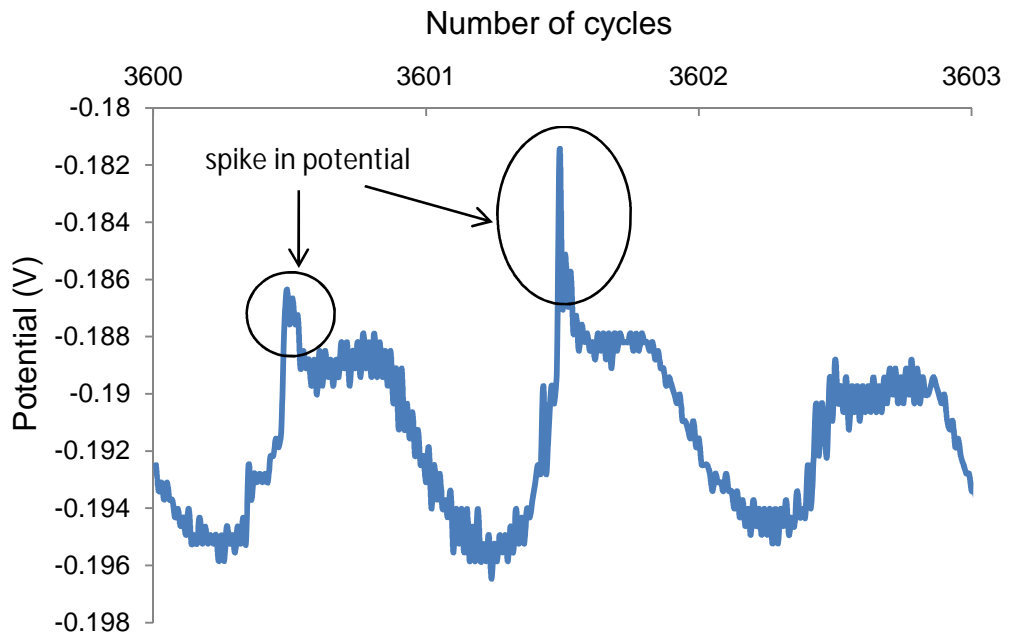
Figure 7.4: OCP measurement over three gait cycles under microseparation gait conditions.

Although the OCP was more negative under microseparation conditions when comparing individual stations independently, there was a large variation between one station to another when comparing the 28mm MoM bearings (Figure 7.5). For the 36mm bearings, there was a distinct difference between the shift in OCP under standard and microseparation conditions during the first 60,000 cycles of testing (Figure 7.6). However, there was a large fluctuation in OCP between 60,000 cycles and 330,000 cycles on all the stations (Figure 7.7). When the machine stopped, the OCP has recovered slightly but not to the free static potential level recorded at the start of the test (Figure 7.8).
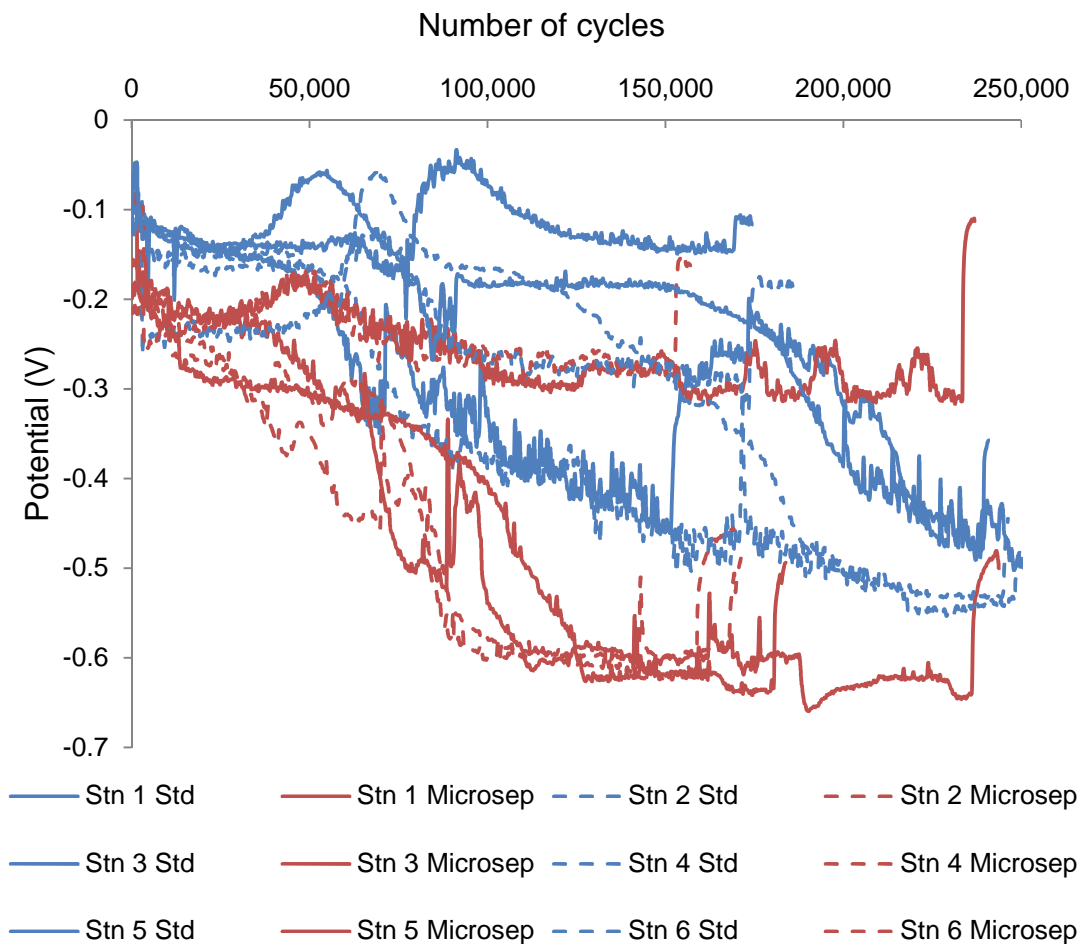
Figure 7.5: OCP measurement for all 28mm MoM bearings under standard and microseparation conditions. Stn= station, Std=Standard conditions, Microsep= microseparation conditions. Odd numbered station= 45° cup inclination angle, even numbered stations= 65° cup inclination angle.
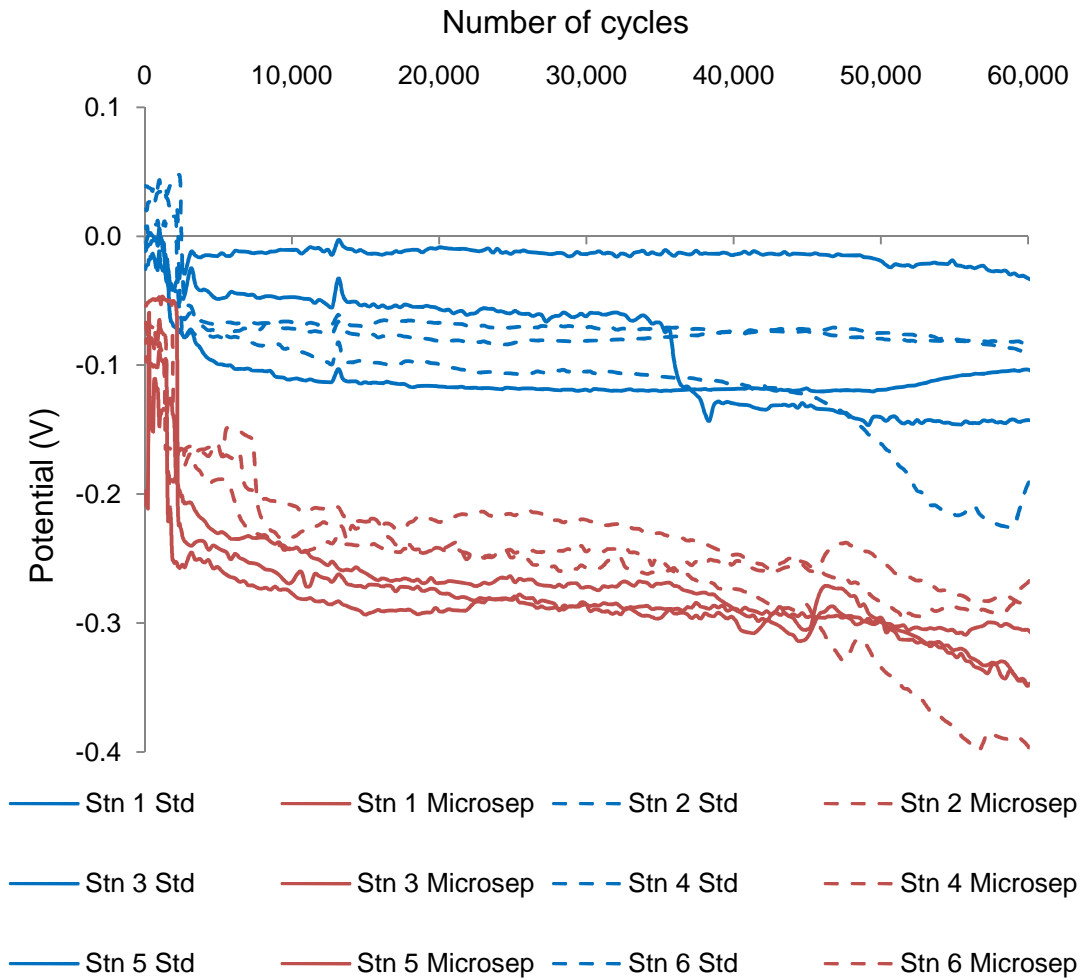
Figure 7.6: OCP measurement for all 36mm MoM bearings under standard and microseparation conditions over the first 60,000 cycles. Stn= station, Std=Standard conditions, Microsep= microseparation conditions. Odd numbered station= 45° cup inclination angle, even numbered stations= 65° cup inclination angle.
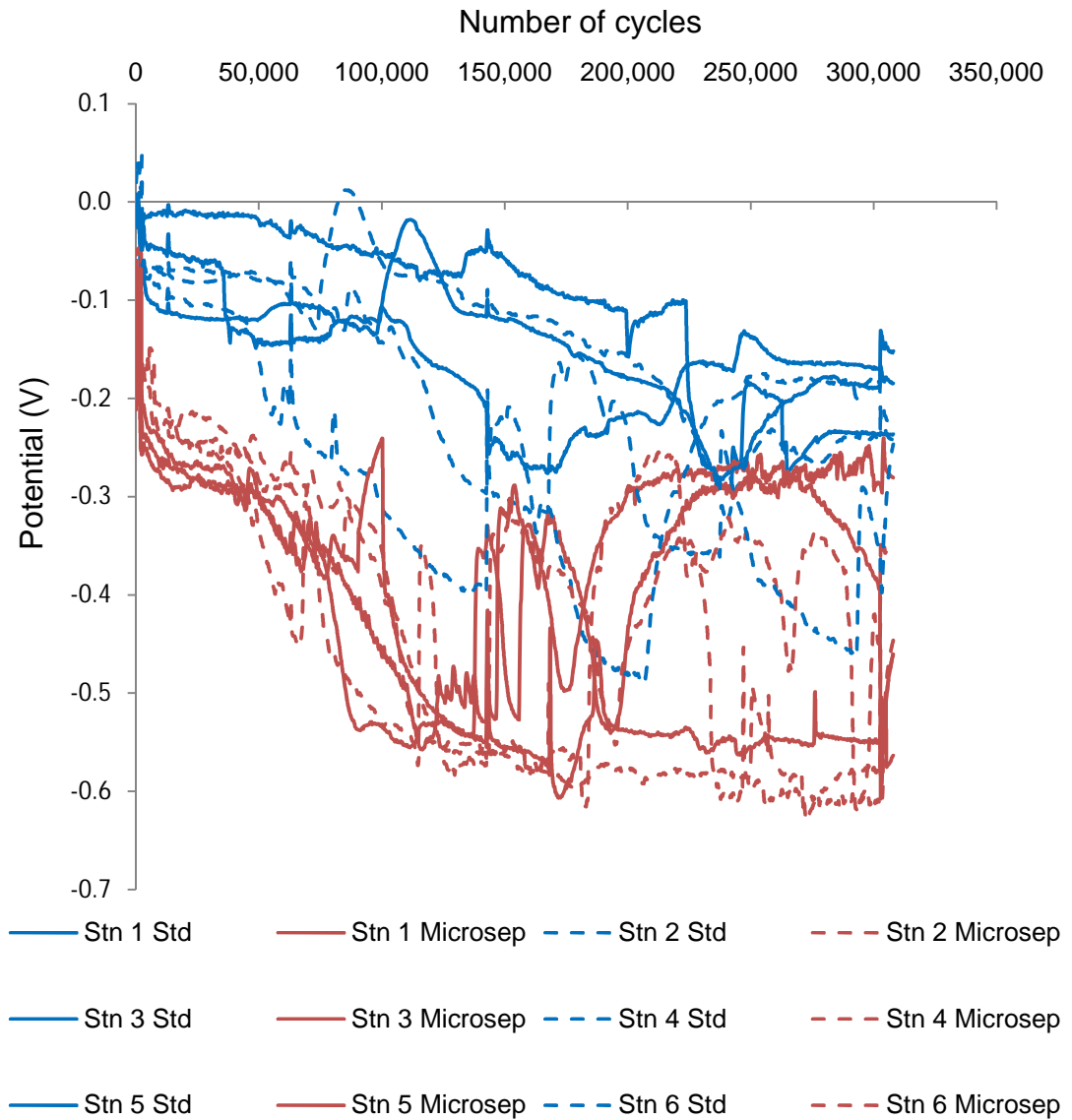
Figure 7.7: OCP measurement for all 36mm MoM bearings under standard and microseparation conditions over the entire test. Stn= station, Std=Standard conditions, Microsep= microseparation conditions. Odd numbered station= 45° cup inclination angle, even numbered stations= 65° cup inclination angle.
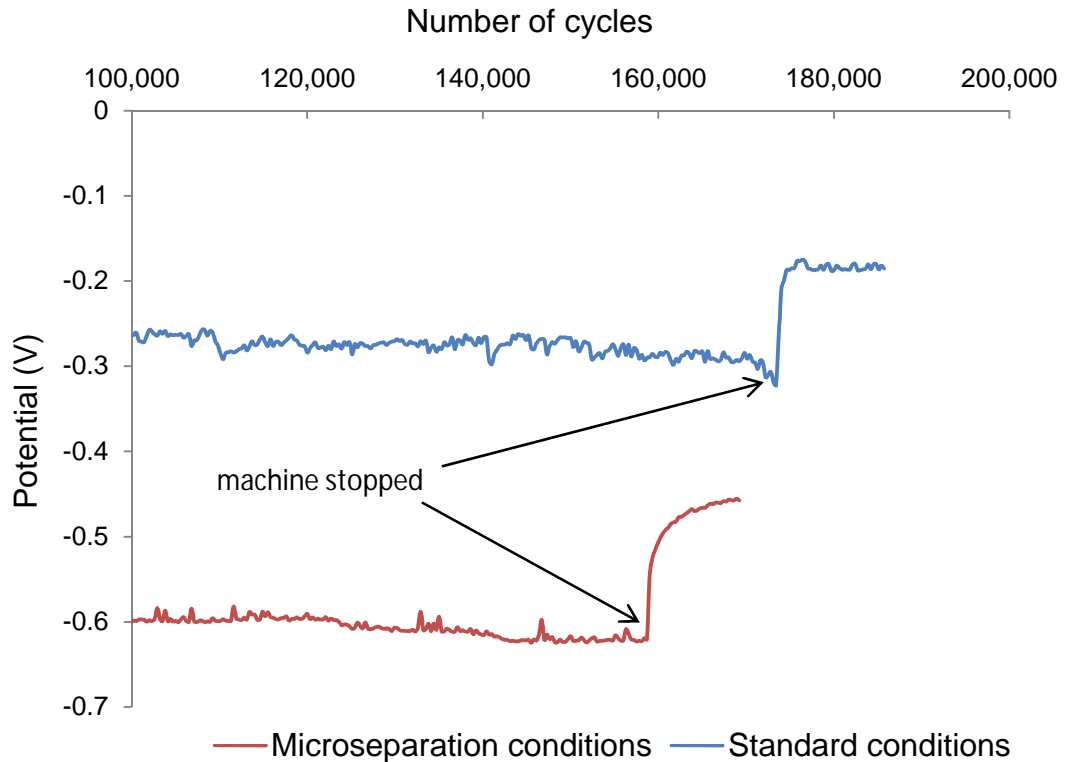
Figure 7.8: Recovery of OCP after stopping the sliding and loading of the bearings surfaces under both standard and microseparation conditions.

For the 28mm bearings, the initial shift to a more negative open circuit potential when the machine started was higher under edge loading conditions compared to standard conditions however, the difference was not statistically different ($p=0.18$ under the 45° cup inclination angle condition and $p=0.94$ under the 65° cup inclination angle condition, Figure 7.9). As the test progressed, the maximum shift in OCP to a more negative value was higher ($p=0.07$) under edge loading conditions (Figure 7.9). Increasing the cup inclination angle from 45° to 65° caused edge loading and increased depassivation of the surface. Under edge loading conditions due to microseparation, the shift in OCP was significantly ($p=0.04$) higher than under standard gait conditions. Moreover, the shift in the potential was higher under edge loading due to translational mal-positioning (microseparation conditions) than under edge loading due to rotational mal-positioning (steep inclination angle conditions).
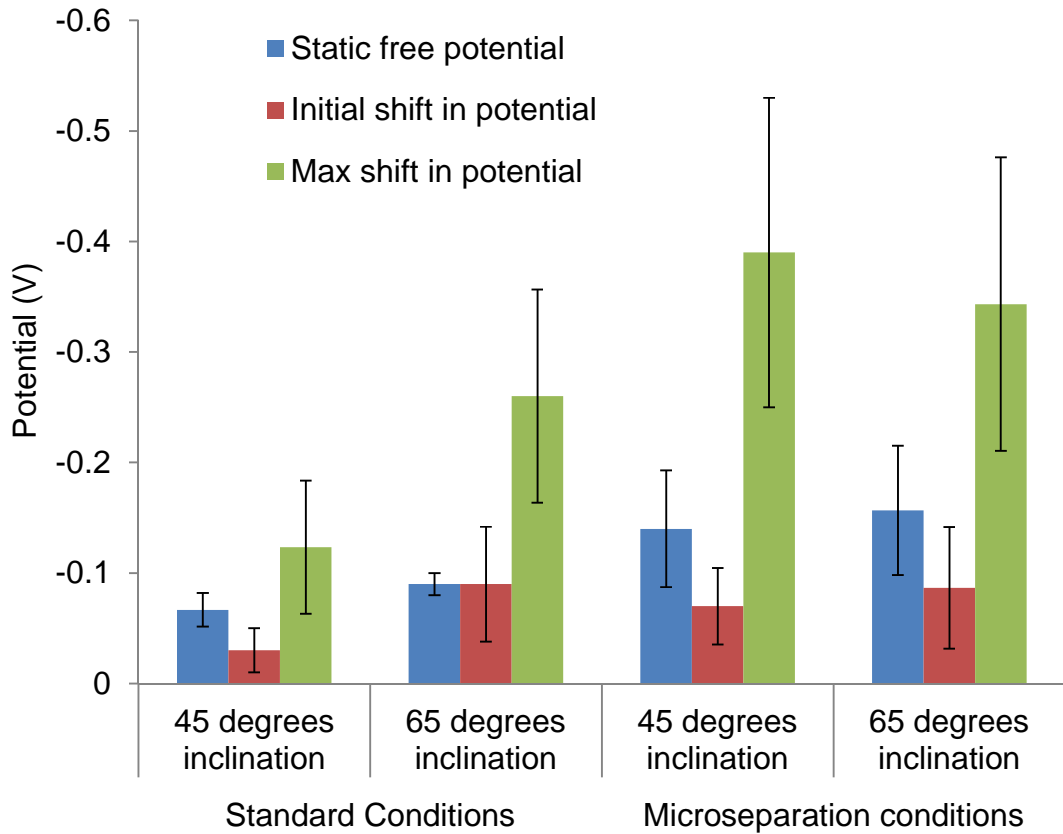
Figure 7.9: The mean static free potential, initial shift in potential and maximum shift in potential under the four different testing conditions for the 28mm MoM bearings.

For the 36mm bearings, the initial shift in OCP at the start of the test and the maximum shift after the 330,000 cycles of testing was significantly (p=0.007) higher under microseparation conditions compared to standard gait conditions (Figure 7.10). Under standard conditions, the wear of the 36mm bearings was below 1mm^3/million cycles. The initial shift in the OCP under standard conditions was lower compared to the initial shift under edge loading conditions due to rotational ma-positioning (p=0.10) and translational mal-positioning (p<0.01). As the test progressed, the maximum shift in OCP was higher under the 65° cup inclination angle conditions compared to the 45° cup inclination angle condition, however, this difference was no statistically significant (p=0.11). However, under microseparation conditions, the maximum shift in OCP was significantly different (p=0.04, Figure 7.10).
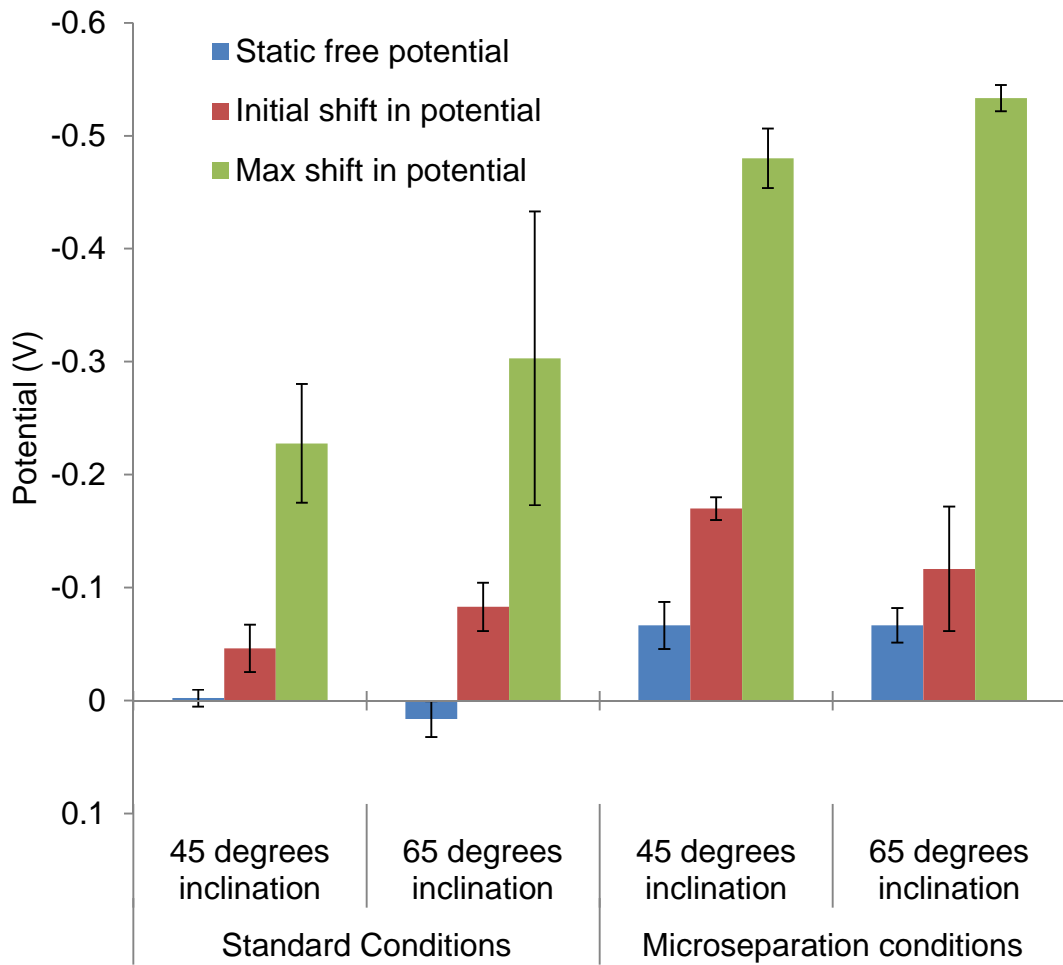
Figure 7.10: The mean static free potential, initial shift in potential and maximum shift in potential under the four different testing conditions for the 36mm MoM bearings.

There was a weak positive correlation between the level of the initial shift in potential and the total wear measured gravimetrically for both bearing sizes (Figure 7.11 and Figure 7.13). However as the test progressed, the shift in potential became more apparent under the edge loading condition where more wear was measured, and the correlation became stronger for both bearing sizes (Figure 7.12 and Figure 7.14).
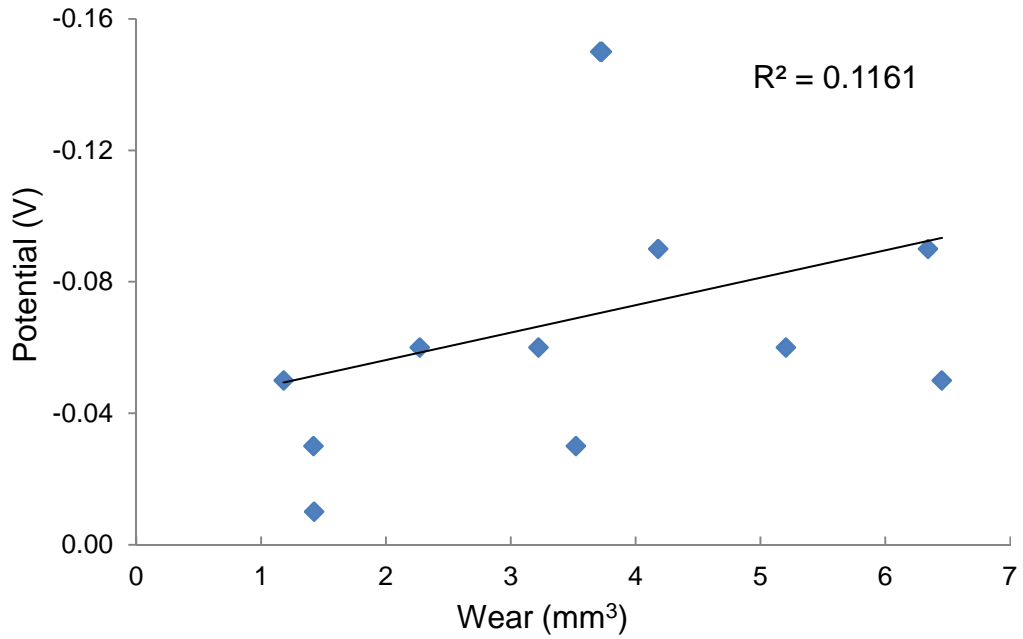
Figure 7.11: Correlation between the wear volume at one million cycles of testing and the initial shift in OCP when the sliding and loading started for the 28mm bearings.
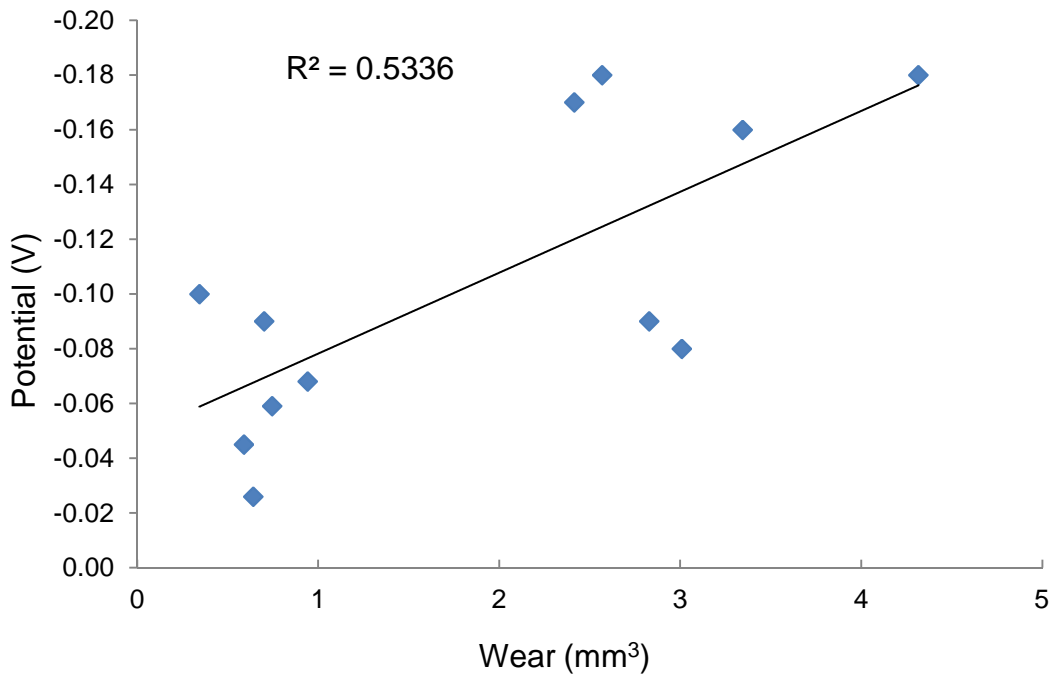
Figure 7.12: Correlation between the wear volume at one million cycles of testing and the initial shift in OCP when the sliding and loading started for the 36mm bearings.
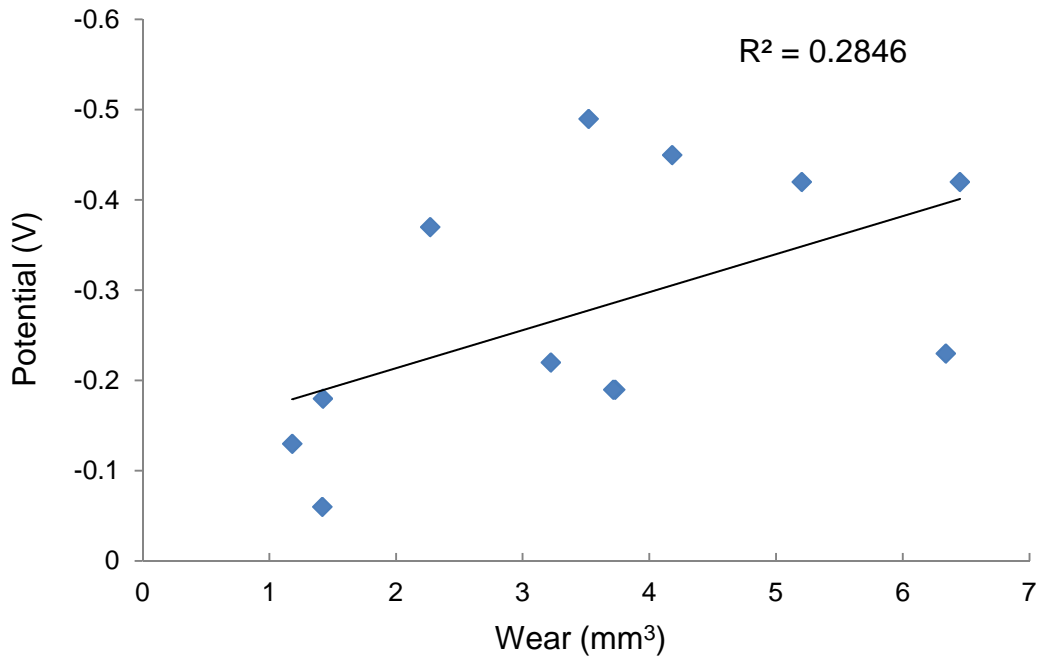
Figure 7.13: Correlation between the wear volume at one million cycles of testing and the maximum shift in OCP for the 28mm bearings.
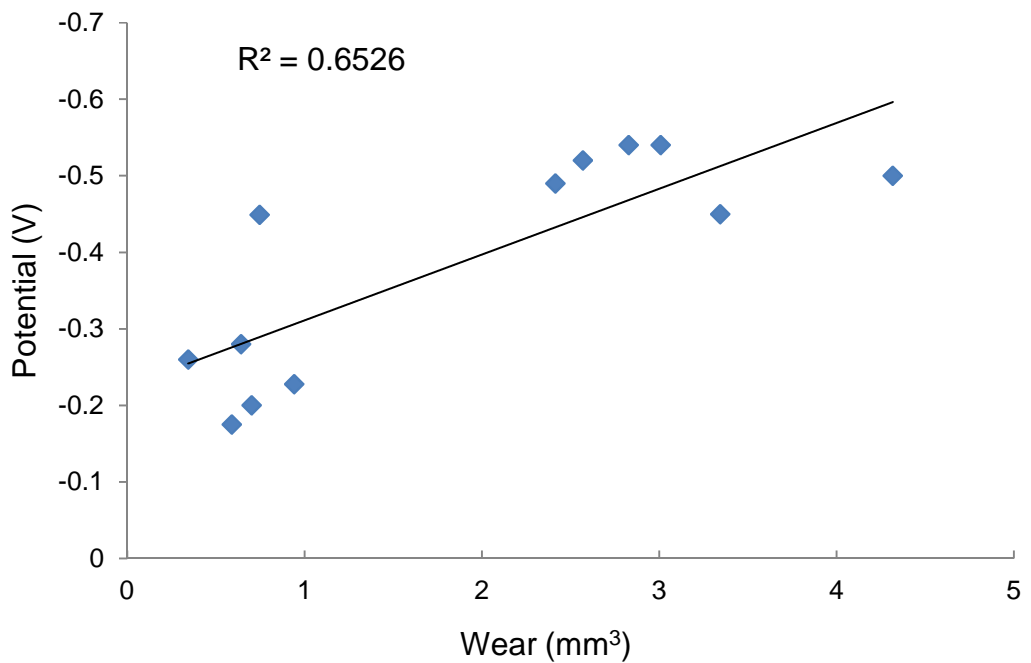
Figure 7.14: Correlation between the wear volume at one million cycles of testing and the maximum shift in OCP for the 36mm bearings.

7.4 Discussion and Conclusion

The total volume of material loss in metal-on-metal bearings is due to complicated phenomena that happen on the surface. Mechanical wear and corrosion are both responsible for this material loss (Totten and Liang, 2004). The mechanical wear has been shown to enhance corrosion rate and also corrosion of the surface could enhance the mechanical wear of the bearings (Yan et al., 2005). When the metal-on-metal bearings are exposed to loading and sliding, the CoCr material gets depassivated enhancing the corrosion on the surface. Previous tribometer studies using metal-on-metal materials have shown that corrosion could contribute up to 44% of the total damage present (Yan et al., 2005). Corrosion enhanced by wear and wear debris dissolution are the main two sources of ion release. Therefore, it is important to understand the corrosion behaviour of metal-on-metal bearings as well as mechanical wear under different loading regimes and kinematics.

As soon as loading and sliding were introduced to the bearing surfaces, the shift of OCP to more negative values indicate depassivation of the surface. This was consistent with previous simple bench tribometers tests (Yan et al., 2007a, Yan et al., 2007b). The original passive chromium oxide layers present at the surface protecting the bulk material were removed producing higher potential differences between the acetabular cup and the reference electrode. This shift was higher under the more severe edge loading conditions.

As the test progressed, the OCP kept shifting to a more negative state indicating the continued depassivation of the surface. The high shift in potential indicated a highly active material that can have a high corrosion rate. The maximum shift in potential was more negative under edge loading conditions, however this shift was not statistically significant for the 28mm bearings whereas it was for the 36mm bearings. This might be due to the high bedding in wear rate of the 28mm bearing to start up with under standard conditions (1.34mm^3 /million cycles) compared to the bedding in wear rate of the 36mm bearings (0.73mm^3 /million cycles).

Under all testing conditions, the OCP measurements were shifting in the negative direction at a steady rate. However, after approximately 60,000

cycles, the OCP on some stations showed recovery for a period of time before then dropping back to the OCP level before the recovery started. This happened at several points during the test in an inconsistent manner. This could be due to the formation of the tribofilm layer passivizing the surface for a short period of time (Hanawa et al., 2001, Hallab et al., 2003, Yan et al., 2006). Once this layer was removed again, the OCP shifted again to a more negative direction. This showed the dynamic nature of hip gait cycles condition. As well the dynamic loading applied, there were two rotational motions present; the internal/external rotation of the acetabular cup and the flexion/extension of the femoral head. This produced complicated contact mechanics of the bearing working in a mixed lubrication regime. These fluctuations in OCP measurements could relate to the fluctuation in the asperity interaction under the mixed lubrication regime. When contact occurred, the bare surface of the material was exposed to the environment surrounding the surface promoting corrosion. However, as the tribofilm was formed again and the lubricant helped separate the asperities, the severity of the contact was reduced and the corrosion rates decreased.

Although, there was a positive correlation between the shift in OCP measurement and the wear rate of the bearing determined gravimetrically, this correlation was not linear. This indicated the complex phenomena that occur on the surface of the bearing surfaces and the complexity of the interactions between mechanical wear and corrosion. Under edge loading conditions, the mechanical wear was significantly increased, producing more wear particle and larger size particles. This study shows that the surface became more active under edge loading conditions however, it was not clear if the proportion of the corrosive wear with respect to the total wear volume was also increased. In order to understand contribution of corrosion to the total damage under different testing conditions, more complex measurements could be undertaken. This was beyond the scope of this Chapter.

CHAPTER 8. GEOMETRIC MEASUREMENTS TECHNIQUE USING COORDINATE MEASUREMENT TECHNIQUES

8.1 Introduction

Geometric measurement techniques using a coordinate measuring machine (CMM) have been used previously to assess the volumetric wear of hip replacement bearings tested *in vitro* or retrieved from patients. These techniques have several advantages over the gravimetric analysis techniques:

- The original measurements of the component before test or implantation are not necessary and an estimate of the original surface can be estimated from any unworn portion of the component.

- The measurement provides a three dimensional construction of the component showing the area, depth and location of the wear patch on the components.

These techniques have also been used to assess the quality of the hip replacement bearings after manufacturing. The diameter and form of the components are assessed to determine the nominal clearance and the waviness of the prosthesis which these have been proven in previous studies to affect the tribological performance of hip replacement bearings, especially metal-on-metal bearings.

There are several factors that can affect the accuracy of these geometric measurement and analysis techniques and few recent publications have discussed wear measurements of retrieved hip bearings using CMM techniques (Bills et al., 2012, Lord et al., 2011). The manufacturers of the Legex 322 coordinate measuring machine (Mitutoyo, UK) used in this study have claimed that the accuracy of the machine is 0.8μm. However, in case of hip replacement bearings, there are several factors that can affect the accuracy of the measurements which can be split into three categories:

1. The machine configuration and set up
2. The components being measured

3. The analysis process
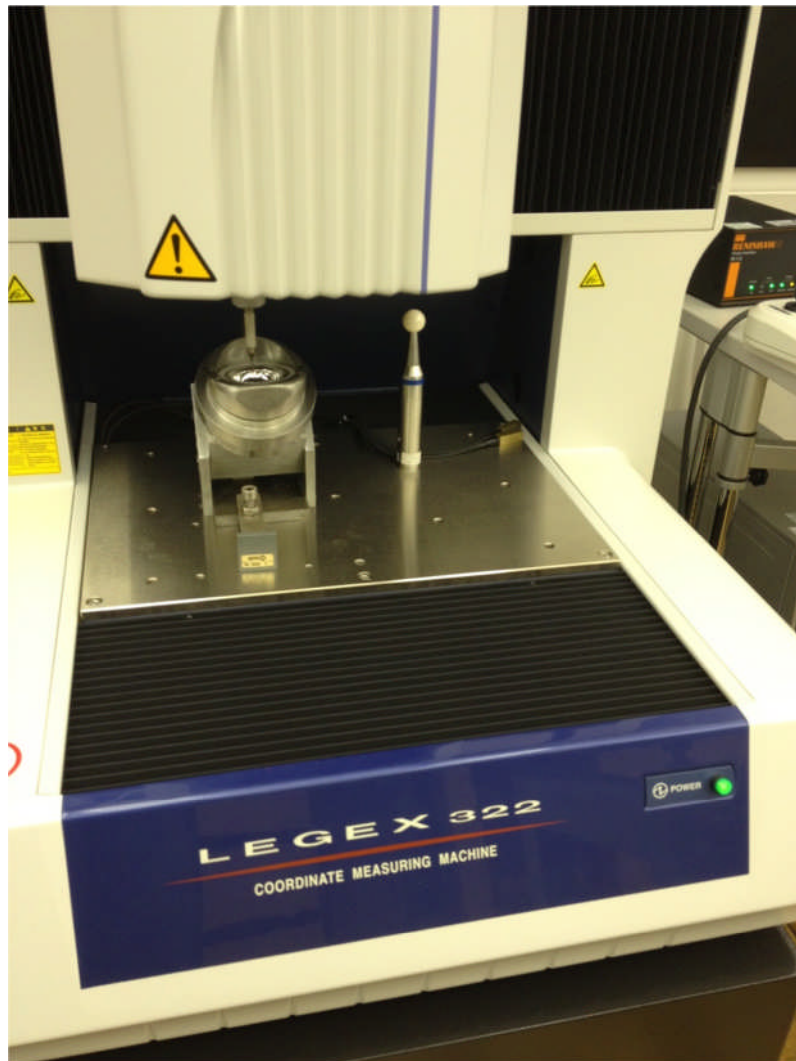
Figure 8.1: Mitutoyo Legex 322 CMM.

8.2 The effect of stylus size and configuration

The machine configuration and set up include the size and length of the stylus, the stylus and probe configurations and the total number of points recorded.

There are many styli sizes, extensions and connection available for CMM measurements (Figure 8.2) and choosing the right configuration for each specific measurement is essential in obtaining the best accuracy possible.

Figure 8.2: Some styli, extensions and connections available for CMM measurements (image taken from Renishaw technical specifications H-1000-3200-15-A).

The smaller the stylus the more details it picks on the surface of the component being measured especially if the components have narrow and shallow wear areas (Figure 8.3). However, a 1mm stylus has a larger form error than a 2mm one, making it more difficult to compensate for the stylus radius when assessing the data points. Also, the assembly of the stylus can also affect the accuracy of the measurement (Figure 8.4). A five-star styli configuration can be used to allow the measurement of larger size femoral heads which have larger curvatures below their equators that a single stylus configuration cannot reach. Also, having a short extension would provide less bending of the tip of the stylus and thus better accuracy (Figure 8.5).
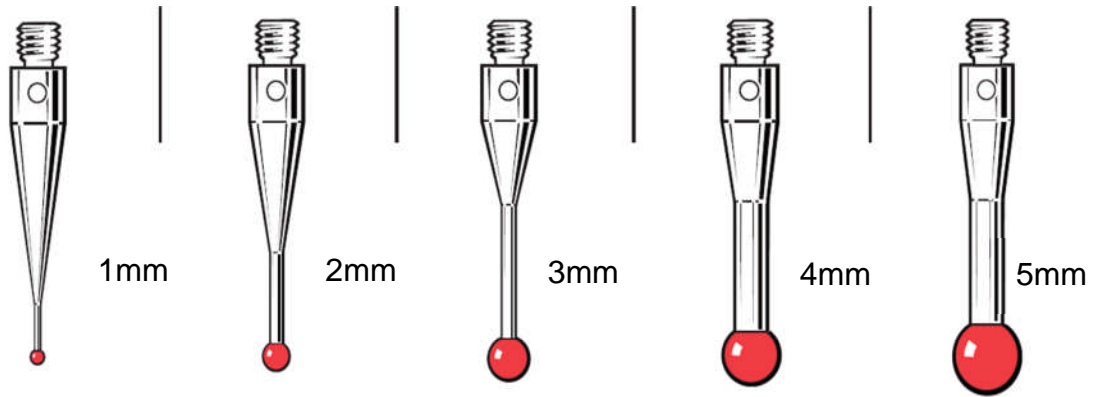
Figure 8.3: Ruby silicon nitride zirconia styli with different diameter sizes.
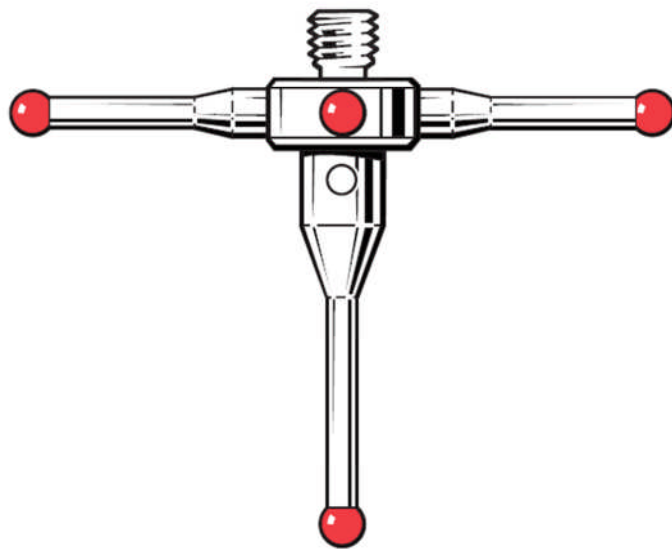
Figure 8.4: A star Styli configuration comprises of 5 styli that can be of the same or different sizes.
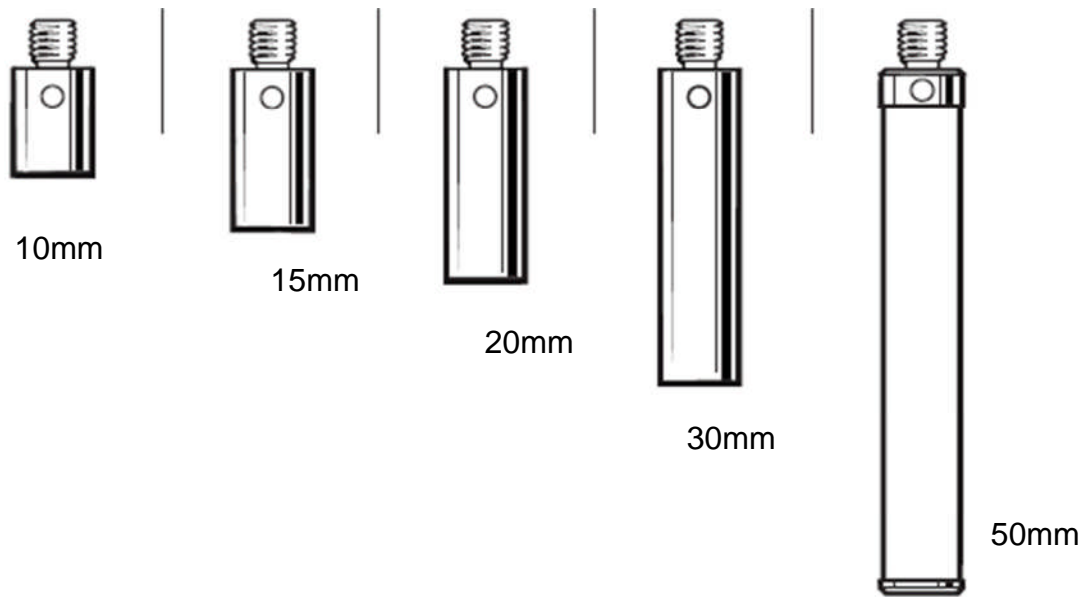
Figure 8.5: Different extension that can be used to allow for greater reach of the stylus.

The number of measurement points is very important when determining the wear volume of the measured components. The more points taken, the more details and information will be picked up from the surface and thus better accuracy (Figure 8.6). However, taking more measurement points is time consuming and processing the data will need large processing power, so it is important to establish a consistent and accurate measurement technique taking all these factors into account.
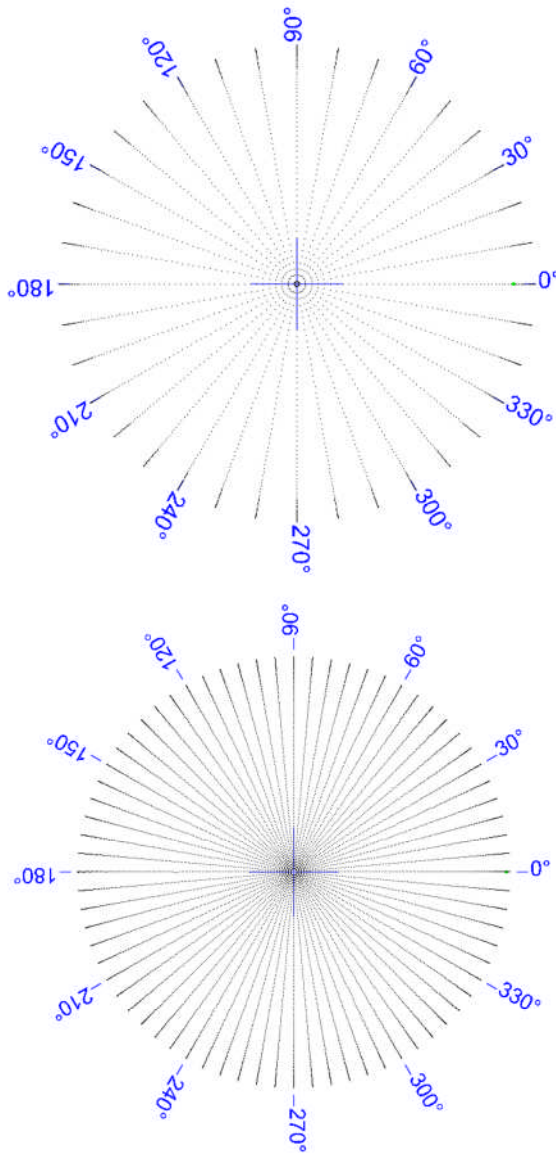
Figure 8.6: Measurement points recorded on a femoral head. The image on the left has 2,808 measurement points whereas the image on the right has 7,704 points picking up more details on the surface.

An unworn ceramic femoral head was used to compare the accuracy of the different size styli and comparing a 1 stylus to 5-star styli configurations. The same femoral head was used with the same measurement parameter. With a single stylus configuration, the 1mm stylus showed a form error that ranged from -2µm to +5µm (Figure 8.7) while the 2mm stylus had a form error in the range of ±2µm (Figure 8.8), and the 3mm stylus showed a form error in the range of ±2µm (Figure 8.9). However, larger form error was

obtained when the 5-star styli configuration was used for both styli sizes. The 1mm 5-star styli configuration showed a form error that ranged from -6µm to +3µm (Figure 8.10) while the 2mm 5-star styli configuration had a form error range from -4µm to +5 µm (Figure 8.11).
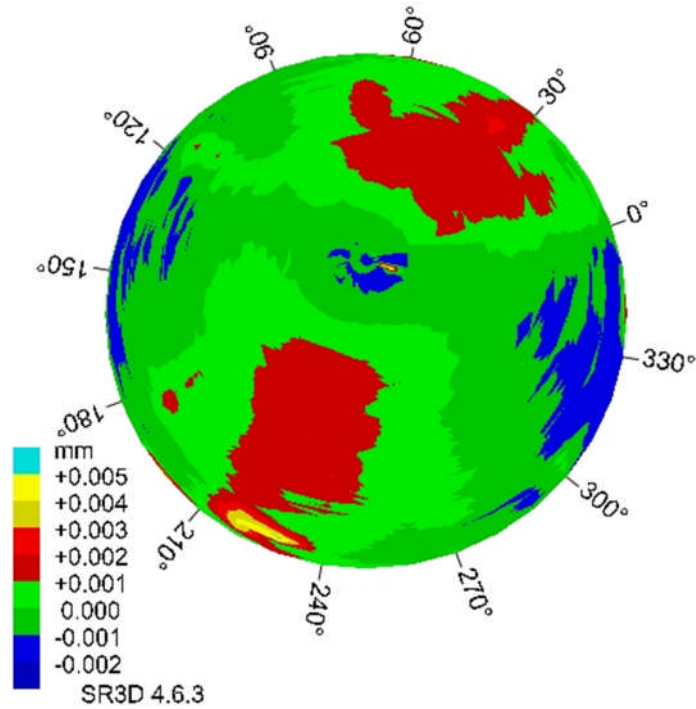
Figure 8.7: Form error on a 28mm ceramic femoral head measured using a 1mm single stylus configuration.
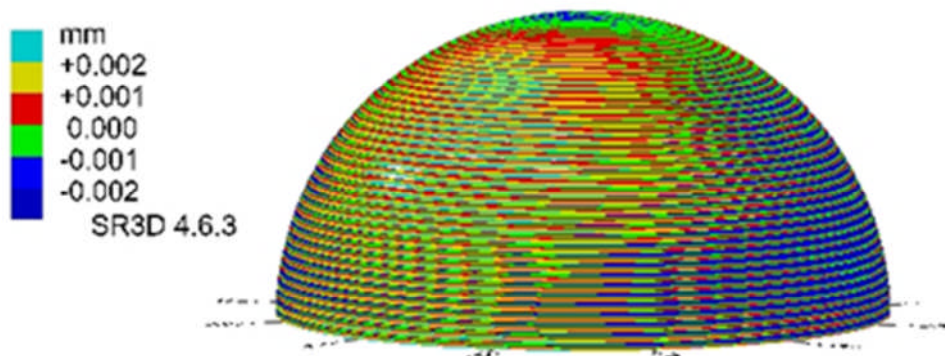
Figure 8.8: Form error on a 28mm ceramic femoral head measured using a 2mm single stylus configuration.
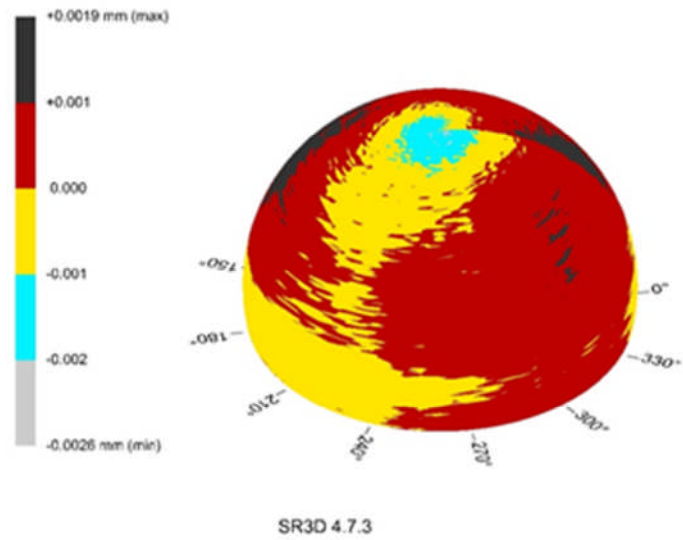
Figure 8.9: Form error on a 28mm ceramic femoral head measured using a 3mm single stylus configuration.
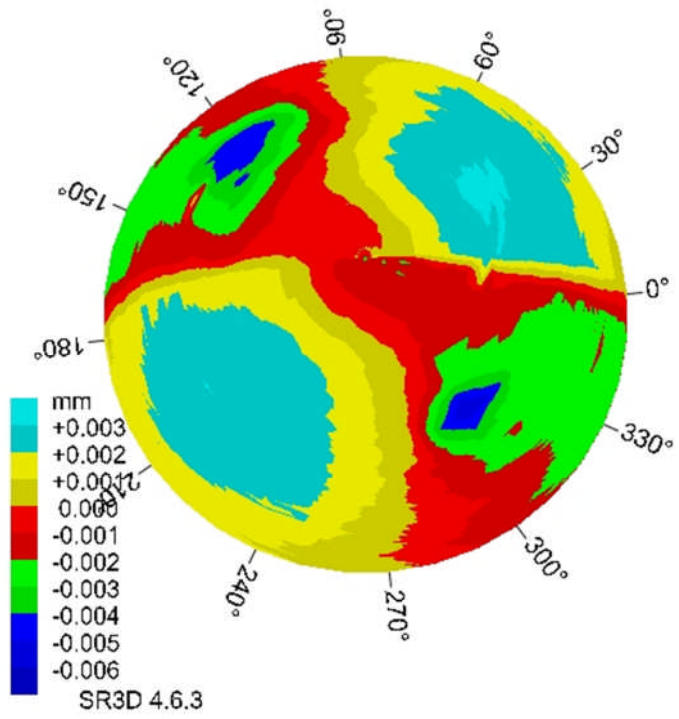
Figure 8.10: Form error on a 28mm ceramic femoral head measured using a 1mm 5-star styli configuration.
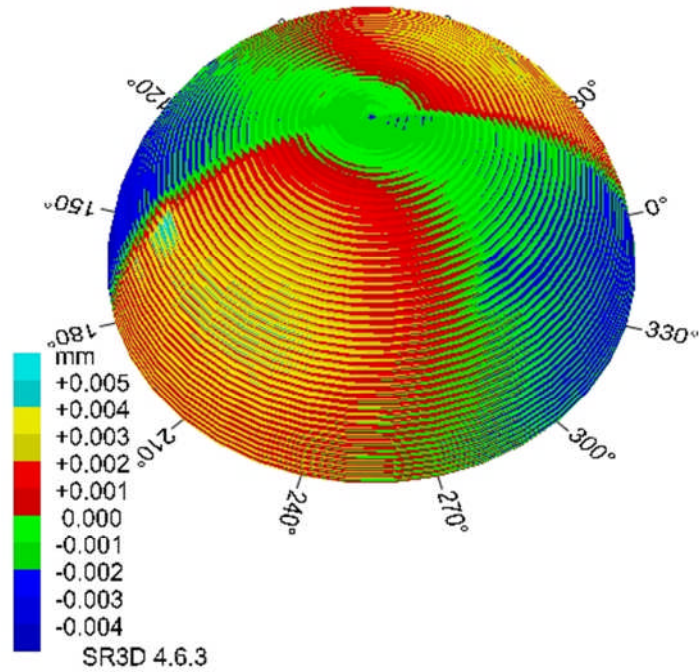
Figure 8.11: Form error on a 28mm ceramic femoral head measured using a 2mm 5-star styli configuration.

8.3 Data Analysis

The coordinate measuring machine was programmed to collect data in the form of traces starting at the pole; the femoral head was placed on a vertical spigot while the acetabular cup was placed with its rim plane parallel to the machine's XY plane. The centre of the component was first determined by taking 25 points over the unworn part of component's surface. Then the traces were taken by revolving the Cartesian coordinate system about the vertical axis passing through the centre of the component (Figure 8.12). The x, y and z coordinates of each measurement point, with the origin taken at the centre of the component, were exported to the SR3D data analysis software developed in collaboration with Tribology solutions Ltd.
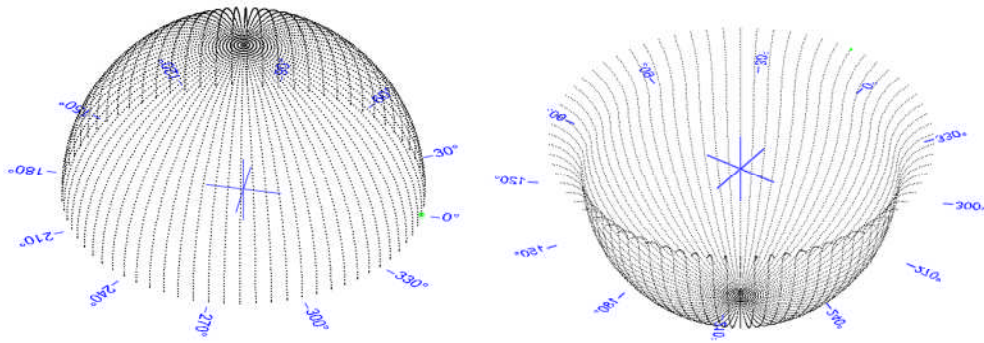
Figure 8.12: Data points taken on the surface of a femoral head (left) and acetabular cup (right) using the CMM by taking traces about the vertical axis.

Once the data points were exported, a nominal sphere was chosen using the data points over the unworn part of the measured surface (Figure 8.13). For the acetabular cup, the nominal sphere was chosen over the unworn surface of the polished bearing surface excluding any points on the chamfer. Then the traces from the unworn region of the surface were revolved about the vertical axis, passing through the centre of the nominal sphere, to form the reference surface (Figure 8.14). A worn acetabular cup was measured and analysed using the SR3D software. Firstly, the nominal sphere was determined using the bearing surface and excluding the chamfer from the fit. The outcome shows the wear area on the bearing surface and the chamfer as well (Figure 8.15 top). By performing the next step where the traces from the unworn region of the surface were revolved about the vertical axis, it was possible to determine the real penetrations and present the wear area accurately (Figure 8.15 bottom).
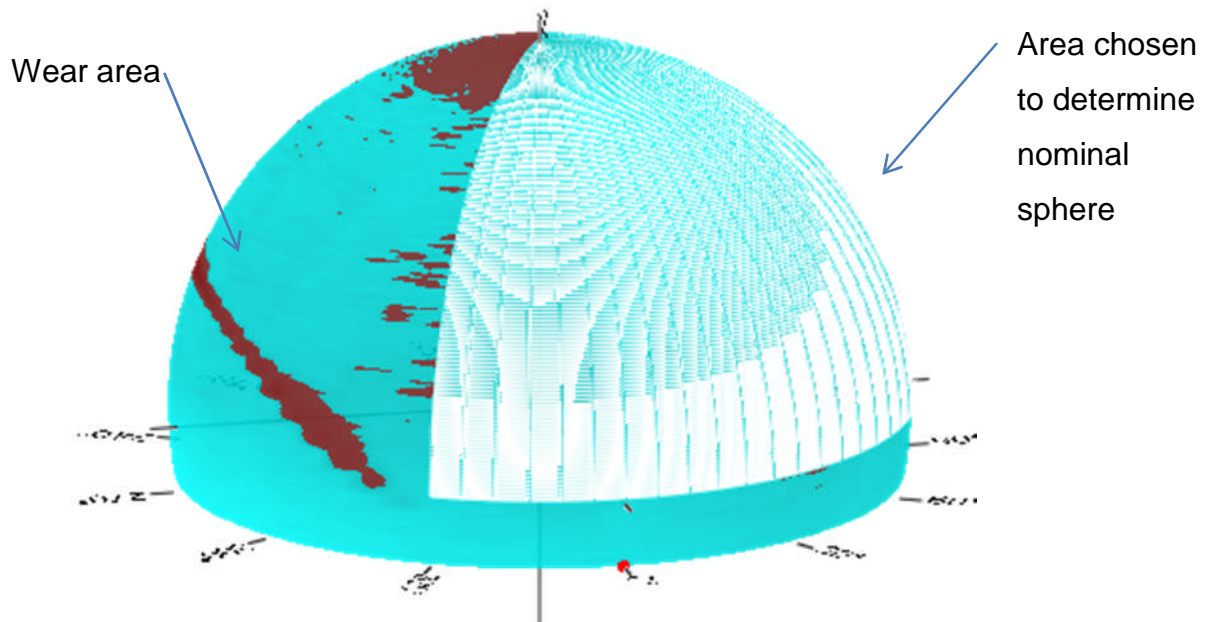
Figure 8.13: the meshed area shows the unworn region chosen to determine the nominal sphere. The grey regions on the surface include points that are below the surface of the nominal sphere.
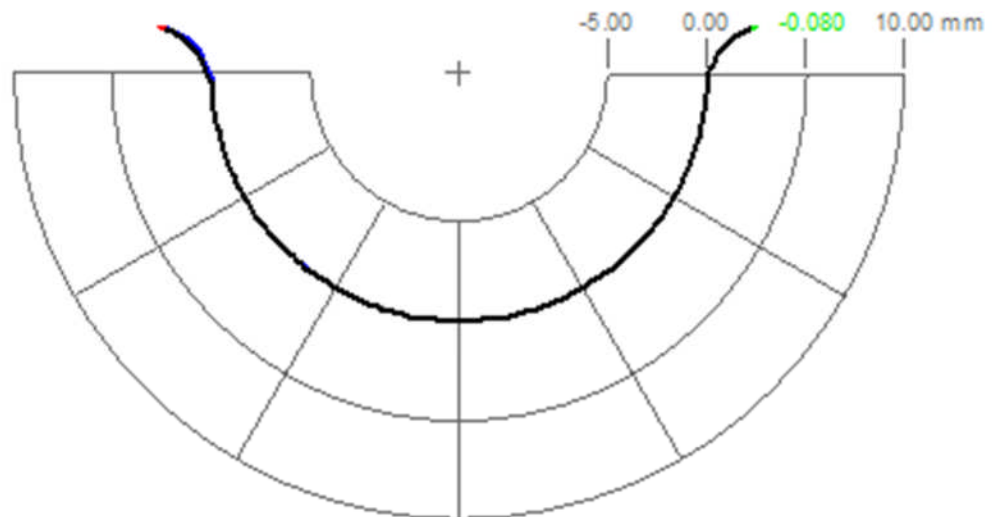
Figure 8.14: Two joined traces at the pole of the component. Few traces from the unworn region are used to form the reference surface.

The chamfer excluded from the nominal sphere fit

Surface representing unworn surface
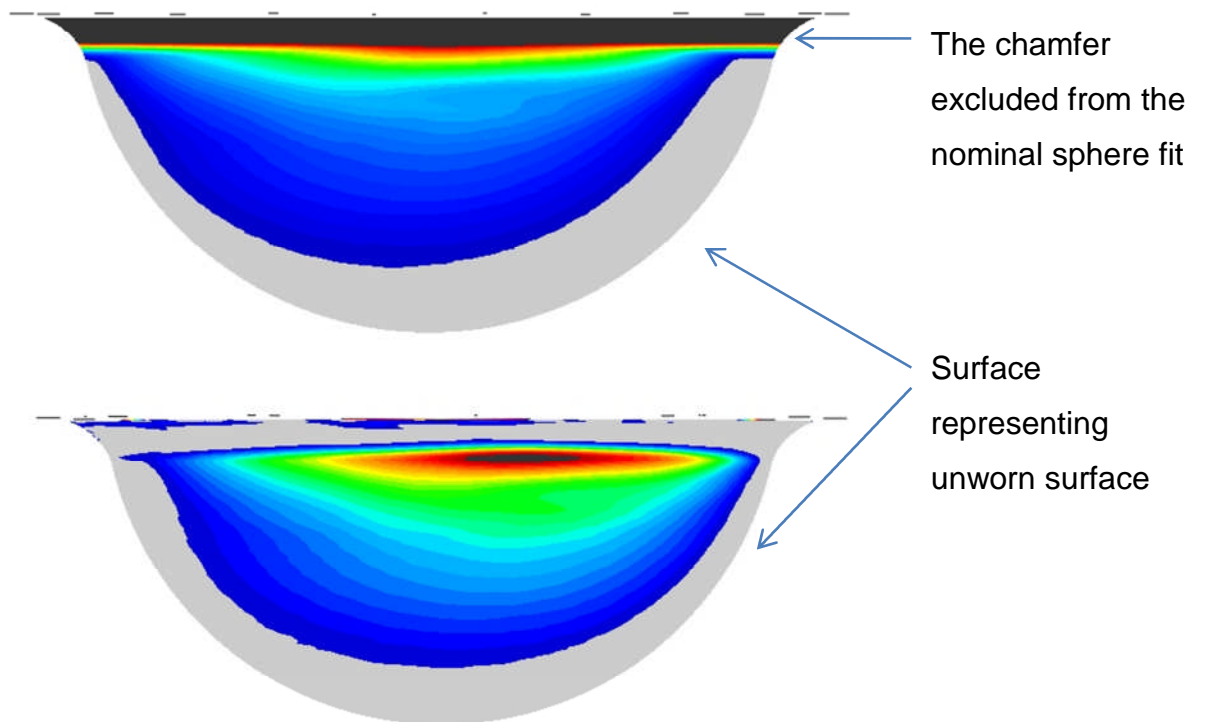
Figure 8.15: An analysed 3D reconstruction of a worn acetabular cup. The top image shows the acetabular cup with the chamfer excluded from the analysis whilst the bottom image shows the wear are with the chamfer taken into account.

8.4 Assessment of Volumetric Wear on Femoral Heads and Acetabular Cups

Before determining the wear volume on worn hip replacement bearing it was important to understand the resolution of the analysis technique. For this purpose ceramic heads were used and 72 traces were taken with 5 degrees spacing about the vertical axis. Each trace consisted of many points with 0.2mm spacing starting at the pole and finishing -2mm below the equator. A 3mm stylus was used.

The calibration ball supplied by the manufacturer of the CMM, Mitutoyo, was assessed. It was a size 20mm diameter ceramic ball with very high quality

surface finish. The measurement showed a form error of ±1μm (Figure 8.16). The contour obtained had a volume 0.01mm^3 lower than the volume of the nominal sphere determined from all the measurement points. However, when assessing worn samples tested on the hip simulators the wear area had to be excluded from the nominal sphere fit. So in order to determine the contour volume deviation from the nominal sphere, only one portion of the measured data points could be used to determine the nominal sphere. This increased the deviation of the contour volume. When the data points from one side of the ball were used, as shown in Figure 8.17, the contour obtained had a volume 0.07mm^3 lower than the volume of the nominal sphere. This means if this ball had a wear area that covered one side of the ball, the wear volume obtained will have an error of 0.07mm^3.

The calibration ball was measured three times. Each time the ball was removed from the machine, then placed back to re-measure. The results are shown in table 8.1.

Table 8.1: Contour volume deviation repeatability. Negative sign indicates that the volume of the contour measured was smaller than the volume of the nominal sphere.

	Volume deviation when all data points were used to determine nominal sphere (mm^3)	Volume deviation when the data points from one side of the ball were used to determine nominal sphere (mm^3)
Repeat 1	-0.010	-0.070
Repeat 2	-0.004	-0.053
Repeat 3	-0.007	-0.036

calibration ball
(contours shown relative to nominal sphere)
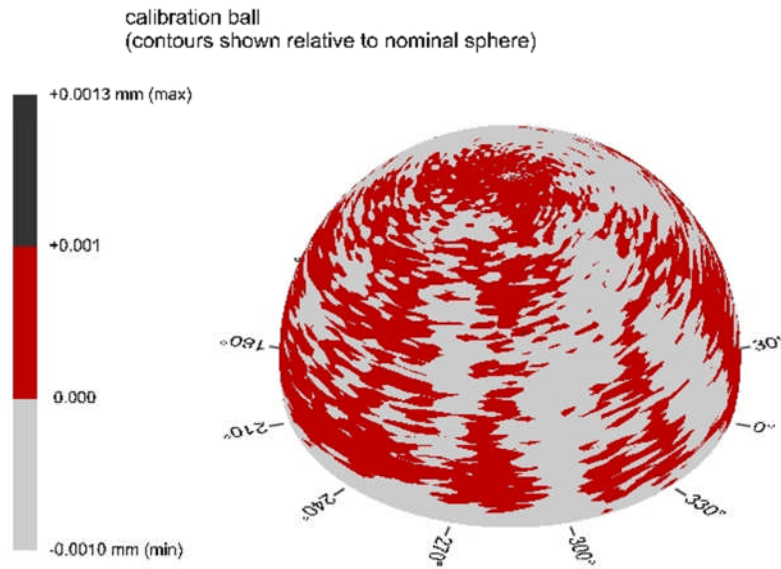
Figure 8.16: The contour of the ceramic calibration ball relative to a nominal sphere determined using all data points.
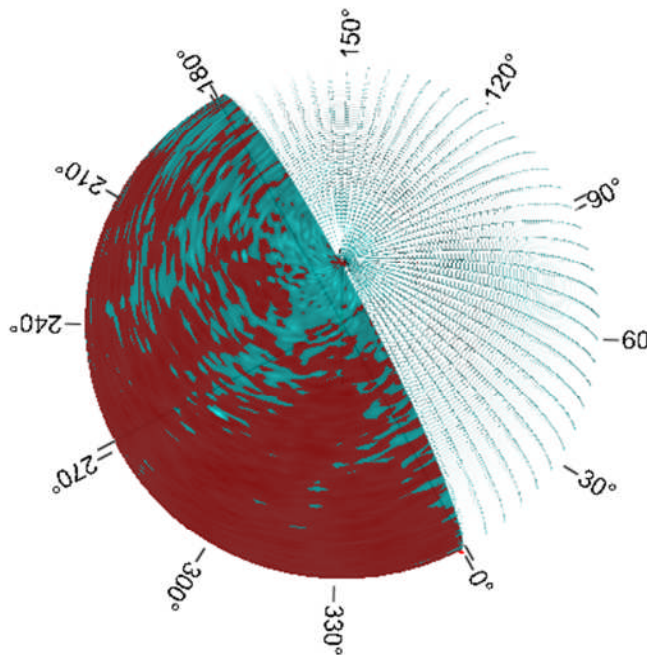
Figure 8.17: The white meshing indicate all the data points chosen to determine the nominal sphere.

An unworn 36mm ceramic head was measured using the same measurement parameters as the calibration ball. The contour variation from the nominal sphere was slightly different from the contour of the calibration

ball (Figure 8.18). Although the range of the form error (-2µm to +1.5µm) was similar to that of the calibration ball, the volumetric analysis would be different due to the difference in the contour pattern. When using all the measurement points to obtain the nominal sphere, the volume difference over the measured femoral head was 0.23mm^3 higher than the nominal sphere. However, when reducing the data points used to obtain the nominal sphere to one side (half) of the femoral head, the volume difference increased to 0.84mm^3. This meant that if this femoral head was to be tested on the hip simulator and the wear volume had to be assessed, the determined wear volume would have an error of up to 0.84mm^3.
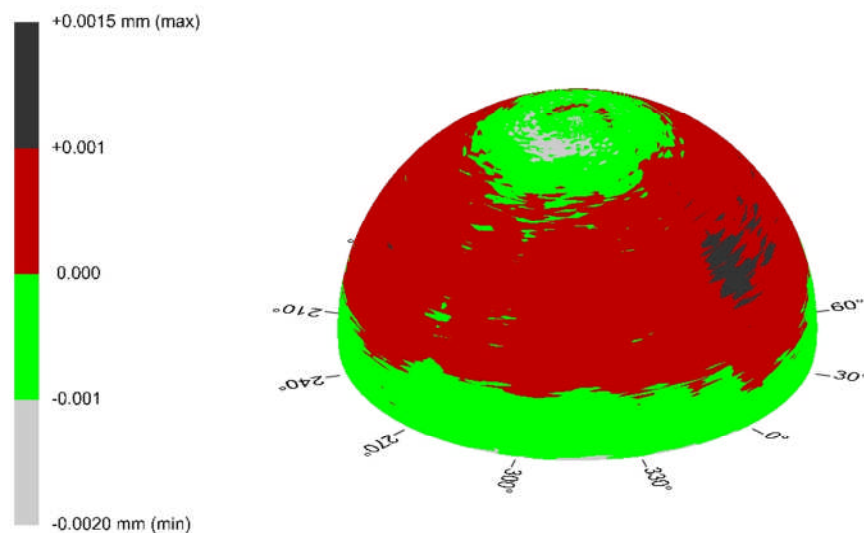
Figure 8.18: Contour of size 36mm BIOLOX delta ceramic head. The contour shows a form error range between -2.0µm to +1.5µm.

Under a hip simulator test the wear area on the ceramic head covered a small proportion of the femoral head surface so in order to determine the volumetric wear, it was possible to exclude a large proportion of the femoral head from the calculations. This reduced the error due to the deviation of the contour of the surface from the nominal sphere. The contour of the ceramic head was split into three regions, the bottom region, the middle region and the top region. The volume difference was assessed when constraining the nominal sphere and volume patch calculation to these three regions.

When choosing the bottom region (Figure 8.19A), the volume of the contour was 0.29mm^3 lower than that of the nominal sphere. This was also the case when choosing a smaller band of data points in the middle region (Figure

8.19B) and top region (Figure 8.19C); the volume difference dropped to 0.29mm^3 and 0.03mm^3 respectively. These analysis steps were repeated three times on the same 36mm head using three consecutive measurements on the CMM, which were done by removing the samples and placing it again on the taper (Table 8.2). The deviation error was lowest at the pole of the head, which could be due to the polishing technique of these femoral heads, which resulted in very small form error at the pole.

Table 8.2: Contour volume deviation repeatability when using data points from different regions on the surface. Negative sign indicates that the volume of the contour measured was smaller than the volume of the nominal sphere.

	Repeat 1	Repeat 2	Repeat 3
Volume deviation when all data points were used to determine nominal sphere (mm^3)	0.23	0.23	0.27
Volume deviation when the data points from one side of the head were used to determine nominal sphere (mm^3)	0.39	0.71	0.47
Volume deviation when the data points from the bottom region of the head were used to determine the nominal sphere (mm^3)	-0.29	-0.01	-0.27
Volume deviation when the data points from the middle region of the head were used to determine the nominal sphere (mm^3)	-0.29	-0.06	-0.25
Volume deviation when the data points from the top region of the head were used to determine nominal sphere (mm^3)	-0.03	-0.03	-0.04
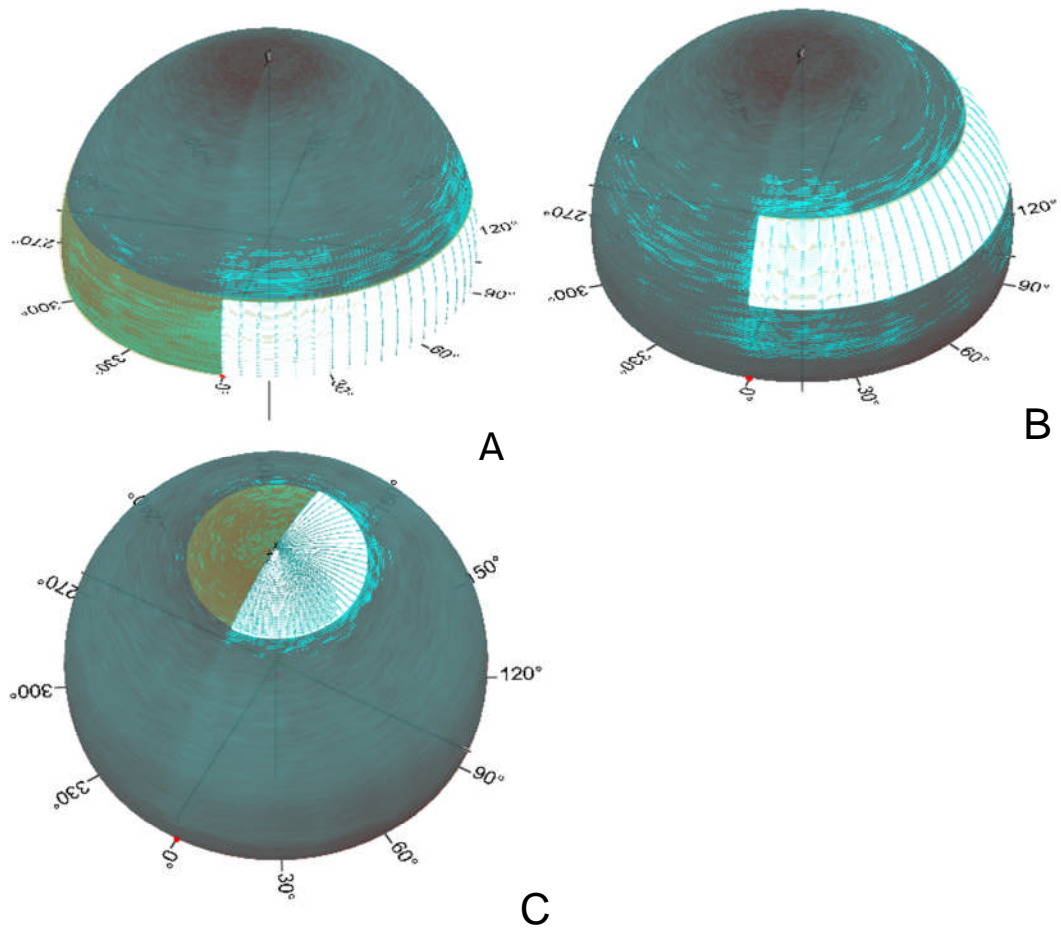
Figure 8.19: The bands of measurement points chosen to construct the nominal sphere which split into three regions, bottom (A), middle (B) and top (C) regions.

The values obtained for this 36mm ceramic head could not be generalised for different femoral head sizes and materials. The finished geometry of each femoral head was highly dependent on the material and the finishing quality. Some femoral heads such as the 36mm ceramic head presented above had very good finished geometry with form error of +/-1.5µm, however, metal femoral heads had different form errors. A 28mm metal head had a form error that ranged from -2.5µm to +2µm (Figure 8.20) and a 36mm metal head had a form error that ranged from -6.8µm to +4.7µm (Figure 8.21). The same analysis to that of the 36mm ceramic head was done on the two metal heads and the volume deviations are summarised in Table 8.3. This affected the contour volume deviation from the nominal sphere showing that the condition of the component before the wear is introduced is crucial

in understanding the minimum wear volume that can be accurately determined. Also it is important to understand the surface profile and use the appropriate data points to generate the nominal sphere so volume of the wear area can be determined as accurately as possible.
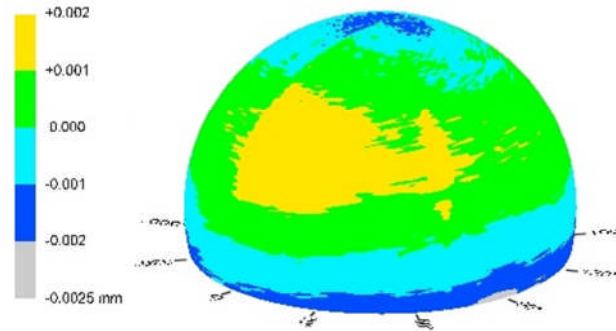
Figure 8.20: Contour of size 28mm metal head. The contour shows a form error range between -2.5µm to +2.0µm.
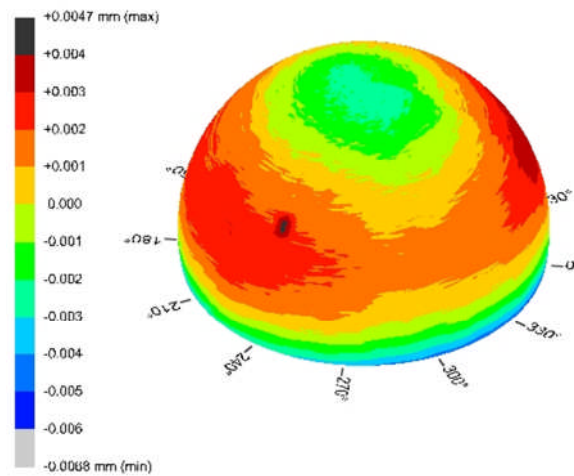
Figure 8.21: Contour of size 36mm metal head. The contour shows a form error range between -6.8µm to +4.7µm.

Table 8.3: Contour volume deviation for the 28mm and 36mm femoral heads using data points from different regions on the surface. Negative sign indicates that the volume of the contour measured was smaller than the volume of the nominal sphere.

	28mm Head	36mm head
Volume deviation when all data points were used to determine nominal sphere (mm^3)	0.24	0.96
Volume deviation when the data points from one side of the head were used to determine nominal sphere (mm^3)	0.46	3.2
Volume deviation when the data points from the bottom region of the head were used to determine the nominal sphere (mm^3)	-0.17	-0.58
Volume deviation when the data points from the middle region of the head were used to determine the nominal sphere (mm^3)	-0.19	-0.32
Volume deviation when the data points from the top region of the head were used to determine nominal sphere (mm^3)	-0.02	-0.02

8.5   Analysis of worn components

The hip replacement bearing couples tested on the Leeds II hip simulator were measured using the CMM and the data was analysed using the SR3D software. The components used in this study were the 28mm and the 36mm ceramic-on-ceramic bearings and the 36mm metal-on-metal bearings tested on the hip simulator for 3 million cycles under standard conditions and 3 million cycles under microseparation conditions. Due to edge loading conditions under microseparation conditions, all femoral heads had stripe wear and the wear area on the acetabular cups was at the rim.

8.5.1   Wear analysis on the metal-on-metal components

The geometric measurement method and analysis technique were developed after the components used in Chapter 4 (28mm MoM bearings) have been used for the tribocorrosion test presented in Chapter 7, which meant the component were not in a condition to be measured on the CMM.

The first set of components measured on the CMM was the 36mm metal-on-metal bearings. The wear area on the femoral head spanned few millimetres below the equator of the head which a 2mm straight stylus could not reach. For this reason a 5 star 2mm stylus configuration (Figure 8.4) was used to measure the femoral heads and a straight 2mm stylus (Figure 8.3) was used to measure the acetabular cups. The 5 star stylus configuration produced a form error 3µm higher than the straight stylus (Figure 8.8 and Figure 8.11), but it was decided that this was acceptable as the measured wear penetration was in the order of tens of microns. The femoral head were measured by taking 2,808 data points taken in the form of 36 traces rotated by 10 degrees from each other about the vertical axis. Each trace consisted of 78 points with a pitch of 0.5mm starting at the pole and finishing 7mm below the equator. Analysis of the unworn part of the femoral heads showed form deviations of ±10µm (Figure 8.22). The acetabular cups were measured by taking 2,052 points in the form of 36 traces rotated by 10 degrees from each other about the vertical axis. Each trace consisted of 57 points with a pitch of 0.5mm starting at the pole and finishing at the rim of the cup. The last three points of each trace lied on the chamfer of the rim.

Three dimensional reconstructions of the femoral head surfaces and the acetabular cups surfaces were obtained using the SR3D software. The unworn region of the surface was given an even grey colour regardless of the scale of the form deviation. The technique used to determine the volumetric wear on the femoral heads and acetabular cups was based on the technique discussed above. The appropriate region of data points was used to determine the nominal sphere and based on the unworn regions of the femoral heads; the accuracy of the calculated volumetric wear was ±1.5mm^3 for the femoral head and ±1.0mm^3 for the acetabular cups. The femoral heads had larger error due to the use of the 5 star stylus

configurations. Taking the error contributed by the form error and the measurement and analysis, the wear volumes obtained by the CMM were in good agreement with that determined gravimetrically (Figure 8.25 and Figure 8.26).
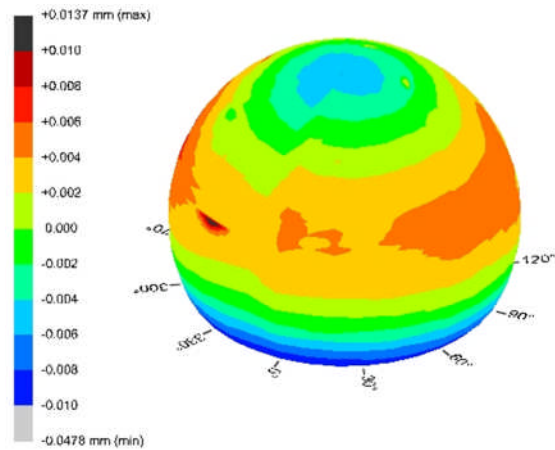
Figure 8.22: Contour of the unworn region of the 36mm metal head measured using the star stylus. The contour shows a form error of ±10μm over the unworn surface.
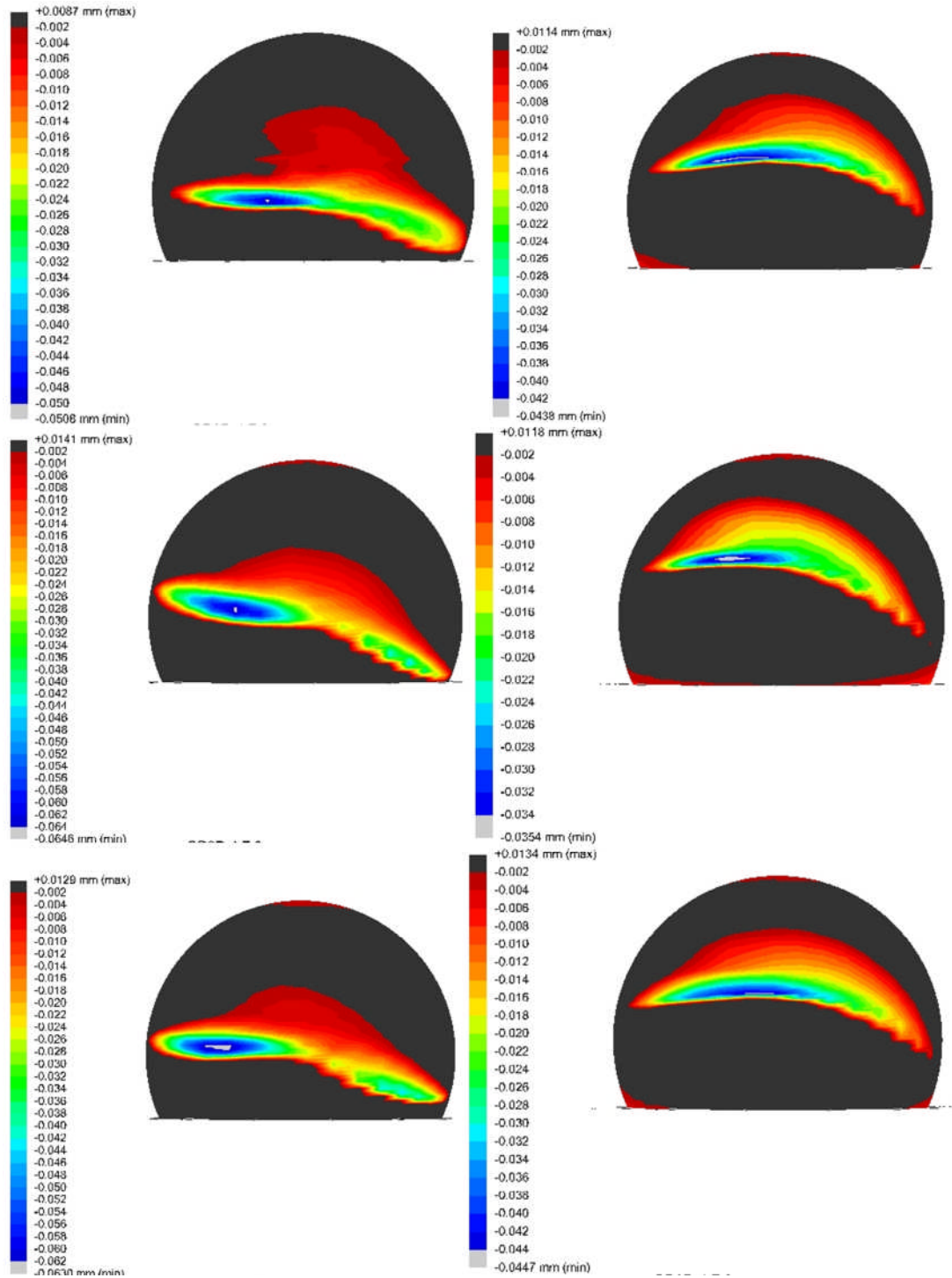
Figure 8.23: Three dimensional reconstruction of the wear are on the femoral heads using the 5 star stylus. The dark grey region represents the unworn area on the femoral head or an area with small penetration which was within the accuracy of the measurement technique.
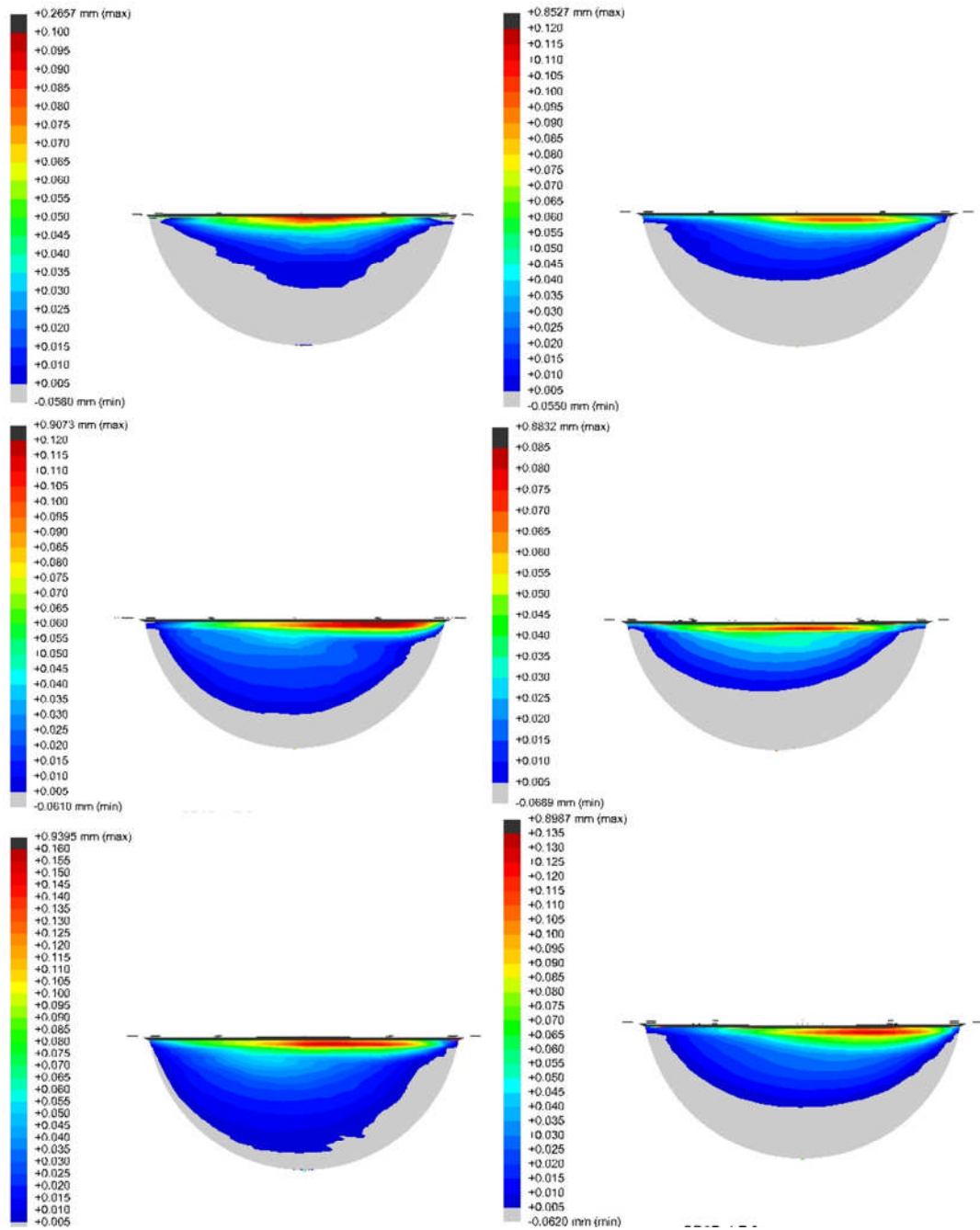
Figure 8.24: Three dimensional reconstruction of the wear are on the acetabular cup using 2mm straight stylus. The light grey region represents the unworn area on the surface of the cup or an area with small penetration which was within the accuracy of the measurement technique.
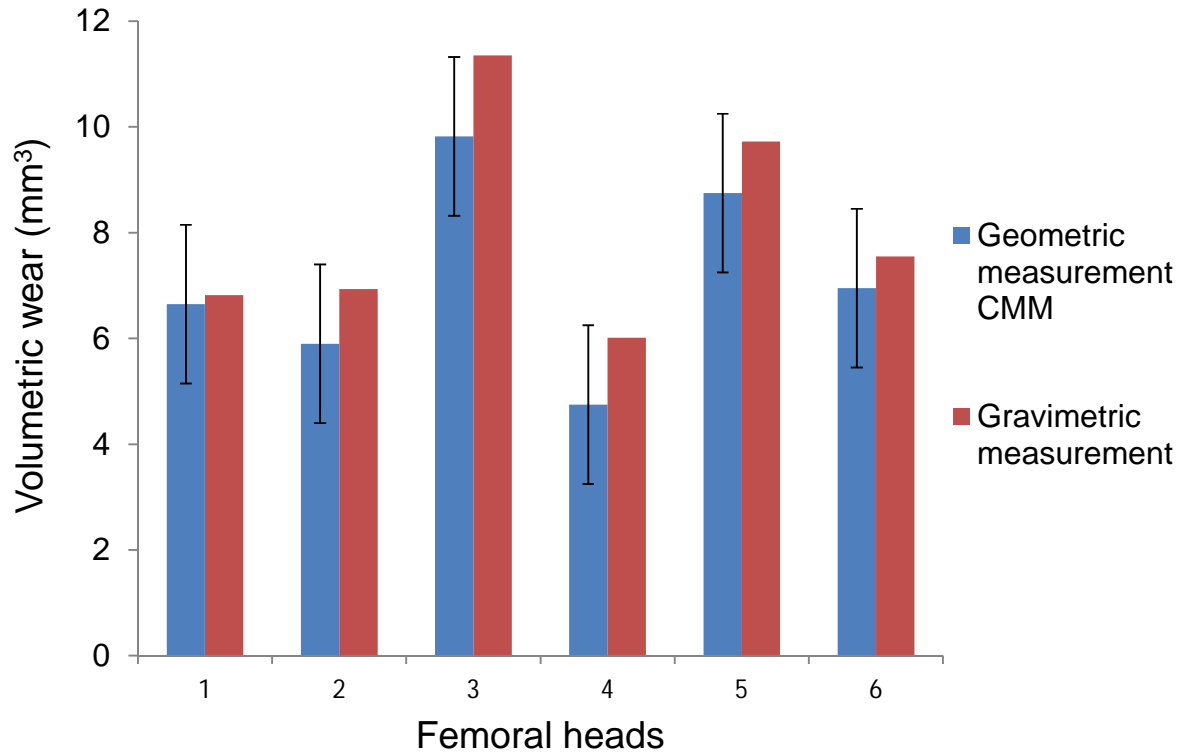
Figure 8.25: Volumetric wear of the 36mm femoral heads determined gravimetrically and measured using the CMM. The error bars represent the volumetric deviation error in the CMM measurements.
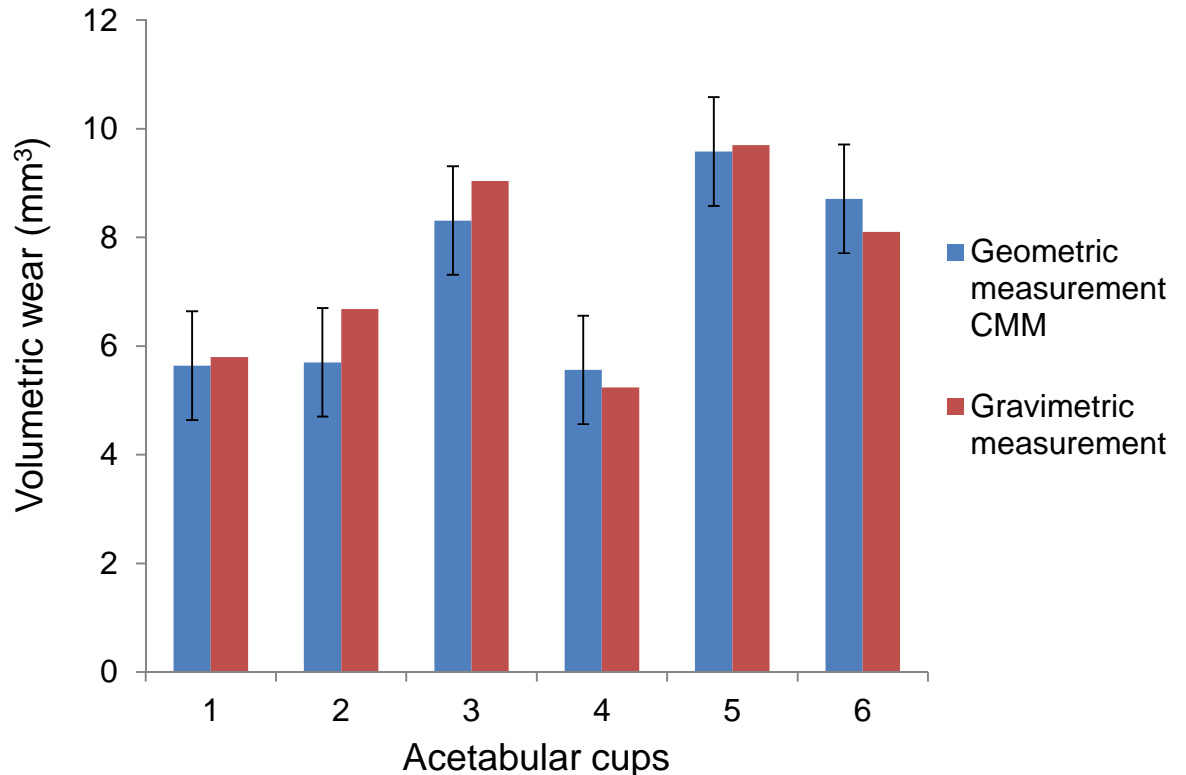
Figure 8.26: Volumetric wear of the 36mm acetabular cups determined gravimetrically and measured using the CMM. The error bars represent the volumetric deviation error in the CMM measurements.

8.5.2 Wear analysis on the ceramic-on-ceramic components

The ceramic femoral heads from the ceramic on ceramic studies on the 28mm and the 36mm bearings were also measured using the CMM to determine the volumetric wear. The penetration wear on the ceramic head are significantly lower than the penetration wear on the metal heads so using the 5 star stylus configuration would not accurately show the wear stripe on the ceramic heads. It was important to use the straight stylus configuration and as the wear area was not very low below the equator, it was possible to reach the wear area using a 3mm stylus. The 28mm femoral heads were measured and 3 dimensional reconstructions of the surfaces (Figure 8.27) were done by taking 9,864 data points in the form of 36 traces rotated by 5 degrees from each other about the vertical axis. Each trace consisted of 137

points with a pitch of 0.2mm starting at the pole and finishing 3mm below the equator. The 36mm femoral heads were measured and 3 dimensional reconstructions of the surfaces (Figure 8.29) were done by taking 12,024 data points in the form of 36 traces rotated by 5 degrees from each other about the vertical axis. Each trace consisted of 167 points with a pitch of 0.2mm starting at the pole and finishing 3mm below the equator. The appropriate region of data points was used to determine the nominal sphere and based on the unworn regions of the femoral heads; the accuracy of the calculated volumetric wear was ±0.2mm^3 for the 28mm femoral head and ±0.4mm^3 for the 36mm femoral head. Taking the error contributed by the form error and the measurement and analysis, the wear volumes obtained by the CMM were in good agreement with that determined gravimetrically (Figure 8.28 and Figure 8.30).
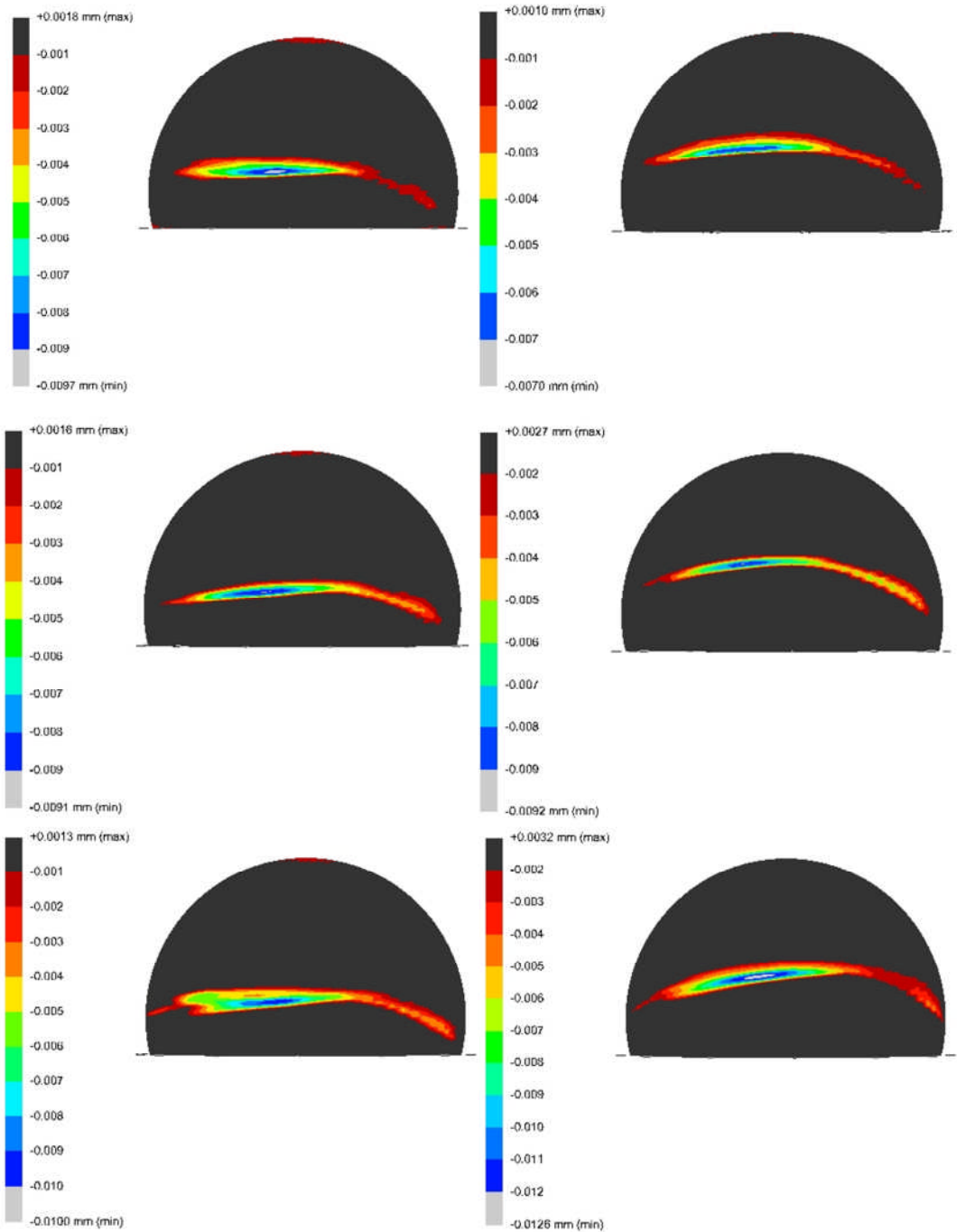
Figure 8.27: Three dimensional reconstruction of the wear are on the 28mm ceramic femoral heads using the 3mm single stylus. The dark grey region represents the unworn area on the femoral head or an area with small penetration which was within the accuracy of the measurement technique.
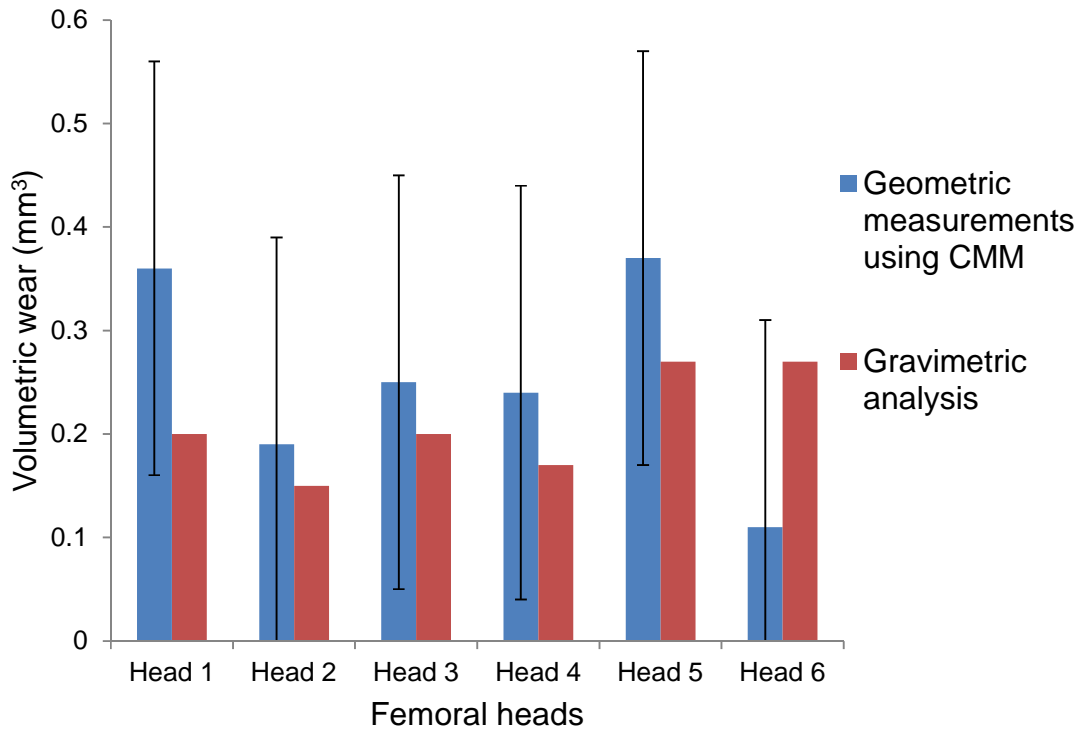
Figure 8.28: Volumetric wear of the 28mm ceramic femoral heads determined gravimetrically and measured using the CMM. The error bars represent the volumetric deviation error in the CMM measurements.
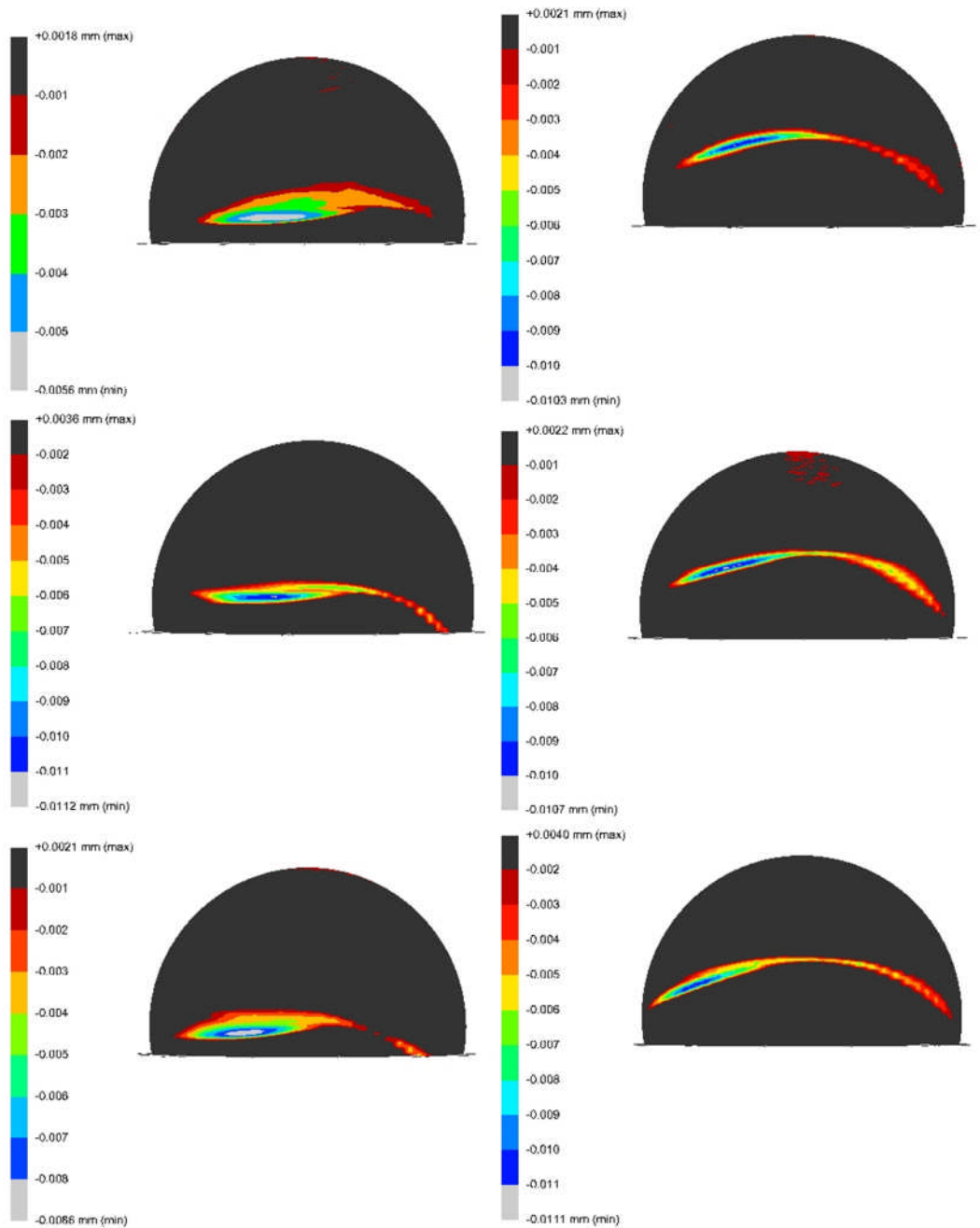
Figure 8.29: Three dimensional reconstruction of the wear are on the 36mm ceramic femoral heads using the 3mm single stylus. The dark grey region represents the unworn area on the femoral head or an area with small penetration which was within the accuracy of the measurement technique.
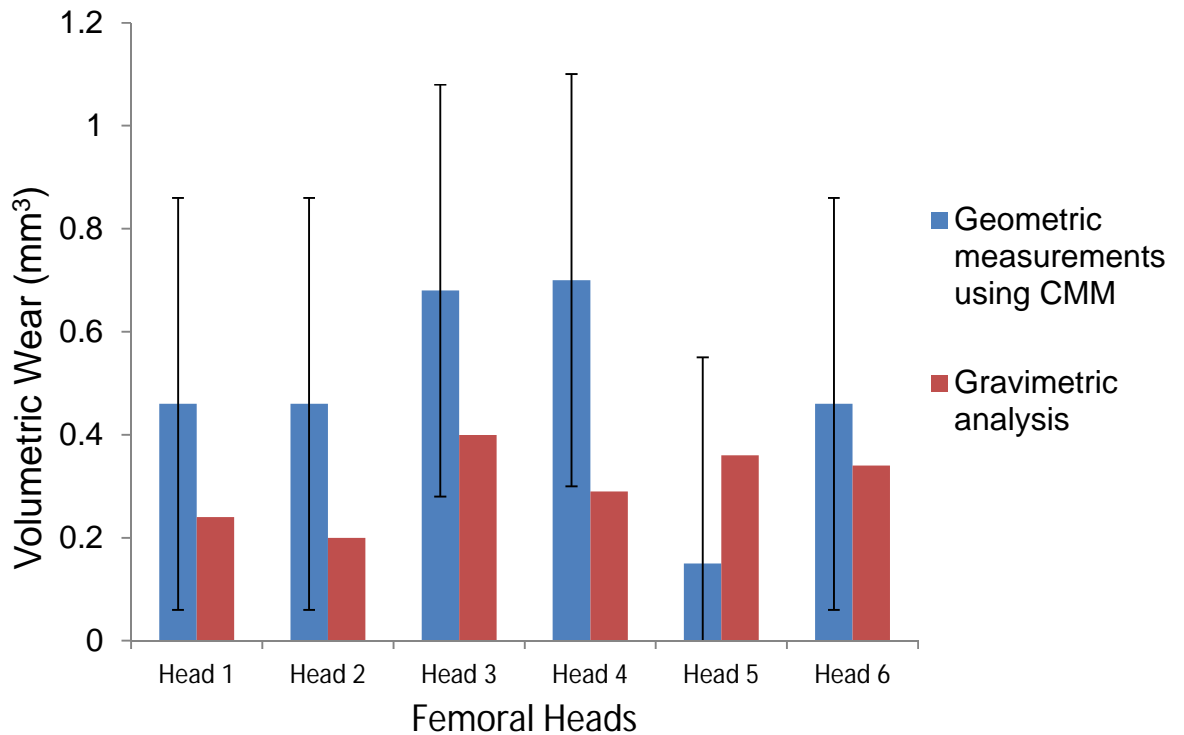
Figure 8.30: Volumetric wear of the 36mm ceramic femoral heads determined gravimetrically and measured using the CMM. The error bars represent the volumetric deviation error in the CMM measurements.

8.6 Conclusion

A novel geometric measurement and analysis techniques was successfully developed to assess the wear of hip replacements bearings tested under standard and edge loading conditions on a hip joint simulator. The volumetric wear assessed using these geometric techniques was compared to the wear volumes determined gravimetrically. Extra information was provided by using geometric analysis including the linear penetration and the location, orientation and the shape of the wear scar. This technique can also be used to assess the wear on retrieved prostheses, which cannot be determined using gravimetric analysis.

CHAPTER 9. OVERALL DISCUSSION, CONCLUSION AND FUTURE WORK

9.1 Rationale

The first successful total hip replacement was designed and implanted by Sir John Charnley in the early 1960s (Charnley, 1961). The bearing surface composed of a metal head articulating against polyethylene liner. The long term results have shown cases of osteolysis resulting in loosening and failure of the prostheses (Charnley, 1982). This was due to the biological reactions induced by the polyethylene wear debris (Willert, 1977). Failures of joint replacement bearings due to wear have triggered the need for preclinical testing and the development of *in vitro* simulators to assess and predict the performance of hip replacement bearings under physiological conditions (Dowson, 1981).

Clinical results did not reflect the predictions of the wear of hard-on-hard bearings from hip simulator tests simulating standard walking cycles. The reason for this unpredicted failure was thought to be due to mal-positioning of the prosthesis *in vivo*. In fact mal-positioning in hip replacement bearings was highlighted many years ago (Nevelos et al., 1999, Nevelos et al., 2000). The paper highlighted an unusual stripe wear area on ceramic-on-ceramic retrievals that had not been observed on components tested on simulators before (Nevelos et al., 1999). In vitro investigations have discovered the conditions that generate such wear mechanisms which involved introducing a medial-lateral displacement to the acetabular cup during the gait cycles producing edge loading (Nevelos et al., 2000). This simulator condition was termed microseparation. Microseparation conditions have been shown to produce the stripe wear mechanism and also generate the bi-modal sized wear particle distribution similar to that observed from retrieved *ex vivo* tissues (Hatton et al., 2002, Nevelos et al., 2000, Nevelos et al., 1999, Nevelos et al., 2001c, Tipper et al., 2002).

Several research papers have reported the wear of ceramic-on-ceramic and metal-on-metal bearings under edge loading conditions due to steep inclination angle and microseparation conditions (Leslie et al., 2010, Leslie et al., 2009, Nevelos et al., 2000, Stewart et al., 2001, Stewart et al., 2003b, Stewart et al., 2003a, Williams et al., 2006, Williams et al., 2008). These developments highlighted the importance of accurate implant positioning to avoid edge loading. Edge loading could occur due to rotational or translational mal-positioning (Fisher, 2011). Rotational mal-positioning is easier to detect clinically which include steep inclination angle and excessive version/ante-version angles. Translational mal-positioning encompasses micro-separation of the centres of rotations of the head and the cup and could occur due to several clinical reasons, such as head offset deficiency, medialised cup, stem subsidence, impingement, subluxation and laxity of the joint/ soft tissue.

This project focused on understanding the wear of different size ceramic-on-ceramic and metal-on-metal bearings under edge loading conditions due to translational and rotational mal-positioning and determining the contribution of each condition to the total wear of the bearing.

9.2   Ceramic-on-ceramic bearings

Ceramic-on-ceramic bearings are an option for high demand patients. Under standard simulator conditions, these bearings produced the lowest wear rates compared to other bearing combinations. Larger ceramic-on-ceramic bearings offer a larger range of motion, thus reducing the risk of impingement and subluxation, providing more flexibility for the active patient (Zagra and Giacometti Ceroni, 2007). The wear of ceramic-on-ceramic bearings is very low under standard *in vitro* simulator testing conditions (Nevelos et al., 2001c, Nevelos et al., 2001a, Clarke et al., 2000). However, retrieval studies have shown stripe wear that was not replicated using these standard conditions (Nevelos et al., 1999). Stripe wear was replicated under edge loading conditions, which resulted from translational mal-positioning, a condition termed "microseparation" (Nevelos et al., 2000).

The latest generation ceramic material called BIOLOX® delta was tested in this thesis under four different conditions; the standard gait conditions with well aligned heads and liners, steep cup inclination angle conditions with well aligned heads and liners, microseparation conditions where translational mal-alignment was introduced between the head and the cup, and the fourth condition was a combination between the latter two conditions.

From Chapters 3 and 4, cup inclination angle did not influence the wear of ceramic-on-ceramic bearings under either standard gait or microseparation conditions. Under standard gait conditions, the wear rate of size 36mm bearings was significantly lower than size 28mm bearings tested on the same simulator. This was reversed when microseparation conditions were introduced to the gait cycle, where the wear rate of the larger size bearings was approximately twice as high (0.23mm^3/million cycles for the 36mm bearing compared to 0.12mm^3/million cycles for the 28mm bearing). This was thought to be due to the larger contact area for the larger bearings and deprived lubrication under edge loading conditions.

The wear rate of BIOLOX® Delta bearings under microseparation conditions was much lower (<0.25mm^3/million cycles) compared to the third generation alumina ceramic-on-ceramic bearings (Stewart et al., 2001) (1.84mm^3/million cycles). Also the mean penetration of the wear stripe, measured by the two dimensional profilometry (Talysurf), was lower for the BIOLOX® delta ceramic bearings (7µm at 3 million cycles) compared to the alumina-on-alumina bearings tested under the same *in vitro* conditions (~90µm at 5 million cycles) (Stewart et al., 2001).

The attempts to determine the size distribution of the wear debris produced under standard and edge loading condition were unsuccessful due to the extremely low wear produced by these BIOLOX® delta ceramic-on-ceramic bearings.

Although BIOLOX® delta ceramic-on-ceramic bearings have shown improved wear resistance, with both bearing sizes under adverse conditions, optimum component positioning cannot be over-emphasised. Current clinical reports related to ceramic-on-ceramic fracture are mainly related to alumina ceramics, and further clinical data is needed to determine the relative

fracture risk of this improved material, however early results are encouraging (Hamilton et al., 2010).

9.3   Metal-on-metal bearings

Under standard gait conditions when the cup inclination angle was at 45°, the wear rate was split into two phases, a bedding in phase and a steady state phase (Dowson, 2001). The larger size bearings, the 36mm reported in Chapter 6, generated a significantly lower steady state wear rate than the 28mm bearings ($0.17mm^3$/ million cycles). The wear results also showed bedding in and steady state phases where the steady state phase occurred at an earlier point for the 36mm bearing compared to the 28mm bearings. In this thesis, the wear rates obtained under standard conditions were lower than previously reported on the 36mm MoM bearings (Williams et al., 2007a). This could be due to the reduced diametrical clearance used in this study (40µm) compared to approximately 80µm in the previous study. Farrar et al. (1997) have shown that decreasing the diametrical clearance reduces the bedding in wear of MoM articulations.

When the cup inclination angle was increased to 65°, the wear rates for the 28mm bearings increased and there was no evidence of a steady state phase after three million cycles. The 36mm bearings showed no increase in wear rate when the cup inclination angle was increased from 45° to 65°. As the inclination angle increased, the contact area approached the rim of the acetabular cup but no head-rim contact occurred. Both bearing sizes used in this study had an included angle (cup coverage) of 160°. A cup design with hemispherical included angle (180°) will have better tolerance to rotational mal-positioning however, this will restrict the range of motion and increase the incidence of impingement (Wang et al., 2011). Decreasing the acetabular coverage will increase the range of motion but will increase the chance of edge loading due to rotational mal-positioning. These results shows that increased wear due to rotational mal-positioning only occurs when edge loading occurs, which in turn is dependent on the combination of several factors such as steep cup inclination angles, excessive version or ante-version angles, and acetabular cup geometries and component size.

Under standard conditions, the wear rates decreased with increasing head size due to improved lubrication regimes. However, when edge loading occurred under microseparation conditions, the wear rate of the 36mm bearings was similar to the 28mm bearings. This was due to a change in the lubrication regime from mixed lubrication, which gave the larger bearings their superior wear resistance under standard gait conditions, to boundary lubrication. For both bearing sizes, the combination of both rotational and translational mal-positioning did not produce higher wear rates compared to translational mal-positioning alone however, reconstructions of the wear area using the CMM showed different wear stripe patterns under the two conditions.

Serum cobalt ion concentrations measured in this study showed a strong correlation with the wear volumes measured gravimetrically. However, chromium ion concentrations showed a weaker correlation with wear volume especially at high wear volumes. Under microseparation and edge loading conditions, metal-on-metal bearings produce micrometer sized particles as well as nanometer sized particles (Leslie et al., 2009). These relatively large particles are rich in chromium oxide and are removed by centrifuging when preparing samples for ion level measurement (Catelas et al., 2006). This could explain the lower than expected chromium ion level at high wear volumes which were obtained under edge loading conditions.

Tribocorrosion measurements have shown that the surface was severely depassivated under edge loading conditions compared to standard simulator conditions. It also showed, through the fluctuation in open circiut potential measurements, the complex wear mechanism that exists in the metal-on-metal articulation.

9.4　Comparison of ceramic-on-ceramic with metal-on-metal bearings

Ceramic-on-ceramic bearings, unlike metal-on-metal bearings, showed no increase in wear due to head-rim contact under increased cup inclination angle. However, microseparation and edge loading conditions have resulted in stripe wear and increased wear in ceramic-on-ceramic bearings. For

28mm BIOLOX$^®$ delta ceramic-on-ceramic bearings, the wear rate under microseparation conditions was 0.12mm^3/ million cycles; approximately 40 times lower than the wear rate of metal on metal bearings under the same conditions using the same simulator. The mean penetration over the wear stripe on the ceramic femoral heads over 3 million cycles of testing was below 8µm (Chapters 3 and 4), compared to a mean of approximately 65µm for the metal-on-metal bearings reported in Chapters 4 and 6. The improved wear properties of the fourth generation ceramic materials under adverse conditions, even with a larger head size, highlighted the resistance of the material to the harsher conditions which, younger and more active patients may exert on a hip prosthesis. It also showed that this material, where wear is concerned, is more forgiving to surgical mal-positioning than metal-on-metal bearings.

9.5 Geometric measurement technique

The improvement in CMM accuracy have allowed the development of geometric measurement and analysis technique that allowed accurate assessment and visualisation of wear scars generated on femoral heads and acetabular cups. The location and the maximum penetration depth could be easily visualised on the reconstructed surfaces using the SR3D software. This showed the advantage of using the CMM over the two dimensional profilometry (Talysurf) to determine the penetration of the wear area. This also allowed the quantification of wear volumes without the need for pre-test measurement, which can also be used to assess the wear on retrieved *ex vivo* bearings.

9.6 Conclusions

The research questions posed in the aims and objectives of this thesis were addressed and the following conclusions were made:

- Rotational mal positioning achieved through steep inclination angles did not influence the wear of BIOLOX$^®$ delta ceramic-on-ceramic bearings.
- The introduction of translational mal positioning, by applying microseparation conditions to the gait cycles, increased the wear of

BIOLOX$^®$ delta ceramic-on-ceramic bearings and resulted in the formation of stripe wear on the femoral heads with associated wear area at the rim of the acetabular cup.

- Increasing the inclination angle did not influence the wear of BIOLOX$^®$ delta ceramic-on-ceramic bearings under microseparation conditions.

- Increasing the bearing size in ceramic-on-ceramic bearings showed a significant increase in the wear rates under microseparation conditions however, this increase was not considered clinically significant.

- The wear rate of metal-on-metal bearings increased under edge loading conditions due to both rotational and translational mal-positioning.

- Unlike the 28mm bearings, the 36mm bearings, edge loading did not occur at the steep angle of 65°, however, the contact area approached the rim of the acetabular cup.

- Increased wear in metal-on-metal bearings only occurred when edge loading conditions were present.

- The increase in wear due to edge loading conditions was more severe under microseparation conditions compared to steep cup inclination angle conditions.

- Edge loading resulted in the formation of stripe like wear on the femoral heads and rim wear on the acetabular cups of metal on metal bearings.

- Increasing the inclination angle under microseparation conditions did not cause any further increase in wear.

- Increasing the femoral head size in metal-on-metal bearings (with diametrical clearances between 40-60µm) resulted in reduced wear rates under standard conditions but no significant difference under microseparation conditions.

- Acetabular cup rim geometries and inclusion angle do not affect the wear rates under standard conditions however; they influence the level of increase in wear under edge loading conditions.

- There was a good correlation between Co and Cr ion level and wear at low levels.

- The correlation of Cr ion levels and wear was weaker under edge loading conditions indicating that larger wear debris were generated under these conditions.

- The corrosion regime with metal-on-metal bearings was more severe under edge loading conditions.

- BIOLOX® delta ceramic-on-ceramic bearings were more resistant to edge loading conditions than metal-on-metal bearings.

- Geometric measurement techniques are useful tools in assessing and visualising the wear areas on hip replacement bearings providing three dimensional representations of the wear areas on the femoral head and acetabular cups.

- The accuracy of the geometric measurements of hip replacement bearings are not only affected by the resolution of the equipment but also by the analysis technique.

9.7   Future work

Under adverse rim loading conditions, other design factors such as rim geometry and cup included angle may impact on the increase in wear for different bearings in total hip replacements. This thesis have shown the necessity of using adverse simulator conditions for preclinical assessments of hip replacement bearings beyond the current ISO standards. However, the full range of conditions which generate mal-positioning *in vivo*, rotational and translational mal-positioning, have not been investigated and future work should study effects of other variations in positioning such as version, the effects of different activities which can cause edge loading, as well as investigations of other design variables. So some research questions that still need to be addressed are:

- What is the effect of changing the version/ ante-version angle as well as the inclination angle on the wear, and wear scar orientation of ceramic-on-ceramic and metal-on-metal bearings under standard and microseparation conditions?

- What is the difference in the wear debris size distribution under edge loading conditions due to rotational and translational mal positioning?

- What is the influence of changing the acetabular cup rim design on the wear and wear mechanisms of metal-on-metal bearings under edge loading conditions?

REFERENCES

AFFATATO, S., BERSAGLIA, G., FOLTRAN, I., EMILIANI, D., TRAINA, F. & TONI, A. 2004. The influence of implant position on the wear of alumina-on-alumina studied in a hip simulator. *Wear,* 256**,** 400-405.

AFFATATO, S., BERSAGLIA, G., ROCCHI, M., TADDEI, P., FAGNANO, C. & TONI, A. 2005. Wear behaviour of cross-linked polyethylene assessed in vitro under severe conditions. *Biomaterials,* 26**,** 3259-67.

AFFATATO, S., LEARDINI, W., JEDENMALM, A., RUGGERI, O. & TONI, A. 2006. Larger Diameter Bearings Reduce Wear in Metal-on-Metal Hip Implants. *Clin Orthop Relat Res.*

AL-HAJJAR, M., LESLIE, I. J., TIPPER, J., WILLIAMS, S., FISHER, J. & JENNINGS, L. M. 2010. Effect of cup inclination angle during microseparation and rim loading on the wear of BIOLOX(R) delta ceramic-on-ceramic total hip replacement. *J Biomed Mater Res B Appl Biomater,* 95**,** 263-8.

AL-SAFFAR, N. 2002. Early clinical failure of total joint replacement in association with follicular proliferation of B-lymphocytes - A report of two cases. *Journal of Bone and Joint Surgery-American Volume,* 84A**,** 2270-2273.

AMSTUTZ, H. C., BEAULE, P. E., DOREY, F. J., LE DUFF, M. J., CAMPBELL, P. A. & GRUEN, T. A. 2004. Metal-on-metal hybrid surface arthroplasty: two to six-year follow-up study. *J Bone Joint Surg Am,* 86-A**,** 28-39.

AMSTUTZ, H. C., CAMPBELL, P., KOSSOVSKY, N. & CLARKE, I. C. 1992. Mechanism and Clinical-Significance of Wear Debris-Induced Osteolysis. *Clinical Orthopaedics and Related Research***,** 7-18.

ANGADJI, A., ROYLE, M., COLLINS, S. N. & SHELTON, J. C. 2009. Influence of cup orientation on the wear performance of metal-on-metal hip replacements. *Proceedings of the Institution of Mechanical Engineers Part H-Journal of Engineering in Medicine,* 223**,** 449-457.

ANGADJI, A., ROYLE, M., HUSSAIN, A., COLLINS, S. N. & SHELTON, J. C. Year. Influence of Cup Orientation on the Wear of Metal-on-Metal Hip Joint Replacements. *In:* Engineers and Surgeons Joined at the Hip, 2007 London, UK. IMechE, 217-220.

ANISSIAN, H. L., STARK, A., GOOD, V., DAHLSTRAND, H. & CLARKE, I. C. 2001. The wear pattern in metal-on-metal hip prostheses. *Journal of Biomedical Materials Research,* 58**,** 673-678.

ANTONY, F. C. & HOLDEN, C. A. 2003. Metal allergy resurfaces in failed hip endoprostheses. *Contact Dermatitis,* 48**,** 49-50.

AUST, S. A., B; SMITH, B; OVERHOLSER, R. Year. Scratch Resistance And Ultra-High-Molecular-Weight-Polyethylene Wear Results For An Amorphous Bulk Metallic Glass. *In:* Society For Biomaterials, 2005. 687.

BARBOUR, P. S., STONE, M. H. & FISHER, J. 1999. A hip joint simulator study using simplified loading and motion cycles generating physiological wear paths and rates. *Proc Inst Mech Eng [H],* 213**,** 455-67.

BARBOUR, P. S., STONE, M. H. & FISHER, J. 2000. A hip joint simulator study using new and physiologically scratched femoral heads with ultra-high molecular weight polyethylene acetabular cups. *Proc Inst Mech Eng [H],* 214**,** 569-76.

BARTZ, R. L., NOBLE, P. C., KADAKIA, N. R. & TULLOS, H. S. 2000. The Effect of Femoral Component Head Size on Posterior Dislocation of the Artificial Hip Joint. *J Bone Joint Surg Am,* 82**,** 1300-.

BASKETTER, D. A., BRIATICOVANGOSA, G., KAESTNER, W., LALLY, C. & BONTINCK, W. J. 1993. Nickel, Cobalt and Chromium in Consumer Products - a Role in Allergic Contact-Dermatitis. *Contact Dermatitis,* 28**,** 15-25.

BIGSBY, R. J. A., HARDAKER, C. S. & FISHER, J. 1997. Wear of ultra-high molecular weight polyethylene acetabular cups in a physiological hip joint simulator in the anatomical position using bovine serum as a

lubricant. *Proceedings of the Institution of Mechanical Engineers Part H-Journal of Engineering in Medicine,* 211**,** 265-269.

BILLS, P., BLUNT, L. & JIANG, X. 2007. Development of a technique for accurately determining clinical wear in explanted total hip replacements. *Wear,* 263**,** 1133-1137.

BILLS, P. J., RACASAN, R., UNDERWOOD, R. J., CANN, P., SKINNER, J., HART, A. J., JIANG, X. & BLUNT, L. 2012. Volumetric wear assessment of retrieved metal-on-metal hip prostheses and the impact of measurement uncertainty. *Wear,* 274**,** 212-219.

BIZOT, P., NIZARD, R., LEROUGE, S., PRUDHOMMEAUX, F. & SEDEL, L. 2000. Ceramic/ceramic total hip arthroplasty. *Journal of Orthopaedic Science: Official Journal of the Japanese Orthopaedic Association,* 5**,** 622-627.

BLACK, J. & HASTINGS, G. W. 1998. *Handbook of Biomaterials properties*, Springer.

BOUTIN, P., CHRISTEL, P., DORLOT, J. M., MEUNIER, A., DEROQUANCOURT, A., BLANQUAERT, D., HERMAN, S., SEDEL, L. & WITVOET, J. 1988. The Use of Dense Alumina Alumina Ceramic Combination in Total Hip-Replacement. *Journal of Biomedical Materials Research,* 22**,** 1203-1232.

BOWSHER, J. G., HUSSAIN, A., WILLIAMS, P., NEVELOS, J. & SHELTON, J. C. 2004. Effect of ion implantation on the tribology of metal-on-metal hip prostheses. *The Journal of Arthroplasty,* 19**,** 107-111.

BOWSHER, J. G., HUSSAIN, A., WILLIAMS, P. A. & SHELTON, J. C. Year. Large head diameters have the potential to reduce ion release in metal-on-metal hip wear simulations. *In:* ORS, 2005 Washington DC. 1626.

BOWSHER, J. G., HUSSAIN, A., WILLIAMS, P. A. & SHELTON, J. C. 2006a. Metal-on-metal hip simulator study of increased wear particle surface area due to 'severe' patient activity. *Proc Inst Mech Eng [H],* 220**,** 279-87.

BOWSHER, J. G., NEVELOS, J., WILLIAMS, P. A. & SHELTON, J. C. 2006b. 'Severe' wear challenge to 'as-cast' and 'double heat-treated' large-diameter metal-on-metal hip bearings. *Proc Inst Mech Eng H,* 220**,** 135-43.

BROCKETT, C., WILLIAMS, S., JIN, Z., ISAAC, G. & FISHER, J. 2006. Friction of total hip replacements with different bearings and loading conditions. *J Biomed Mater Res B Appl Biomater*.

BROCKETT, C. L., HARPER, P., WILLIAMS, S., ISAAC, G. H., DWYER-JOYCE, R. S., JIN, Z. & FISHER, J. Year. The influence of clearance on friction, lubrication and squeaking in large diameter metal-on-metal hip replacements. *In:* 21st European Conference on Biomaterials, Sep 09-13 2007 Brighton, ENGLAND. Springer, 1575-1579.

BRODNER, W., GRUBL, A., JANKOVSKY, R., MEISINGER, V., LEHR, S. & GOTTSAUNER-WOLF, F. 2004. Cup inclination and serum concentration of cobalt and chromium after metal-on-metal total hip arthroplasty. *J Arthroplasty,* 19**,** 66-70.

BROWN, C., WILLIAMS, S., TIPPER, J. L., FISHER, J. & INGHAM, E. 2006. Characterisation of wear particles produced by metal on metal and ceramic on metal hip prostheses under standard and microseparation simulation. *J Mater Sci Mater Med*.

BRUMMITT, K. & HARDAKER, C. S. 1996. Estimation of wear in total hip replacement using a ten station hip simulator. *Proc Inst Mech Eng [H],* 210**,** 187-90.

BURGER, W. & RICHTER, H. G. 2000. High strength and toughness alumina matrix composites by transformation toughening and 'in situ' platelet reinforcement (ZPTA) - The new generation of bioceramics. *In:* GIANNINI, S. M. A. (ed.) *Bioceramics.*

BUTTERFIELD, M., STEWART, T., WILLIAMS, S., INGHAM, E., STONE, M. & FISHER, J. Year. Wear of metal-metal and ceramic-ceramic hip prostheses with swing phase microseparation. *In:* 48th Annual Meeting of the Orthopaedic Research Society, 2002 Texas, USA.

CALES, B. 2000. Zirconia as a sliding material - Histologic, laboratory, and clinical data. *Clinical Orthopaedics and Related Research*, 94-112.

CALLAGHAN, J. J., ROSENBERG, A. G. & RUBASH, H. E. 2007. *The Adult Hip*, Lippincott Williams & Wilkins.

CAMPBELL, P., BEAULE, P. E., EBRAMZADEH, E., LEDUFF, M., DE SMET, K., LU, Z. & AMSTUTZ, H. C. 2006. The John Charnley Award: a study of implant failure in metal-on-metal surface arthroplasties. *Clin Orthop Relat Res,* 453**,** 35-46.

CAPELLO, W. N., D'ANTONIO, J. A., FEINBERG, J. R., MANLEY, M. T. & NAUGHTON, M. 2008. Ceramic-on-ceramic total hip arthroplasty: update. *J Arthroplasty,* 23**,** 39-43.

CATELAS, I., CAMPBELL, P. A., BOBYN, J. D., MEDLEY, J. B. & HUK, O. L. 2006. Wear particles from metal-on-metal total hip replacements: effects of implant design and implantation time. *Proc Inst Mech Eng [H],* 220**,** 195-208.

CATELAS, I. & WIMMER, M. A. 2011. New insights into wear and biological effects of metal-on-metal bearings. *J Bone Joint Surg Am,* 93 Suppl 2**,** 76-83.

CHAN, F. W., BOBYN, J. D., MEDLEY, J. B., KRYGIER, J. J. & TANZER, M. 1999. The Otto Aufranc Award. Wear and lubrication of metal-on-metal hip implants. *Clin Orthop Relat Res***,** 10-24.

CHAN, F. W., BOBYN, J. D., MEDLEY, J. B., KRYGIER, J. J., YUE, S. & TANZER, M. 1996. Engineering issues and wear performance of metal on metal hip implants. *Clin Orthop Relat Res***,** 96-107.

CHARLISH, A. 1994. *The Complete Arthritis Handbook,* London, Carnell Ltd.

CHARNLEY, J. 1961. Arthroplasty of the hip. A new operation. *Lancet,* 1**,** 1129-32.

CHARNLEY, J. 1982. Long-term results of low-friction arthroplasty. *Hip***,** 42-9.

CLARKE, I. C., GOOD, V., WILLIAMS, P., SCHROEDER, D., ANISSIAN, L., STARK, A., OONISHI, H., SCHULDIES, J. & GUSTAFSON, G. 2000.

Ultra-low wear rates for rigid-on-rigid bearings in total hip replacements. *Proceedings of the Institution of Mechanical Engineers Part H-Journal of Engineering in Medicine,* 214**,** 331-347.

CLARKE, I. C., GREEN, D., WILLIAMS, P., PEZZOTTI, G. & DONALDSON, T. 2007. Wear performance of 36mm Biolox (R) forte/delta hip combinations compared in simulated 'severe' micro-separation test mode. *Bioceramics and Alternative Bearings in Joint Arthroplasty***,** 33-43.

CLARKE, I. C., PEZZOTTI, G., GREEN, D. D., SHIRASU, H. & DONALDSON, T. 2006. Severe Simulation Test for run-in wear of all-alumina compared to alumina composite THR *Bioceramics and Alternative Bearings in Joint Arthroplasty.* Steinkopff.

CLARKE, M. T., LEE, P. T., ARORA, A. & VILLAR, R. N. 2003. Levels of metal ions after small- and large-diameter metal-on-metal hip arthroplasty. *J Bone Joint Surg Br,* 85**,** 913-7.

CORR, M. 2003. Rheumatoid arthritis. Introduction. *Springer Semin Immunopathol,* 25**,** 1-2.

CROWNINSHIELD, R. D., MALONEY, W. J., WENTZ, D. H., HUMPHREY, S. M. & BLANCHARD, C. R. 2004. Biomechanics of large femoral heads - What they do and don't do. *Clinical Orthopaedics and Related Research***,** 102-107.

D'LIMA, D. D., HERMIDA, J. C., CHEN, P. C. & COLWELL, C. W. 2003. Polyethylene cross-linking by two different methods reduces acetabular liner wear in a hip joint wear simulator. *Journal of Orthopaedic Research,* 21**,** 761-766.

DANIEL, J., ZIAEE, H., SALAMA, A., PRADHAN, C. & MCMINN, D. J. 2006. The effect of the diameter of metal-on-metal bearings on systemic exposure to cobalt and chromium. *J Bone Joint Surg Br,* 88**,** 443-8.

DAVIES, A. P., WILLERT, H. G., CAMPBELL, P. A., LEARMONTH, I. D. & CASE, C. P. 2005. An unusual lymphocytic perivascular infiltration in tissues around contemporary metal-on-metal joint replacements. *J Bone Joint Surg Am,* 87**,** 18-27.

DE HAAN, R., PATTYN, C., GILL, H. S., MURRAY, D. W., CAMPBELL, P. A. & DE SMET, K. 2008. Correlation between inclination of the acetabular component and metal ion levels in metal-on-metal hip resurfacing replacement. *J Bone Joint Surg Br,* 90**,** 1291-7.

DENNIS, D. A., KOMISTEK, R. D., NORTHCUT, E. J., OCHOA, J. A. & RITCHIE, A. 2001. "In vivo" determination of hip joint separation and the forces generated due to impact loading conditions. *Journal of Biomechanics,* 34**,** 623-629.

DOORN, P. F., MIRRA, J. M., CAMPBELL, P. A. & AMSTUTZ, H. C. 1996. Tissue reaction to metal on metal total hip prostheses. *Clin Orthop***,** S187-205.

DOWSON, D. 1981. Wear Processes and Test Procedures. *In:* DOWSON, D. A. W., V. (ed.) *Introduction to the Biomechanics of Joints and Joint Replacements.* London: Mechanical Engineers Pub. Ltd.

DOWSON, D. 2001. New joints for the Millennium: wear control in total replacement hip joints. *Proc Inst Mech Eng [H],* 215**,** 335-58.

DOWSON, D., HARDAKER, C., FLETT, M. & ISAAC, G. H. 2004a. A hip joint simulator study of the performance of metal-on-metal joints: Part I: The role of materials. *J Arthroplasty,* 19**,** 118-23.

DOWSON, D., HARDAKER, C., FLETT, M. & ISAAC, G. H. 2004b. A hip joint simulator study of the performance of metal-on-metal joints: Part II: Design. *J Arthroplasty,* 19**,** 124-30.

DOWSON, D., MCNIE, C. M. & GOLDSMITH, A. A. 2000. Direct experimental evidence of lubrication in a metal-on-metal total hip replacement tested in a joint simulator. *Journal of Mechanical Engineering Science,* 214**,** 175-86.

ENDO, M., TIPPER, J. L., BARTON, D. C., STONE, M. H., INGHAM, E. & FISHER, J. 2002. Comparison of wear, wear debris and functional biological activity of moderately crosslinked and non-crosslinked polyethylenes in hip prostheses. *Proc Inst Mech Eng [H],* 216**,** 111-22.

ESSNER, A., SUTTON, K. & WANG, A. 2005. Hip simulator wear comparison of metal-on-metal, ceramic-on-ceramic and crosslinked UHMWPE bearings. *Wear,* 259**,** 992-995.

FAGERSON, T. L. 1998. *The Hip Handbook,* London, Butterworth-Heinemann.

FARRAR, R. & SCHMIDT, M. B. Year. The Effect of Diametral Clearance on wear between head and cup for metal on metal Articulations. *In:* Orthopaedic Research Society, 1997 San Francisco. 7112.

FIRKINS, P. J., TIPPER, J. L., INGHAM, E., STONE, M. H., FARRAR, R. & FISHER, J. 2001a. Influence of simulator kinematics on the wear of metal-on-metal hip prostheses. *Proceedings of the Institution of Mechanical Engineers, Part H: Journal of Engineering in Medicine,* 215**,** 119-122.

FIRKINS, P. J., TIPPER, J. L., INGHAM, E., STONE, M. H., FARRAR, R. & FISHER, J. 2001b. A novel low wearing differential hardness, ceramic-on-metal hip joint prosthesis. *J Biomech,* 34**,** 1291-8.

FIRKINS, P. J., TIPPER, J. L., SAADATZADEH, M. R., INGHAM, E., STONE, M. H., FARRAR, R. & FISHER, J. 2001c. Quantitative analysis of wear and wear debris from metal-on-metal hip prostheses tested in a physiological hip joint simulator. *Biomed Mater Eng,* 11**,** 143-57.

FISHER, J. 2011. Bioengineering reasons for the failure of metal-on-metal hip prostheses: an engineer's perspective. *J Bone Joint Surg Br,* 93**,** 1001-4.

FISHER, J., BELL, J., BARBOUR, P. S., TIPPER, J. L., MATTHEWS, J. B., BESONG, A. A., STONE, M. H. & INGHAM, E. 2001. A novel method for the prediction of functional biological activity of polyethylene wear debris. *Proc Inst Mech Eng [H],* 215**,** 127-32.

FISHER, J., HU, X. Q., STEWART, T. D., WILLIAMS, S., TIPPER, J. L., INGHAM, E., STONE, M. H., DAVIES, C., HATTO, P., BOLTON, J., RILEY, M., HARDAKER, C., ISAAC, G. H. & BERRY, G. 2004. Wear

of surface engineered metal-on-metal hip prostheses. *J Mater Sci Mater Med,* 15**,** 225-35.

FISHER, J., HU, X. Q., TIPPER, J. L., STEWART, T. D., WILLIAMS, S., STONE, M. H., DAVIES, C., HATTO, P., BOLTON, J., RILEY, M., HARDAKER, C., ISAAC, G. H., BERRY, G. & INGHAM, E. 2002. An in vitro study of the reduction in wear of metal-on-metal hip prostheses using surface-engineered femoral heads. *Proc Inst Mech Eng [H],* 216**,** 219-30.

FISHER, J., JIN, Z., TIPPER, J., STONE, M. & INGHAM, E. 2006. Tribology of alternative bearings. *Clin Orthop Relat Res,* 453**,** 25-34.

FREEMAN, M. A. R., SWANSON, S. A. V. & HEATH, J. C. 1969. Study of the Wear Particles produced from Cobalt-chromium-molybdenum-manganese Total Joint Replacement Prostheses. *Annals of the Rheumatic Diseases,* 28 (suppl 5).

GALVIN, A. L., TIPPER, I. L., JENNINGS, L. M., STONE, M. H., JIN, Z. M., INGHAM, E. & FISHER, J. 2007. Wear and biological activity of highly crosslinked polyethylene in the hip under low serum protein concentrations. *Proceedings of the Institution of Mechanical Engineers Part H-Journal of Engineering in Medicine,* 221**,** 1-10.

GAWKRODGER, D. J. 2003. Metal sensitivities and orthopaedic implants revisited: the potential for metal allergy with the new metal-on-metal joint prostheses. *Br J Dermatol,* 148**,** 1089-93.

GERMAIN, M. A., HATTON, A., WILLIAMS, S., MATTHEWS, J. B., STONE, M. H., FISHER, J. & INGHAM, E. 2003. Comparison of the cytotoxicity of clinically relevant cobalt-chromium and alumina ceramic wear particles in vitro. *Biomaterials,* 24**,** 469-79.

GISPERT, M. P., SERRO, A. P., COLACO, R., PIRES, E. & SARAMAGO, B. 2007. Wear of ceramic coated metal-on-metal bearings used for hip replacement. *Wear,* 263**,** 1060-1065.

GLASER, D., KOMISTEK, R. D., CATES, H. E. & MAHFOUZ, M. R. 2008. Clicking and squeaking: in vivo correlation of sound and separation

for different bearing surfaces. *J Bone Joint Surg Am,* 90 Suppl 4**,** 112-20.

GOLDSMITH, A. A. & DOWSON, D. 1999a. Development of a ten-station, multi-axis hip joint simulator. *Proc Inst Mech Eng [H],* 213**,** 311-6.

GOLDSMITH, A. A., DOWSON, D., ISAAC, G. H. & LANCASTER, J. G. 2000. A comparative joint simulator study of the wear of metal-on-metal and alternative material combinations in hip replacements. *Proc Inst Mech Eng [H],* 214**,** 39-47.

GOLDSMITH, A. A. J. & DOWSON, D. 1999b. A multi-station hip joint simulator study of the performance of 22 mm diameter zirconia-ultra-high molecular weight polyethylene total replacement hip joints. *Proceedings of the Institution of Mechanical Engineers Part H-Journal of Engineering in Medicine,* 213**,** 77-90.

GOOD, V., RIES, M., BARRACK, R. L., WIDDING, K., HUNTER, G. & HEUER, D. 2003. Reduced wear with oxidized zirconium femoral heads. *J Bone Joint Surg Am,* 85-A Suppl 4**,** 105-10.

GRAY 2000. *Gray's Anatomy of the Human Body,* New York, Bartleby.com.

GREEN, T. R., FISHER, J., STONE, M., WROBLEWSKI, B. M. & INGHAM, E. 1998. Polyethylene particles of a 'critical size' are necessary for the induction of cytokines by macrophages in vitro. *Biomaterials,* 19**,** 2297-302.

HALLAB, N., MERRITT, K. & JACOBS, J. J. 2001. Metal sensitivity in patients with orthopaedic implants. *J Bone Joint Surg Am,* 83-A**,** 428-36.

HALLAB, N. J., SKIPOR, A. & JACOBS, J. J. 2003. Interfacial kinetics of titanium- and cobalt-based implant alloys in human serum: Metal release and biofilm formation. *Journal of Biomedical Materials Research Part A,* 65A**,** 311-318.

HALLING, J. 1975. *Principles of Tribology*, Macmillan Press Ltd.

HAMILTON, W. G., MCAULEY, J. P., DENNIS, D. A., MURPHY, J. A., BLUMENFELD, T. J. & POLITI, J. 2010. THA With Delta Ceramic on

Ceramic Results of a Multicenter Investigational Device Exemption Trial (vol 10, doi # 10.1007/s11999-009-1091-4, 2010). *Clinical Orthopaedics and Related Research,* 468**,** 909-909.

HANAWA, T., HIROMOTO, S. & ASAMI, K. 2001. Characterization of the surface oxide film of a Co-Cr-Mo alloy after being located in quasi-biological environments using XPS. *Applied Surface Science,* 183**,** 68-75.

HASEGAWA, M., SUDO, A., HIRATA, H. & UCHIDA, A. 2003. Ceramic acetabular liner fracture in total hip arthroplasty with a ceramic sandwich cup. *The Journal of Arthroplasty,* 18**,** 658-661.

HATTON, A., NEVELOS, J. E., NEVELOS, A. A., BANKS, R. E., FISHER, J. & INGHAM, E. 2002. Alumina-alumina artificial hip joints. Part I: a histological analysis and characterisation of wear debris by laser capture microdissection of tissues retrieved at revision. *Biomaterials,* 23**,** 3429-40.

HOWIE, D. W., MCCALDEN, R. W., NAWANA, N. S., COSTI, K., PEARCY, M. J. & SUBRAMANIAN, C. 2005. The Long-Term Wear of Retrieved McKee-Farrar Metal-on-Metal Total Hip Prostheses. *J Arthroplasty,* 20**,** 350-7.

HU, X. Q., ISAAC, G. H. & FISHER, J. 2004. Changes in the contact area during the bedding-in wear of different sizes of metal on metal hip prostheses. *Biomed Mater Eng,* 14**,** 145-9.

INGRAM, J. H., STONE, M., FISHER, J. & INGHAM, E. 2004. The influence of molecular weight, crosslinking and counterface roughness on TNF-alpha production by macrophages in response to ultra high molecular weight polyethylene particles. *Biomaterials,* 25**,** 3511-3522.

JACOBS, J. J., GILBERT, J. L. & URBAN, R. M. 1994. Corrosion of metallic implants. *In:* STAUFFER, R. N. (ed.) *Advances in Operative Orthopaedics.* St Louis: Mosby.

JACOBS, J. J., GILBERT, J. L. & URBAN, R. M. 1998. Corrosion of metal orthopaedic implants. *J Bone Joint Surg Am,* 80**,** 268-82.

JACOBS, J. J., HALLAB, N., SKIPOR, A., URBAN, R. M., MIKECZ, K. & GLANT, T. 1999. Metallic Wear and Corrosion Products: Biological Implications. *In:* REIKER, E., WINDLER, M. & WYSS, U. (eds.) *Metsul: A Metal-on-Metal Bearing.* Bern: Hans Huber.

JARRETT, C. A., RANAWAT, A., BRUZZONE, M., RODRIGUEZ, J. & RANAWAT, C. 2007. The Squeaking Hip: An Underreported Phenomenon of Ceramic-On-Ceramic Total Hip Arthroplasty. *The Journal of Arthroplasty,* 22**,** 302-302.

JIN, Z. M., DOWSON, D. & FISHER, J. 1997. Analysis of fluid film lubrication in artificial hip joint replacements with surfaces of high elastic modulus. *Proceedings of the Institution of Mechanical Engineers. Part H - Journal of Engineering in Medicine,* 211**,** 247-56.

JIN, Z. M., MEAKINS, S., MORLOCK, M. M., PARSONS, P., HARDAKER, C., FLETT, M. & ISAAC, G. 2006a. Deformation of press-fitted metallic resurfacing cups. Part 1: Experimental simulation. *Proc Inst Mech Eng H,* 220**,** 299-309.

JIN, Z. M., STONE, M., INGHAM, E. & FISHER, J. 2006b. (v) Biotribology. *Current Orthopaedics,* 20**,** 32-40.

KEURENTJES, J. C., KUIPERS, R. M., WEVER, D. J. & SCHREURS, B. W. 2008. High incidence of squeaking in THAs with alumina ceramic-on-ceramic bearings. *Clinical Orthopaedics and Related Research,* 466**,** 1438-1443.

KOTHARI, M., BARTEL, D. L. & BOOKER, J. F. 1996. Surface geometry of retrieved McKee-Farrar total hip replacements. *Clinical Orthopaedics and Related Research***,** S141-S147.

KUNTZ, M., SCHNEIDER, N. & HEROS, R. 2006. Controlled zirconia phase transformation in Biolox delta- a feature of safety. *Ceramics in orthopeadics.* Steinkopff.

KWON, Y.-M., GLYN-JONES, S., SIMPSON, D. J., KAMALI, A., MCLARDY-SMITH, P., GILL, H. S. & MURRAY, D. W. 2010. Analysis of wear of retrieved metal-on-metal hip resurfacing implants revised due to pseudotumours. *J Bone Joint Surg Br,* 92-B**,** 356-361.

KWON, Y., OSTLERE, S., MCLARDY-SMITH, P., GUNDLE, R., WHITWELL, D., GIBBONS, C. L. M., TAYLOR, A., PANDIT, H., GLYN-JONES, S., ATHANASOU, N., BEARD, D., GILL, H. S. & MURRAY, D. W. Year. Asymptomatic Pseudotumours in Patients with metal-on-metal hip resurfacing: Prevelance and metal ion study. *In:* British hip Society, 2009 Manchester.

LANGTON, D. J., JOYCE, T. J., JAMESON, S. S., LORD, J., VAN ORSOUW, M., HOLLAND, J. P., NARGOL, A. V. & DE SMET, K. A. 2011. Adverse reaction to metal debris following hip resurfacing: the influence of component type, orientation and volumetric wear. *J Bone Joint Surg Br,* 93**,** 164-71.

LESLIE, I., WILLIAMS, S., BROWN, C., ISAAC, G., JIN, Z. M., INGHAM, E. & FISHER, J. 2008. Effect of bearing size on the long-term wear, wear debris, and ion levels of large diameter metal-on-metal hip replacements - An in vitro study. *Journal of Biomedical Materials Research Part B-Applied Biomaterials,* 87B**,** 163-172.

LESLIE, I. J., CAMPBELL, P., WILLIAMS, S., MCKELLOP, H., INGHAM, E. & FISHER, J. Year. Edge Loading and Wear of Hip Surface Replacements, a Comparison of Clinical Retrievals and Simulator Samples. *In:* Orthopaedic research Society, 2010 New Orleans, USA.

LESLIE, I. J., WILLIAMS, S., ISAAC, G., INGHAM, E. & FISHER, J. 2009. High Cup Angle and Microseparation Increase the Wear of Hip Surface Replacements. *Clinical Orthopaedics and Related Research,* 467**,** 2259-2265.

LIAO, Y. & HANES, M. Year. The relationship of metal-on-metal wear and metal ion release in the serum lubricant. *In:* Orthopaedic Research Society, 2006 Chicago. 0506.

LIU, F., JIN, Z., ROBERTS, P. & GRIGORIS, P. 2006. Importance of head diameter, clearance, and cup wall thickness in elastohydrodynamic lubrication analysis of metal-on-metal hip resurfacing prostheses. *Proc Inst Mech Eng [H],* 220**,** 695-704.

LIVERMORE, J., ILSTRUP, D. & MORREY, B. 1990. Effect of femoral head size on wear of the polyethylene acetabular component. *J Bone Joint Surg Am,* 72**,** 518-28.

LORD, J. K., LANGTON, D. J., NARGOL, A. V. F. & JOYCE, T. J. 2011. Volumetric wear assessment of failed metal-on-metal hip resurfacing prostheses. *Wear,* 272**,** 79-87.

LUSTY, P. J., WATSON, A., TUKE, M. A., WALTER, W. L., WALTER, W. K. & ZICAT, B. 2007. Orientation and wear of the acetabular component in third generation alumina-on-alumina ceramic bearings: AN ANALYSIS OF 33 RETRIEVALS. *J Bone Joint Surg Br,* 89-B**,** 1158-1164.

MAI, M. T., SCHMALZRIED, T. P., DOREY, F. J., CAMPBELL, P. A. & AMSTUTZ, H. C. 1996. The contribution of frictional torque to loosening at the cement-bone interface in Tharies hip replacements. *J Bone Joint Surg Am,* 78**,** 505-11.

MAK, M. M., BESONG, A. A., JIN, Z. M. & FISHER, J. 2002. Effect of microseparation on contact mechanics in ceramic-on-ceramic hip joint replacements. *Proc Inst Mech Eng [H],* 216**,** 403-8.

MALLORY, T. M., LOMBARDI, A. V., DENNIS, D. A., KOMISTEK, R. D., FADA, R. A. & NORTHCUT, E. J. 1999. Do total hip arthroplasties piston during leg length maneuvers and gait? An in vivo determination of total hip arthroplasty separation during abduction/adduction leg lift and gait. *Scientific Exhibit 66, American Academy of Orthopaedic surgeons.*

MANAKA, M., CLARKE, I. C., YAMAMOTO, K., SHISHIDO, T., GUSTAFSON, A. & IMAKIIRE, A. 2004. Stripe wear rates in alumina THR - Comparison of microseparation simulator study with retrieved implants. *Journal of Biomedical Materials Research Part B-Applied Biomaterials,* 69B**,** 149-157.

MASSON, B. 2009. Emergence of the alumina matrix composite in total hip arthroplasty. *International Orthopaedics,* 33**,** 359-363.

MCBRYDE CW, THEIVENDRAN K, TREACY RBC & PB, P. Year. Is the outcome of Birmingham hip resurfacing influenced by gender? *In:* British Hip Society Proceedings, 11-13 March 2009.

MCKELLOP, H., CLARKE, I. C., MARKOLF, K. L. & AMSTUTZ, H. C. 1978. Wear Characteristics of Uhmw Polyethylene - Method for Accurately Measuring Extremely Low Wear Rates. *Journal of Biomedical Materials Research,* 12**,** 895-927.

MCKELLOP, H., PARK, S. H., CHIESA, R., DOORN, P., LU, B., NORMAND, P., GRIGORIS, P. & AMSTUTZ, H. 1996. In vivo wear of three types of metal on metal hip prostheses during two decades of use. *Clin Orthop***,** S128-40.

MCMINN, D., TREACY, R., LIN, K. & PYNSENT, P. 1996. Metal on metal surface replacement of the hip. Experience of the McMinn prothesis. *Clin Orthop***,** S89-98.

MEDLEY, J. B., CHAN, F. W., KRYGIER, J. J. & BOBYN, J. D. 1996. Comparison of alloys and designs in a hip simulator study of metal on metal implants. *Clin Orthop***,** S148-59.

MITTELMEIER, H. & HEISEL, J. 1992. Sixteen-years' experience with ceramic hip prostheses. *Clin Orthop***,** 64-72.

MORLOCK, M., DELLING, G., RÜTHER, W., M., H. & BISHOP, N. 2006a. In-vivo wear of hip surface replacements - a comparison of retrievals and simulator results. *Journal of Biomechanics,* 39 Suppl. 1**,** S121.

MORLOCK, M. M., BISHOP, N., RUTHER, W., DELLING, G. & HAHN, M. 2006b. Biomechanical, morphological, and histological analysis of early failures in hip resurfacing arthroplasty. *Proc Inst Mech Eng [H],* 220**,** 333-44.

MORLOCK, M. M., BISHOP, N., ZUSTIN, J., HAHN, M., RUTHER, W. & AMLING, M. 2008. Modes of implant failure after hip resurfacing: Morphological and wear analysis of 267 retrieval specimens. *Journal of Bone and Joint Surgery-American Volume,* 90A**,** 89-95.

MULLER, M. E. 1995. The benefits of metal-on-metal total hip replacements. *Clin Orthop***,** 54-9.

NEVELOS, J., INGHAM, E., DOYLE, C., STREICHER, R., NEVELOS, A., WALTER, W. & FISHER, J. 2000. Microseparation of the centers of alumina-alumina artificial hip joints during simulator testing produces clinically relevant wear rates and patterns. *J Arthroplasty,* 15**,** 793-5.

NEVELOS, J. E., INGHAM, E., DOYLE, C., FISHER, J. & NEVELOS, A. B. 1999. Analysis of retrieved alumina ceramic components from Mittelmeier total hip prostheses. *Biomaterials,* 20**,** 1833-40.

NEVELOS, J. E., INGHAM, E., DOYLE, C., NEVELOS, A. B. & FISHER, J. 2001a. The influence of acetabular cup angle on the wear of "BIOLOX Forte" alumina ceramic bearing couples in a hip joint simulator. *J Mater Sci Mater Med,* 12**,** 141-4.

NEVELOS, J. E., INGHAM, E., DOYLE, C., NEVELOS, A. B. & FISHER, J. 2001b. Wear of HIPed and non-HIPed alumina-alumina hip joints under standard and severe simulator testing conditions. *Biomaterials,* 22**,** 2191-7.

NEVELOS, J. E., PRUDHOMMEAUX, F., HAMADOUCHE, M., DOYLE, C., INGHAM, E., MEUNIER, A., NEVELOS, A. B., SEDEL, L. & FISHER, J. 2001c. Comparative analysis of two different types of alumina-alumina hip prosthesis retrieved for aseptic loosening. *J Bone Joint Surg Br,* 83**,** 598-603.

ONEGA, T., BARON, J. & MACKENZIE, T. 2006. Cancer after total joint arthroplasty: a meta-analysis. *Cancer Epidemiol Biomarkers Prev,* 15**,** 1532-7.

PALASTANGA, N. P., FIELD, D. & SOAMES, R. 2006. *Anatomy and Human Movement: Structure and Function*, Butterworth Heinemann.

PANDIT, H., GLYN-JONES, S., MCLARDY-SMITH, P., GUNDLE, R., WHITWELL, D., GIBBONS, C. L. M., OSTLERE, S., ATHANASOU, N., GILL, H. S. & MURRAY, D. W. 2008. Pseudotumours associated with metal-onmetal hip resurfacings. *Journal of Bone and Joint Surgery-British Volume,* 90B**,** 847-851.

PARK, Y.-S., HWANG, S.-K., CHOY, W.-S., KIM, Y.-S., MOON, Y.-W. & LIM, S.-J. 2006. Ceramic Failure After Total Hip Arthroplasty with an Alumina-on-Alumina Bearing. *J Bone Joint Surg Am,* 88**,** 780-787.

PAUL, J. P. 1966. Forces transmitted by joints in the human body. *Proceedings of Institution of Mechanical Engineers,* 181**,** 8-15.

PAVOOR, P. V., GEARING, B. P., MURATOGLU, O., COHEN, R. E. & BELLARE, A. 2006. Wear reduction of orthopaedic bearing surfaces using polyelectrolyte multilayer nanocoatings. *Biomaterials,* 27**,** 1527-33.

PRIA, P. D. 2007. Evolution and new application of the alumina ceramics in joint replacement. *European Journal of Orthopaedic Surgery and Traumatology,* 17**,** 253-256.

RABINOWICZ, E. 1965. *Friction and Wear of Materials,* New York, John Wiley & Sons.

REFIOR, H. J., PLITZ, W. & WALTER, A. 1997. Ex vivo and in vitro analysis of the alumina/alumina bearing system for hip joint prostheses. *Bioceramics, Vol 10*, 127-130.

RIEKER, C., KOETTIG, P., REIDER, V. & SHEN, M. Year. In-vivo Volumetric Wear Rate Of Modern Metal-metal Bearings. *In:* Society For Biomaterials, 2005a. 84.

RIEKER, C., KONRAD, R. & SCHON, R. 2001. In vitro comparison of the two hard-hard articulations for total hip replacements. *Proc Inst Mech Eng [H],* 215**,** 153-60.

RIEKER, C. B., SCHON, R., KONRAD, R., LIEBENTRITT, G., GNEPF, P., SHEN, M., ROBERTS, P. & GRIGORIS, P. 2005b. Influence of the clearance on in-vitro tribology of large diameter metal-on-metal articulations pertaining to resurfacing hip implants. *Orthopedic Clinics of North America,* 36**,** 135-+.

RIEKER, C. B., SCHON, R. & KOTTIG, P. 2004a. Development and validation of a second-generation metal-on-metal bearing: Laboratory studies and analysis of retrievals. *J Arthroplasty,* 19**,** 5-11.

RIEKER, C. B., SCHÖN, R. & KÖTTIG, P. 2004b. Development and validation of a second-generation metal-on-metal bearing: Laboratory studies and analysis of retrievals. *The Journal of Arthroplasty,* 19**,** 5-11.

ROTER, G., MEDLEY, J., CHENG, N., PARE, P., KRYGIER, J. J. & BOBYN, J. D. Year. Intermittent motion: A clinically significant protocol for metal-metal hip simulator testing. *In:* 48th Annual Meeting Orthopaedic Research Society, 2002 Dallas, Texas.

SAARI, H., SANTAVIRTA, S., NORDSTROM, D., PAAVOLAINEN, P. & KONTTINEN, Y. T. 1993. Hyaluronate in total hip replacement. *J Rheumatol,* 20**,** 87-90.

SAIKKO, V. 2005. A 12-station anatomic hip joint simulator. *Proc Inst Mech Eng [H],* 219**,** 437-48.

SAVARINO, L., GRANCHI, D., CIAPETTI, G., CENNI, E., GRECO, M., ROTINI, R., VERONESI, C. A., BALDINI, N. & GIUNTI, A. 2003. Ion release in stable hip arthroplasties using metal-on-metal articulating surfaces: a comparison between short- and medium-term results. *J Biomed Mater Res A,* 66**,** 450-6.

SCHEY, J. A. 1996. Systems view of optimizing metal on metal bearings. *Clin Orthop***,** S115-27.

SCHMALZRIED, T. P., FOWBLE, V. A., URE, K. J. & AMSTUTZ, H. C. 1996a. Metal on metal surface replacement of the hip. Technique, fixation, and early results. *Clin Orthop***,** S106-14.

SCHMALZRIED, T. P., PETERS, P. C., MAURER, B. T., BRAGDON, C. R. & HARRIS, W. H. 1996b. Long duration metal-on-metal total hip arthroplasties with low wear of the articulating surfaces. *Journal of Arthroplasty,* 11**,** 322-331.

SCHMALZRIED, T. P., SHEPHERD, E. F., DOREY, F. J., JACKSON, W. O., DELA ROSA, M., FA'VAE, F., MCKELLOP, H. A., MCCLUNG, C. D., MARTELL, J., MORELAND, J. R. & AMSTUTZ, H. C. 2000. Wear is a function of use, not time. *Clinical Orthopaedics and Related Research***,** 36-46.

SCHMIDT, M., WEBER, H. & SCHON, R. 1996. Cobalt chromium molybdenum metal combination for modular hip prostheses. *Clin Orthop*, S35-47.

SCHOLES, S. C., GREEN, S. M. & UNSWORTH, A. 2001. The wear of metal-on-metal total hip prostheses measured in a hip simulator. *Proc Inst Mech Eng [H],* 215, 523-30.

SEEDHOM, B. B. & WALLBRIDGE, N. C. 1985. Walking Activities and Wear of Prostheses. *Annals of the Rheumatic Diseases,* 44, 838-843.

SIEBER, H.-P., RIEKER, C. B. & KOTTIG, P. 1999a. Analysis of 118 second-generation metal-on-metal retrieved hip implants. *J Bone Joint Surg Br,* 81-B, 46-50.

SIEBER, H. P., RIEKER, C. B. & KOTTIG, P. 1999b. Analysis of 118 second-generation metal-on-metal retrieved hip implants. *The Journal of Bone and Joint Surgery. British Volume,* 81, 46-50.

SILVA, M., HEISEL, C., MCKELLOP, H. & SCHMALZRIED, T. 2007. Bearing Surfaces. *In:* CALLAGHAN, J. J. (ed.) *The Adult Hip.* Philadelphia: Lippincott Williams & Wilkins.

SILVA, M., SHEPHERD, E. F., JACKSON, W. O., DOREY, F. J. & SCHMALZRIED, T. P. 2002. Average patient walking activity approaches 2 million cycles per year: pedometers under-record walking activity. *J Arthroplasty,* 17, 693-7.

SMITH, S. L., DOWSON, D. & GOLDSMITH, A. A. 2001. The effect of femoral head diameter upon lubrication and wear of metal-on-metal total hip replacements. *Proc Inst Mech Eng [H],* 215, 161-70.

SMITH, S. L. & UNSWORTH, A. 1999. A comparison between gravimetric and volumetric techniques of wear measurement of UHMWPE acetabular cups against zirconia and cobalt-chromium-molybdenum femoral heads in a hip simulator. *Proceedings of the Institution of Mechanical Engineers Part H-Journal of Engineering in Medicine,* 213, 475-483.

SPECTOR, B. M., RIES, M. D., BOURNE, R. B., SAUER, W. S., LONG, M. & HUNTER, G. 2001. Wear performance of ultra-high molecular

weight polyethylene on oxidized zirconium total knee femoral components. *J Bone Joint Surg Am,* 83-A Suppl 2 Pt 2**,** 80-6.

STACHOWIAK, G. W. & BATCHELOR, A. W. 2005. *Engineering tribology,* Amsterdam ; London, Elsevier Butterworth-Heinemann.

STEWART, T., TIPPER, J., STREICHER, R., INGHAM, E. & FISHER, J. 2001. Long-term wear of HIPed alumina on alumina bearings for THR under microseparation conditions. *J Mater Sci Mater Med,* 12**,** 1053-6.

STEWART, T. D., TIPPER, J. L., INSLEY, G., STREICHER, R. M., INGHAM, E. & FISHER, J. 2003a. Long-term wear of ceramic matrix composite materials for hip prostheses under severe swing phase microseparation. *J Biomed Mater Res B Appl Biomater,* 66**,** 567-73.

STEWART, T. D., TIPPER, J. L., INSLEY, G., STREICHER, R. M., INGHAM, E. & FISHER, J. 2003b. Severe wear and fracture of zirconia heads against alumina inserts in hip simulator studies with microseparation. *J Arthroplasty,* 18**,** 726-34.

STEWART, T. D., WILLIAMS, S., TIPPER, J. L., INGHAM, E., STONE, M. D. & FISHER, J. 2002. Advances in simulator testing of orthopaedic joint prostheses. *Leeds Lyon*.

STREICHER, R. M., SEMLITSCH, M., SCHON, R., WEBER, H. & RIEKER, C. 1996. Metal-on-metal articulation for artificial hip joints: laboratory study and clinical results. *Proc Inst Mech Eng [H],* 210**,** 223-32.

TIPPER, J. L., FIRKINS, P. J., BESONG, A. A., BARBOUR, P. S. M., NEVELOS, J., STONE, M. H., INGHAM, E. & FISHER, J. 2001. Characterisation of wear debris from UHMWPE on zirconia ceramic, metal-on-metal and alumina ceramic-on-ceramic hip prostheses generated in a physiological anatomical hip joint simulator. *Wear,* 250**,** 120-128.

TIPPER, J. L., FIRKINS, P. J., INGHAM, E., FISHER, J., STONE, M. H. & FARRAR, R. 1999. Quantitative analysis of the wear and wear debris from low and high carbon content cobalt chrome alloys used in metal on metal total hip replacements. *J Mater Sci Mater Med,* 10**,** 353-62.

TIPPER, J. L., HATTON, A., NEVELOS, J. E., INGHAM, E., DOYLE, C., STREICHER, R., NEVELOS, A. B. & FISHER, J. 2002. Alumina-alumina artificial hip joints. Part II: characterisation of the wear debris from in vitro hip joint simulations. *Biomaterials,* 23**,** 3441-8.

TIPPER, J. L., INGHAM, E., HAILEY, J. L., BESONG, A. A., FISHER, J., WROBLEWSKI, B. M. & STONE, M. H. 2000. Quantitative analysis of polyethylene wear debris, wear rate and head damage in retrieved Charnley hip prostheses. *J Mater Sci Mater Med,* 11**,** 117-24.

TOTTEN, G. E. & LIANG, H. 2004. *Mechanical tribology : materials, characterization, and applications,* New York, Marcel Dekker.

UDOFIA, I., LIU, F., JIN, Z., ROBERTS, P. & GRIGORIS, P. 2007. The initial stability and contact mechanics of a press-fit resurfacing arthroplasty of the hip. *J Bone Joint Surg Br,* 89**,** 549-56.

VASSILIOU, K., ELFICK, A. P., SCHOLES, S. C. & UNSWORTH, A. 2006. The effect of 'running-in' on the tribology and surface morphology of metal-on-metal Birmingham hip resurfacing device in simulator studies. *Proc Inst Mech Eng [H],* 220**,** 269-77.

VASSILIOU, K. E., APD; SCHOLES, SC; UNSWORTH, A. Year. The Effect Of "Running-in" On The Tribology Of Metal-on-metal Hip Resurfacing Device. *In:* Society For Biomaterials, 2005. 83.

VISURI, T., PUKKALA, E., PAAVOLAINEN, P., PULKKINEN, P. & RISKA, E. B. 1996. Cancer risk after metal on metal and polyethylene on metal total hip arthroplasty. *Clin Orthop***,** S280-9.

VISURI, T., PUKKALA, E., PULKKINEN, P. & PAAVOLAINEN, P. 2003. Decreased cancer risk in patients who have been operated on with total hip and knee arthroplasty for primary osteoarthrosis: a meta-analysis of 6 Nordic cohorts with 73,000 patients. *Acta Orthop Scand,* 74**,** 351-60.

WAGNER, H. 1978. Surface replacement arthroplasty of the hip. *Clin Orthop***,** 102-30.

WALKER, P. S. & GOLD, B. L. 1971. The tribology (friction, lubrication and wear) of all-metal artificial hip joints. *Wear,* 17**,** 285-299.

WALTER, W. L., INSLEY, G. M., WALTER, W. K. & TUKE, M. A. 2004. Edge loading in third generation alumina ceramic-on-ceramic bearings: stripe wear. *J Arthroplasty,* 19**,** 402-13.

WALTER, W. L., O'TOOLE G, C., WALTER, W. K., ELLIS, A. & ZICAT, B. A. 2007. Squeaking in ceramic-on-ceramic hips: the importance of acetabular component orientation. *J Arthroplasty,* 22**,** 496-503.

WANG, L., WILLIAMS, S., ISAAC, G., JIN, Z. & FISHER, J. Year. Effect of acetabular cup orientation and design on the contact mechanics and range of motion of metal-on-metal hip resurfacing prostheses. *In:* Orthopaedic Research Society, 2011 Long Beach, California, USA.

WILLERT, H. G. 1977. Reactions of the articular capsule to wear products of artificial joint prostheses. *J Biomed Mater Res,* 11**,** 157-64.

WILLERT, H. G., BUCHHORN, G. H., FAYYAZI, A., FLURY, R., WINDLER, M., KOSTER, G. & LOHMANN, C. H. 2005. Metal-on-metal bearings and hypersensitivity in patients with artificial hip joints. A clinical and histomorphological study. *J Bone Joint Surg Am,* 87**,** 28-36.

WILLIAMS, J. A. 2005. *Engineering tribology,* Cambridge, Cambridge Univ. Press.

WILLIAMS, S. 2003. *Surface Engineered Total Hip Replacements.* University of Leeds.

WILLIAMS, S., BUTTERFIELD, M., STEWART, T., INGHAM, E., STONE, M. & FISHER, J. 2003a. Wear and deformation of ceramic-on-polyethylene total hip replacements with joint laxity and swing phase microseparation. *Proc Inst Mech Eng [H],* 217**,** 147-53.

WILLIAMS, S., ISAAC, G., HARDAKER, C., INGHAM, E. & FISHER, J. Year. Ceramic-on-Metal Hip Replacements: A Novel Bearing Combination. *In:* Orthopaedic Research Society, 2007a San Diego, USA., 1672.

WILLIAMS, S., ISAAC, G., HATTO, P., STONE, M. H., INGHAM, E. & FISHER, J. 2004a. Comparative wear under different conditions of surface-engineered metal-on-metal bearings for total hip arthroplasty. *J Arthroplasty,* 19**,** 112-7.

WILLIAMS, S., JALALI-VAHID, D., BROCKETT, C., JIN, Z., STONE, M. H., INGHAM, E. & FISHER, J. 2006. Effect of swing phase load on metal-on-metal hip lubrication, friction and wear. *J Biomech,* 39**,** 2274-81.

WILLIAMS, S., LESLIE, I., ISAAC, G., JIN, Z., INGHAM, E. & FISHER, J. 2008. Tribology and wear of metal-on-metal hip prostheses: influence of cup angle and head position. *J Bone Joint Surg Am,* 90 Suppl 3**,** 111-7.

WILLIAMS, S., SCHEPERS, A., ISAAC, G., HARDAKER, C., INGHAM, E., JAGT, D. V., BRECKON, A. & FISHER, J. 2007b. THE 2007 OTTO AUFRANC AWARD: Ceramic-on-Metal Hip Arthroplasties: A Comparative In Vitro and In Vivo Study. *Clin Orthop Relat Res,* 465**,** 23-32.

WILLIAMS, S., STEWART, T. D., INGHAM, E., STONE, M. H. & FISHER, J. 2004b. Metal-on-metal bearing wear with different swing phase loads. *J Biomed Mater Res,* 70B**,** 233-9.

WILLIAMS, S., TIPPER, J. L., INGHAM, E., STONE, M. H. & FISHER, J. 2003b. In vitro analysis of the wear, wear debris and biological activity of surface-engineered coatings for use in metal-on-metal total hip replacements. *Proc Inst Mech Eng [H],* 217**,** 155-63.

WIMMER, M. A., ARTELT, D., KUNZE, J., MORLOCK, M. M., SCHNEIDER, E. & NASSUTT, R. 2001. Friction and wear properties of metal/metal hip joints - Application of a novel testing and analysis method. *Materialwissenschaft Und Werkstofftechnik,* 32**,** 891-896.

YAN, Y., NEVILLE, A. & DOWSON, D. 2005. Understanding the role of corrosion in the degradation of metal-on-metal implants. *Proceedings of the Institution of Mechanical Engineers Part H-Journal of Engineering in Medicine,* 220**,** 173-181.

YAN, Y., NEVILLE, A. & DOWSON, D. 2006. Biotribocorrosion - an appraisal of the time dependence of wear and corrosion interactions: I. The role of corrosion. *Journal of Physics D-Applied Physics,* 39**,** 3200-3205.

YAN, Y., NEVILLE, A. & DOWSON, D. 2007a. Tribo-corrosion properties of cobalt-based medical implant alloys in simulated biological environments. *Wear,* 263**,** 1105-1111.

YAN, Y., NEVILLE, A., DOWSON, D. & HOLLWAY, F. 2007b. Biotribocorrosion of CoCrMo orthopaedic implant materials - Assessing the formation and effect of the biofilm. *Tribology International,* 40**,** 1728-1728.

YAN, Y., NEVILLE, A., DOWSON, D., WILLIAMS, S. & FISHER, J. 2010a. Electrochemical instrumentation of a hip simulator: a new tool for assessing the role of corrosion in metal-on-metal hip joints. *Proceedings of the Institution of Mechanical Engineers Part H-Journal of Engineering in Medicine,* 224**,** 1267-1273.

YAN, Y., NEVILLE, A., DOWSON, D., WILLIAMS, S. & FISHER, J. 2010b. Tribofilm formation in biotribocorrosion – does it regulate ion release in metal-on-metal artificial hip joints? *Proceedings of the Institution of Mechanical Engineers, Part J: Journal of Engineering Tribology,* 224**,** 997-1006.

YEW, A., JIN, Z. M., DONN, A., MORLOCK, M. M. & ISAAC, G. 2006. Deformation of press-fitted metallic resurfacing cups. Part 2: Finite element simulation. *Proc Inst Mech Eng H,* 220**,** 311-9.

ZAGRA, L. & GIACOMETTI CERONI, R. 2007. Ceramicâ€"ceramic coupling with big heads: clinical outcome. *European Journal of Orthopaedic Surgery & Traumatology,* 17**,** 247-251.

APPENDIX

List of publications

Journal publications

- Mazen Al Hajjar, Ian J. Leslie, John Fisher, Sophie Williams, Joanne L. Tipper, Louise M. Jennings. Effect of cup inclination angle during microseparation and rim loading on the wear of BIOLOX$^{®}$ delta ceramic-on-ceramic total hip replacement. Journal of Biomedical Materials Research Part B: Applied Biomaterials. Wiley Subscription Services, Inc., A Wiley Company. 95B: 263-268.

- Manuscript in press: Mazen Al-Hajjar, John Fisher, Sophie Williams, Joanne L. Tipper, Louise M. Jennings. Effect of Femoral Head Size on the Wear of Metal on Metal Bearings in Total Hip Replacements under Adverse Edge Loading Conditions. Journal of Biomedical Materials Research: part B.

- Manuscript in press: Mazen Al-Hajjar, John Fisher, Sophie Williams, Joanne L. Tipper, Louise M. Jennings. Wear of 36mm BIOLOX Delta Ceramic-on-Ceramic Bearings in Total Hip Replacement under Edge Loading Conditions. Proceedings of Institute of Medical and Biological Engineering: Part H, Journal of Engineering in Medicine.

- Jennings LM, Al-Hajjar M, Brockett CL, Williams S, Tipper JL, Ingham E, Fisher J,. Enhancing the safety and reliability of joint replacement implants. Orthopaedics and Trauma, 2012, 26(4):246-252.

- Fisher J, Al Hajjar M, Williams S, Tipper J.L, Jennings L.M, Ingham E. Simulation and measurement of wear in metal-on-metal bearings in vitro-understanding the reasons for increased wear. Orthopaedics and Trauma, 2012, 26(4):253-258.

Conference proceedings

- M. Al-Hajjar, S. Williams, J. Fisher, L.M. Jennings. Cobalt and Chromium Ion Level Analysis from Metal-on-Metal Hip Replacements Tested under Adverse In Vitro Conditions. Orthopaedic Research Society (ORS), San Francisco California USA, 2012. Chapters 4 and 6

- M. Al-Hajjar, S. Williams, J. Fisher, L.M. Jennings. Geometric Wear Measurement of Metal-on-Metal Hip Replacements Tested Under Adverse In Vitro Simulator Conditions. Orthopaedic Research Society (ORS), San Francisco California USA, 2012. Chapter 8

- M. Al-Hajjar, J. Fisher, S. Williams, J.L. Tipper, L. M. Jennings. Effect of Head Size on Wear of Ceramic-on-Ceramic Bearings in THRs under Steep Cup Inclination Angle and Adverse Edge Loading and Microseparation Conditions. Engineers and Surgeons Joined at the Hip III, IMechE, 2011. Chapters 3 and 5

- M. Al-Hajjar, J. Fisher, S. Williams, J.L. Tipper, L. M. Jennings. Effect of Head Size on Wear in Metal-on-Metal Bearings in THRs under Steep Cup Inclination Angle and Adverse Edge Loading and Microseparation Conditions. Engineers and Surgeons Joined at the Hip III, IMechE, 2011. Chapters 4 and 6

- M. Al-Hajjar, J. Fisher, S. Williams, J.L. Tipper, L. M. Jennings. Wear of Ceramic-on-Ceramic Bearings in THRs: Effect of Head Size under Steep Cup Inclination Angle and Microseparation and Edge Loading Conditions. International Society for Technologies in Arthroplasty (ISTA), 2011. Chapters 3 and 5

- M. Al-Hajjar, J. Fisher, S. Williams, J.L. Tipper, L. M. Jennings. Wear of Metal-on-Metal Bearings in THRs: Effect of Head Size under Steep Cup Inclination Angle and Microseparation and Edge Loading

Conditions. International Society for Technologies in Arthroplasty (ISTA), 2011. Chapters 4 and 6

- M. Al-Hajjar, J. Fisher, S. Williams, J.L. Tipper, L. M. Jennings. Metal on Metal Total Hip Replacement: Influence of Head Size Under Adverse Hip Simulator Conditions. British Orthopaedic Research Society (BORS), Cambridge UK, 2011. Chapters 4 and 6

- M. Al-Hajjar, S. Williams, J. Fisher, L.M. Jennings. Effect of Head Size on Wear in Metal-on-Metal Bearings in Total Hip Replacements under Steep Cup Inclination Angle and Adverse Edge Loading and Microseparation Conditions. Orthopaedic Research Society (ORS), Long Beach California USA, 2011. Chapters 4 and 6

- M. Al-Hajjar, J. Tipper, S. Williams, J. Fisher, L.M. Jennings. Wear of Metal-on-Metal Bearings in Total Hip Replacements: Influence of Head size and Surgical Positioning. Furlong HCA25, London, 2010. Chapters 4 and 6

- M. Al-Hajjar, S. Williams, J. Fisher, L. M. Jennings. The Influence of Cup Inclination Angle and Head Position on the Wear of Metal-on-Metal Bearings in Total Hip Replacements. 6th World Congress of Biomechanics, Singapore, 2010. Chapter 4

- M. Al-Hajjar, L.M. Jennings, I.J. Leslie, S. Williams, T. Stewart, J. Fisher. The Influence of Edge Loading on the Wear of Fourth Generation Ceramic-on-Ceramic Bearing in Total Hip Replacements. Orthopaedic Research Society (ORS), New Orleans USA, 2010. Chapter 3

- M. Al-Hajjar, L.M. Jennings, I.J. Leslie, A.L. Galvin, S. Williams, J. Fisher. The Influence Of Surgical Positioning And Function On The Wear Of Ceramic-On-Ceramic Total Hip Replacement. The 13th BIOLOX® Symposium, Edinburgh UK, 2009. Chapter 3

- M. Al-Hajjar, L. M. Jennings, I. J. Leslie, J. Fisher. Ceramic-On-Ceramic Total Hip Replacement: Influence of Cup Inclination Angle And Head Position. British Orthopaedic Research Society (BORS), Newcastle UK, 2009. Chapter 3

- L M Jennings, M Al-Hajjar, I J Leslie, J Fisher. The Influence Of Cup Inclination Angle And Head Position On The Wear Of Ceramic-On-Ceramic Total Hip Replacements. British Hip Society (BHS), Manchester UK, 2009. Chapter 3